An investigation of peptide-based translocating systems and their potential for gene therapy

Nwachuku, Julia Nonyelum Lucille

Award date:
2000

Awarding institution:
University of Bath

An Investigation of Peptide-Based Translocating Systems and their Potential for Gene Therapy

Submitted by Julia Nonyelum Lucille Nwachuku
for the degree of Doctor of Philosophy
of the University of Bath
2000

ProQuest LLC
789 East Eisenhower Parkway
P.O. Box 1346
Ann Arbor, MI 48106-1346

SUMMARY

The discovery of peptide domains, which can facilitate translocation of polypeptides or nucleic acids across biological membranes, has important implications for the therapeutic use of recombinant proteins, oligonucleotides and plasmid DNA.

The initial aim involved the synthesis of a cell penetrating peptide sequence based on the homeodomain of the *Drosophila* protein Antennapedia (pAntp) which has been found to translocate through the membrane of neurons *in vitro* and accumulates in their nuclei. The challenge of the project was to work out how these peptides function and the kinetics involved in their translocation. A selection of fluorescent probes was incorporated in the peptide sequence to allow analysis of the cellular uptake of the peptide(s) using techniques such as electron, confocal and low light microscopy. Both electron and confocal microscopy gave evidence to suggest that the uptake and intracellular movement of the peptides in B16 cells was due to endocytosis. The other translocating system was VP22 from the herpes simplex virus, which is found to exhibit the unusual property of intercellular transport. This function was investigated *in vitro* and in animal tissues, namely muscle and tumour. Although spread of VP22 was observed in mouse tumour tissue, this effect was not seen in muscle. The methods of gene delivery that have been studied include viral and non-viral methods. While viral vectors are efficient transfection agents *in vivo*, they exhibit a number of significant disadvantages including immunogenicity and the production of replication competent viruses. Although the efficiency of non-viral methods *in vivo* is relatively low compared with viral vectors, such methods display low toxicity and are unlikely to provoke inflammation. The ability of the peptides to transfer DNA into cells was tested using *in vitro* transfection techniques. Conditions were optimised in B16 cells and the transfection efficiency varied between a series of mammalian cell lines. The level of gene expression was enhanced by the addition of 25 lysine residues to penetratin particularly in the presence of chloroquine. This implies that uptake is mostly by endocytosis. However, the overall transfection efficiency was not better than endosomolytic agents. The assembly of virus-like particles to facilitate gene delivery was achieved by using synthetic components. These particles accomplished cellular uptake and efficient endosomal escape, fulfilling some of the useful attributes of viral vectors.

Dedication

For Leonora Haynes, mum, dad and Julia Haynes

"Fear is a darkroom for developing negatives"

-Jess Stock

Acknowledgements

My sincere gratitude must go to Dr. Colin W. Pouton for his never ending optimism and lively enthusiasm as my supervisor throughout my time at the University of Bath. Thanks also to Dr. Steve Moss and Dr. Mike Tobyn for their advice on many occasions.

I am grateful to some academic staff for their advice and assistance with various aspects of the project: Dr. Graham Bloomberg at the University of Bristol for peptide synthesis, Ursula Potter for electron microscopy experiments, Dr. Stewart Abbot for flow cytometry analysis, Dr Charareh Pourzand for numerous advice on molecular biology techniques, Dr. Pauline Wood for her help with animal experiments, Dr. Paul Mapp and colleagues for immunohistochemistry techniques, Dr. Mick Arnott for his molecular biology experience, Kim Dora for UV microscopy experiments. I am particularly grateful to Ian Jones and Dave Tosh for numerous advice with confocal microscopy techniques. Last but not the least, thanks to Mike Holton at GlaxoWellcome for his assistance with zeta potential and particle size measurements.

In addition, thanks to the EPSRC, Bath University and AstraZeneca (case award) for financial assistance, which is gratefully acknowledged. I especially wish to thank Dr. Marianne Ashford, Dr. Keith Horspool, Dr. John Smith and other AstraZeneca employees for their interest and useful discussions.

Many thanks must go to my family and friends. Your continued support and encouragement is greatly appreciated.

Table of Contents

Tables

Figures

Abbreviations

A	absorbance
AAV	adeno-associated virus
ADA	adenosine deaminase
β-gal	β-galactosidase
BSA	bovine serum albumin
cm	centimetres
CMV	cytomegalovirus
C-terminus	carboxy end of a peptide
Da	daltons
DABCO	diazabicyclo[2,2,2]octane
DMF	dimethylformamide
DMSO	dimethylsuphoxide
DOTAP	N-[1-(2,3-dioleoyloxy)propyl]-N,N,N-trimethylammonium chloride
DNA	deoxyribonucleic acid
DTT	dithiothreitol
EDTA	ethylene diamine tetra-acetic acid
EGFP	enhanced green fluorescent protein
EM	electron microscopy
FACS	fluorescence activated cell sorting
FCS	foetal bovine serum
FITC	fluoresecin isothiocyanate
Fmoc	N-(-9-fluorenyl)methoxycarbonyl
FPE	fluorescein phosphatidylethanolamine
g	acceleration due to gravity (= 9.81 m/s^2)
g	gram(s)
GDV	gene delivery vector
HBS	hepes buffered saline
HD	homeodomain
HEPES	N-(2-hydroxyethyl)piperazine-N-2'-ethane sulphonic acid
HPLC	high performance liquid chromatography
HIV	human immunodeficiency virus
LB	Luria Bertani
Luc	luciferase gene
μ	micro
M	mole(s) per liter
MEM	minimum essential medium
mg	milligram(s)
ml	milliliter(s)
MTT	1-[4,5-dimethylthiazol-2-yl]-3,5-diphenylformazan
N-terminus	amino end of a peptide
NEAA	non essential amino acid

ng	nanogram(s)
NHS	N-hydroxysuccinimide
NLS	nuclear localization signal
nm	nanometre(s)
OD	optical density
Opfp	O-pentafluorophenyl
pAntp	antennapedia protein
PBS	phosphate buffered saline
PCS	photon correlation spectroscopy
PE	phosphatidylethanolamine
PEG-PS	polyethylene glycol-polystyrene
PEI	polyethyleneimine
PVP	polyvinylpyrrolidone
RNA	ribonucleic acid
rpm	revolutions per minute
RSV	Rous Sarcoma Virus
SD	standard deviation
TAE	tris-acetate-EDTA buffer
TBE	tris-borate-EDTA buffer
TE	tris-EDTA buffer
TEM	transmission electron microscopy
TFA	trifluoroacetic acid
Tris	tris(hydroxymethylaminomethane)
Triton X-100	t-octylphenoxypolyethoxyethanol
UV	ultraviolet
V	volts
VP22	viral protein 22
v/v	volume by volume
w/v	weight by volume
λ	wavelength
X-gal	5-bromo-4-chloro-3-indolyl-β-D-galactopyranoside

CHAPTER 1

INTRODUCTION

1.1 THE PROMISE OF GENE THERAPY

Over the past several decades the development of methods for delivering genes to mammalian cells has stimulated great interest in the possibility of treating human disease by gene-based therapies. The gene therapy concept is based on the assumption that definitive treatment for genetic diseases should be possible by directing treatment to the site of the defect itself, the mutant gene, rather than to secondary effects of mutant gene products. Somatic gene therapy involves the process of inserting specific genetic information into a cell in order to replace, augment or eliminate an absent or defective gene and holds promise as a major innovation in medical science. The new gene serves as the code enabling the patient's cells to produce a specific protein that prevents or fights a disease. There are several reasons for this expanding interest in the discovery and development of gene delivery systems. Firstly, aimed at treating diseases at the most basic level, gene therapy could represent an important advance in the treatment of genetic disorders, such as haemophilia, cystic fibrosis, Duchenne muscular dystrophy and acquired multifactorial diseases, such as metabolic disorders, different forms of cancer and HIV infection (Anderson, 1992; Crystal, 1995; Friedmann *et al.*, 1997; Ledley, 1994; Hodgson *et al.*, 1995). Secondly, the clinical use of conventional protein drugs presents various limitations including formulation difficulties leading to low bioavailability and poor pharmacokinetics as well as a high cost of scale-up and manufacture. Hence gene therapy methods show high promise in aiming to overcome these limitations. Gene therapy can be used potentially to, (i) restrict expression of a therapeutic protein to specific cells within the body, (ii) control the level of expression in response to clinical needs, and (iii) achieve expression for a sustained time after a single administration. The intracellular distribution of therapeutic proteins can also be controlled by gene therapy. Successful development of gene therapy technologies will require a multidisciplinary approach for the design and optimization of delivery systems. There would also be a need to adjust gene-dosing regimens according to the needs of the patient. Different

biological targets and diseases will require different therapeutic technologies. Although gene therapy offers several new and promising approaches to disease treatment, there remains the issue of relatively low efficacy experienced in various clinical trials (Williams, 1995). Thus, it is critical to identify ways to improve the efficiency of gene delivery and expression in order to broaden the clinical opportunities of gene therapy. There are a number of obstacles (extracellular and intracellular), which can potentially reduce the amount of DNA getting through to its target site. To optimize and combine the different functions for extracellular and intracellular requirements is a major challenge. The significance of each of these barriers will depend on the intended route of administration and the location of target cells. Any advance in gene delivery will require a better understanding of these barriers at a fundamental level in an attempt to improve efficiency.

1.2 APPROACHES TO SOMATIC GENE THERAPY

Finding the right method or vector for introducing new genetic material into the cell remains a substantial challenge in the development of gene therapy. Scientists are working on ways to deliver therapeutic genes to enough of the right types of cells to achieve the desired treatment outcome. Multiple methods have been developed to transfer genes into cells of patients and various research groups have explored these options (Miller, 1992; Kay *et al.*, 1993; Ledley, 1995; Knowles *et al.*, 1995; Mendell *et al.*, 1995). The efficiency of transfer, whether or not persistence of expression is desired, and the levels of expressed gene product that can be achieved, are some of the characteristics that will determine the type of vector employed. The principle strategies for gene delivery can be classified according to the nature of the product to be administered to a patient. There are two basic ways by which genes can be provided to patients. Both methods involve the introduction of genes into vectors that are capable of transporting genes into cells. More commonly, cells are removed from a selected tissue in a patient, exposed to gene delivery vectors *in vitro* (*ex vivo*) and the genetically corrected cells are returned to the patient. Other methods involve introduction of vectors directly into the tissue to be treated (*in vivo*).

1.2.1 *Ex vivo* gene therapy (cell-based)

Early clinical trials involved transfer of *ex vivo* adenosine deaminase (ADA) gene into lymphocytes of a patient having an otherwise lethal defect in this enzyme, which produces immune deficiency (Miller, 1992). The results of this trial were relatively limited due to relatively small amounts of cells containing the therapeutic gene and subsequent low levels of expression of ADA. Other approaches to gene therapy used either implanted cells or modified viruses for gene transfer. The first approved trial of gene transfer involved an *ex vivo* approach (Culver and Blaese, 1994). There have been safety and efficacy issues concerning the applications of both cell- and viral-mediated strategies for the treatment of other diseases, including cystic fibrosis (Marshall, 1995). There are other *ex vivo* gene therapy strategies based on the introduction of genes into bone marrow cells and these are being used in clinical trials for the treatment of Gaucher's disease (Ohashi *et al.*, 1992), AIDS (Yu *et al.*, 1995; Riddell *et al.*, 1992) and to protect bone marrow from chemotherapy toxicity (Deisseroth *et al.*, 1994). More recently, exciting results have been obtained by successful human gene therapy clinical trials for the treatment of inherited severe combined immunodeficiency (SCID), which can occur when mutations in several different genes of immune cells exist (Cavazzana-Calvo *et al.*, 2000), treatment of haemophilia (Kay *et al.*, 2000) and growth of new blood vessels to treat cardiovascular disease (Isner and Asahara, 1999).

1.2.2 Viral-based *In vivo* gene therapy

Viral vectors are based on natural viruses where at least one viral gene has been replaced by the therapeutic gene. Viral vectors are widely used since the molecular biology of viruses is well understood and they give high levels of RNA uptake and expression. Introduction of DNA into the target cell is performed via optimized and highly evolved pathways of infection without further viral spread post transduction. Such pathways provide these vectors with access to a number of target cells, uptake via receptor-mediated endocytosis and efficient intracellular trafficking from the endosomes to the

nucleus. Hence, a number of viruses have been explored for gene delivery *in vivo* (Rosenfeld *et al.*, 1992).

1.2.2.1 Retroviral vectors

Retroviruses were the first viral vectors used in gene therapy. They splice copies of their genes permanently into the chromosomes of the cells they invade (Miller, 1990). This permanent integration of therapeutic genes reduces the ability of physicians to terminate therapy as a result of adverse effects. Retroviral genes stably integrate and this process is not transient. Other factors may shut down expression. Although retroviruses have been used for direct administration to patients, this has been limited by the rapid inactivation by human complement. Recently, some groups have attempted to modify retroviruses by inhibiting complement activation and complement-mediated elimination (Rother *et al.*, 1995; Rother *et al.*, 1995). Other challenges include the random splicing of DNA into host chromosomes that may lead to activation of cellular oncogenes. Also, there is an inherent inability to characterize completely the retroviral vector preparations used for gene transduction generating replication-competent retroviruses (Temin, 1990).

1.2.2.2 Adenoviral vectors

These vectors are of interest because of their potential for *in vivo* gene delivery. Adenoviruses are capable of infecting non-dividing and dividing cells efficiently, expressing large amounts of gene products (Trapnell, 1993; Addison *et al.*, 1995; Chen *et al.*, 1994). Integration of adenoviral DNA sequences does not appear to be an integral part of their life cycle. This feature avoids the possibility of disturbing vital cellular genes. Because the DNA eventually disappears, there would have to be repeated administration of treatments for chronic diseases such as cystic fibrosis. The more serious obstacle to the use of adenoviral vectors in patients is the activation of host immune responses and inflammation in target tissues (Dai *et al.*, 1995). Various reports have described cellular immune responses against transduced cells (Yang *et al.*, 1995; Yei *et al.*, 1994; Brody *et al.*, 1994). Such responses have perhaps contributed to a lack

of gene expression using adenoviral vectors in patients (Knowles *et al.*, 1995; Eissa *et al.*, 1994; Fang *et al.*, 1995).

1.2.2.3 Adeno-associated viral vectors

Adeno-associated viruses (AAV) are DNA viruses capable of permanently inserting their genome into the chromosomes of the host cell (Kotin, 1994). AAV vectors can infect both dividing and non-dividing cells (Podsakoff *et al.*, 1994). AAV vectors are appealing because they cause no known diseases in people and have been shown to produce efficient long-term gene transfer (Xiao *et al.*, 1996; Kessler *et al.*, 1996). However, due to their smaller size, they may not be able to accommodate large genes compared to retroviruses. The requirement for a helper virus to produce sufficient titers of the virus for clinical use has negatively impacted the success of AAV vector production (Flotte *et al.*, 1995).

1.2.2.4 Other viral vectors

There are several other viruses being explored as vectors as well including herpesviruses, alphaviruses and poxviruses. None is perfected yet, but each is likely to have its own therapeutic niche. For example, herpesviruses have potential as vectors for therapy aimed at neurological disorders. They are attracted to neurons, some of which retain the virus in a harmless state for the lifetime of the affected person. Alphaviruses have several features, which make them suited for use as expression vectors. The RNA genome is infectious due to its positive polarity, that is, naked genomic RNA is able to initiate an infection when introduced into the cytoplasm of a cell (Liljestrom, 1995). The alphaviruses upon which today's vectors are based (Semliki Forest and Sindbis virus) are not widespread, vector proteins are not produced and therefore there will be no pre-existing immunity against the vector (Liljestrom, 1995).

1.2.3 Bacterial-mediated gene delivery

One requirement for bacteria to transfer genetic material into mammalian cells is the ability to invade the host cell. Certain intracellular pathogens have developed specific mechanisms for cell entry and growth within cells. Several groups have reported direct introduction of DNA from bacteria to mammalian cells. Work by Grillot-Courvalin *et al.*, 1998 showed that an invasive strain of *E. coli* could express EGFP in both dividing and quiescent cells. This strain of *E coli* is unable to synthesize cell wall and lyse without the presence of diaminopimelic acid (DAP). These DAP-ve *E. coli* were modified by the incorporation of two separate genes. The first was the invasin gene from *Yersinia pseudotuberculosis*, which is necessary for entry of *E. coli* into nonphagocytic cells that express a subset of β1-integrins. The second gene, hly, encodes for the listeriolysin O gene from *Listeria monocytogenes* and allows *E. coli* (and DNA) to escape from the entry vesicle.

Bacterial transfer of DNA for stimulation of the mucosal immune response holds some potential and has been reported by Dietrich *et al.*, 1998. An attenuated self-destructive strain of *Listeria monocytogenes* was shown to express a listeria-specific phage lysin from the ActA promoter. The suicide lysin is expressed once the promoter is activated, causing the bacteria to lyse and release plasmid DNA into the cytosol. This system has potential for oral administration since the bacteria invades its host through the intestinal mucosal surface. Also, antigen presentation occurs shortly after infection, presenting an opportunity for DNA vaccine development.

Lemmon *et al.*, 1997 described introduction of a gene for *E. coli* nitroreductase, using the obligate anaerobe *Clostridium beijerinckii*. This enzyme activates a nontoxic drug CB 1954 to a bifunctional anticancer agent. Significant nitroreductase activity was detected only in tumours. This selectivity is thought to be due to the hypoxic environment required for growth of these bacteria since the oxygen tension in normal tissues is sufficiently high to prevent germination of clostridia. These hypoxic regions typically occur in many solid tumours in humans.

1.2.4 Non-viral gene delivery

A non-viral gene medicine is composed of a gene encoding a therapeutic protein, a synthetic gene delivery system that controls the location of the gene within the body and a plasmid-based gene expression system that controls both the function of a gene within a target cell and secretion of the produced therapeutic protein (Tomlinson and Rolland, 1996). Gene medicines are designed to be administered to a patient by conventional routes using conventional methods such as direct injection into target tissues (e.g., muscle and tumours), inhalation or intravenous injection. They are intended to have low toxicity due to the use of synthetic material for gene delivery and non-integrating plasmids. The plasmids degrade within the body, leading to a finite duration of gene expression. At the doses applied, there is no report so far of plasmid integration into host chromosomes *in vivo*. Thus they should not lead to insertional mutagenesis or oncogenesis as compared to the risks associated with the use of several viral vectors. Several groups have described non-viral approaches for gene transfer (Ledley, 1995; Perales *et al.*, 1994; Baker *et al.*, 1997; Cotten and Wagner, 1997; Wolff *et al.*, 1990). These systems are attractive for various reasons: (I) they can be generated by assembly of few, defined components, (II) they can be very flexible regarding the size of DNA to be transported, (III) the whole diversity of chemical reactions and physical interactions may be utilized for the synthesis and assembly of transfection material, (IV) plasmid DNA and transfection reagents can be produced at a large scale with rather low costs, and (V) safety testing of synthetic material is less laborious than testing of recombinant material.

1.2.4.1 Naked DNA gene transfer

Plasmids are colloidal systems of specific hydrodynamic size, very hydrophilic macromolecules and have a highly negative surface charge. These properties determine their biological distribution, cellular uptake, intracellular trafficking and nuclear translocation (Lew *et al.*, 1995; Liu *et al.*, 1995; Ledley *et al.*, 1994; Thierry *et al.*, 1995). Wolff *et al.*, 1990 reported efficient gene transfer in rodent muscle cells, mainly in the myofibres, after intramuscular application of naked DNA in saline without any cationic

lipids or retroviruses. This was a surprising finding that led to subsequent studies on the use of naked DNA to express therapeutic proteins. The slow turnover rate of myofibre nuclei is thought to allow plasmid DNA to persist for up to several months. Wolff *et al.*, 1992 showed that expression of luciferase DNA under regulation by the rous sarcoma viral (RSV) promoter lasts for at least 19 months postinjection. Hence, plasmid DNA appears to exhibit significant stability when injected into muscle tissue (Utvik *et al.*, 1999). Elicitation of a greater degree of efficiency of plasmid uptake may be achieved by combining DNA transfer with myotoxic agents that selectively destroy myofibres (Davies *et al.*, 1993).

Conditions have been worked out for the local gene transfer of naked DNA in a number of animal tissues including skin (Hengge *et al.*, 1996). Budker *et al.*, 1996 reported high levels of luciferase expression by injecting naked plasmid DNA into the portal veins of mice. However, the levels were achieved with hyperosmotic injection solutions and occlusion of the blood outflow from the liver. These conditions widen the sinusoid fenestrae and enhance extravasation of plasmid DNA. Again Budker *et al.*, 1998 demonstrated efficient expression of plasmid DNA within muscle when all blood vessels leading into and out of the hindlimb were occluded. Vile and Hart, 1993 described injection of DNA, encoding the β-gal gene expressed from two promoters, into B16 melanomas resulted in extensive transduction of tumour cells in B16s whereas no expression was seen in other cell types, due to the inclusion of cell type-specific expression cassette into the vector. The transfection efficiency appears to be species-dependent with less expression observed in animals bigger than mice. Also, very large amounts of DNA have to be injected. Nevertheless, Mumper *et al.*, 1996 developed polymeric gene delivery systems as an example of optimization of formulation for gene delivery to muscle. They showed that plasmid DNA formulated in 5% polyvinyl pyrrolidone was better dispersed in the tissue as compared to plasmid DNA formulated in saline. These systems are designed to disperse and retain the DNA throughout the muscle as well as protect it from nuclease degradation.

Alternatives to injection by needle include administration involving propelling the solution by needle-free jet injection, (Furth *et al.*, 1992). Also, Yang *et al.*, 1990 demonstrated *in vitro* and *in vivo* gene transfer by particle bombardment using the gene

gun where gold microparticles are loaded with DNA and fired into the target tissue. Also, improved local expression was obtained by delivering electrical pulses to the DNA-loaded area (Aihara and Miyazaki, 1998; Heller *et al.*, 1996).

Following characterization of the expression and pharmacokinetics of plasmid DNA delivered alone or complexed with cationic liposomes, reports by Meyer *et al.*, 1995 attempted to elucidate the mechanism of DNA uptake by cells. They showed that reduced gene expression in the presence of dextran sulfate and saturation of the dose-expression relationship supported receptor-mediated DNA uptake.

The high relative efficiency of plasmid DNA in all situations encourages more applications of this method to problems of therapeutic strategies for various diseases and DNA-based vaccination protocols (Ulmer *et al.*, 1993). Isner, 1998 reported early clinical trial results of treatment of an ischaemic limb after intraarterial gene transfer of naked DNA encoding for vascular endothelial growth factor (VEGF). Improvements in levels of serum VEGF, proliferation of new blood vessels and increase in capillary density were observed. Long *et al.*, 1999 reported higher plasma insulin concentrations and significantly reduced hyperglycaemia in diabetic mice after naked plasmid was injected into skeletal muscle.

1.2.4.2 Expression plasmids

Expression plasmids for non-viral gene therapy should direct the synthesis of therapeutic proteins in a manner that is accurate, achieves a level sufficient for therapeutic effect, and is controlled in duration. In plasmids, the size of the inserted DNA fragment that contains the therapeutic gene(s) is unlimited. Plasmids of high quality (>90% supercoiled DNA, 99% purity) can be purified from bacterial fermentations in high yield and in a cost-effective manner. Conditions for maintaining the chemical stability of plasmids at or near ambient temperatures are known, and plasmids may be stored for long time periods as aqueous suspensions or lyophilized material (Nordstrom, 1999). Improvements in the persistence of gene expression will further help to overcome the limitations in gene delivery and create new therapeutic opportunities. The single most important influence of plasmid expression levels in transfected cells is the

enhancer/promoter. Hartikka *et al.*, 1996 reported significant superiority of the cytomegalovirus (CMV) promoter to RSV when plasmids were injected into mouse muscle. A comparison of both promoters showed that expression by CMV was two-fold greater than with the RSV promoter and four-fold greater than simian virus (SV40) promoter (Qin *et al.*, 1997). The most active constructs contain a CMV promoter, a cleavable intron (int), and an improved bovine growth hormone-derived terminator and polyadenylation signal (BGH) (Felgner, 1996). Wheeler *et al.*, 1996 found that similar constructs gave at least 50 times higher expression in mouse lung compared to previous CMV based vectors.

Different groups have considered factors that affect the persistence of plasmid expression. Although integration of expression plasmids into genomic DNA would be the most effective way to ensure plasmid persistence in transfected cells, it is not desirable since random integration into genomic sites may result in activation of oncogenes. Wolff *et al.*, 1990 reported no integration into host chromosomes *in vivo*. In addition, lack of persistent expression *in vivo* could result from destruction of transfected cells by the immune system (Davies *et al.*, 1997). Loss or degradation of transfected DNA may be overcome by the introduction of replication elements. Although the best-characterized origins are from viral sources, research is moving towards characterizing mammalian origins of replication (Wohlgemuth *et al.*, 1996) to avoid the risks of immunogenicity associated with viral origins. Another mechanism that may be responsible for short-lived expression *in vivo* is promoter shutdown and this is thought to be due to short-lived transcription factors. Generally, immunological issues are significantly reduced in comparison with viral vector approaches.

1.2.4.3 Lipid-based gene delivery systems

Liposome-mediated gene delivery has been used successfully by various groups to transfer both reporter and physiologically relevant genes *in vitro* and *in vivo* (Caplen *et al.*, 1995; Alton *et al.*, 1993; Conary *et al.*, 1994; Hyde *et al.*, 1993; Leventis and Silvius, 1990; Logan *et al.*, 1995). The prototype cationic lipid for gene transfer is DOTMA (Felgner *et al.*, 1994). Formulations of DNA with cationic lipids such as DOTMA and a

neutral phospholipid, commonly DOPE, produce lipid/plasmid DNA complexes that are capable of introducing DNA into cells at high efficiency (Felgner *et al.*, 1989). Commercially available cationic lipid mixtures (Lipofectin and Lipofectamine) are used routinely for basic research. Cationic lipids that have been investigated more recently for gene transfer *in vitro* (Jiao *et al.*, 1992; McLachlan *et al.*, 1994; Cheng, 1996; Walker *et al.*, 1996) include variations of quaternary amine-based cationic lipids including DMRIE (Wheeler *et al.*, 1996) and covalent linkage of polylysine (Zhou and Huang, 1994) or polycations such as spermine and spermidine (Behr *et al.*, 1989; Loeffler *et al.*, 1990) onto the diacylated backbone or sterol.

Neutral lipids such as DOPE and cholesterol are generally included in plasmid/lipid complexes and are thought to effect the release of plasmids from the endosomes after endocytic uptake of the plasmid/lipid complex by the cells (Farhood *et al.*, 1995). Different structures have been described for the resulting complex formed when plasmids interact with cationic lipids, which can be micellar or liposomal in structure. Gustafsson *et al.*, 1995 used cryoelectron microscopy to show that plasmid/lipid systems resembled multilamellar vesicles suggesting that lipid bilayers were able to maintain their structure and form stacks of bilayers with DNA intercalated between the bilayers. Gao and Huang, 1995 reported that plasmid/DC-Chol:DOPE complexes appeared as 'spaghetti and meatball' structures. Another proposed model involves the reorganization of the initial lipid structure by fusion of adjacent lipid structures induced by the polyanionic plasmid. This results in the coating of the DNA with a lipid bilayer along the entire length of the plasmid and possible hexagonal packed structures (Sternberg *et al.*, 1994; Gershon *et al.*, 1993).

The processes by which plasmids are able to access the nucleus for expression to be initiated after transfection of the cells are still unclear. Only a few mechanistic studies have been initiated with the aim of elucidating the processes that enable plasmids to dissociate from a plasmid/lipid complex and translocate to the nucleus of the transfected cells. Many factors influence the pathway of entry including the colloidal and surface properties of the system and the type of transfected cell. Most experimental results now support that the uptake of complexes occurs by an endocytic pathway (Wrobel and Collins, 1995; Zhou and Huang, 1994). Zabner *et al.*, 1995, presented direct evidence of

endocytic uptake by following the entry of unlabeled and gold particle-labeled plasmids condensed with cationic lipids into different cell types *in vitro*. Indirect evidence has been obtained by showing that chloroquine, a lysosomotrophic agent which raises the pH of the endosomal compartment and prevents fusion of endosomes with lysosomes, was able to increase *in vitro* transfection efficiency of plasmid/lipid complexes (Felgner *et al.*, 1994; Zhou and Huang, 1994; Legendre and Szoka, 1992). *In vitro* uptake of plasmid/lipid complexes has been reported to require 4-6 hours of incubation to achieve maximal gene transfer into cells (Van der Woude *et al.*, 1995).

Cationic lipids have been used extensively over the recent years in preclinical studies to deliver genes to the lung epithelium of various species, including rats, by aerosol delivery (Stribling *et al.*, 1992). They used a 1: 1 molar ratio of cationic: neutral lipid to generate DNA-lipid complexes suitable for delivery to the mouse airway in aerosol form. The first clinical trial using cationic lipid-based systems was initiated by Nabel *et al.*, 1993. DC-chol/DOPE-based systems were used to complex a gene expression system containing the HLA B7 gene. The plasmid/lipid complex was injected into melanomas to induce an immune response against the antigen and potentially enhanced presentation of tumour-specific antigens. Studies in five patients demonstrated uptake and expression of plasmid in the tumours and a partial local response against the tumour. The consistently growing number of clinical trials indicates the promise of such approaches.

1.2.4.4 Polymer-based gene delivery system

1.2.4.4.1 Condensing cationic polymers

Dendrimers are a class of polymers in which an amine starting material is repeatedly substituted at its amino termini to provide a branched structure. At each round of synthesis, another layer of branched chains is added and termed a 'generation'. For example, a dendrimer with three layers is a 3rd generation dendrimer. Application of cationic polymers, such as polybrene has been solely restricted to *in vitro* gene transfer due to their relative low efficiency, cytotoxicity or non-biodegradability. As a result, novel polycationic polymers have recently been investigated for *in vitro* gene transfection

by several groups (Kabanov and Kabanov, 1995; Haensler and Szoka, 1993; Kukowska-Latallo *et al.*, 1996; Boussif *et al.*, 1995). Non-linear cationic polymers, such as polyamidoamine cascade dendrimers (e.g., Starbust™ dendrimers) can be produced by controlled synthesis with either ammonia or an ethylenediamine core by successive addition of methyl acrylate and ethylenediamine. Because each layer should be fully substituted, the resulting spheroidal dendrimer has a precise diameter, molecular weight and number of terminal amines. Dendrimers can condense plasmids through electrostatic interactions of their terminal primary amines with the DNA phosphate groups. Tomlinson and Rolland, 1996 examined the effect of the colloidal and surface characteristics of plasmid/dendrimer complexes on gene delivery efficiency. Plasmid/dendrimer complexes have been shown to have different zeta potential values depending on the concentration of the dendrimers in the complex. Kukowska-Latallo *et al.*, 1996 reported the efficient *in vitro* transfer of plasmids into various mammalian cells using higher generation dendrimers (5^{th} to 10^{th}), which was enhanced by addition of chloroquine. Tang *et al.*, 1996 showed data to suggest that transfection activity is dramatically enhanced using degraded dendrimers that are capable of causing endosomal escape due to the presence of titratable amines on these polymers.

There has been enormous interest in the use of the cationic polymer, polyethyleneimine (PEI) for gene delivery. PEI is not only among the best vectors currently available *for in vitro* work but is proving to be a versatile and effective carrier for different *in vivo* situations. PEI has the highest cationic charge density of any known organic macromolecule (Kichler *et al.*, 1999) since one in every three nitrogens is in an amine group and the overall protonation level increases from 20% to 45% between pH values of 7 and 5 (Suh *et al.*, 1994). PEI has been shown to mediate gene transfer into a variety of cells and primary cultures with an efficiency at least as high as that of cationic liposomes (Boussif *et al.*, 1995), without the addition of any cell-binding ligand or endosomolytic moiety. In contrast to polylysine, PEI combines DNA binding and condensing activity with a high pH-buffering capacity almost over the entire pH range (Tang and Szoka, 1997). Marshall *et al.*, 1999 showed that PEI was better than polylysine at condensing and transfecting yeast artificial chromosomes (YACs). PEI has also been found to enhance the delivery of adenovirus-bacterial artificial chromosome (BAC) DNA

complexes to cultured cells (Baker and Cotten, 1997). Chemical modification of PEI does not interfere with its high buffering capacity and ability to cause endosomal lysis and several cell-binding ligands have been successfully coupled with PEI to mediate selective gene transfer. Zanta *et al.*, 1997 reported efficient transfection in hepatocyte-derived cell lines using galactosylated PEI. Transferrin and antiCD3 antibody were both incorporated by covalent linkage to PEI. The resulting conjugates achieved up to 1000-fold increase in transfection efficiency (Kircheis *et al.*, 1997). More recently, the integrin-binding peptide CYGGRGDTP was coupled via a disulphide bridge to dithiopyridine-derivatized PEI 25 kDa (Erbacher *et al.*, 1999b). Grafting an RGD-containing peptide to PEI condensed plasmid DNA into a homogeneous population of 30-100 nm toroidal particles and improved transfection in fibroblast and epithelial cells by two orders of magnitude. Exchange of aspartic acid (D) by glutamic acid (E) in the peptide sequence reduced the transfection levels to those of non-targeting complexes indicating the involvement of integrins in gene delivery with RGD complexes.

Observations by Pollard *et al.*, 1998 demonstrated that DNA complexed with PEI was transferred to the nucleus after microinjection into the cytoplasm, a property that is not seen with cationic lipids. In additional contrast to cationic lipid complexes, trafficking through the nuclear envelope appeared to be the rate-limiting step as opposed to the disassembly of PEI/DNA complexes in the nucleus.

One of the most promising aspects of PEI-based gene transfer comes from results *in vivo* that show PEI to have the edge on the other vectors. Intraventricular injection of PEI/DNA complexes formulated in 5% glucose showed the complexes to be highly diffusible in the cerebrospinal fluid of newborn and adult mice, diffusing from a single site of injection throughout the entire brain ventricular spaces (Goula *et al.*, 1998). Abdallah *et al.*, 1996 showed extremely high levels of transgene expression in the mature mouse brain. Intravenous delivery of cationic polymer/DNA complexes was found to induce clearance by the reticuloendothelial system (Plank *et al.*, 1996). A delivery system produced by Ogris *et al.*, 1999 involving polyethylene glycol (PEG) conjugation after transferrin-PEI/DNA formation, prevented interactions with plasma proteins, complement factors and erythrocytes. Also, modification with PEG did not interfere with *in vitro* transfection activity and interaction with the transferrin receptor was still

possible. Similar work done by Erbacher *et al.*, 1999a showed that conjugation of PEG to PEI/DNA complexes protected the complexes from parasitic interactions but interfered with condensation of DNA. In this case, conjugation of PEG occurred before DNA was condensed with the ligand-PEI conjugate.

1.2.4.4.2 Non-condensing cationic polymers

Gene delivery systems have been designed to control the distribution of gene expression systems in muscle tissue after direct intramuscular administration and consequently enhance their cellular bioavailability (Mumper *et al.*, 1995; Mumper *et al.*, 1996). Such systems increase the steady-state levels of both reporter and therapeutic genes expressed in muscle as compared to gene expression systems injected in isotonic saline.

One of the most effective muscle delivery system is based on protective, interactive, non-condensing polymers. These colloidal polymers include polyvinyl derivatives that interact with a plasmid via hydrogen bonding and hydrophobic interactions, facilitating uptake and reducing net negative surface charge of the plasmid. Immunohistochemical staining of rat muscle sections after intramuscular injection of either naked DNA or a polyvinyl pyrrolidone-based (PVP) formulation of plasmid showed that the polymeric gene delivery system increased the number and distribution of cells expressing a β-galactosidase gene (Mumper *et al.*, 1996). Kinetic studies also demonstrated that formulation of plasmids with PVP extends the range of dose responsiveness. Levy *et al.*, 1996 showed that the injection of 50-100 μg of plasmid in saline into rodent muscles provided maximal levels of gene expression, whereas Mumper *et al.*, 1996 reported that using PVP in the same models increased levels with doses higher than 100 μg of plasmid.

1.3 FACTORS LIMITING POLYCATION-BASED DNA DELIVERY.

In some applications, the delivery of RNA or oligonucleotides into the cytoplasm is sufficient for obtaining the desired biological effect. The majority of gene transfer approaches, however, aims at the delivery of DNA into the nucleus of the cell, where gene expression results from transcription into RNA, processing and delivery of RNA

into the cytoplasm, followed by translation into the corresponding protein. In any case the nucleic acid has to be delivered across cellular membranes: the cell surface membrane, the endosomal or lysosomal membranes, or the nuclear envelope. Basically, gene delivery can be envisaged as a series of hurdles (both extracellular and intracellular) that successively deplete the mass of DNA that progresses towards the target site. Improvement in the efficiency of any individual step would be expected to improve the overall efficiency.

1.3.1 Extracellular

The presence of serum nucleases rapidly degrades plasmid DNA. Kawabata *et al.*, 1995 reported a half-life of less than 10 minutes to degradation. DNA is found in blood at very low levels that varies among species due to the range of deoxyribonuclease activity found in these species. Various groups have shown that some cationic polymer-DNA complexes prevent such degradation and so could potentially solve this problem (Dash *et al.*, 1997; Kayatose and Kataoka, 1998; Leong *et al.*, 1998). It has also been found that serum inhibits association of complexes with the cell membrane. However, this can be improved by increasing the charge ratio, which allows the polyplexes to overcome the serum proteins (Mastrangeli *et al.*, 1996). The inhibition may also be overcome by allowing complexes to incubate in polyanion-containing media before addition to serum-transfecting media.

Hashida *et al.*, 1996 have reviewed the biodistribution of macromolecules and particles from the systemic circulation. The main uptake route of DNA was through scavenger receptors found on nonparenchymal cells in the liver. These data indicate the need to neutralize the polyanionic nature of DNA to avoid uptake by these liver cells. Several groups have published studies involving intravenous administration using polypeptide DNA-condensing agents, often targeted to the liver (Wu and Wu, 1993; Perales *et al.*, 1994b). However, these systems have been found to show variable transfection activity. The particle size of complexes is likely to be a major determinant of activity, since access to the liver probably requires particles smaller than 100 nm in diameter (Perales *et al.*, 1994a). Often, DNA-polylysine particles are reported to be greater than 100 nm in

diameter. The circulatory system is bounded by endothelium, which is mostly characterized as continuous endothelium. This implies that cells are held tightly together, and are located upon a basement membrane that structurally prevents molecules with diameters greater than 15 nm from passing through. Hence, in most tissues, exit of materials from the circulation becomes progressively difficult as molecular weight increases. Exception to this is tissues that contain leaky endothelium such as some tumours, inflamed tissues, spleen and liver. For 100 nm particles extravasation is likely to be highly dependent on blood pressure within the liver (Pouton, 1998). Systemically, such particles are almost invariably opsonized by serum proteins such as albumin, and are taken up by macrophage populations, mainly in the liver and spleen, unless they have a hydrophilic coating to reduce the level of opsonization and recognition (Stolnik *et al.*, 1995). In addition, the binding of albumin to cationic particles is known to reduce the zeta potential and promote aggregation of particles. Studies by Nishida *et al.*, 1991 suggest that cationic macromolecules are more readily taken up by the liver and spleen than are neutral polymers. Other studies on particles (Tabata and Ikada, 1988) postulate that particles with the lowest surface potential have lowest uptake by phagocytosis.

A few studies utilizing non-viral gene delivery systems have described considerable lung expression, which was also accompanied by severe systemic toxicity with up to 50% of the animals dying from lung embolism (Kircheis *et al.*, 1999; Ogris *et al.*, 1999). Obstruction of the lung capillaries is not surprising considering that the lung provides the first capillary bed encountered by the transfection complexes after intravenous injection. Particle sizes of 300-400 nm or less should not cause obstruction of the lung capillaries but the positive charge of the particles can be responsible for broad non-specific interaction with plasma components, extracellular matrix and cell membranes (Kircheis *et al.*, 1999). These interactions with serum or salt are likely to lead to growth of the particles, which finally are retained in the capillaries. Avid binding of positively charged complexes to cell membranes, e.g. binding to the lung capillary endothelium can enhance this process. Plank *et al.*, 1996 have investigated opsonization of different DNA-polycationic delivery systems through the ability of these complexes to cause complement activation. It was found that complement activation relates to the positive charge on the complexes with potency of activation being chain-length specific for

polylysine. Condensation with DNA reduced the activation of complement in all cases, with higher charge ratios resulting in greater complement activation. Similar activation was reported for all polycations tested including, polylysine, PEI, and dendrimers. Cationic lipids gave lower complement activation than polycations, but short chain oligolysines had similar properties to the lipids. Modifying complexes with PEG resulted in reduction in complement activation activity.

1.3.2 Intracellular

1.3.2.1 Membrane binding and internalization

The binding force of polycation-mediated delivery is thought to be the electrostatic interaction between the positive charges of the complex and the negative charges of the cellular membrane. The uptake of most macromolecules or particles into cells by passive diffusion across the plasma membrane is limited by their low solubility in lipid bilayers. Some polypeptides such as herpes simplex virus tegument protein VP22 (Elliott and O'Hare, 1997) and the Drosophila homeoprotein, Antennapedia (pAntp) (Derossi *et al.*, 1996) have the ability to translocate directly across the plasma membrane by mechanisms which are not fully understood. These polypeptides may have a role in the delivery of macromolecules (Prochiantz, 1996; Fahraeus *et al.*, 1996) but have not yet been harnessed for delivery of DNA plasmids. Uptake of most macromolecules or particles occurs into membrane-bound compartments by pinocytosis, adsorptive endocytosis, receptor-mediated endocytosis or phagocytosis (Gruenberg and Maxfield, 1995; Robinson *et al.*, 1996). The default pathway in the absence of an escape or trafficking mechanism will be fusion with lysosomes and ultimately degradation. Consequently, DNA taken up into a vesicle must have a means of escape or much of the internalized DNA will be lost through degradation. The plasma membranes extracellular surface has a net negative charge, which allows cationic particles to bind by electrostatic interaction. Adsorptive endocytosis is then likely to occur regardless of what complex provides the excess cationic charge. Moreover, there is no guarantee than endocytosis will lead to

transfection. Polylysine-DNA complexes are internalized, provided the net charge is positive, and even then only in the presence of chloroquine (Pouton, 1998).

A specific interaction with the extracellular surface may result in tighter binding and offers the possibility of cell-specific targeting of DNA delivery systems. Targeting ligands have been incorporated into DNA complexes to aid (1) targeting specific cell types and (2) enhancing intracellular delivery. One simple form of receptor-mediated transfection makes use of the binding of integrins to the tripeptide Arg-Gly-Asp (RGD). Hart *et al.*, 1996 reported increased transfection of polylysine-DNA complexes incorporating an RGD sequence, probably by promoting internalization following integrin binding, in the same pathway as that followed by adenoviruses. Another useful ligand is transferrin, because its receptor is ubiquitously expressed and readily internalized upon binding to its ligand. Hence, a rapid rate of uptake could be exploited. Also, transferrin is known to recycle through the endosomal compartment without necessarily being routed to the lysosome (Wagner *et al.*, 1994). In these cases, internalization is by the efficient cellular process of receptor-mediated endocytosis. For this purpose conjugates with polylysine, protamines, histones, PEI, cationic lipids and other polycations have been generated and tested. Data from these experiments suggest that the nature of the cationic carrier can strongly influence which of the cellular barriers are most limiting for gene delivery.

1.3.2.2 Cytoplasmic trafficking

A general association between cytotoxicity and transfection suggests that a degree of membrane-damage must be mediated for DNA to get access to the cytoplasm. Successful transfection relies on achieving the correct balance between gaining adequate access of DNA into the cytoplasm and causing excessive and lethal damage to the cell (Pouton and Seymour, 1998). The ability of chloroquine to promote transfection activity of polycation-DNA complexes against a variety of target cells suggests that a vesicular stage with acidification is probably involved. Although the mechanism by which chloroquine mediates escape from the endosome has not been established beyond doubt, it seems likely that a major disruption of endosomal function is required due to osmotic swelling

(Pouton, 1998). This is challenged by reports that other lysosomotrophic bases, such as ammonium sulphate, which are similarly capable of buffering the endosomal pH, do not promote transfection. Observations by Erbacher *et al.*, 1996 postulated an alternative explanation, which is that chloroquine mediates its action via complex dissociation.

Viruses have acquired special mechanisms to release their genome from endosomes into the cytoplasm. In the case of membrane-free viruses such as adenoviruses, the endosomal acidification process specifically activates viral coat protein domains that trigger disruption of the endosomal membrane. In the case of enveloped viruses such as influenza virus the viral membrane fuses with the endosomal membranes. Several authors have explored viral means of endosomal escape (Wagner *et al.*, 1991; Plank *et al.*, 1992; Cotten *et al.*, 1990). Cotten *et al.*, 1990 reported that inactivated adenoviral particles used to mediate complex escape from the endosome increased transfection efficiency dramatically. The disadvantage of a single administration using viral systems led to a synthetic approach for delivery. Wagner *et al.*, 1992b utilized a peptide derived from the fusogenic N-terminus of the influenza virus haemagglutinin HA-2. Employment of pH sensitive peptides as endosomal-releasing agents for DNA-peptide complexes, have since been reported by several groups (Gottschalk *et al.*, 1996; Wilke *et al.*, 1996; Wyman *et al.*, 1997). These peptides may have specificity for endosomal pH due to acidic residues (glutamic and aspartic acids) aligning on one side of an amphipathic helix. At neutral pH the negatively charged carboxylic groups destabilize the alpha helical structure; acidification of the carboxylic group shifts the equilibrium towards amphipathic helical structure, which promotes multimerization of peptides and/or membrane interaction. By introduction of additional glutamic acids into the peptide sequence the pH specificity can be enhanced. The concept that peptide-mediated endosome disruption is essential for an efficient delivery of nucleic acids may also be relevant for the delivery of other biologically active compounds such as antisense oligonucleotides, drugs, peptides, or proteins.

Boussif *et al.*, 1995; Abdallah *et al.*, 1996; Kircheis *et al.*, 1997 have all incorporated PEI to promote escape from the endosome. Another system currently available is dendrimers (Haensler and Szoka, 1993; Tang *et al.*, 1996).

Much research activity has focused on endosomal escape, the implication being that delivery to the cytoplasm would enable the particle to approach the nuclear envelope. However, the cytoplasm is a viscous fluid and diffusion of macromolecular particulate systems within this medium may be extremely slow (Luby-Phelps *et al.*, 1987; Meyer *et al.*, 1997). Escape from the endosome may leave a condensed particle of DNA stranded at a site some distance from the nuclear envelope. Vesicles, organelles, and other colloidal structures are transported actively using molecular motors associated with the microtubule network or actin microfilaments (Cole and Lippincott-Schwartz, 1995; Hamm-Alvarez, 1998). Movement along microtubules is mediated by two classes of motor proteins in an oriented manner. Kinesins (and associated proteins) direct movement in an outward direction, usually linked to the secretory pathway. Dyneins (dynactin) move vesicles in the inward direction, normally associated with the endocytic pathway, towards the perinuclear region (Pouton and Seymour, 1998). Coonrod *et al.*, 1997 noted inhibition of transfection when vinblastine and cytochalasin B were used to depolymerise microtubules. This implies that nuclear transport of DNA requires routing endosomes.

1.3.2.3 Decomplexation

For transcription factor to bind with the plasmid DNA, it is assumed that the cationic moieties have to be removed. In other words, the plasmid DNA may have to be 'naked' or partially uncondensed for transcription to take place. Erbacher *et al.*, 1996 have postulated that part of the mode of action of chloroquine may be to promote dissociation of DNA and polylysine within the endosome, resulting in improved translocation of DNA to the nucleus, or improved rates of transcription. This is contradicted by Wolfert and Seymour, 1998 who found that microinjection of polylysine-DNA complexes into the cytoplasm of Xenopus oocytes in the absence of chloroquine achieved higher levels of gene expression than equivalent injections of free DNA. However, intranuclear injection of polylysine-DNA complexes achieved expression levels comparable to those of free DNA. These data imply that the cationic moiety of the complexes may have some nuclear localizing effects.

1.3.2.4 Nuclear localization

The nuclear membrane is a barrier preventing uptake of most macromolecules greater than 70 kDa into the nucleus, unless they are able to interact with the nuclear pore active transport system (Pante and Aebi, 1996; Jans and Hubner, 1996). Dowty *et al.*, 1995 and Fritz *et al.*, 1996 have observed that only <1% NIH 3T3 cells expressed β-galactosidase after cytoplasmic injection of a lacZ reporter gene, whereas lacZ was efficiently expressed when injected into the cytoplasm of primary rat muscle cells. Both data suggest that transport of naked DNA into the nucleus of cells is inefficient in a large number of some cell types. Intracellular macromolecular transport into and out of the nucleus occurs through the nuclear pore complex (NPC), which has a functional diameter of 26 nm. The current model for nuclear import is a two-step process. The first step is energy-dependent binding of proteins to the nuclear pore complex. The second step is energy-independent, temperature-sensitive translocation through the NPC. There are no strict consensus sequences but there are similarities between most nuclear localization signals (NLSs). They typically include clusters of four or more cationic residues and are often flanked by the α helix breakers, proline or glycine (Pouton, 1998). The motif -PKKKRKV-, has been shown to direct the nuclear import of the SV40 large tumour antigen (Kalderon *et al.*, 1984). Another recently found NLS is required for the efficient nuclear import of the human immunodeficiency virus type-1 (HIV-1) core into quiescent cells (Bukrinsky *et al.*, 1993). Substitution of one of the lysine residues from the HIV-1 matrix protein NLS -KKKYKLK- results in total abolition of nuclear import of the HIV core (Bukrinsky *et al.*, 1993).

Several groups speculated that polylysine may act as a nuclear targeting signal due to the fact that most of these signals are composed of an array of highly basic amino acids (K and R). Furthermore, the small diameter of compact toroid forms of DNA achieved by interaction of DNA with polylysine may also permit the direct entry of the complexes into the nucleus via nuclear pores which are smaller than 30 nm in diameter (Bukrinsky *et al.*, 1993). One indication for a nuclear targeting capacity of polylysine comes from results presented by Page *et al.*, 1995 who reported that the injection of polylysine-DNA mixtures into the cytoplasm of mouse embryonic stem cells led to transgenic animals

with about 50% efficiency compared to intranuclear injection of naked DNA. In contrast, injection of naked DNA into the cytoplasm did not lead to transgenesis. However, it is unclear whether polylysine acts as a transport signal or as a protective agent in these experiments.

Nuclear trafficking may become a major barrier for successful gene transfer, considering that *in vivo*, many cells and cell types are resting. Rosenkranz *et al.*, 1992 showed nuclear localization of FITC-labeled insulin-polylysine conjugate after transfection with plasmid-insulin-polylysine particles, suggesting that polylysine may indeed be able to promote entry of material into the nucleus. In growing cells, plasmid DNA may passively enter the nucleus during cell division after the nuclear membrane is broken down (Zauner *et al.*, 1998).

The effect of membrane-active peptides and related agents may help to elucidate the mechanisms and to overcome membrane barriers of different gene transfer systems.

1.4 MEMBRANE TRANSLOCATING SEQUENCES

The membrane of eukaryotic cells represents a barrier normally impermeable to non-lipophilic substances. Introducing large hydrophilic molecules into the cytoplasmic or nuclear compartments of live cells without disrupting the plasma membrane seems an unattainable goal. In consequence, internalization of extracellular compounds requires the presence of specific channels, or specialized endocytic mechanisms. Recently, several groups have reported that some transcription factors can be internalized by cells in culture and addressed to the cytoplasmic and nuclear compartments. Among these factors are homeodomain-containing polypeptides and Tat protein.

A 60-amino-acid long DNA-binding domain of Antennapedia, has been found to have unexpected properties which opens up new possibilities for cellular delivery. Antennapedia is a drosophila homeoprotein. Homeoproteins are transcription factors involved in several important biological processes occurring primarily, but not exclusively, during development. The DNA binding domain of these transcription factors is highly conserved and is called the homeodomain. It consists of 60 amino acids arranged in three α-helices. It was also demonstrated that a 16-amino acid long peptide

that corresponds to the third helix is capable of translocating through biological membranes (Joliot *et al.,* 1991a). Internalization occurred in various cell types at both 37°C and 4°C, hence eliminating classical endocytosis (energy-independent mechanism) (Derossi *et al.*, 1994). A proposed model for Antennapedia third helix internalization involves the interaction of the peptide with charged phospholipids on the outer side of the membrane. Destabilization of the bilayer results in the formation of inverted micelles that travel across the membrane and eventually open on its cytoplasmic side (Figure 1.1).

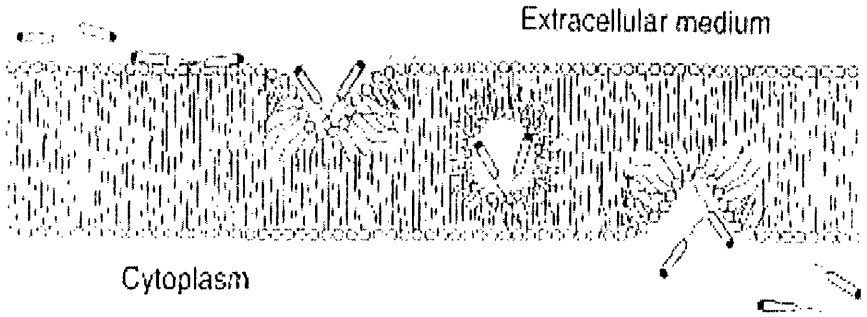

Figure 1.1. A model for Antennapedia third helix internalization (Derossi *et al.*, 1998).

This 16 amino acid sequence has since been patented and is called Penetratin peptide. It has a number of advantages; it represents a non-disruptive procedure for introducing molecules into various types of cells, which is probably not targeted to the lysosome. Also, it has been found that for internalization to take place, only low concentrations of Penetratin are required. The amount of internalized peptide was found to increase with an increase in the external concentration without any cytotoxic effect (Appligene product information, 1997).

Various experiments were carried out to determine the effect of point mutations of the antennapedia-homeodomain (Antp-HD) on its biological properties. Induction of a biological effect (neurite elongation) requires internalization, transcription regulation and specific binding to a cognate homeoprotein target site. Also, tryptophan present within the third helix was found to be vital for internalization (Prochaintz, 1997) since studies of protein-lipid interaction reported that tryptophans are known inducers of inverted micelles (de Kruijff *et al.*, 1985). Antp-HD has been used *in vivo* where it was injected

into the developing nervous system of chick embryos (Joliot *et al.*, 1991a). *In vitro*, however, a high efficiency of translocation has been observed, significant enough to require dilution of the peptide before use. Antp-HD displays high stability as it can be recovered intact from the nucleus with fully conserved DNA-binding properties, four days after cell internalization. Several groups have now used penetratin to internalize peptides, phosphopeptides, full-length proteins, and antisense oligonucleotides inside live cells. Penetratin was coupled to a small synthetic peptide and added to tissue culture medium of human keratinocyte-derived HaCaT cells where entry into the G1/S phase was blocked (Fahraeus *et al.*, 1996). The penetratin sequence was used as a vector for the intracellular addressing of a protein kinase C inhibitor which provoked rapid modification of growth cone morphology (Theodore *et al.*, 1995). The coupling of the penetratin sequence to superoxide dismutase 1 (SOD1) antisense oligonucleotide not only caused efficient cellular uptake even in the presence of serum, but also caused inhibition of SOD1 activity and promotion of cell death at low concentrations of the oligonucleotide (Troy *et al.*, 1996). Pooga *et al.*, 1998 described experiments to demonstrate that peptide nucleic acid (PNA) oligomer coupled to the cell-penetrating peptide, pAntp, can enter Bowes melanoma cells and suppress galanin receptor expression. PNAs though effective binders of RNA are particularly difficult to ferry across the plasma membrane. By linking a 21-mer PNA that interacts with galanin receptor type mRNA to a naturally occurring penetratin, they have been able to down regulate the receptors in rats, leading to decreased galanin binding and a resultant increased tolerance to pain. This unique translocating system allows direct targeting to the cytoplasm and nucleus, is non-cell-type specific and highly efficient. It also presents a natural, poorly immunogenic system that would be a preferred choice to viruses or bacterial toxins, for injection into humans for therapeutic purposes.

Another example of a transcription factor internalized by cells in culture and capable of driving exogenous polypeptides into the cells is the Tat protein of human immunodeficiency virus (HIV) (Fawell *et al.*, 1994). This protein is internalized by an unknown mechanism. However, the basic residues present between positions 37 and 72 seem to play a role in the binding to the cells.

37 72

---CFITKALGISYG**RKKRRQRRR**PPQGSQTHQVSLS**K**Q-----

Figure 1.2. Tat peptide amino acid sequence (37-72).

In addition, lysosomotrophic agents, such as chloroquine, enhance the amount of polypeptide found in the cells implying that Tat-driven internalization involves the endocytic pathway and allows for targeting of high molecular weight proteins. Currently, delivery of therapeutic compounds *in vivo* can only be achieved when the molecules are small (typically <600 Da). For instance, delivery of bioactive peptides across the blood brain barrier is generally restricted to small, lipophilic peptides. Schwarze *et al.*, 1999 showed that intraperitoneal injection of the 120-kDa β-gal protein, fused to the protein transduction domain from the HIV-Tat protein, results in delivery of the biologically active fusion protein to all tissues in mice, including the brain. These results open new possibilities for direct delivery of proteins into patients in the context of protein therapy. HIV-Tat peptides have only recently been shown to ferry magnetic particles efficiently into haematopoietic and neural progenitor cells (Lewin *et al.*, 2000). The peptide vectors derived from these proteins also contain a relatively high number of positively charged amino acids (lysine and arginine), as do most proteins with nuclear localization signals.
Rojas and colleagues, 1998 also presented a novel approach that allows the efficient delivery of proteins into living cells. They demonstrated that proteins of up to 41 kDa become cell-membrane permeable simply after their attachment to a short membrane-translocating peptide sequence (MTS). The MTS is a 12-residue hydrophobic peptide sequence modified from an h region of the signal sequence of Kaposi fibroblast growth factor. They genetically engineered *Schistosoma japonicum* glutathione S-transferase (GST) to contain the 12-residue MTS at its C-terminus. The resulting fusion protein, GST-MTS, was efficiently imported into every cell *in vitro* by a process mediated by free membrane penetration facilitated by the strong interactions between the MTS and the lipids of the cell membrane lipid bilayer. Previously, the largest molecule transported in this way was a 25-residue peptide.

One of the major obstacles to the development of any successful gene therapy lies in the delivery of a target protein to sufficient numbers of cells to elicit a therapeutic response. Although viral delivery strategies have proven to be very efficient, high immunogenicity coupled with the inefficiency of *in vivo* transfection still limit the extent of gene transfer. The potentially detrimental effects of the increased host immune response may however, outweigh the therapeutic benefit achieved by virally targeting a greater proportion of cells. A novel approach reported by Dilber *et al.*, 1999, which harnesses the unique ability of the herpes simplex virus type 1 (HSV-1) VP22 protein to spread from cell to cell, may provide a means to overcome this.

The HSV-1 VP22 protein forms part of the viral tegument, a poorly understood region of the virion located between the capsid and the envelope. The recent discovery that VP22 possesses novel trafficking properties has aroused significant interest in its potential as a protein delivery vehicle (Elliott and O'Hare, 1997) since transport was observed after introduction of the VP22 gene by several routes, including transfection or microinjection of the isolated gene in plasmid constructs or by infection with a non-replicating herpesvirus encoding the VP22 gene. In infected cells, cytoplasmically located VP22 is rapidly excreted via a golgi-independent pathway and is subsequently imported into neighbouring uninfected cells by a process requiring an intact actin cytoskeleton. Imported VP22 accumulates in the nucleus, where it may affect the regulation of cellular factors, increasing susceptibility to HSV infection (Elliott and O'Hare, 1997). The intercellular spread of VP22 appears to be a highly efficient process, with VP22 synthesized in one microinjected cell capable of reaching up to 200 surrounding cells (Elliott and O'Hare, 1997). In addition, this transport activity was retained in a fusion protein consisting of VP22 linked to green fluorescent protein (GFP) which behaved essentially like the native protein with respect to expression, localization and spread (Elliott and O'Hare, 1997). A short C-terminal deletion mutant of VP22 lacking 34 residues was expressed normally and exhibited unaltered cytoplasmic localization in the primary cells expressing VP22 but failed to spread to the surrounding cells implying its importance in the transport of VP22. The widespread delivery of functional p53 protein using VP22 (VP22-p53 fusion protein) to a human tumour cell line induced apoptosis in targeted cells (Phelan *et al.*, 1998). Dilber *et al.*, 1999 showed that the spread of VP22

was consistent with the enhanced biological activity of VP22-thymidine kinase (TK) fusion proteins in one of the most commonly used suicide gene therapy strategies. Recent work has shown that gap junctions are important mediators of the bystander effect both *in vitro* and *in vivo* (Vrionis *et al.*, 1997). Dilber *et al.*, 1999 demonstrated that in VP22-TK expressing cells devoid of gap junction activity, the addition of ganciclovir resulted in a cytotoxic bystander effect *in vitro*, and cytotoxicity leading to tumour regression *in vivo*. This makes the VP22 system an attractive delivery vehicle for numerous gene therapy strategies, including those with restricted delivery.

1.5 AIMS AND OBJECTIVES

Internalization of exogenous macromolecules by live cells provides a powerful approach for studying cellular functions. More significantly, understanding the mechanism of transfer from the extracellular milieu to the cytoplasm and nucleus could also contribute to the development of new therapeutic approaches. The first part of this study was to investigate the properties of two membrane-translocating sequences, penetratins and VP22.

Penetratins are a class of peptides with translocating properties capable of carrying hydrophilic compounds across the plasma membrane by an 'energy-independent' phenomenon that is poorly understood. As part of this project to understand the translocation mechanism of fluorescent derivatives of penetratin, further studies attempted to investigate the kinetic efficiency of cellular uptake as well as the nature of the interaction of the peptide with membranes. One potential way to improve the efficacy of gene therapy is to construct plasmids, which express fusions of therapeutic proteins with membrane translocating peptide sequences (MTPs). Such fusion proteins may be able to translocate from transfected cells to other cells in the locality, producing a bystander effect, or generally improving the biodistribution of the gene product within the target tissue. The intercellular transport of EGFP fusion constructs incorporating the cell-permeable peptide, penetratin and its mutant derivative, were examined in order to further elucidate their translocation.

The introduction of nucleic acids, peptides/proteins, and small molecules into the appropriate target cells and tissues is being developed as a therapeutic approach to a range of diseases. Elliott and O'Hare, 1997 demonstrated the remarkable ability of herpes simplex virus-1 protein VP22 to ferry proteins between cells. VP22 is efficiently transported from the cytoplasm of the original expressing cell and subsequently imported to many neighbouring cells, where it accumulates in the nucleus. Following direct injection into muscle and tumour tissue, the transport of VP22 was investigated, in an attempt to exhibit delivery *in vivo* since *in vitro* models are often markedly different to those *in vivo*, thus making correlation difficult.

Several proteins and polypeptides have been proposed as vectors for the delivery of macromolecules into living cells. In contrast, toxins and proteins from pathogenic agents, capable of translocating across the membrane and reaching the cytoplasm, have been relatively efficient in protein delivery (Fawell *et al.*, 1994), but of limited applicability in gene delivery. Since the discovery of the ability of penetratin to internalize cells in culture, reaching the cytoplasm and nucleus, part II of this project examined the possibility of using penetratin as a vector for the intracellular transport of plasmid DNA. In an attempt to elucidate the interaction of penetratin with DNA in complexed systems, comparisons are made with other cationic/plasmid DNA systems and endosomolytic agents currently used as effective non-viral gene delivery systems. A limited panel of cell lines including epithelial, fibroblast and tumour cell lines are included to study the influence of different membrane structures on peptide uptake.

The future of gene therapy of various diseases is dependent on delivery of DNA to cells *in vivo,* driven by the rapid advancement of both viral and non-viral modes of gene transfer. Although the use of viral vectors constitutes the most efficient process for gene transfer, their use is limited due to safety issues. Hence, the assembly of synthetic virus-like particles is a credible strategy, since these particles may possess some of the useful attributes of viral vectors but are completely devoid of infective capacity in mammalian cells. Cell-surface integrins are interesting potential targets for gene delivery by polycation-DNA complexes since they are exploited for cell entry by a number of viruses. This section of the project investigates construction of synthetic virus-like particles that can accomplish selective receptor-binding function, and efficient endosomal escape. Although a cationic particle is required for DNA condensation, a polylysine/ligand-binding moiety is utilized in this study to create targeting particles that are electrically neutral or slightly negative in order to avoid tissue interactions *in vivo*, which often immobilize cationic particles. Further investigations are done to attempt to correlate the *in vitro* biological activity of complexes with their physical attributes such as particle size since ideal transfection particles for in vivo gene transfer should not only be small but also electroneutral.

CHAPTER 2

GENERAL MATERIALS AND METHODS

2.1 PEPTIDE SYNTHESIS

The peptides were assembled using Fmoc (Atherton and Sheppard, 1989) chemistry on a Perseptive Biosystems 9050+ automatic peptide synthesiser with customised protocols. Amino acids, with side chain protection where necessary, were protected at the primary amino acid end with N-(-9-fluorenyl)methoxycarbonyl (Fmoc) and activated as O-pentafluorophenyl (Opfp) esters, (Perseptive Biosystems). The amino acids were coupled in the specified order to a polyethylene glycol-polystyrene resin (PEG-PS)™, with polyethylene glycol units attached as spacers building from C to N terminus. The resin was obtained with the C-terminal amino acid already attached via a cleavable ester bond with a typical substitution of 0.2 mMol/gram. Side chain protections used were t-butyl for ser, thr, glu, asp; trityl for cys, asn; 2,2,5,7,8-pentamethylchroman-6-sulfonyl (pmc) for arg, t-butoxycarbonyl for lys and trp. A 4-fold excess of amino acid to resin substitution was used.

Coupling was performed using HBTU (benzotriazol-N,N,N,N-tetramethyluronium hexafluorophosphate) chemistry-1 equivalent of HBTU, 1-hydroxybenzotriazole (HOBt) and 2 equivalents of N-methylmorpholine are dissolved with the protected amino acid in dimethylformamide (DMF) and added to the DMF solvated resin where the previous amino acid has been N-α-deprotected (Fmoc removed with 20% piperidine solution in DMF) exposing a free amino terminus. Figure 2.1 shows a general schematic representation of reactions. The final Fmoc group was removed and the resin washed in succession with methanol and dichloromethane and dried under high vacuum.

2.2 PEPTIDE PURIFICATION

The peptide was released from the resin (500 mg) during 2 h with a cocktail (50 ml) of trifluoroacetic acid (TFA) 92.5%, phenol 2%, water 2%, ethanedithiol 2%, anisole 1% and triisobutylsilane 1%. Concentration and ether precipitation yielded the white peptide, which was collected by centrifugation, washing three times with ether and vacuum drying for 30 minutes.

Characterization was performed using reverse-phase HPLC on a C18 silica wide-pore column (15 cm x 2.1 mm) with an elution gradient of 10%-50% acetonitrile containing 0.1% TFA over 40 minutes at 217 nm and 277 nm simultaneously. The peptides were purified to a single peak on analytical HPLC. Further purification where necessary was performed on a 25 cm x 22 mm column using the same conditions. Purity was estimated at greater than 90%. Samples of by-products were of similar peptides and present in trace amounts. The molecular weight was confirmed by mass spectrometry performed on a VG Quattro triple quadruple instrument with electrospray ionisation. The purified peptides were then lyophilized for use in biological assays. Although the peptides are chemically synthesized from the C – N terminus, they have been written in the opposite direction to how they are synthesized.

The following cationic peptides were synthesized and employed at different stages of this project:

- Penetratin (pAntp)

H_2N-RQIKI**W**FQNRRMK**W**KK-COOH

- Mutant penetratin (mutant pAntp)

H_2N-RQIKIW**F**QNRRMK**F**KK-COOH

- Bifunctional penetratin (K_{25}penetratin)

H_2N-K_{25}-RQIKIWFQNRRMKWKK-COOH

- RGD-containing peptide couple to oligolysine (K_{25}-RGD)

H_2N-K_{25}-GACDC**RGD**CFCA-COOH

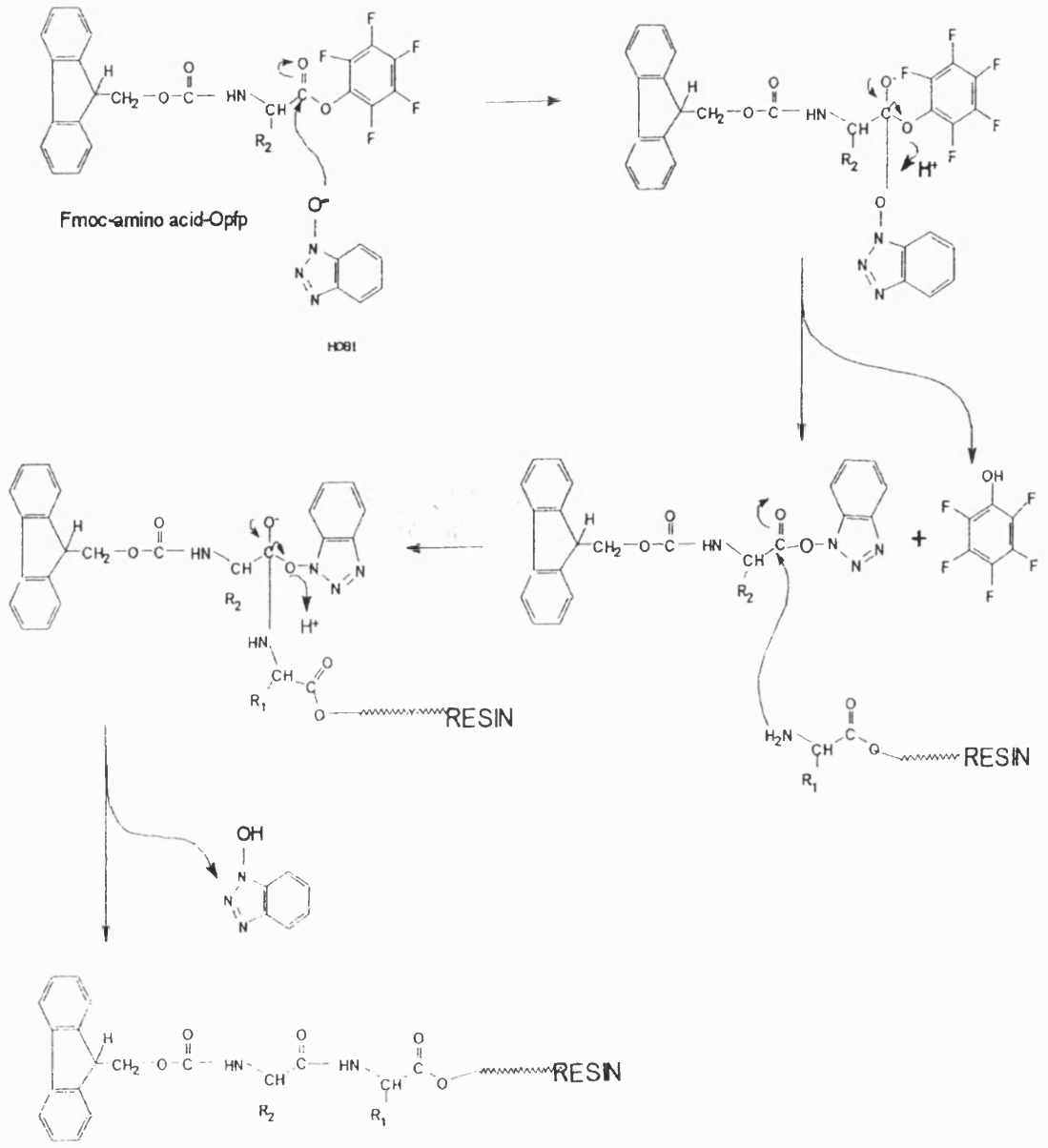

Figure 2.1. Schematic representation of the coupling reaction of peptide synthesis

2.3 CELL CULTURE TECHNIQUES

2.3.1 Solutions

2.3.1.1 Water

Milli-Q water used for the preparation of all culture solutions was obtained from a Milli-Q PF Plus system with ultrafiltration cartridge (Millipore, UK, Ltd).

2.3.1.2 Phosphate buffered saline

Phosphate buffered saline (PBS) tablets without magnesium or calcium ions were obtained from Oxoid Ltd, UK. This solution was made by dissolving one tablet per 100 ml milli-Q water at a pH of 7.3. PBS solutions were sterilized by autoclaving at 121°C for 15 minutes.

2.3.1.3 Sodium Bicarbonate and sodium hydroxide

Solutions of 7.5% (w/v) sodium bicarbonate and 1 M sodium hydroxide were prepared individually using milliQ water and sterilised by autoclaving.

2.3.1.4 Ethylene Diamine Tetraacetic Acid (EDTA)

A 0.02% (w/v) solution of ethylenediamine tetraacid (EDTA) was prepared in PBS. EDTA in PBS solutions was also sterilised by autoclaving.

2.3.1.5 Trypan Blue

This dye, made as a 0.1% (w/v) solution in PBS, was used to assess cell viability. It was obtained from BDH laboratory Reagents Ltd.

2.3.1.6 Culture media and additives

All solutions used for the preparation of culture medium for cells were obtained from GIBCO BRL, Paisley, unless prepared as above. Eagle's Minimum Essential Medium (MEM) with Earle's salts, without sodium bicarbonate and L-glutamine was obtained as 10x concentrates. MEM non-essential amino acids solution (MEM-NEAA), L-glutamine (200 mM), and penicillin (10000 iu/ml)-streptomycin (10000 μg/ml) were obtained as 100x concentrates. Foetal calf serum (FCS) from various suppliers was batch tested to determine which provided optimum growth of cells. As a result, FCS with batch numbers 06Q5262A, 30Q5262A and 06Q7554F from GIBCO were used. Growth media were prepared aseptically according to the formulae below, stored at 4°C and used within three weeks of preparation.

Table 2.1 below shows formulae for making MEM

ADDITIVE	VOLUME (ml)
Eagle's MEM 10x	50
Foetal calf serum	50
MEM-NEAA	5
L-glutamine	5
Penicillin-streptomycin	5
7.5% w/v $NaHCO_3$	15
MilliQ water	to 500
1 M NaOH	Adjust to pH 7.4 ~ 2 ml

2.3.2 Equipment and disposable items

All aseptic techniques were carried out in a laminar flow cabinet (MDH Ltd) designed for vertical re-circulation of air. Cells were cultured in an LEEC PF2 anhydric incubator (Laboratory and Engineering Company) with a set temperature of 37°C.

Growing cell cultures were viewed daily under an inverted light microscope (WILD M4, Wild Heerburg Ltd). For determination of cell concentration in suspension, a double grid haemocytometer (Neubauer 0.1mm Dept, Weber, UK) was used to count appropriately diluted samples.

Sterile 75 cm^2 and 175 cm^2 filter top tissue culture flasks were obtained from Falcon, Becton Dickinson and Co, UK. Six- and 96-well plates were obtained from Nunc, Denmark. Cryopreservation ampoules used for storing frozen cells in liquid nitrogen were obtained from Corning, UK.

2.3.3 Cell Culture methods

All cells were grown in Eagle's MEM containing 10% FCS and maintained at 37°C in a LEEC anhydric incubator in a humidified atmosphere of 95%/5% carbon dioxide. Daily check ups were made to check cell cultures for evidence of bacterial and fungal contamination. All cell lines were grown as monolayer cultures and subcultured at 80-100% confluence. The medium was changed every 48 hours.

For subculture, used culture medium was discarded and the 175 cm^3 flask was rinsed three times with 10 ml aliquots of PBS and then incubated at 37°C with 2 ml of 0.02% EDTA for approximately 5 minutes. Detached cells were diluted to 10 ml with complete culture medium, and an appropriate aliquot of suspension transferred to a sterile 175 cm^3 flask containing 50 ml of fresh culture medium. Cells treated with EDTA solution were similarly diluted to 10 ml after detachment but were then centrifuged at 1000 rpm for 6 minutes, the supernatant discarded and then resuspended in 10 ml of culture medium before transfer into flasks for subsequent culture.

2.3.3.1 Determination of cell concentration

After cells are detached from flask, the cell suspension was briefly vortexed in a whirlimixer. To 100 µl of suspension was added 200 µl of PBS and 200 µl of Trypan Blue solution all in a microcentrifuge tube. A sample was loaded on to a grid

haemocytometer overlaid with a coverslip. Viable cells could be seen by a bright 'halo' light around their cellular membrane as opposed to dead cells which were permeabilised and stained blue by the dye. The viable cell numbers in the four squares surrounding the central square were counted and this was repeated for the other side of the haemocytometer grid, using an inverted light microscope.

The viable cell concentration in the original suspension was calculated as follows:

$$\text{Cells/ml} = \text{Av. cell count per chamber} \times 10^4 \times \text{dilution factor} \quad (5)$$

Equation 2.1.

2.3.3.2 Cell storage and recovery

Cells were prepared for storage by detachment of a confluent monolayer according to the protocol mentioned in the previous section followed by centrifugation at 200 *g* (1000 rpm) for 8 minutes. The supernatant was then discarded and the cells resuspended in filter sterilised (0.2 μm acrodisc) solution of culture medium supplemented with 10% v/v dimethylsulphoxide (spectrophotometric grade, Aldrich, UK) as a cryopreservative. Cell suspensions were then dispensed in 1.8 ml aliquots into corning tubes, transferred to a Union Carbide BF6 biological freezer unit plug which fitted into a Union Carbide LR-40 liquid nitrogen freezer. This permitted the cells to be cooled down to -70°C at a rate of approximately 1°C per minute. The cells were then transferred to a Union Carbide LR-40 liquid nitrogen freezer where they were stored at approximately -148°C.

For cell recovery, the contents of an ampoule was thawed rapidly by brief incubation in a 37°C water bath followed by dilution with 10 ml of fresh medium added dropwise. Cells were centrifuged for 8 minutes at 200 *g* and the supernatant was discarded. The cells were then resuspended in 10 ml of fresh medium and the transferred into a 175 cm^2 flask containing 50 ml of medium and then incubated under standard culture conditions. Cells were cultured for at least two passages in order to establish them before they were used for experiments.

2.4 TRANSFECTION OF CELLS

One hour prior to transfection, monolayers of rapidly dividing cells were washed once with warm Opti-MEM™, which is a serum-free medium specifically designed for transfection experiments and then 1.5 ml of this medium was added to each well. Five hundred microlitres of complex containing 2 μg of DNA and variable quantities of gene transfer agent were added to each well. Transfection was carried out for four hours at 37°C after which time the transfection medium was replaced with fresh complete culture medium and cells were cultured for a further 24 hours before harvesting for analysis. For all transfection studies, each data point represents the mean ± standard deviation (SD) of triplicate samples and each experiment was repeated on at least two occasions (often three times).

2.5 MOLECULAR BIOLOGY METHODS

2.5.1 DNA preparation

The following three reporter plasmid constructs were used for transfection experiments (Appendix D). pCMVβ (Clontech) is a 7.2 kb reporter plasmid, which contains the *E.coli* β-galactosidase gene under the transcriptional control of the human cytomegalovirus (CMV) immediate early promoter/enhancer element. pEGFP-N1 (Clontech, UK) contains the enhanced GFP under the control of CMV promoter. EGFP expressing cells can readily be detected by visualization using a fluorescence microscope or by FACS analysis. The plasmid, pCMV*luc* (a kind gift from J.-P Behr) contains the firefly luciferase reporter gene encoding luciferase under the transcriptional control of the cytomegalovirus (CMV) promoter. The following steps were used to produce milligram quantities of all plasmids used throughout this project.

2.5.2 Preparation of competent *E.coli* DH5α cells

Escherichia coli strain DH5α was used for the propagation of all plasmids.
Competent *E.coli* DH5α cells were prepared and transformed with the appropriate plasmid using the heat shock technique as described by Sambrook *et al.*, 1989:

TfbI buffer		
30 mM KCl		3 ml of a 1 M solution
100 mM RbCl		1.209 g
10 mM $CaCl_2$		12.5 ml of 80 mM solution
50 mM $MnCl_2$		5 ml (1 M solution)
Water	to	100 ml

Adjust to pH 5.8 with 0.2 M acetic acid and filter sterilise.

TfbII buffer		
10 mM MOPS		0.209 g
75 mM CaCl2		1.100 g
10 mM RbCl		0.1209 g
15% (v/v) glycerol		15 ml
Water	to	100 ml

Adjust to pH 6.6 with 1 M KOH and filter sterilise.

A single colony of *E.coli* DH5∝ was picked from a fresh agar plate and inoculated into 5 ml of LB medium and incubated at 37°C overnight in a shaking incubator. The following morning, 1 ml of culture was diluted to 100 ml with LB and grown under standard conditions until the optical density ($OD_{550\ nm}$) of the solution reached 0.48 (2.5 – 3 hours). The cell suspension was then chilled on ice for 5 minutes and centrifuged in sterile falcon tubes for 5 minutes, 600 rpm (Beckham J2-MC) at 4°C. The supernatant was discarded and the cells re-suspended in 40 ml of TfbI buffer ($2/5^{th}$ volume of culture) and chilled on

ice for 5 minutes. Cells were centrifuged at 6000 rpm for 5 minutes at 4°C and the supernatant discarded. Cells were subsequently re-suspended in 4 ml ($1/25^{th}$ volume of culture) of TfbII buffer and chilled on ice for 15 minutes. Cells were stored in 200 µl aliquots, snap frozen in a dry-ice/methanol bath and stored at -70°C until required.

2.5.3 Transformation of competent *E.coli* DH5∝ cells

200 µl of competent cell suspension was thawed at room temperature and then placed on ice for 10 minutes. Plasmid DNA (<100 ng) was then added and gently mixed followed by incubation on ice for 30-45 minutes. The cells were shocked by incubating at 37°C for 2 minutes or 42°C for 90 seconds and then returned to ice for 20 minutes. The cell suspension was then diluted to 800 µl with LB followed by incubation at 37°C for 1 hour. After this time, 200 µl of this suspension was plated out on an LB-agar plate (Appendix C) containing ampicillin and tetracycline (Appendix B) at concentrations of 50 µg/ml and 12.5 µg/ml respectively. Plates were inverse incubated overnight at 37°C.

2.5.4 Plasmid propagation, isolation and purification

A single colony of *E.coli* DH5α containing the desired plasmid was isolated from an LB-agar plate supplemented with ampicillin and tetracycline (50 µg/ml and 12.5 µg/ml respectively) and inoculated into 10 ml of LB broth containing the same antibiotics (primary culture). This primary culture was grown for 8 hours at 37°C on a shaking incubator at 300 rpm (New Brunswick Scientific, UK) and then a 5 ml aliquot was expanded in 500 ml of LB broth, also containing the appropriate antibiotics, and grown overnight.

The plasmids were isolated by the alkaline lysis method (Birnboim and Doly, 1979) and the cell lysate purified by anion exchange chromatography using the Plasmid Maxi kit (Qiagen Inc., Surrey, UK) according to the manufacturers' protocol. The isolated DNA was dissolved in TE buffer (Tris 10 mM, EDTA 1 mM), pH 8 and stored at -20°C.

2.5.5 Purification of DNA by phenol/chloroform extraction

One volume of phenol: chloroform: isoamyl alcohol (25: 24: 1) was added to the DNA solution and the two solutions mixed by 'flicking' the microcentrifuge tube. The tube was then centrifuged at 14000 rpm for 1 minute (Jouan A14 microfuge, France) to separate the phases, and the upper aqueous phase removed without disturbing the interface. This process was repeated once, followed by the addition of 1 volume of 24: 1 chloroform-isoamyl alcohol to precipitate the remaining protein and reduce the amount of dissolved phenol, which is in the aqueous phase. Once again the upper aqueous phase was removed and the DNA within this phase precipitated using one of the following precipitation methods.

2.5.6 Ethanol precipitation of DNA

To a volume of DNA solution in a centrifuge tube was added 0.1 volumes of 3 M sodium acetate solution and 2 volumes of absolute ethanol. The sample was then chilled overnight at -70°C or for 15 minutes in an ethanol/dry-ice bath. After this time, the sample was centrifuged at 14000 rpm for 10 minutes at 4°C, the supernatant was discarded and the DNA pellet washed once with 70% ethanol. The sample was again centrifuged at 14000 rpm for 10 minutes, the supernatant discarded and the pellet air dried for 5 minutes, being careful not to over dry. The pellet of DNA was then re-suspended in 10 mM Tris-Cl buffer, pH 8.5.

2.5.7 Isopropanol precipitation of DNA

The salt concentration of the DNA solution was adjusted with sodium acetate 0.3 M and 0.7 volumes of isopropanol added at room temperature. The DNA solution was immediately centrifuged at 14000 rpm for 20 minutes at 4°C. After carefully decanting the supernatant the pellet was washed in 70% ethanol at room temperature and centrifuged for a further 10 minutes at 4°C. Once again the supernatant was removed and

the pellet air-dried for 5 minutes. The DNA pellet was then re-suspended in 10 mM Tris-Cl buffer, pH 8.5.

2.5.8 Sample purity and quantification

For quantification of plasmid DNA, a 10-20 µl aliquot of sample was diluted to 1 ml with distilled water and the absorbance of the solution measured at 260 nm (A_{260}) and 280 nm (A_{280}). The concentration of DNA in the original solution was calculated as follows:

$$\text{Concentration of DNA (µg/ml)} = \text{Dilution factor} \times 50^{1} \times A_{260}$$

[1]based on the assumption that 50 µg/ml solution of double stranded DNA has an absorbance of 1 at 260 nm (Sambrook *et al.,* 1989; Laboratory manual).
The purity of DNA was calculated as follows:

$$\text{Ratio} = A_{260} / A_{280}$$

Ratios between 1.8 and 2.0 (indicates high purity) were consistently obtained.

2.5.9 Sample identification

A sample of purified DNA was linearised with a restriction endonuclease (New England Biolabs, UK) for 2 hours at 37°C and then loaded on to a 1% w/v agarose gel in 0.5x TBE. The gel was then electrophoresed in the same buffer at 80 volts for one hour against marker DNA (*Eco*R I/Hind III cut λ DNA) of variable length to confirm the size of isolated DNA. At the end of a run, gels were stained with ethidium bromide in 0.5x TBE at a concentration of 0.5 µg/ml for 10 minutes. The DNA bands were visualised using an ultraviolet light box. The gel verified that the majority of the DNA was supercoiled and free from contaminating nucleic acids (genomic DNA or RNA).

2.5.10 Calculation of cationic polymer to DNA charge ratio

The calculation of negative charge provided by the DNA was determined on the basis that each nucleotide in the DNA sequence is associated with a single negative charge. A mean value of 330 was used as the molecular weight of a monophosphorylated nucleotide, as established from data given by Sambrook *et al.*, 1989; Felgner *et al.*, 1994).

$$\text{No. of mols of positive charges} = \frac{\text{Mass of peptide x No. of positively charged groups}}{\text{Molecular weight of peptide}}$$

$$\text{No. of mols of negative charges} = \frac{\text{Mass of DNA}}{330}$$

$$(+/-)\text{ charge ratio} = \frac{\text{No. of molecules of positive charges}}{\text{No. of molecules of negative charges}}$$

The complexation of plasmid DNA with PEI introduced a concept of N/P ratio. This is the ratio of nitrogens from PEI to phosphates from DNA. According to the protonation profile of PEI, every sixth nitrogen atom is protonated under physiological conditions (Boussif *et al.*, 1995). Hence only a theoretical charge ratio can be calculated from a pH titration of PEI. More recent literature (Erbacher *et al.*, 1999a) has reported a shift in the protonation profile of PEI complexation with DNA. Here a significantly higher percentage of PEI (about 10% more than was previously found) becomes charged at physiological pH.

2.6 METHODS OF ANALYSIS

2.6.1 Preparation of cell extracts post transfection for analysis

Solutions

Phosphate buffered saline (PBS)

0.1 M sodium phosphate buffer (pH 7.3)

Lysis buffer (see section 2.6.2).

2.6.1.1 Detergent Lysis Method

After the appropriate period of incubation post transfection, the cell monolayer was washed twice with 2 ml of PBS. Washed monolayers were treated with 250 µl of lysis buffer per well and the plates were frozen at -70°C. After thawing at room temperature for 30 minutes, the cell extracts were collected and transferred into sterile micro-centrifuge tubes and centrifuged for 10 minutes at 200 g and the supernatant used for analysis.

2.6.2 Assay methods

2.6.2.1 Luciferase Assay

Luciferase levels within cells were quantified using the Promega luciferase assay system (Promega, UK) according to the manufacturer's instructions. As little as 10^{-20} moles (0.001 pg) of firefly luciferase can be measured using this kit. A standard curve of light units vs. relative enzyme concentration was produced using purified firefly luciferase (Appendix E). The Promega lysis buffer (1x: 25 mM Tris-phosphate, pH 7.8; 2 mM DTT; 1, 2-diaminocyclohexane-N, N, N', N'-tetraacetic acid; 10% glycerol; 1% Triton® X-100 and BSA 1 mg/ml) was employed. Supplementation with 1 mg/ml BSA ensures that luciferase is not lost from solution by adsorption onto container walls. After centrifugation of the cell lysate, 20 µl of room temperature cell extract (supernatant) were mixed with 100 µl of luciferase assay reagent (luciferase assay substrate + 10 ml of assay buffer) again at room temperature. The disposable test tube containing the reaction mixture was then immediately placed into the luminometer. Light output was measured

using a Turner Designs TD-20/20 luminometer. The instrument settings were as follows: a delay of 2 seconds, integrate for 10 seconds, sensitivity level 25.1%.
The time course for the expression of luciferase in B16 cells was studied. Appendix J shows the sensitivity of the luminescent assay. Expression of luciferase peaked at around 24 hours, after which there was a decline in expression. Hence all transfection experiments were analysed after 24 hours of incubation.

2.6.2.2 Protein assay

The luciferase figures were converted to relative values by dividing the assay level per well by the amount of protein (mg) in the well at the end of the transfection. The protein content in cell extracts was measured using the Bio-Rad Dc protein assay kit. Samples were prepared according to the manufacturer's protocol (macro-assay) and calibration curves were constructed using bovine serum albumin as a standard. Spectrophotometric measurements were made at 750 nm. A typical standard curve is shown in appendix F.

2.7 CHARACTERIZATION METHODS

2.7.1 Particle size analysis

Photon Correlation Spectroscopy (PCS) was used to obtain the mean hydrodynamic diameter of complexes using the ZetaPlus particle sizing software (Brookhaven Instruments Corporation). Measurements were made using an argon laser of wavelength 633 nm at a temperature of 20°C and an angle of 90°. To reduce particulate contamination all glassware for sample preparation and measurements were washed three times with prefiltered Millipore water and left to dry in a laminar flow cabinet. All complexes were prepared in 5% glucose. Briefly, 102 μg of plasmid DNA were mixed with various quantities of peptides to produce a range of charge ratios. The complexes were incubated for 20 minutes at room temperature prior to measurements being made.

PART I

A STUDY OF PEPTIDE TRANSLOCATION

ACROSS CELLULAR MEMBRANES

CHAPTER 3

INVESTIGATION OF INTERNALIZATION AND CELLULAR TRAFFICKING OF FLUORESCENT PEPTIDE DERIVATIVES

3.1 INTRODUCTION

Classically, direct cytoplasmic access is usually attained by membrane disrupting techniques, such as microinjection, electroporation or toxin-based techniques. Hence, the reported ability of the *Drosophila* protein, pAntp, to enter cells without rupturing the plasma membrane, where it appears to reach the cytoplasm and target the nucleus, is of great interest. This discovery of membrane translocation can provide a useful tool for investigating and influence various intracellular processes in cellular systems. Also, it presents potential applications in cell biology and may form the foundation of a delivery system, which can be used to internalize different molecules into cells. So far, the mechanism by which penetratin performs this cellular internalization has not been confirmed. One suggestion for its mechanism of translocation is the formation of inverted micelles as a result of destabilization of the lipid bilayer. One aspect of this chapter looks at the transport of penetratin peptides across cells in culture in an attempt to elucidate its mechanism of translocation. Fluorescent derivatives of wildtype penetratin and a published mutant (reported to be inactive) were synthesized. A number of fluorescent dyes were coupled separately to the peptides in order to follow the mobility of these fluorescent derivatives within cells. To achieve this, laser scanning confocal microscopy and transmission electron microscopy techniques were both employed. This chapter also describes studies of the interactions between various peptides of interest and the lipid bilayer of plasma membranes in an attempt to explain the mechanisms of membrane translocation that these peptides utilize. This involved studies of peptide-membrane interactions using a novel fluorescence technique. Fluorescence measurements were made using a spectrophotometer with software for collection of data against time. Hence, it was possible to probe the affinity of these peptides and their derivatives for the membranes.

3.2 MATERIALS AND METHODS

Peptide syntheses and cell culture techniques have been described in Chapter 2.

3.2.1 Preparation of labelled peptides

3.2.1.1 Fluorescent dyes

A number of fluorescent labels were used during the course of this study.
The green fluorescent dye, BODIPY FL CASE, was supplied as 1 mg orange powder by Molecular Probes, Inc, USA.
Biotin was obtained from SigmaAldrich, UK. It appeared as a white powder and has a molecular weight of 341.4.
Amersham Life Science, UK, supplied fluorescein-linked streptavidin (-FITC) and human transferrin biotin-labelled. Both were obtained in solution and were stored at 2 – 8 °C. Colloidal gold-labelled streptavidin (10 nm) was obtained from SigmaAldrich, UK. It was supplied as a red liquid suspension. Aliquots of 100 µl were prepared and stored at -20°C.

3.2.1.1.1 Synthesis of ADMP.

The other dye employed was ADMP (Bennett *et al.*, 1999), a coumarin-based amino acid. This dye was described by Dr Sukhi Bansal and was synthesized at King's College, University of London. The synthesis involved wet chemistry techniques and was under the supervision of Dr Bansal. It was obtained as a light brown powder and with a molecular weight of 264.

The synthetic strategy involved four steps:

The first step involved the synthesis of chloromethoxycoumarin, a reaction between equimolar quantities of the phenol (40 mM, 6.16 g) and the acetoacetate (40 mM, 5.40 ml) using toluene (200 ml) as solvent in the presence of an ion exchange catalyst, Amberlyst 15 (4 g). The reaction was allowed to proceed over 24 hours after which TLC was used to confirm completion. The TLC solvent system was ethylacetate: hexane (2: 1) (BDH, Ltd.). Recrystallization was carried out to ensure purity for step 2, using boiling ethanol. A 60% yield was achieved (Scheme 1).

STEP 1

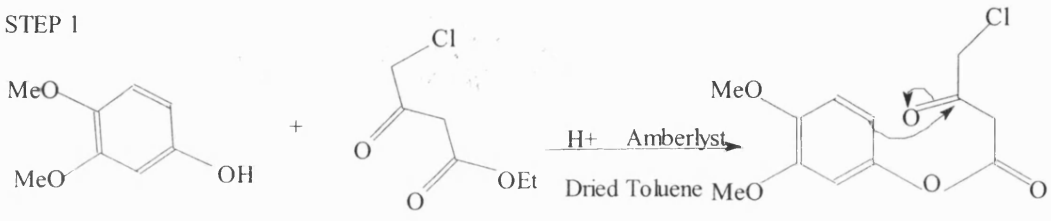

3, 4-dimethoxyphenol

Ethyl-4-chloroacetoacetate

\+

EtOH

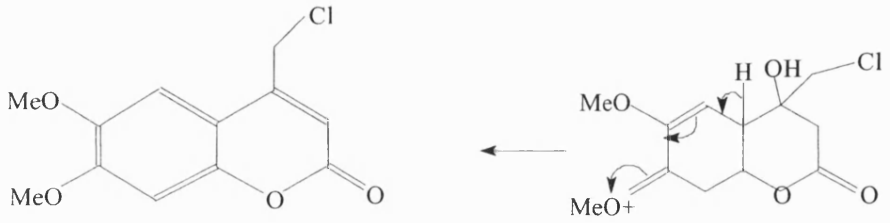

Chloromethylcoumarin

Scheme 1

STEP 2

Dried sodium hydride (0.036 mol) was dissolved in 30 ml DMF, cooled to between –10 and -30°C and stirred under nitrogen. To the suspension was added

diethylacetamidomalonate (0.039 mol) dissolved in 50 ml DMF. The mixture was stirred at room temperature for one hour. This mixture was then added to a solution of chloromethoxycoumarin dissolved in one litre of DMF, stirring overnight at room temperature. The DMF was removed using a rotatory evaporator, after which the mixture was washed to remove sodium chloride. Again, TLC was used to confirm identity and ensure completion. An extraction was carried out with ethylacetate and 0.1 M HCl and the sample was dried using anhydrous sodium sulphate (Scheme 2). The product was recrystallized from ethanol, and analyzed by TLC, which showed the presence of impurities. Column chromatography with silica gel was employed to remove impurity fractions. The solvent system was ethylacetate: hexane (2: 1).

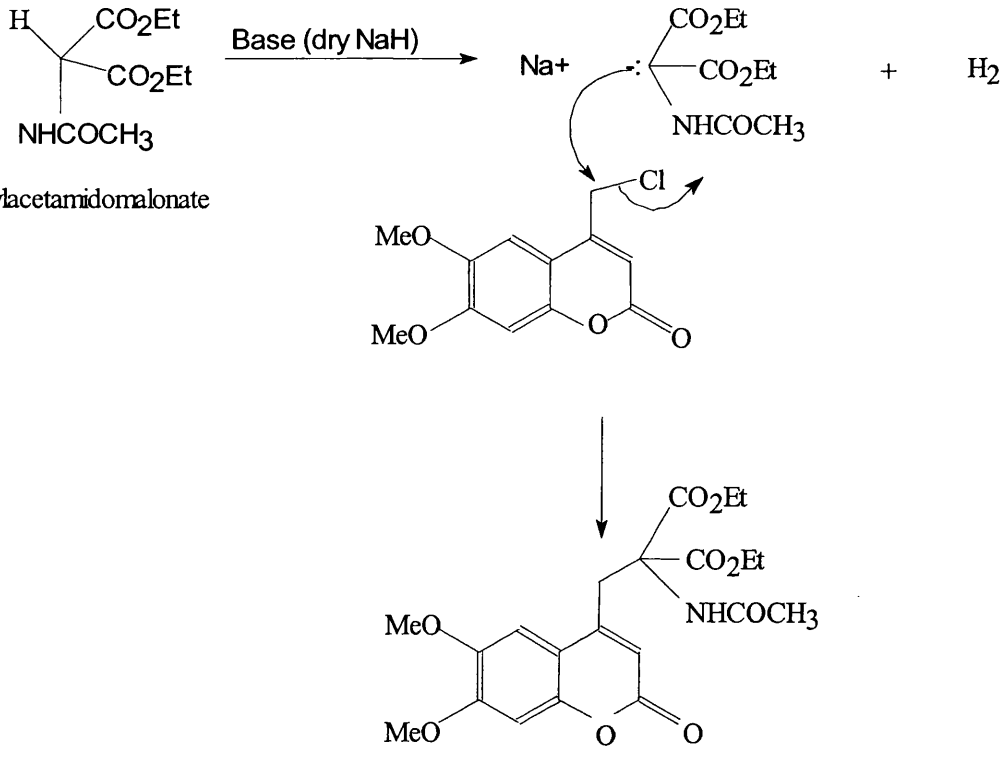

Diethylacetamidomalonate

Step 2

Ethylacetatedimethoxycoumarin (Scheme 2)

Step three was an acidification step. Hydrochloric acid (6 M) was added to the product from step two and refluxed overnight at 250°C. The sample was evaporated to dryness using a vacuum. The TLC solvent system was n-butanol: water: acetic acid (4: 1: 1). Recrystallization procedures involved boiling in ethanol (15 ml) and 1 M NaOH (6 ml). The product was then acidified with acetic acid (2.5 ml) leaving a brown precipitate.

STEP 3

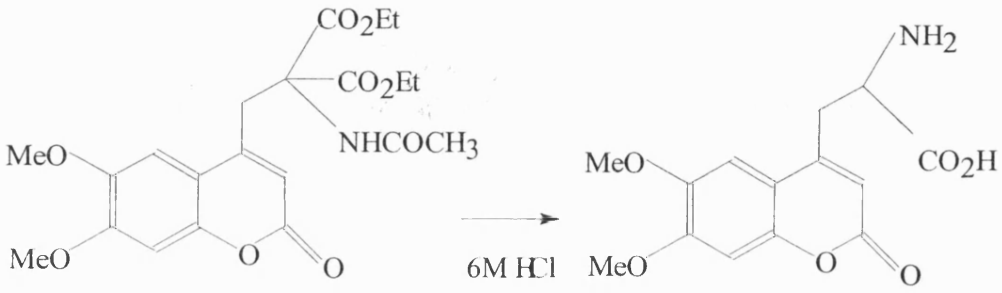

Step four involved the addition of fmoc N-hydroxysuccinimide (1.15 g) (NovaBiochem) to the amino acid (1.0 g) in a mixture of acetonitrile (Rathburn, Ltd): water (1: 1). DIPEA (1.25 ml) (Fluka) was added as a coupling agent. The mixture was stirred overnight, after which 1 M HCl (40 ml) was added. The TLC solvent system was chloroform: methanol (3: 1). The product was extracted with ethylacetate, and evaporated to dryness.

STEP 4

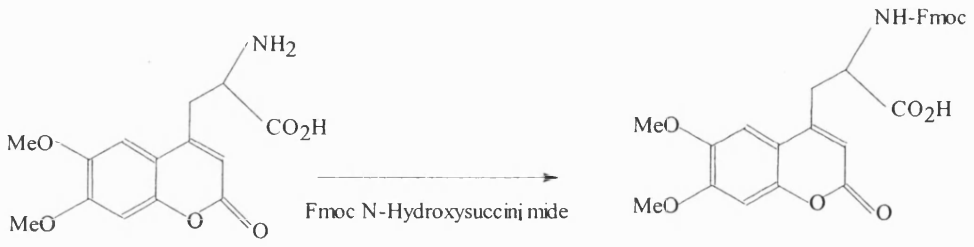

(6,7-dimethoxy-4-coumaryl)alanine (ADMP) ADMP Fmoc derivative

A ninhydrin test was carried out on ADMP. The detector system was a mixture of 0.3 g ninhydrin, 100 ml 1-butanol and 3 ml glacial acetic acid. The absence of a purple stain confirmed the coupling of the fmoc to the coumarin compound. ADMP has the following properties:

Absorbance maximum at 345 nm, $\varepsilon = 11000\ M^{-1}cm^{-1}$

Fluorescence emission at 429 nm

The purity of the label was carried out with HPLC and its identity confirmed using Nuclear Magnetic Resonance (NMR) (appendix H).

3.2.1.2 Coupling of fluophores to peptides

The coupling reactions of both ADMP and Biotin to the peptides were as follows:
Into an eppendorf, 1 ml of DMF was added, after which 40 mg of the fluophores was added. A combination of coupling agents was used: equal molarities of 1, 3 diisopropylcarbodiimide (DIPCIDI) (Fluka, UK) and N-hydroxybenzotriazole (HOBt) (PerSeptive Biosystems, UK) were added to the eppendorf. Then the peptide coupled to dry resin was added. The reaction mixture was left for one hour while shaking at 15-minute intervals. The quantities of reagents used in this protocol varied according to the fluorescent dye in question. Although it is usual to have a 4: 1 molar ratio of dye to peptide for each coupling reaction, this ratio could not be achieved with the BODIPY FL CASE/peptide reaction due to the cost and therefore lack of availability of BODIPY. Hence a ratio of 1: 1 was used for BODIPY. 2 mg of BODIPY was added to 250 µl of DMF in an eppendorf, after which equivalent molar quantities of the coupling reagents were added followed by the peptide on dry resin. The reaction was left overnight on a shaker. The coupling efficiencies of each reaction are shown in table 3.1.

Peptides	**Biotin**	**BODIPY FL**	**ADMP**
PenetratinK_{25}	-	++	++++
Penetratin	++++	++	++++
Penetratin mutant	++++	++	++++

Table 3.1 shows the efficiencies (+) of the various coupling reactions. These pluses (+) were allocated arbitrarily. Four (+) indicated 100% coupling. Two (+) indicated 50% coupling.

The following tests were carried out to confirm that the fluophore had been linked to the peptide, as evidenced by the absence of amine groups. A sample of the resin was washed with dimethylformamide (DMF), dichloromethane (DCM) and methanol (MeOH) in succession prior to the following two tests.

A) Kaiser Test

The most widely used qualitative test for the presence or absence of free amino groups was devised by Kaiser *et al.*, 1970. The following solutions were prepared:

1. Dissolve 5 g of ninhydrin in 100 ml ethanol
2. Dissolve 80 g of liquefied phenol in 20 ml of ethanol.
3. Add 2 ml of a 0.001 M aqueous solution of potassium cyanide to 98 ml pyridine.

A few resin beads were washed several times with ethanol. The resin was transferred to a small glass tube and two drops of each of the above solutions were added. The solutions were mixed well and then heated in an oven to 120°C for 4-6 minutes. Blue resin beads indicated a positive test for the presence of amines.

B) 2, 4, 6-trinitrobenzenesulfonic acid (TNBS) test

In an eppendorf, the following were added: 0.5 ml DMF, 50 µl Diisopropylethylamine (DIPEA) and two drops of 2, 4, 6-trinitrobenzenesulfonic acid (SigmaAldrich, UK). A

sample of resin beads was placed on a white ceramic tile. A few drops of test solution were placed over the resin. A positive result was a distinct red colour indicating the presence of amines while a lack of colour change indicated the absence of amines (Hancock and Battersby, 1976). The percentage of beads that change colour gave an indication of how far the coupling has gone.

If these tests proved negative, dry nitrogen gas was bubbled through the reaction mixture for about a minute to keep the atmosphere dry, the eppendorf was then immediately covered with parafilm and foil, and the mixture was left to proceed overnight. If tests were positive, the resin was cleaved and the peptide purified as described in chapter 2.

3.2.2 Confocal Microscopy

3.2.2.1 Preparation of samples

To facilitate the examination of B16 mouse melanoma cells under the microscope, the cells were grown on glass coverslips. These glass coverslips 22 cm x 22 cm, were thoroughly cleaned by soaking them in distilled water overnight, rinsing them twice in 96% ethanol and then finally drying in air. The coverslips were then sterilized by autoclaving for 15 minutes at 121°C before using them in cell culture. A single sterile coverslip was placed into each well of a six-well plate and the wells filled with 2 ml of MEM containing FCS and lacking phenol red. B16 cells were plated onto the coverslips at a density of 2 x 10^5 cells and the plates were placed in an incubator overnight. During this period, the cells were allowed to adhere to the coverslips and become about 60% confluent. After 24 hours, the used medium was removed and the cells were then washed twice in PBS. Fresh MEM (1.5 ml) but without phenol red was placed in each well to replace the old medium. For addition to B16 cells, the peptides were diluted in MEM supplemented with 10% FCS, to a volume of 500 µl. Following addition of the peptides, the cells were returned to the incubator for a fixed time. At the end of this time course, the cells were washed three times in MEM and then fixed for five minutes with 100% ethanol at -20°C. The cells were then washed three times in PBS, and incubated for 30

minutes with fluorescein-linked streptavidin which was diluted 10 times into PBS containing 10% FCS. At the end of the incubation the cells were washed three times in PBS. To prepare cells for visualizing under the microscope, the coverslip was placed, cells facing downwards, onto a dimple microscope slide (Fisher). An antioxidant, DABCO (100 mg/ml, SigmaAldrich, UK) in 10% PBS/90% glycerol had already been spotted onto the dimple so that the cells were bathed in this solution. The excess DABCO solution was removed from around the edges of the coverslips, which were sealed with clear nail polish. The slides were left for 24 hours to dry.

3.2.2.2 Peptide visualization

Fluorescence images were obtained with a Zeiss LSM-510 confocal laser-scanning microscope (Zeiss LSM-510 system with inverted Axiovert 100M microscope) equipped with a krypton-argon laser. Excitation was set at 488 nm for fluorescein isothiocyanate, and the emitted light was filtered with an appropriate filter set at 510 nm. Photomultiplier gain and laser power were identical within each experiment to allow comparison of samples against untreated samples.

3.2.3 Transmission Electron Microscopy (TEM)

3.2.3.1 Preparation of cell sections for visualization by TEM

TEM processing involved a number of steps, which needed to be completed in order to prepare the cell specimens for TEM investigation. The main steps included fixation, dehydration, infiltration/embedding, sectioning, staining and viewing under the microscope. Two replicates of each sample were prepared, as a result of the difficulties of cell adhesion and growth on filter wells. After several preliminary experiments, B16 mouse melanoma cells were grown on cell culture inserts incorporating polyethylene terephthalate (PET) track-etched membranes, with a pore size of 0.4 μM (Becton Dickinson). Both sides of the membrane were tissue culture treated. B16 cells were cultured in MEM containing 10% FCS and one insert was placed in each well of a

multiwell cell culture insert six-well plate with centering ribs. The top (apical surface) of each filter insert was filled with 1.5 ml of medium while the basolateral compartment was filled with 2.6 ml of MEM medium. Cells were seeded at a density of 2 x 10^5 cells per well and allowed to reach 85% confluence. Cells were then incubated with the appropriate amounts of biotinylated peptide and then immediately followed with gold-labelled streptavidin in HBS for four hours at 37°C, which revealed the presence of the biotinylated peptide. The cells were washed with PBS and then fixed with 2.5% glutaraldehyde in 2 x PBS overnight at 37°C to ensure that cells had enough time to adhere to the filters. The fixative was added to the inside and outside of the insert. The cells were then washed three times (5 minutes each) with PBS. Post-fixation was done in 1% osmium tetraoxide in PBS for one hour at room temperature. This was followed by another stage of washing in triple distilled water. At this point the filter membranes were cut out from the culture insert. This procedure was carried out in the presence of PBS to prevent the filters from drying out. Each filter was placed in vials to facilitate the dehydration stage. This involved exposing the filters to an acetone dehydration gradient: 50%, 70%, 80%, 90%, 95% (three changes for each were made and each change lasted 10 minutes) and 100% dry acetone. This final change was made six times for 20 minutes. The dry acetone was then replaced by 100% propylene oxide with two changes for 15 minutes. Infiltration/embedding initially involved replacement of 100% propylene oxide with 3: 1 propylene oxide to epoxy resin for an hour. Subsequently, this mixture was replaced with 1: 1 propylene oxide to epoxy resin for an hour. Then the filters were completely embedded in 100% epoxy resin overnight at 60°C so that the resin was allowed to completely surround the cells. The resin was used as a premix kit (TAAB) which included the resin and hardener already mixed to give medium hardness. After 24 hours, the filters were rolled around a cocktail stick and placed into a capsule mould prefilled with fresh resin. These were allowed to set overnight at 60°C. Following curing the blocks were trimmed, faced and sectioned to produce thin sections of approximately 50 nm (silver colour). Sectioning was carried out on an OmU3, Reichert (Austria) ultramicrotome using both glass, and finally diamond knives. The sections were placed onto palladium sprayed copper grids (300 mesh, Agar Scientific) coated with pioloform using 0.3% w/v pioloform solution in chloroform as described by Robards and

Wilson, 1989. Sections were then washed in distilled water and left to dry. The grids were then placed, sections facing downward, onto drops of Reynold's lead citrate for 5 minutes. The Reynold's lead citrate was freshly filtered and surrounded by a few sodium hydroxide pellets to absorb carbon dioxide and prevent the conversion of lead citrate to the carbonate precipitate. The sections were given a final wash and left to dry on filter paper ready for examination. Specimen grids were examined using a Jeol 1200EX II transmission electron microscope operating at an accelerated voltage of 80 kV. Photographs were taken of the areas on the grid showing cell ultrastructure and gold particles.

3.2.4 Cell culture preparation for ADMP-peptide conjugates

B16 melanoma cells were grown for 24 hours on coverslips in six-well plates as in section 3.2.2.1. ADMP-penetratin and ADMP-mutant penetratin were incubated with B16 cells both for two different time points, five minutes and three hours. After these respective time points, the cells were washed twice with PBS and then treated for 15 minutes with CellScrub buffer (Gene Therapy Systems, San Diego, CA) to remove extracellular conjugates. Cells were then fixed with 100% ethanol for 5 minutes and mounted on slides using the antibleaching agent DABCO for viewing with a low light microscope.

3.2.4.1 Low light microscopy for viewing ADMP-peptide conjugates

Cells were examined with an Olympus IX70 fluorescence microscope incorporating a 100W Hg lamp and an Olympus PlanApo x40 water immersion objective. The samples were exposed to only a small percentage of the fluorescent light due to the presence of neutral density filters in the light path. The excitation was recorded between 330 – 385 nm and the emission wavelength was at 420 nm. The microscope was also equipped with a PentaMax cooled digital intensified CCD (charge-coupled device) camera system (Princeton Instruments). Images were captured by using Improvison Openlab v2.2.1 image analysis software.

3.2.5 Membrane preparations for investigation of peptide interactions

The fluorescent dye 1-(3-Sulfonatopropyl)-4[β[2-(di-*n*-octylamino)-6-naphthyl]vinyl] pyridinium betaine (di-8-ANEPPS) was purchased from Molecular Probes, Inc. Egg phosphatidylethanolamine (PE) was purchased from SigmaAldrich, UK. Fluoresceinphosphatidylethanolamine (FPE) was purchased from Molecular Probes, Inc.

3.2.5.1 Labelling membranes with FPE and Di-8-ANEPPS

Phosphatidylcholine dissolved in chloroform and di-8-ANEPPS (as required) were mixed in a round bottom flask, and the solution was dried under a stream of nitrogen to deposit a thin lipid film on the inside of a glass tube. Large unilamellar vesicles (LUV) were prepared by hydrating the dried lipid film with the sucrose buffer (280 mM sucrose, 10 mM Tris, pH 7.5), then repeatedly freezing and thawing the suspension five times, and finally extruding it ten times through two polycarbonate filters of pore size 0.1 μm (Nucleopore Corp., Pleasanton, CA) using an extruder (Lipex Biomembranes Inc., Vancouver, Canada) according to the extrusion procedure of Mayer *et al.*, 1986. LUVs were labelled exclusively in the outer bilayer leaflet with FPE using the following procedure. LUVs were incubated with FPE dissolved in ethanol at 37°C for one hour in the dark. Any remaining unincorporated FPE was removed by gel filtration on a PD10 sephadex column equilibrated with the appropriate buffer. FPE-liposomes were used immediately and any remaining FPE was stored at 4°C for up to two weeks.

3.2.5.2 Fluorescence measurements and analysis

Fluorescence time courses were obtained by adding the desired amount of peptide to 2 ml lipid suspensions (200 μm lipid) on an SLM-Aminco model spectrofluorimeter. For FPE experiments excitation and emission wavelengths were set at 490 nm and 518 nm, respectively. For di-8-ANEPPS measurements, excitation and emission wavelengths were set at 460 nm and 520 nm.

3.3 RESULTS

3.3.1 Fluorescent labelling of peptides using BODIPY FL CASE, Biotin and ADMP

3.3.1.1 Labelling with BODIPY

The Kaiser test and the TNBS test for the presence of free amines, both showed positive results for the labelling reaction as evidenced by the absence of free amines. The labelled peptide was then cleaved from the resin and purified by methods described in chapter 2. BODIPY FL CASE is a water-soluble succinimidyl (N-hydroxysuccinimide or NHS) ester of BODIPY FL cysteic acid with a molecular weight of 641. Its fluorescence excitation spectrum has an excitation at 504 nm with an extinction of 72300 $M^{-1}cm^{-1}$ and an emission centred at 511 nm.

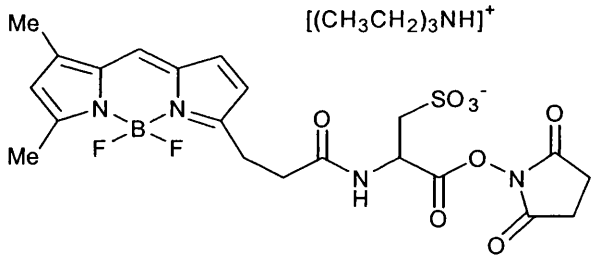

Figure 3.1. Structure of BODIPY FL CASE.

BODIPY FL CASE contains a sulphonated spacer that appears to decrease the interaction between the fluophore and the protein to which it is being conjugated. The reaction between a protein and BODIPY FL CASE results in split of the N-hydroxysuccinimide (NHS) ester part of the molecule, which acts as a leaving group, creating the formation of an amide bond with the protein.

The fluorescence spectrum of BODIPY alone and BODIPY linked to a peptide in this study indicated a significant shift in the excitation wavelength from 504 nm to 460 nm. Also, there was a dramatic reduction in the absorbance maximum in comparison to BODIPY. Three separate measurements confirmed that the absorbance of the fluophore linked to a peptide was approximately 12 times less than that of BODIPY (Figure 3.2).

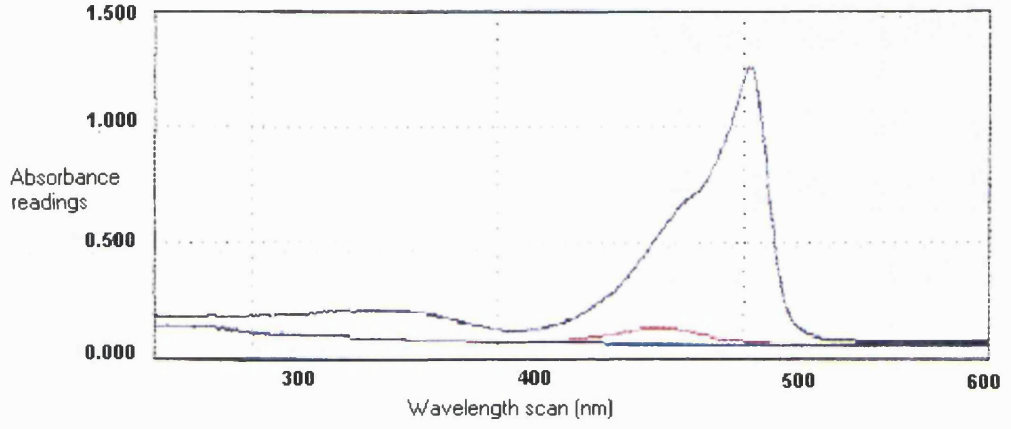

Figure 3.2. Fluorescence spectra of BODIPY FL CASE (dark blue line), BODIPY FL CASE conjugated to a peptide (red line) and peptide without fluorescence label (light blue line). The concentration of each sample was 1 mg/ml. These spectra are representative of three evaluations carried out on different occasions.

These observations of significant differences in the fluorescence spectra of BODIPY samples compared to BODIPY-peptide samples led to an investigation of the mass spectrometry of these samples by electrospray. Figure 3.3 indicates the mass spectrometry of BODIPY alone. The spectrum indicated a significant reduction in the observed mass compared to the expected mass of BODIPY. Cysteic acid succinimidyl esters are water-soluble and can undergo hydrolysis releasing either the carboxylic acid or more likely the succinimide alcohol accounting for the difference of 199 from the mass spectrometry results. The mass spectrometry of BODIPY linked to penetratin is shown in figure 3.4. There also appeared to be a reduction in the mass observed compared to that expected for the structure. This is discussed in section 3.4.1.

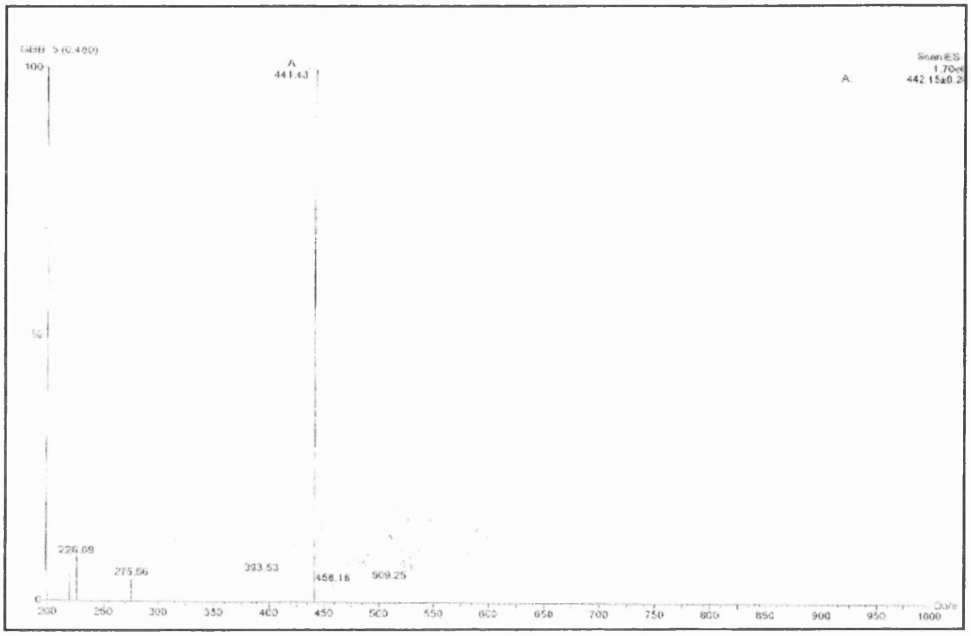

Figure 3.3. Electrospray mass spectrometry of BODIPY FL CASE.

Expected mass = 641 Observed mass = 442

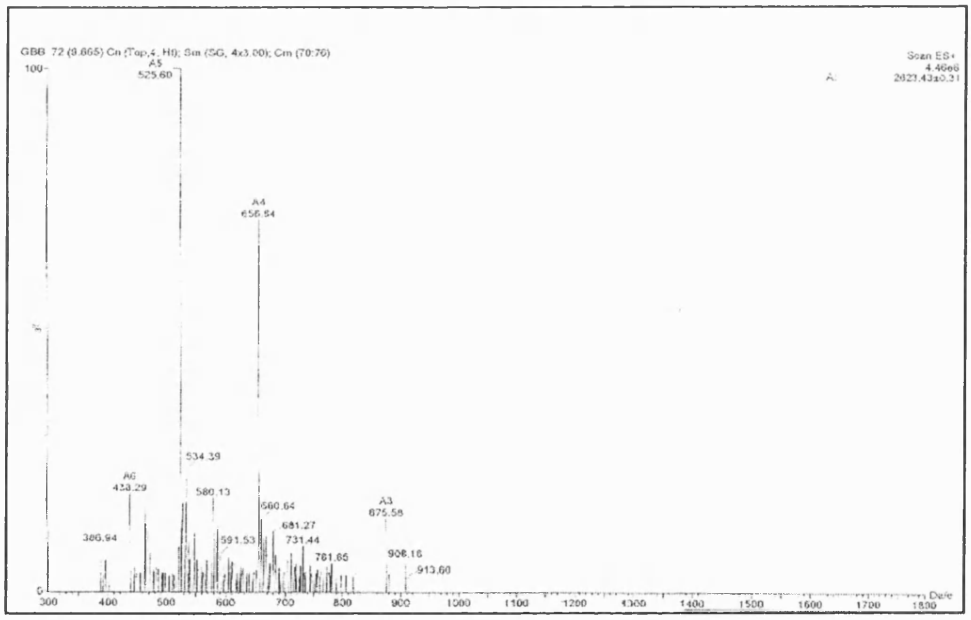

Figure 3.4. Electrospray mass spectrometry of BODIPY-penetratin.

Expected mass = 2688 Observed mass = 2623

The mass spectrum is a plot of abundance (the relative amounts of the different positively charged fragments) against the mass-charge ratio of the fragments. Each major peak (numbered) in the spectrum represents a fragment of the molecule. The smaller peaks represent impurities from the sample. The fragments are scanned so that the peaks are arranged by increasing mass-charge from left to right in the spectrum. The intensities of the peaks are proportional to the relative abundance of the fragments, which in turn depends on their relative stabilities.

3.3.1.2 Labelling with ADMP and Biotin

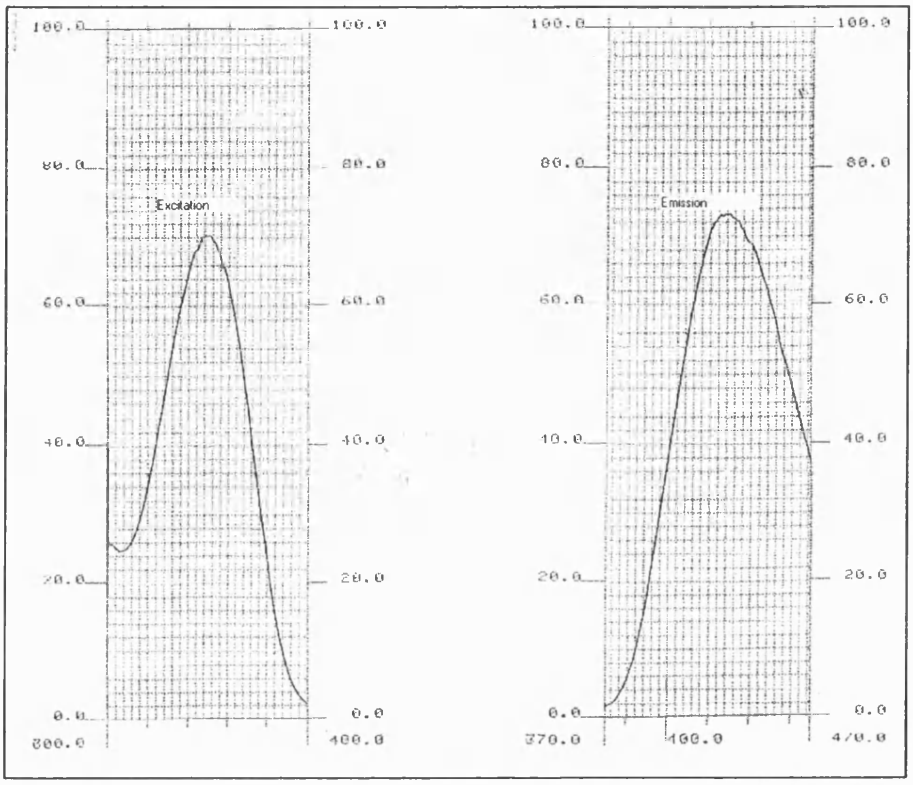

Figure 3.5. UV-VIS scan of ADMP at a concentration of 1 mg/ml. The spectrum shows an emission of 429 nm and an excitation wavelength of 345 nm. An initial UV scan employed water as a standard to confirm that the equipment was suitably calibrated.

For all labelling reactions with ADMP and Biotin, the amine tests always proved negative, as evidenced by the absence of amine groups indicating a fully coupled peptide (section 3.2.1.2). The peptides were cleaved from the resin and then purified before further analysis was undertaken. The peptides are labelled with both ADMP and biotin selectively at their N-termini. The fluorescence properties of the labelled peptides were compared to the unmodified fluorescent labels to ensure that the process of labelling did not have a detrimental effect on the spectral properties of the fluophores. Figure 3.5 and 3.6 show observed spectral properties of unmodified ADMP and ADMP coupled to peptide.

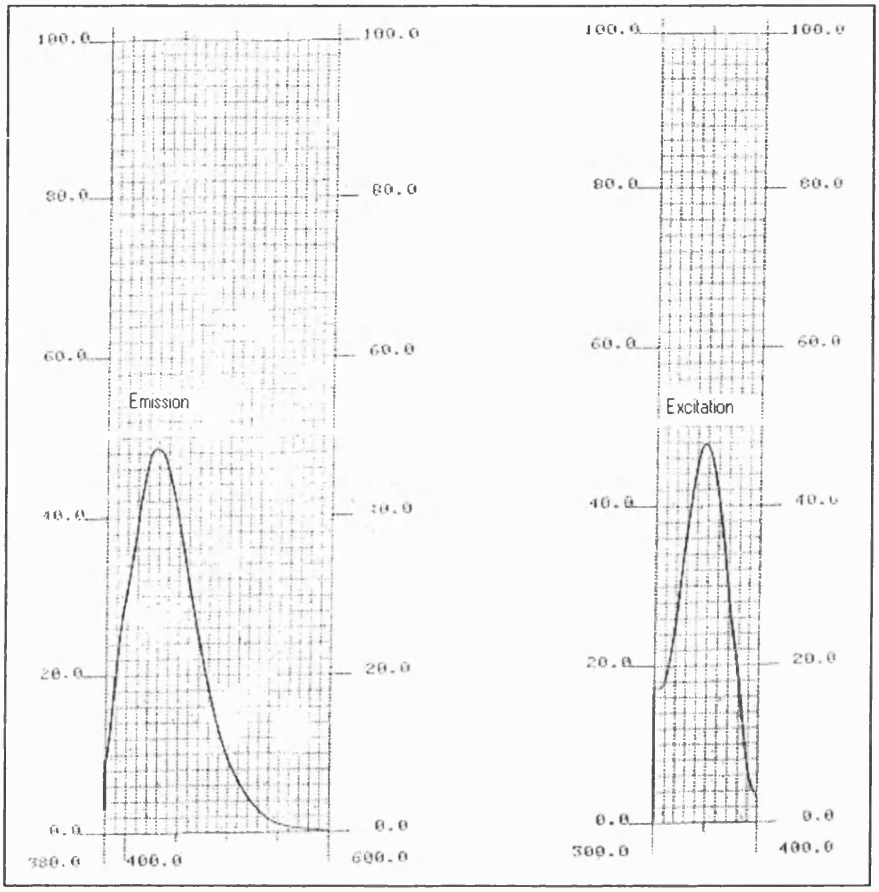

Figure 3.6. UV-VIS scan of ADMP linked to penetratin at a concentration of 1 mg/ml. The spectrum shows an emission of 429 nm and an excitation of 345 nm.

The UV scan for ADMP-penetratin confirmed that the labelling process was successful since the labelled peptide exhibited the same spectral properties as the unmodified fluophore.

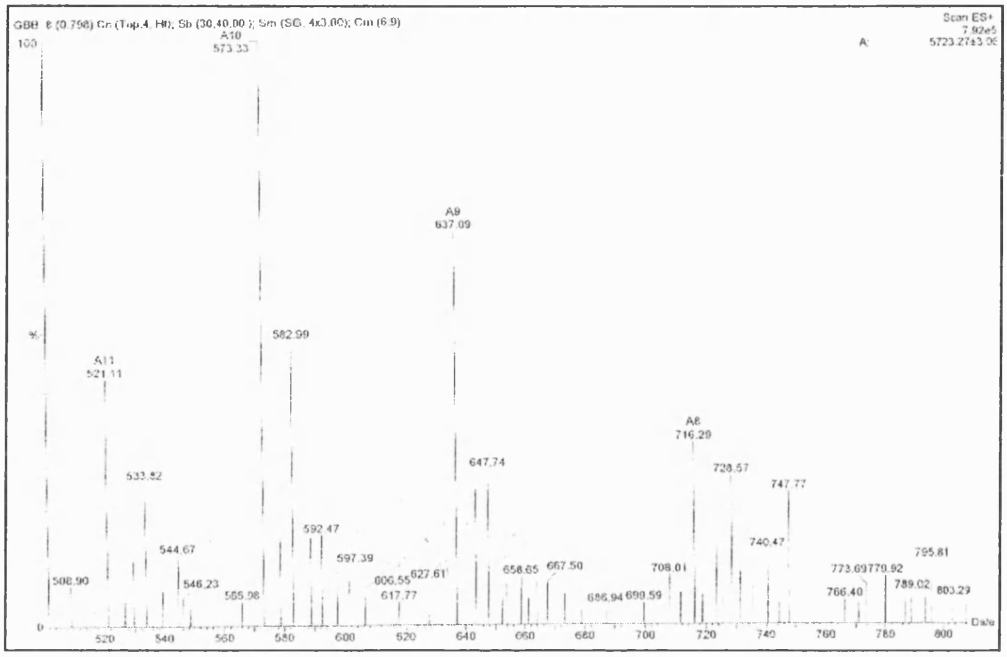

Figure 3.7. Electrospray mass spectrometry for ADMP linked to K_{25}penetratin.

Expected mass = 5725 Observed mass = 5723

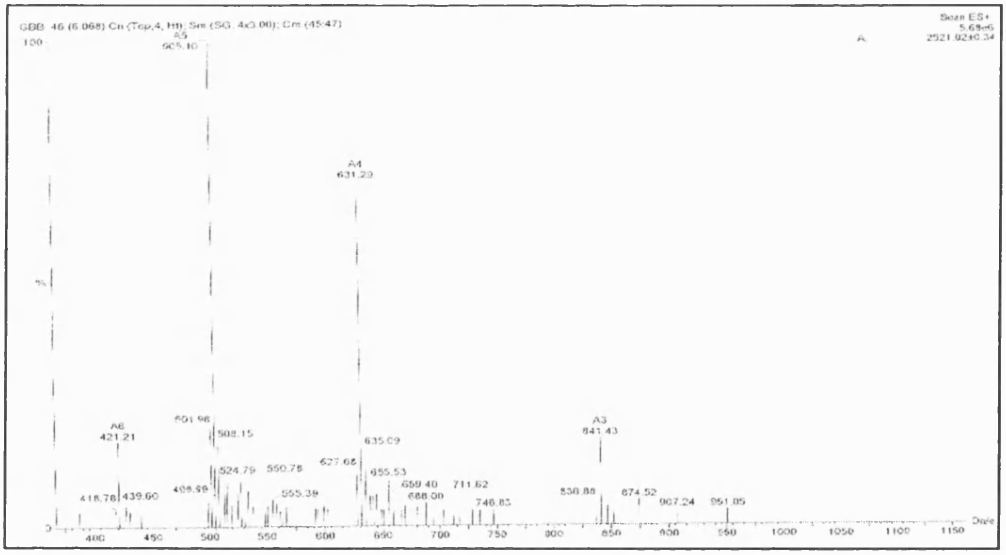

Figure 3.8. Electrospray mass spectrometry for ADMP linked to penetratin.

Expected mass = 2520 Observed mass = 2521

The expected masses were calculated from the carbon skeleton and functional groups of samples. The observed masses shown in Figure 3.7 and 3.8 are both equivalent to the average of the main peaks obtained for each sample.

3.3.2 Visualization of intracellular peptides using confocal microscopy

To follow the cellular entry and fate of penetratin as a translocating peptide, confocal microscopy was employed. B16 murine melanoma cells were exposed to biotin-labelled penetratin or mutant penetratin, which has been reported to be poorly translocated. Cells were exposed for four hours, after which the peptides were removed by rinsing with several washes using PBS. The cells were then fixed and the presence of biotin revealed with fluorescein isothiocyanate-labelled streptavidin.

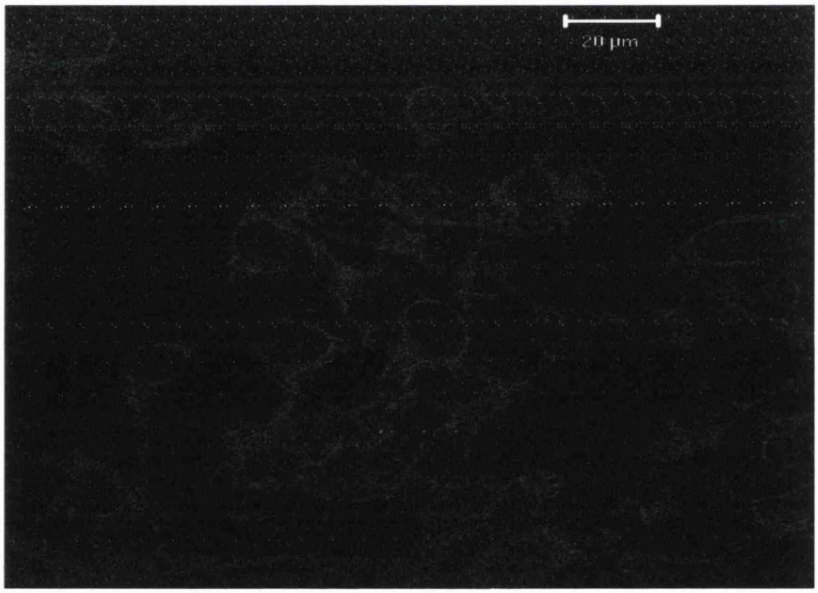

Figure 3.9. Confocal image showing B16 melanoma cells, which were not incubated with either peptide or streptavidin FITC. Excitation at 488 nm, FITC emission filter. Scale bar: 20 µm.

The control image shown in Figure 3.9 indicates the level of autofluorescence observed under the FITC filter set of the microscope. A comparison in peptide distribution was achieved by maintaining fixed conditions for all scans. The confocal images displayed in Figure 3.9 - 3.12 are representative of B16 cell sections observed using replicates of slides ($n \geq 2$).

A

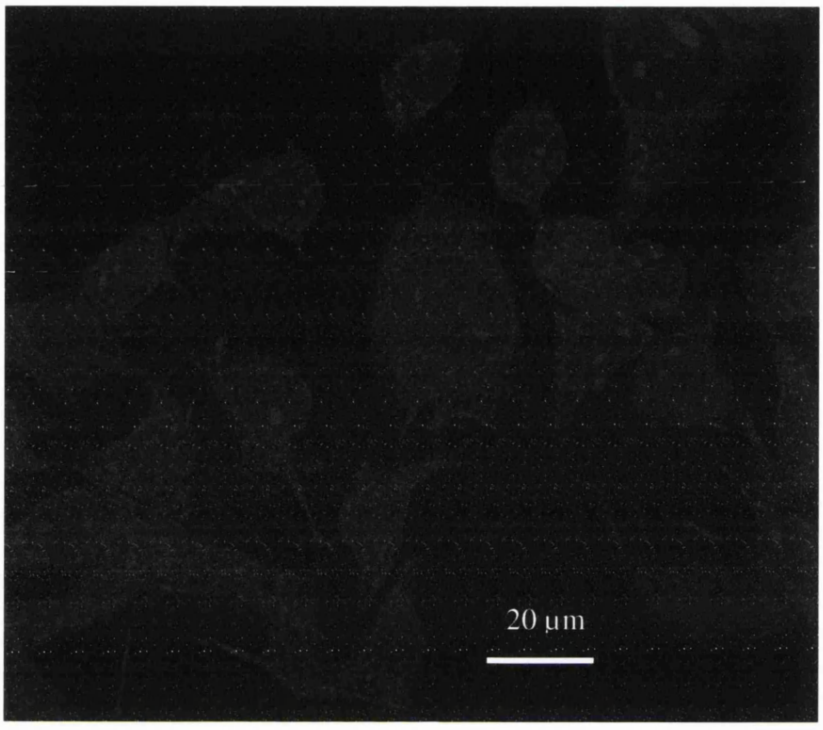

B

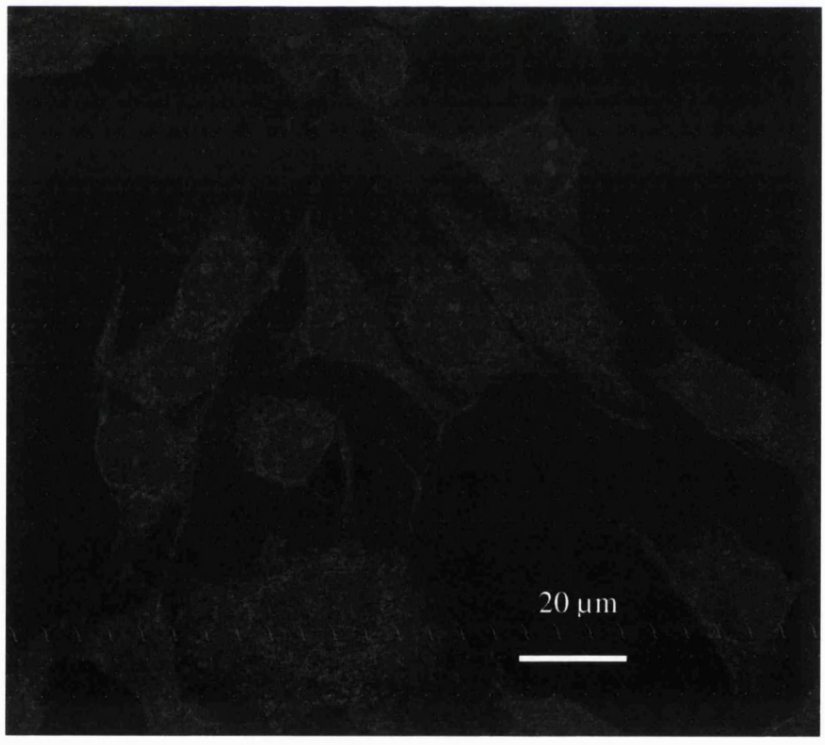

C

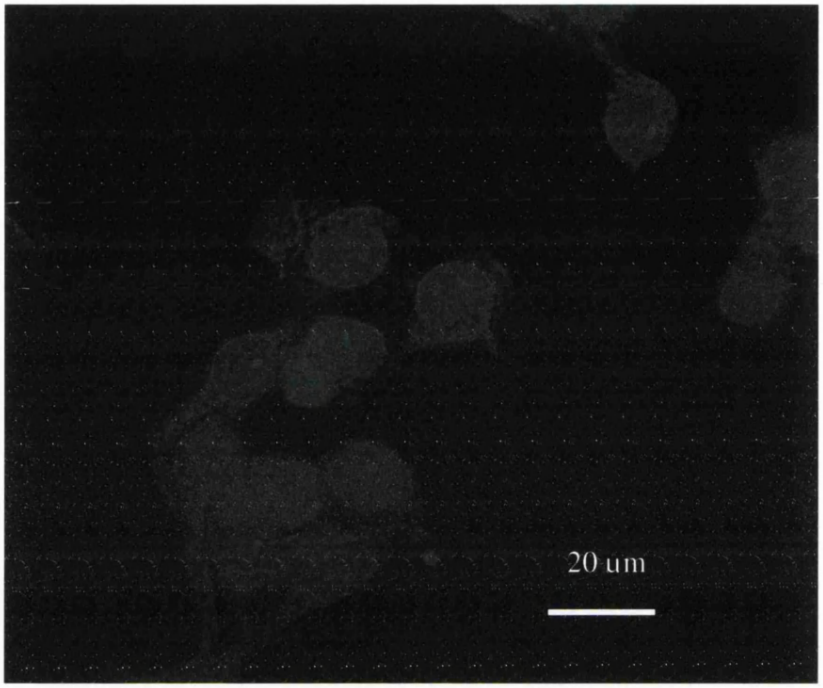

D

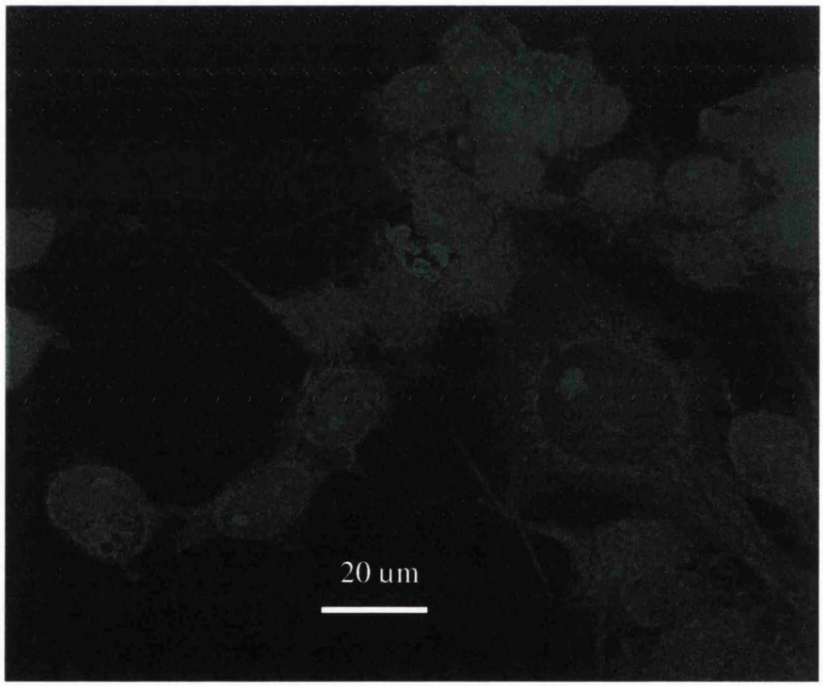

Figure 3.10. Confocal images showing B16 cells that have been incubated for different times with the biotin-labelled mutant penetratin [22 μM] for up to four hours at 37°C and subsequently treated with FITC-streptavidin. Image A (5 minutes), B (30 minutes), C (2 hours), D (4 hours). Excitation at 488 nm, FITC emission filter. Scale bar: 20 μm.

A

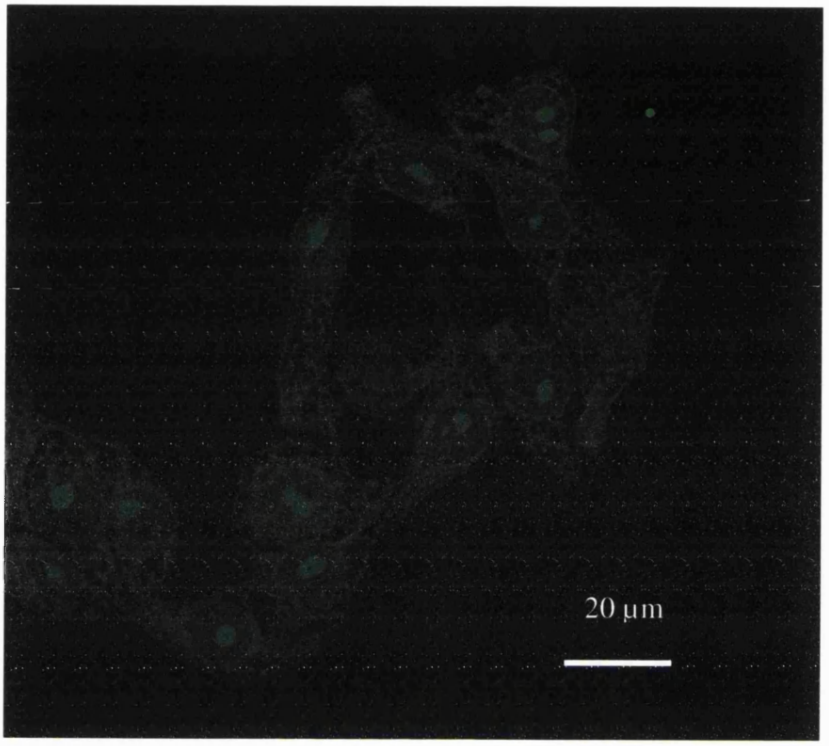

B

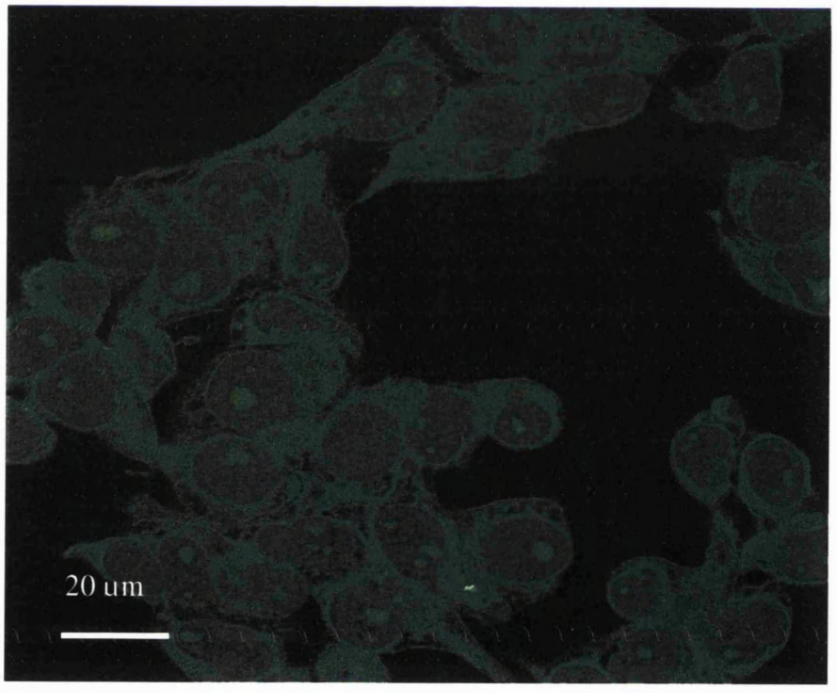

C

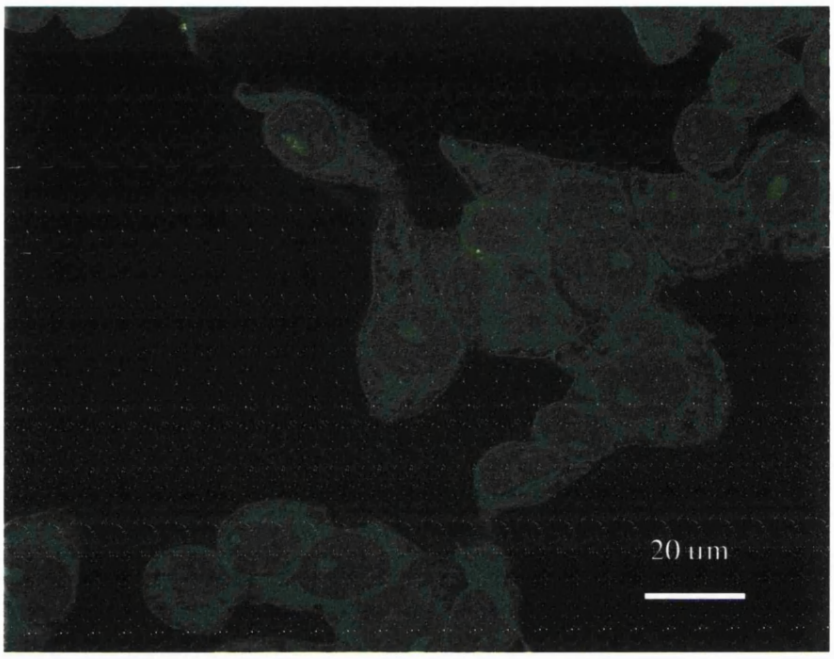

D

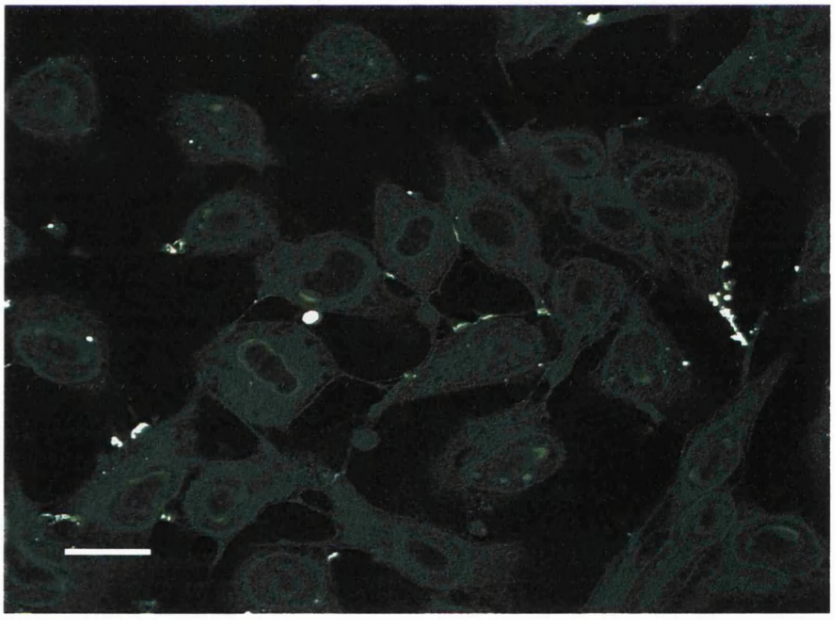

Figure 3.11. Confocal microscopy visualisation of biotin-labelled penetratin [22 μM] incubated with B16 cells for up to four hours at 37°C and subsequently treated with FITC-streptavidin. Image A (5 minutes), B (30 minutes), C (2 hours), D (4 hours).Excitation at 488 nm, FITC emission filter. Laser power and photomultiplier gain is identical within each experiment. Scale bar: 20 μm.

A

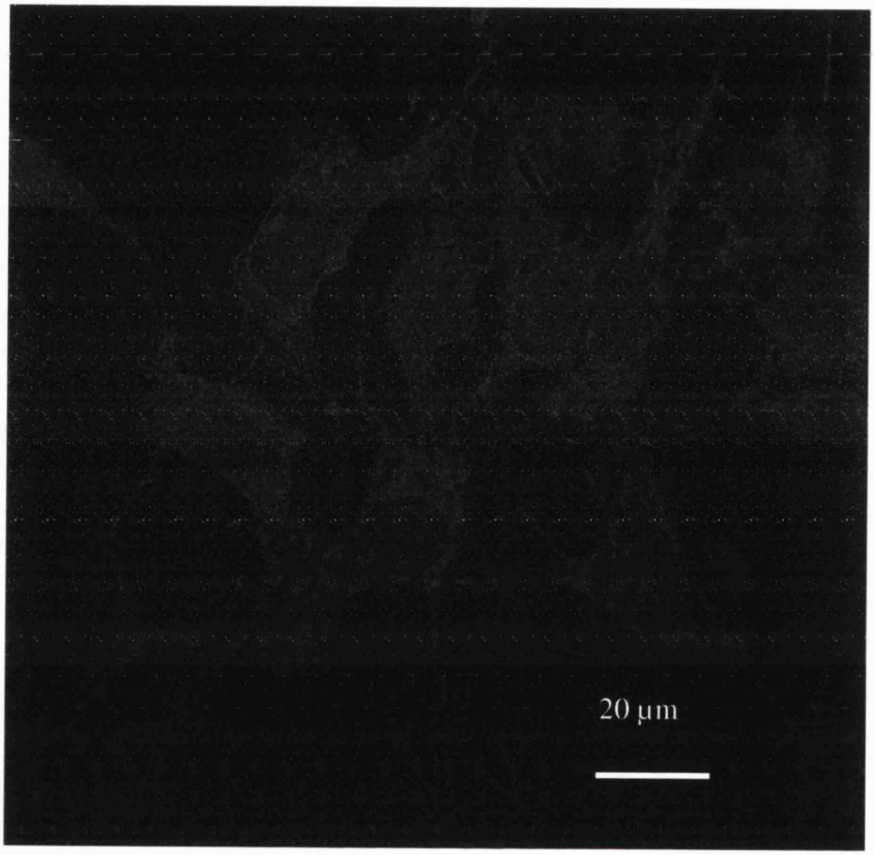

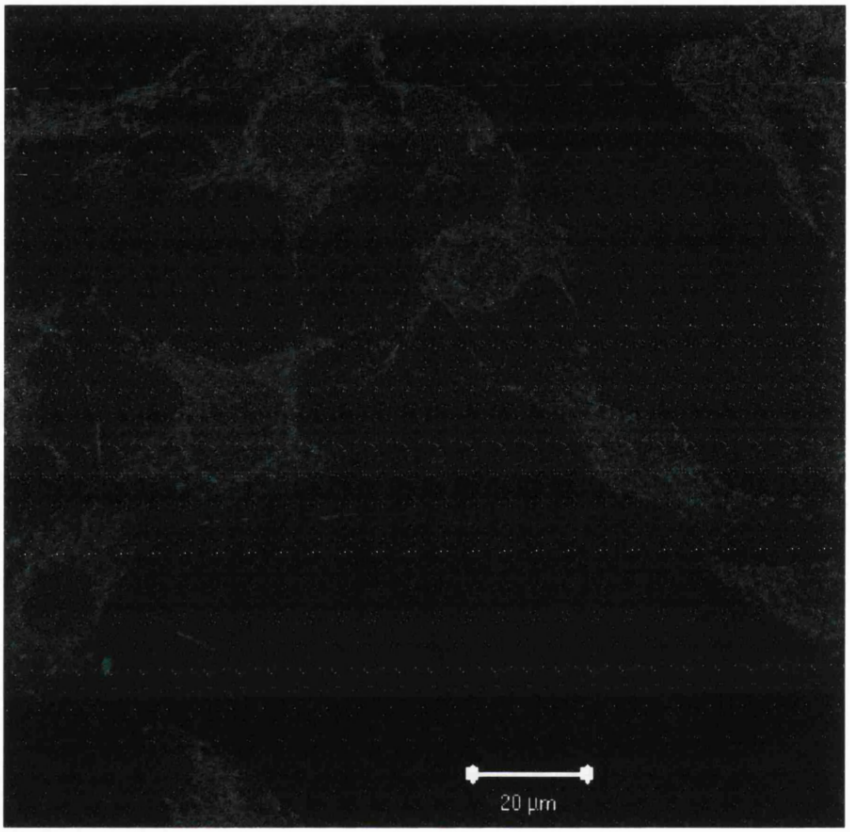

B

Figure 3.12. Confocal microscopy images of B16 cells incubated with biotin-labelled mutant penetratin (A) and penetratin (B) for four hours at 4°C with subsequent detection using FITC-streptavidin.

3.3.3 Transmission electron microscopy examination of peptide uptake.

The use of the transmission electron microscopy (TEM) provides a very powerful tool for examining cells at the ultrastructural level. In addition to confocal microscopy, TEM was employed to further evaluate the cellular mechanisms of uptake and trafficking of penetratin and its derivative. These techniques, used in conjunction, are more powerful than either technique alone. The final results achieved with TEM can be very dependent on the methods of sample preparation. All the stages of sample preparation need to be optimised as much as possible to ensure that the images are free from artefacts and that there is homogeneity between sample populations. Direct methods of detection can be achieved using colloidal gold particles, which act as very electron-dense markers and can easily be observed under an electron beam. Gold particles form complexes with proteins such as streptavidin by means of a non-covalent interaction. Colloidal gold particles of 10 nm in diameter were chosen for these experiments to ensure easier visibility in low magnification electron micrographs. The following representative EM images were eventually obtained after transfection and the EM process was repeated two occasions. Consequently, 30 sections were prepared and repeatedly studied on numerous occasions under the microscope.

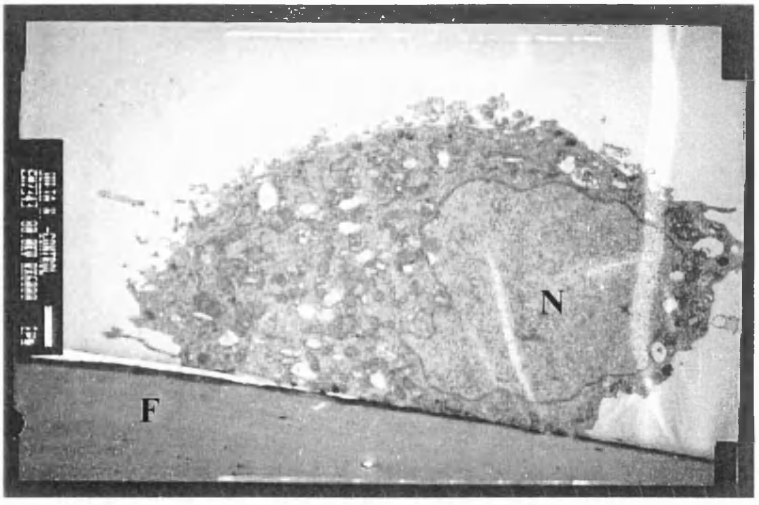

Figure 3.13. Electron micrograph showing an untreated B16 murine melanoma cell (N = nucleus) attached to a filter (F) from the cell culture insert plate (x 6000). Scale bar indicates 1 μm.

A

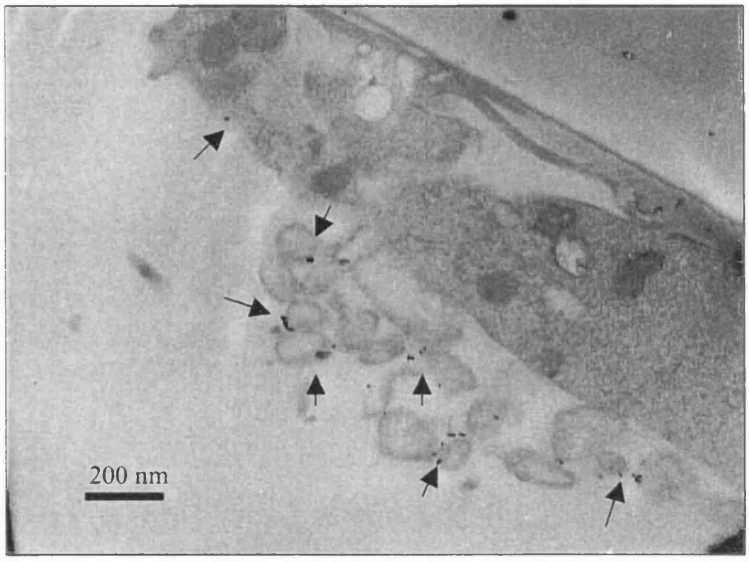

B

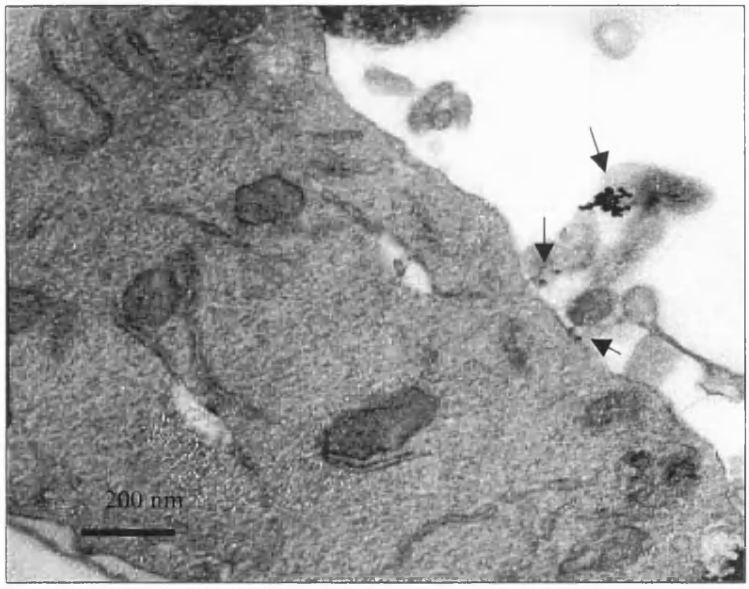

Figure 3.14. Electron micrographs showing sections of B16 cells which were treated with streptavidin colloidal gold particles without biotinylated peptide. The cells were fixed in glutaraldehyde, post-fixed in osmium tetroxide, dehydrated and embedded and finally stained with uranyl acetate and lead acetate. (A) Electron micrograph with no evidence of gold particles inside the cell, (x 20,000). (B) Cluster of gold particles at cell surface, (x 30,000). Arrows pinpoint gold particles.

A

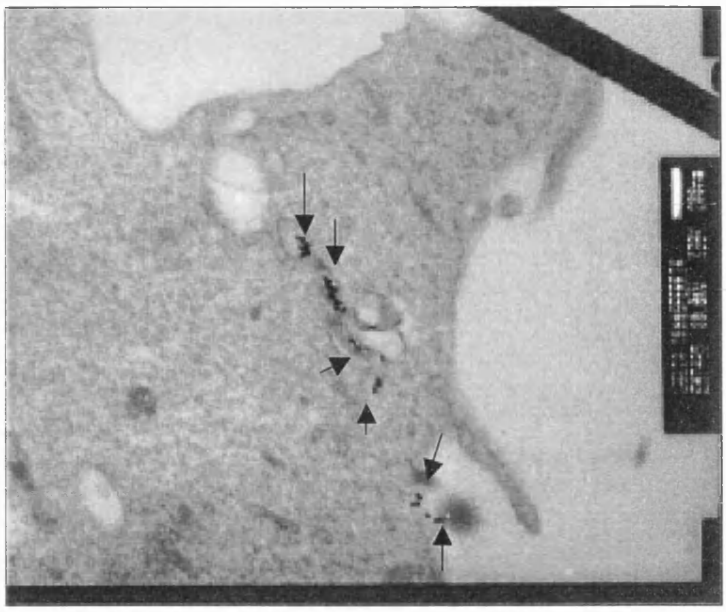

B

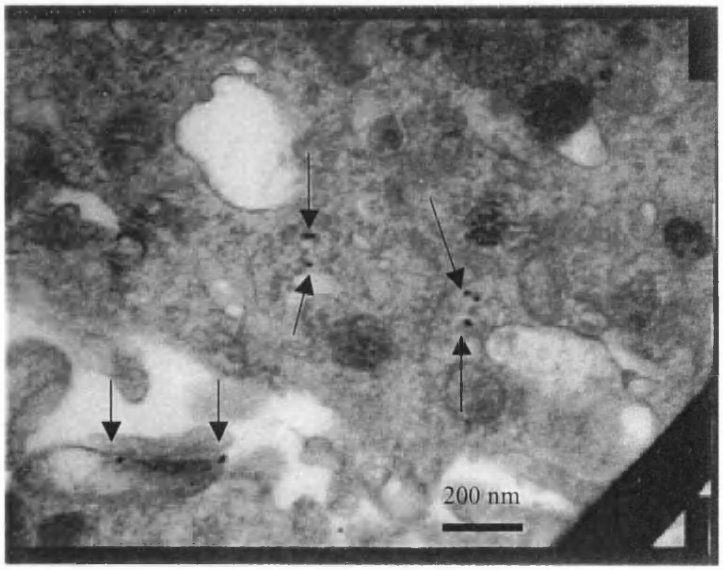

Figure 3.15. Uptake of streptavidin-gold labelled transferrin molecules by B16 cells. Cells were fixed 4 hours post-incubation. After fixation in glutaraldehyde, postfixation in osmium tetroxide, dehydration and embedding, the sections were stained with uranyl acetate and lead citrate. (A) Electron micrograph of gold labelled particles moving through vesicular structures immediately beneath the cell surface, (x 30,000). Scale bar 200 nm. (B) Intracellular vesicular structures containing gold-labelled transferrin particles (x 40,000). Both images show cytoplasmic cell sections.

A

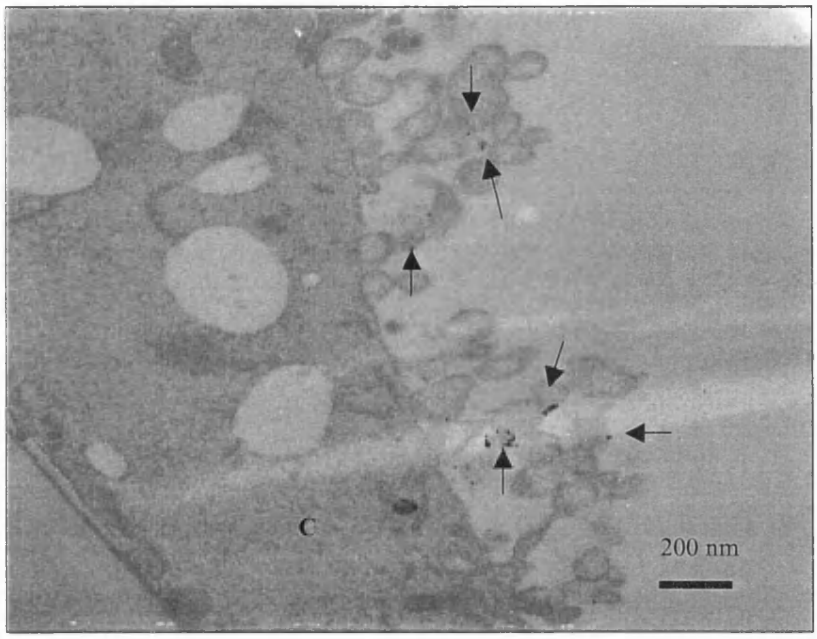

B

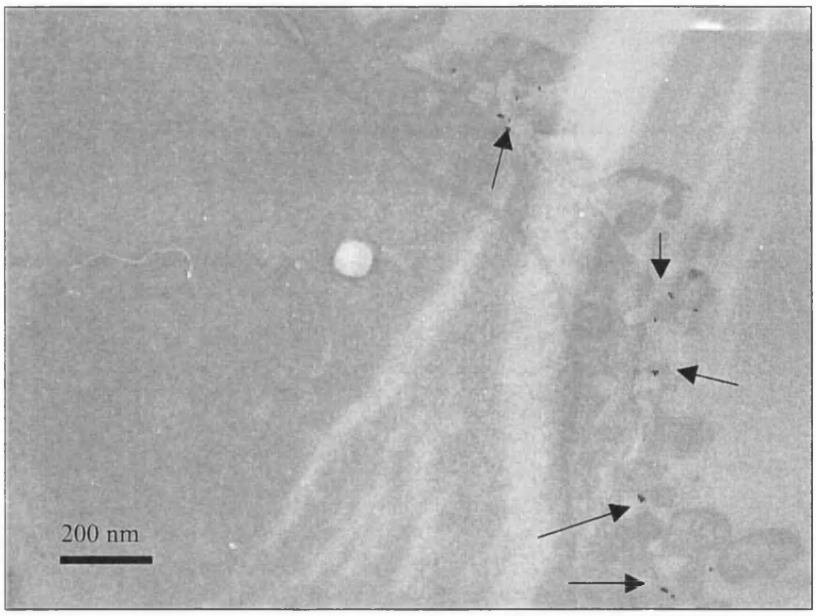

Figure 3.16. Electron micrographs showing B16 cells incubated with biotinylated mutant penetratin, after which cells were rinsed several times and incubated with streptavidin gold-labelled particles. Cells were fixed and stained four hours post-incubation. Gold particles (pinpointed by arrows) remain on the surface of the cells. No particles visible in the cytoplasm (C) (A x 10,000), (B x 20,000).

A

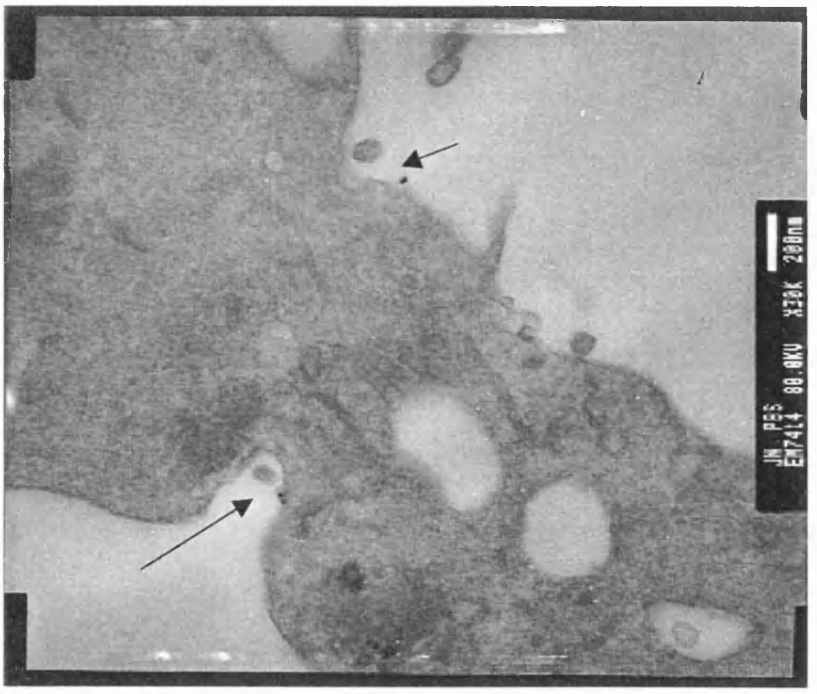

B

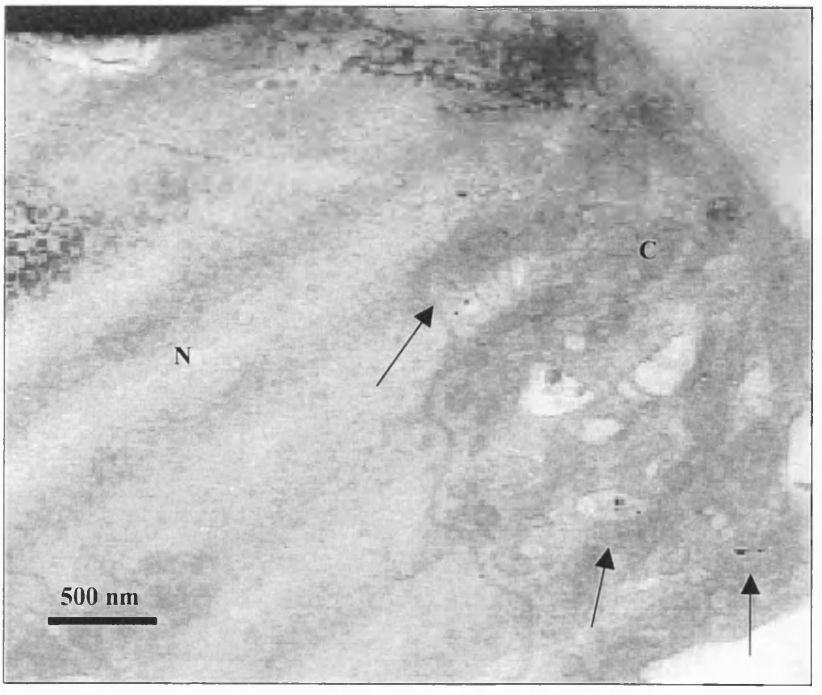

C

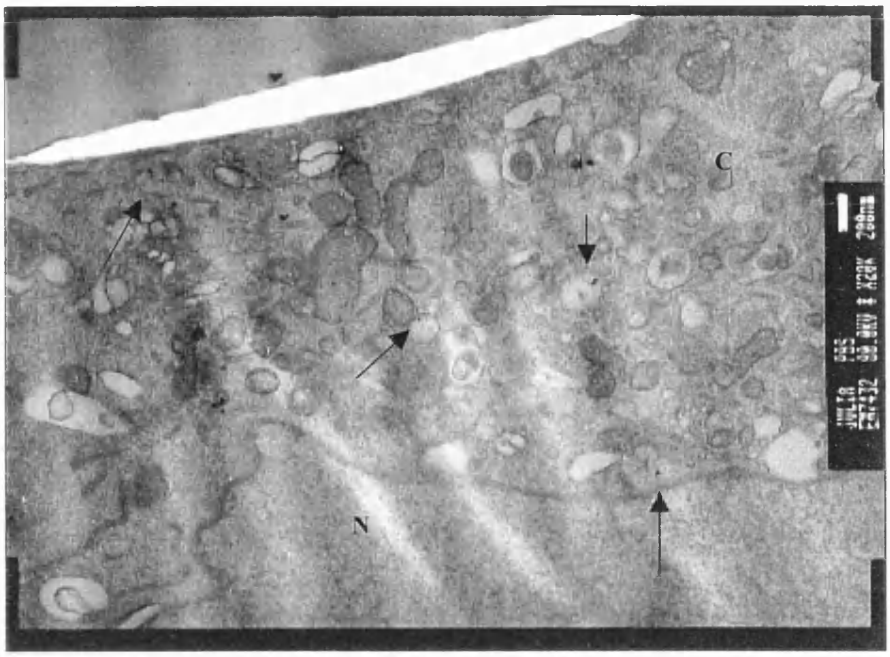

D

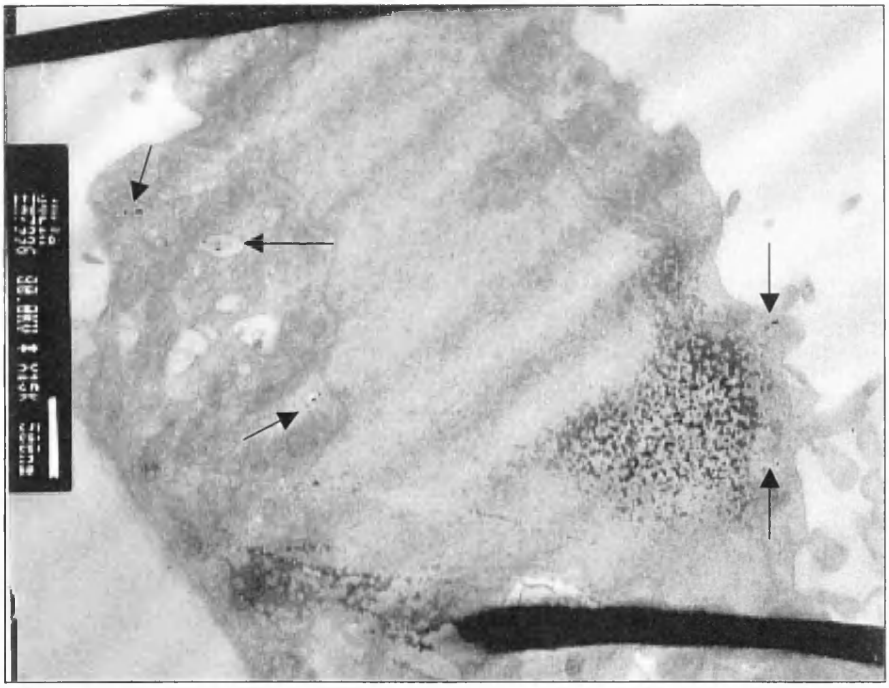

Figure 3.17. Uptake of gold particles with biotinylated penetratin by B16 cells. The arrows indicate gold particles internalized by cellular vesicles in the cytoplasm (C). There were no gold particles visible in the nucleus (N). Cells were fixed four hours post-incubation. (A) Cell projections engulfing gold-labelled peptide particles. (B), (C) and

(D) represent sections that have been incubated with biotinylated penetratin. All have gold particles enclosed in vesicular vacuoles within the cytoplasmic regions. These images were not seen with other samples including the biotinylated mutant penetratin. However, no gold particles were observed in nuclear compartments of the images taken. The TEM images shown in this chapter are representative sections for each sample tested. Hence, the distribution pattern of gold particles for each sample was consistently observed in all batches of cells examined.

3.3.4 Visualization of ADMP-peptide conjugates

All images of B16 cells incubated with ADMP-conjugates were taken using identical settings with the microscope. The detector gain remained at 49.9 for all pictures.

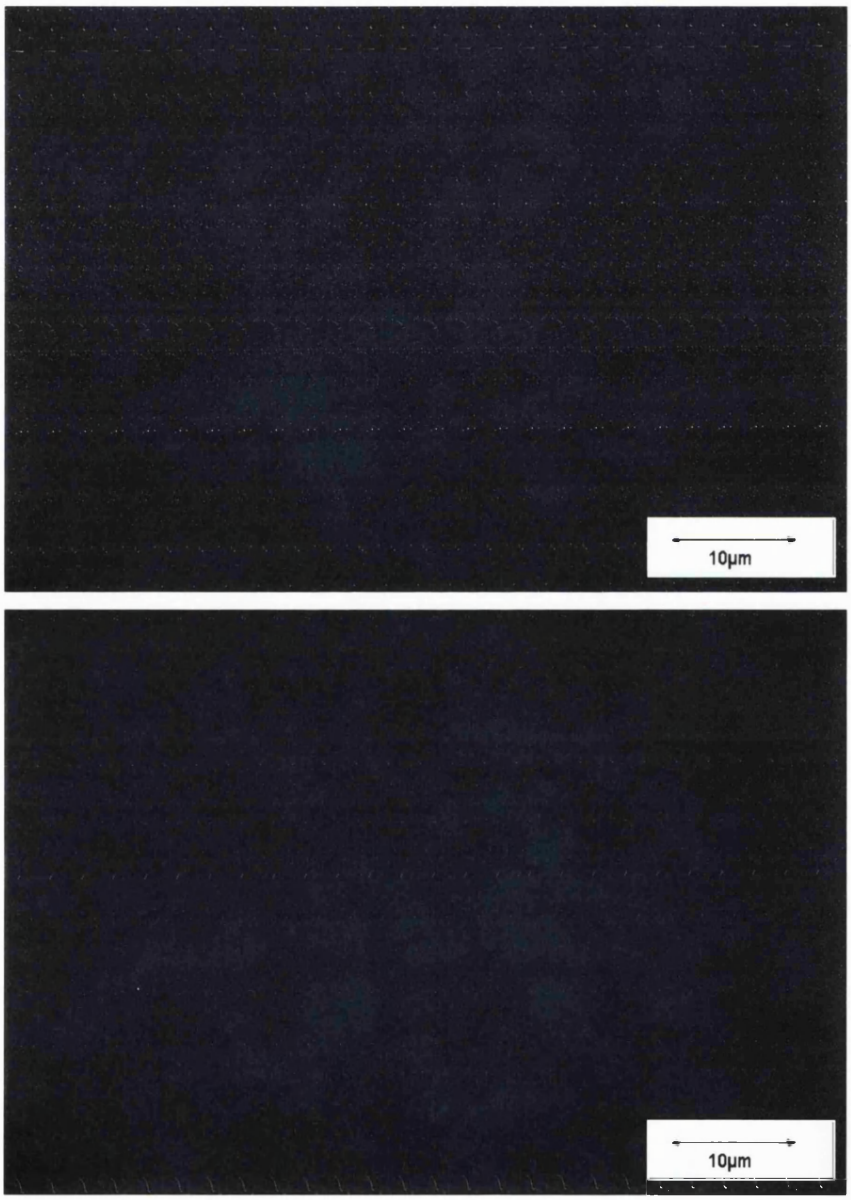

Figure 3.18. B16 cells that have not been exposed to labelled peptides (untreated). Cells were washed after incubation, with PBS and examined with a microscope equipped with a UV laser and a CCD camera system.

A

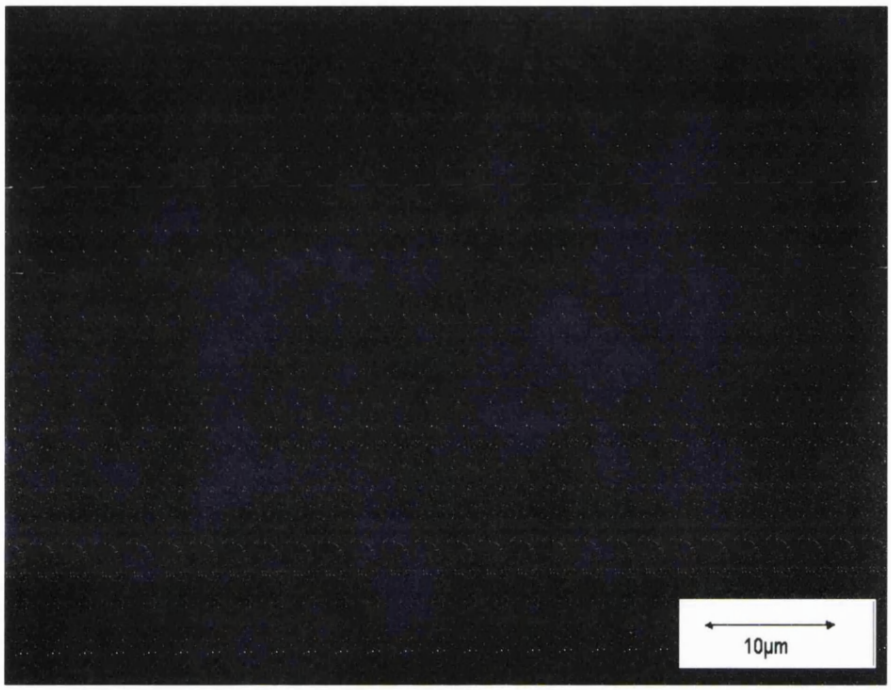

B

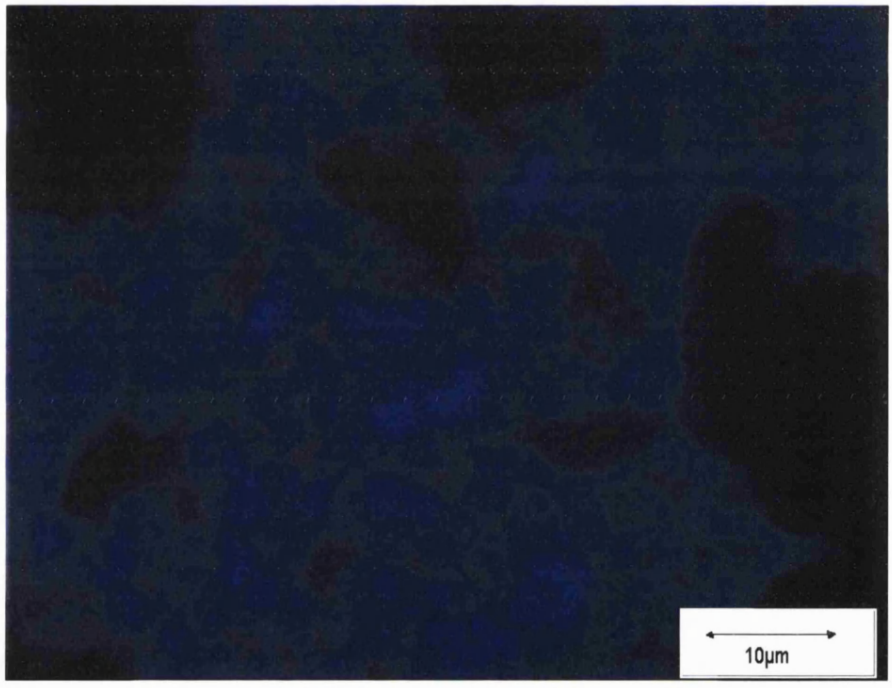

Figure 3.19. Microscopic images showing B16 cells which were incubated with ADMP-labelled conjugates after a 5-minute incubation period. (A) represents cells that were exposed to ADMP-mutant penetratin and (B) shows cells exposed to ADMP-penetratin. Both images were taken using the same settings.

A

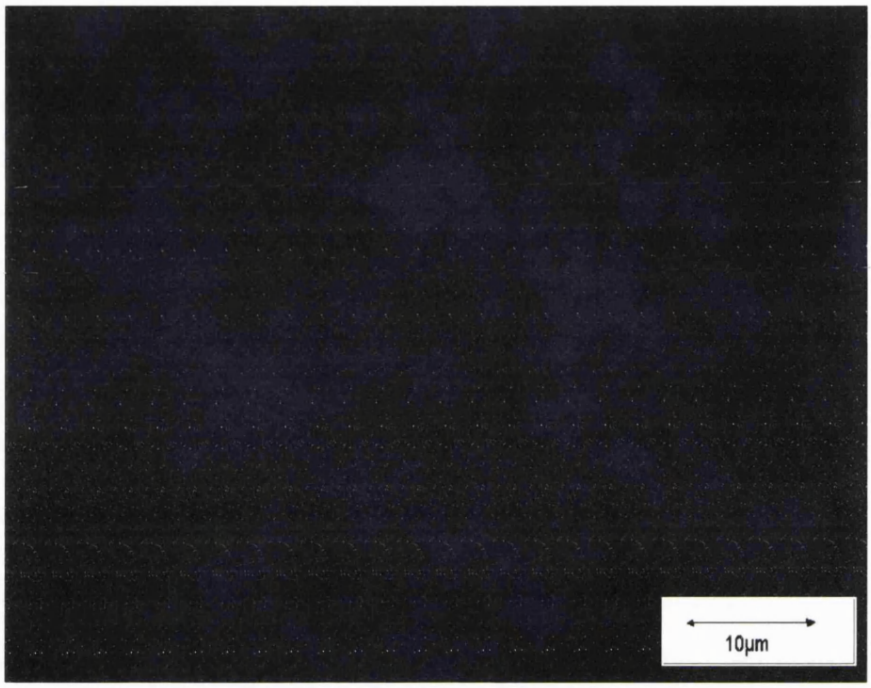

B

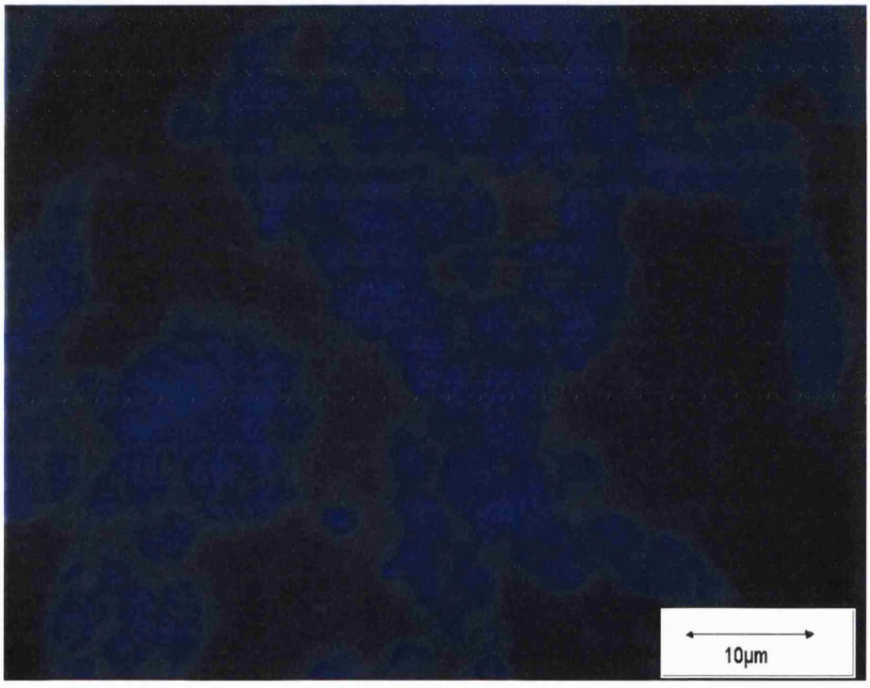

Figure 3.20. Microscopic images showing B16 cells, which were incubated with ADMP-labelled conjugates after a three-hour incubation period. (A) displays cells that were incubated with ADMP-mutant penetratin while (B) shows cells that were exposed to ADMP-penetratin. Pictures were taken at identical detector gain.

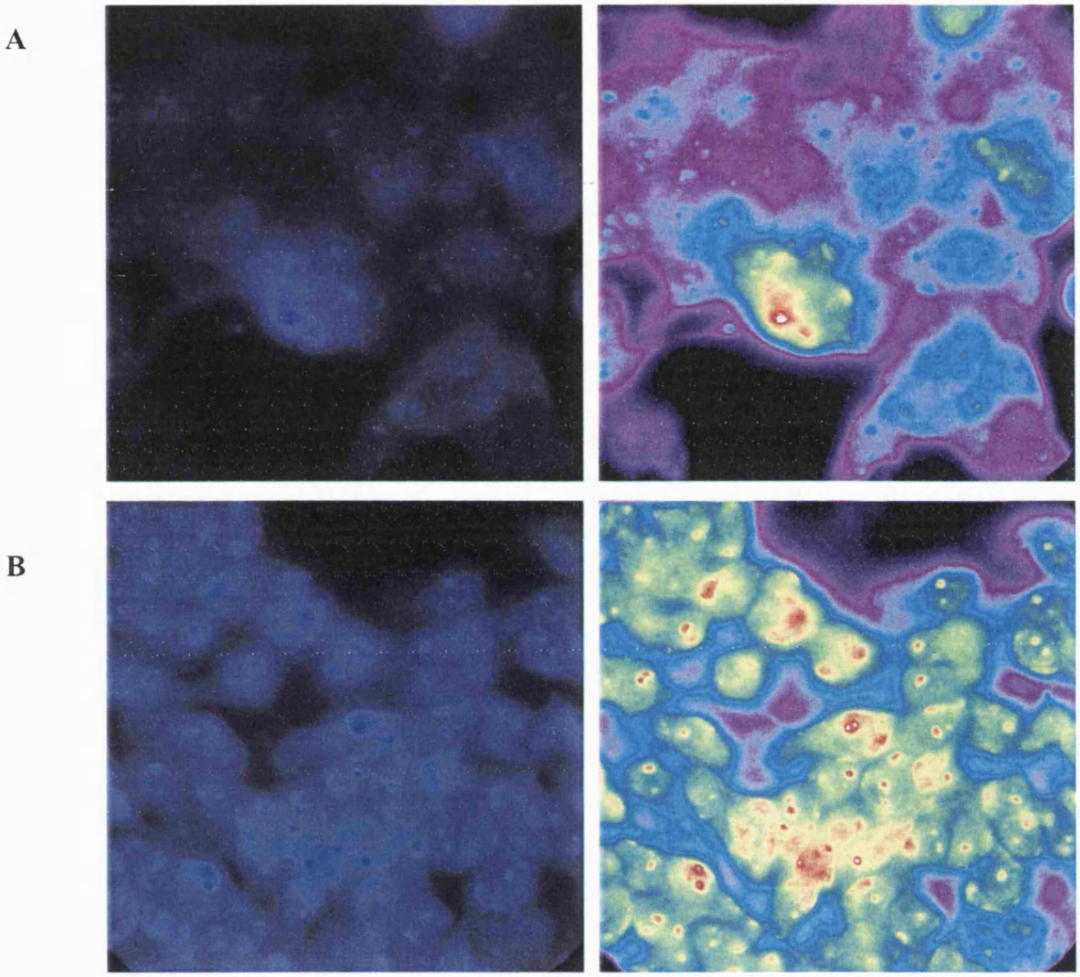

Scale bar 10μm

Figure 3.21. Images represent cells exposed to ADMP-penetratin conjugates for five minutes (A) and three hours (B). The images on the right side are corresponding contour analysis of the amount of fluorescence. A x 60 oil immersion objective was used to take these images.

Cells treated with ADMP-penetratin conjugates consistently revealed intense cellular staining. Staining was predominantly surface-associated after short, 0 – 5 minutes incubation period with progressive accumulation in intracellular staining up to three hours.

3.3.5 Interactions of penetratin and its derivatives with phospholipid vesicles

The measurements of fluorescence changes can indicate a clear interaction between charged peptides and the lipid membranes. The technique involved labelling membranes with small amounts of FPE, which is sensitive to the membrane surface electrostatic potential. Addition or removal of a charged peptide resulted in a corresponding increase or decrease in the fluorescence intensity of the probe. The response observed on interaction of Ca^{2+} ions served as a positive control for integrity of the membrane preparation.

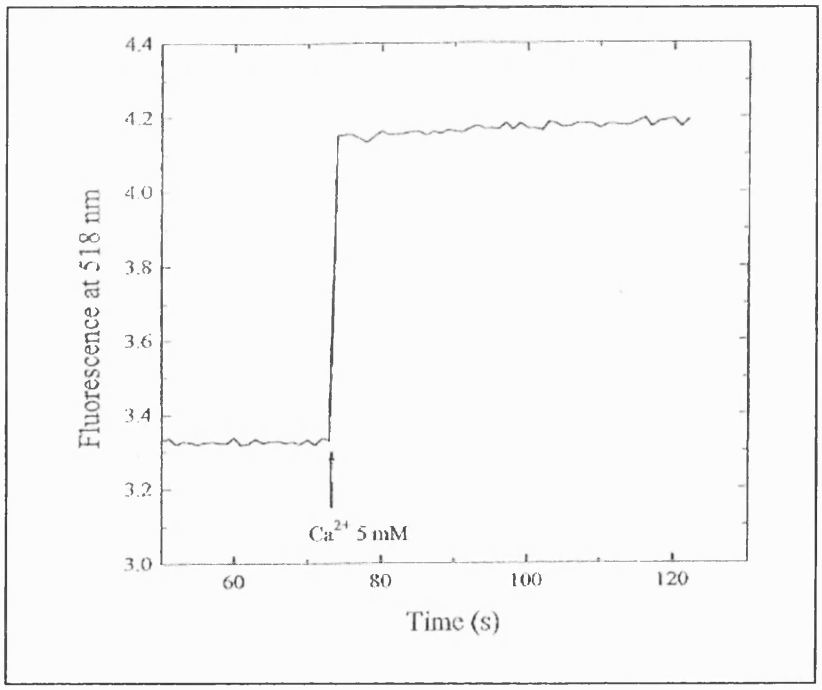

Figure 3.22. The introduction of Calcium ions [5 mM] to phospholipid vesicles, which have been labelled with FPE, caused a fluorescence change due to the ionisation of fluorescein. Total lipid concentration was typically 200 μM. The liposomes had a diameter of approximately 100 nm after preparation. Fluorescence measurements were made using an SLM-Aminco model spectrofluorometer. Excitation and emission wavelengths were set at 490 nm and 518 nm, respectively. This Ca^{2+} profile acted as a diagnostic tool. All experiments were carried out at room temperature.

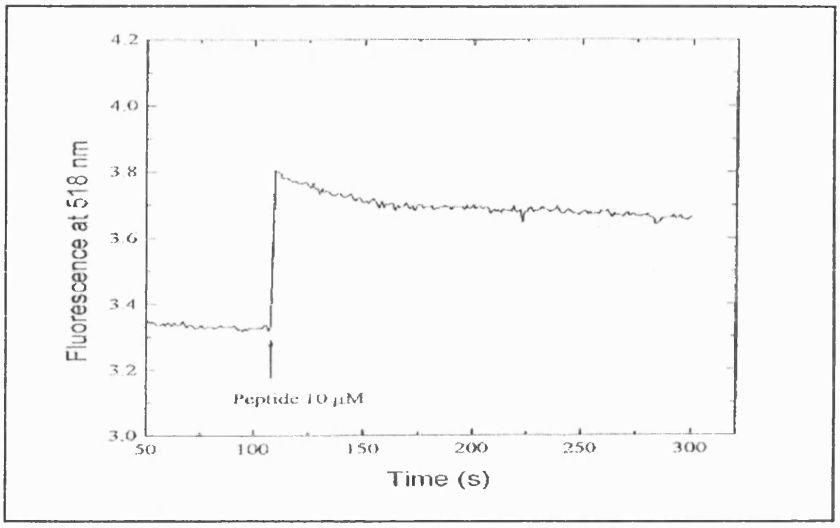

Figure 3.23. Typical fluorescence changes after introduction of penetratin to FPE-labelled phosphatidylcholine vesicles. Lipid concentration was 200 μM and the sample volume was 2 ml. Fluorescence measurements were made on an SLM-Aminco spectronic instrument: 500 V, Excitation λ = 495 nm, Emission λ = 518 nm.

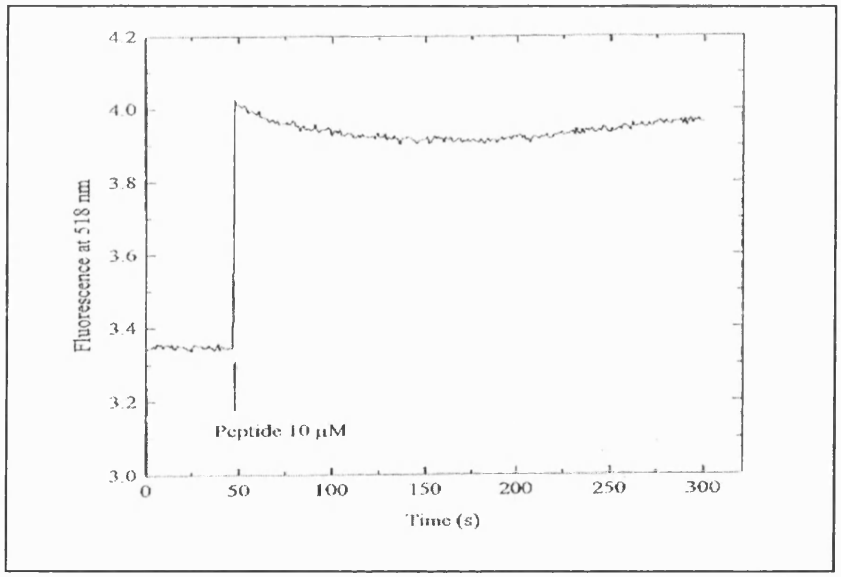

Figure 3.24. Time course of the interaction of mutant penetratin with 100 nm diameter phospholipid vesicles as revealed by fluorescence of FPE-labelled membranes. Fluorescence measurements were made under similar experimental conditions as in figure 3.23. Experiments were performed at room temperature.

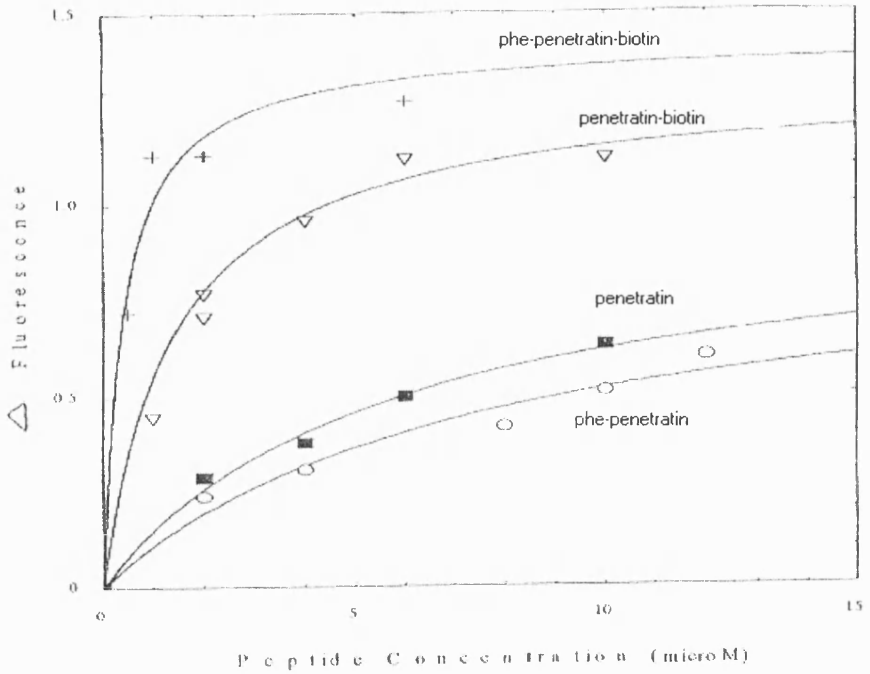

Figure 3.25. FPE measurements: The lipid concentration was 200 μM. FPE-phospholipid vesicles were subjected to various concentration of peptide with a single excitation wavelength of 490 nm and emitted light recorded at 520 nm. The relative magnitude of the initial change in fluorescence was plotted against concentration of peptide to produce an adsorption isotherm for each peptide. The fluorescence changes were measured against increasing peptide concentrations.

The equation used to fit the data is as follows: $y = (a\,x)/(b + x)$

Table 3.2 below shows the corresponding a and b values for each peptide.

Peptide	a	σ_a	b	σ_b
Penetratin	0.945	0.100	5.250	1.200
Phe-penetratin (mutant)	0.879	0.162	6.940	2.790
Penetratin-biotin	1.310	0.060	1.370	0.269
Phe-penetratin-biotin (mutant)	1.420	0.067	0.405	0.098

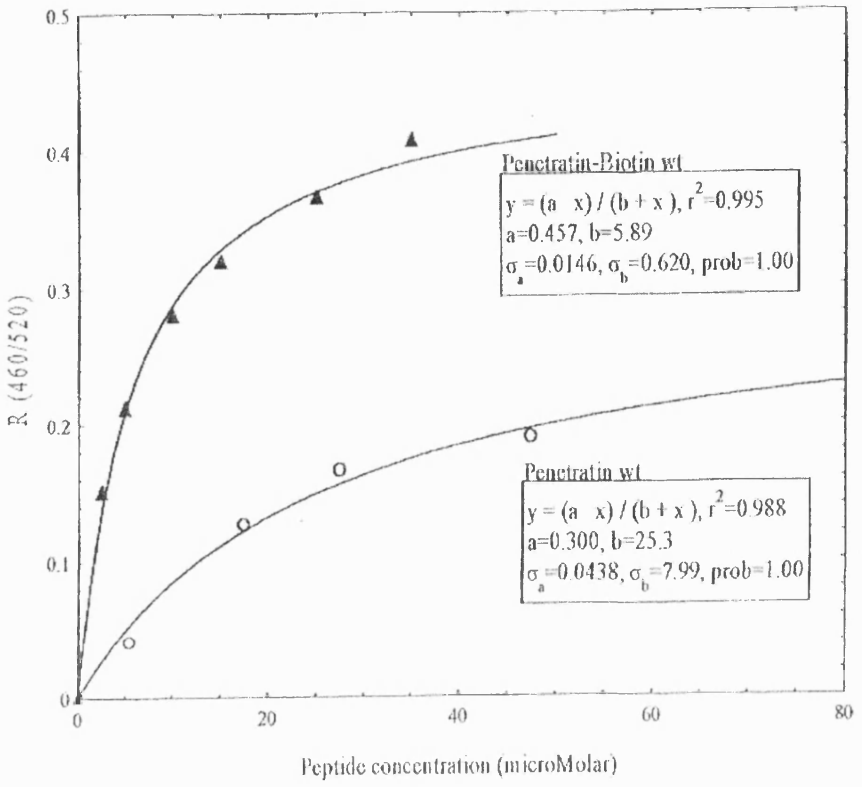

Figure 3.26. Di-8-ANEPPS measurements: Phospholipid vesicles labelled with di-8-ANEPPS were subjected to fluorescence investigation with a stopped-flow spectrophotometer. The plot shows the effect of peptide concentration on the fluorescence signal amplitude following normalization by background subtraction. Lipid concentration was 200 μM. Increasing volumes of peptide were added to the suspensions containing the vesicles to achieve the desired final concentration.

The data obtained from the measurement of R (460/520) in the di-8-ANEPPS measurements and the fluorescence at 518 nm for the FPE measurements, as a function of peptide concentration was fitted to a hyperbolic function equivalent to those which describe the single site binding model curves;

$$R = \text{capacity}.[\text{peptide}]/(Kd + [\text{peptide}])$$

Where Kd is the dissociation constant and the capacity corresponds to the maximum value of R.

From both graphs, the equation of each curve is given by:

$$Y = (a\ x)/(b + x)$$

where a = capacity, a value which is proportional to the number of binding sites and b = Kd, the dissociation constant for the binding process, a measure of the affinity of the peptide for the membrane. The smaller the constant, the higher the affinity. Sigma values that accompany each parameter in the graphs represent the standard error for each parameter.

3.4 DISCUSSION

3.4.1 Fluorescent labelling of peptides

Although fluorescein isothiocyanate (FITC) remains one of the most popular fluorescent labelling reagents, the green fluorescent BODIPY FL CASE, was first choice as a fluorescent label in this study for a number of reasons. Some of the characteristics BODIPY displayed that made it potentially superior to fluorescein include:

- A higher fluorescent intensity per dye molecule.
- Insensitivity to solvent polarity and pH. It was important that no quenching of fluorescence occurred once the label was within the intracellular environment.
- Labelling with BODIPY should not adversely affect the properties of the molecule in question since it is not a charged fluophore.
- Greater photostability.

BODIPY FL was purchased as a succinimidyl ester of BODIPY FL cysteic acid. Succinimidyl esters form amide bonds, with free amine groups. The fluorescence spectra obtained after linking BODIPY to the peptide indicated that there was a detrimental effect on the fluorescence intensity of BODIPY. A significant shift in the excitation wavelength occurred as well, which indicated a chemical change after coupling. This problem was probably due to the cleaving conditions, which were required to deprotect and detach the peptide from the resin. It was desirable to conjugate the fluophore to the N-terminus of a resin-bound peptide before the removal of other protecting groups and release of the peptide from the resin. This removed any ambiguity about the position of the coupling, which could only occur at the N-terminus. The cleavage mixture always required the presence of trifluoroacetic acid (TFA) 95%, a reagent used for the deprotection of peptides, which are synthesized using fmoc chemistry, creating relatively harsh conditions, which were assumed to cause the breakdown of BODIPY. This hypothesis was supported by the electrospray mass spectrometry results for the labelled peptides, which indicated the loss of chemical groups equivalent to the breakdown of the

chromophore structure of BODIPY. Appendix A shows electrospray mass spectrometry results for the peptides alone confirming their high level of purity. Unfortunately the electrospray mass spectrometry result for BODIPY coupled to peptide indicated a loss of mass. It seems certain that some degradation occurred judging from the fluorescence spectrum of BODIPY-peptide.

The labelling problems encountered with BODIPY encouraged the introduction of ADMP as an alternative fluophore. ADMP is a coumarin-based amino acid derivative. The coumarin itself is not fluorescent but the addition of various electron-donating substituents on the molecule results in increased fluorescence intensity. The advantages of using ADMP include its relatively similar structure and size with amino acids (MW = 264). This fluophore has been used to label peptides in experiments aimed at determining how the structures of peptides influence their alveolar permeability (Dodoo *et al.*, 2000). ADMP is relatively small compared with other fluorescent probes, being only slightly larger than tryptophan. ADMP also absorbs at longer wavelengths than the naturally occurring amino acids. More significantly, ADMP was found to be stable to repetitive treatment with TFA during peptide cleavage. The synthetic route of ADMP allowed the products of each stage of synthesis to be easily checked for yield and purity. Each stage had to be optimized to ensure that the final product was of a high yield and purity. The coupling of ADMP to a peptide did not have any detrimental effects on the structural stability of the peptide. The spectral properties of the labelled peptide were identical to the spectral properties of ADMP. The integrity of the fluophores were further confirmed by electrospray mass spectrometry data which yielded equivalent observed masses to the expected masses of the labelled peptides.

3.4.2 Peptide internalization and trafficking.

Confocal laser scanning microscopy confirmed that the internalization of penetratin led to its intracellular localization rather than a non-specific association with extracellular membranes. B16 cells generally have dendritic morphology. However, some of the cells appeared to be more rounded after the internalization experiments. This effect was seen clearly in images showing cells that had extended incubation with penetratin for up to

four hours. There are two possible explanations for this observation. Despite the versatility of B16 cells, the process of preparation for microscopy and incubation for as long as four hours may have caused them to change structurally leading to this rounded state. Also, the presence of these peptides may have induced cytotoxicity. Fawell *et al.*, 1994 reported that Tat conjugates showed some cytotoxicity when HeLa cells in culture were found to round up with incubation of these conjugates. During the four-hour incubation period, most of the fluorescence was cytoplasmic in distribution although only a few cells showed nuclei fluorescence. Cells incubated with penetratin showed very bright halos in the cytoplasmic regions and around the nuclear membranes of cells. This was more evident at four hours where fluorescence appeared as distinct rings around the nuclei and plasma membranes. In addition, the distribution of fluorescence in the cell images was of a punctate appearance. This was indicative of an endocytotic movement through the cell by the peptides. Other investigators have described this appearance, which is characteristic of endocytotic vesicles using confocal microscopy (Thierry and Dritschilo, 1992; Thierry *et al.*, 1997). Nuclear staining in cells incubated with penetratin did not appear as widespread as cytoplasmic staining. It is likely that a longer incubation period was needed to see more fluorescence in the nuclei as was reported by other groups including Zelphati *et al.*, 1999. The nucleoli were strongly stained in cells incubated with penetratin compared to control cells and cells incubated with the mutant penetratin. The confocal images presented here show cell sections that were incubated at 37°C. There was little or no fluorescence (background levels) when the peptides were incubated at 4°C. The fluorescence intensity of cell images was more widespread and brighter at 37°C. Similar findings were reported by Derossi *et al.*, 1994. At 4°C, most cellular metabolic processes shut down or take place at very slow rates. Hence, only binding tends to take place since diffusion occurs at a very low rate. The results demonstrate the importance of membrane fluidity and active metabolism in the cellular transport of penetratin.

Transmission electron microscopy was employed as a further confirmation of the mode of cell entry undertaken by penetratin and its derivatives. Similar controls were used in these experiments as those of confocal microscopy. In addition biotin-labelled transferrin was employed in TEM, as it is a well-known marker for receptor-mediated endocytosis

(Zabner *et al.*, 1995). In all the images taken of cells without peptide incubation, all the streptavidin gold particles observed always appeared on the surface of the cells (Figure 3.14). There were no gold particles seen inside any cell. A similar pattern was also observed with cells incubated with mutant penetratin, where all the gold particles remained on the cell surface at the end of the incubation time of four hours (Figure 3.16). There was a very obvious difference seen in cells incubated with biotin-labelled penetratin. Firstly, there was clear cell entry of penetratin-gold particles with a few seen also on the cell surface (Figure 3.17). It was possible to capture an image of particles on the cell surface being engulfed by cellular projections (Figure 3.17A). A significant observation was that penetratin-gold internalized particles were consistently found in vesicular structures in the cytoplasm of cells. This pattern of distribution was also observed in cells incubated with biotin-labelled transferrin-streptavidin gold particles (Figure 3.15) and was indicative of endocytosis taking place. These data contradict the suggestions for mechanism of internalization proposed by Derossi *et al.*, 1996. Although there appeared to be a small amount of fluorescence reaching the nucleus in the confocal images, it was not possible to see any peptide-gold particles in the nucleus of cells from TEM. It is thought that a longer incubation and a higher concentration of peptide may be necessary to observe nuclear uptake.

The images obtained from the ADMP-labelled conjugates clearly showed uptake of penetratin in a short time, 5 minutes (figure 3.19B, 3.20B and 3.21A). Then there was a gradual increase in intracellular trafficking between 5 minutes and three hours (figure 3.19A, 3.20A and 3.21B). Hence, penetratin does not appear to undergo instant intracellular trafficking. This is consistent with the data obtained from confocal microscopy with the streptavidin fluorescein and biotinylated peptides.

3.4.3 Peptide-membrane interaction

It is of significant interest to gain an understanding of some of the factors, which predispose the interactions of peptides with membranes. Previous studies investigating the ability of these translocating peptides to bind to membranes have involved the conjugation of a chromophoric indicator to the peptides or the synthesis of radio

derivatives (Rapaport and Shai, 1994; Shai, 1995). The localization of fluoresceinphosphatidylethanolamine (FPE) at the membrane surface can present the possibility of measuring in real time, the interactions of peptides with membranes in a sensitive and virtually non-invasive manner (Wall *et al.*, 1995). This technique relies on the fact that most peptides possess a net charge and, as the charged peptide comes into contact with the membrane surface, it interferes with the electrostatic potential of the membrane surface. By locating a fluophore, which is sensitive to the membrane surface potential precisely at the membrane-solution interface, it is possible to monitor the binding and insertion of the peptide into the membrane to very high sensitivity and in real time. Figure 3.23 and 3.24 represented typical patterns of fluorescence changes: an increase in fluorescence followed by a gradual decrease in fluorescence. The change in fluorescence may be positive or negative depending on the resulting change in the microenvironment at the surface of the membrane. The initial rapid phase which leads to an increase in fluorescence intensity is consistent with the addition of positive charge to the membrane surface. This phase has been previously established as the binding of the peptide to the membrane surface (Golding *et al.*, 1996). The much slower decay of the fluorescence intensity indicates loss or removal of positive charge from the membrane surface and represents peptide insertion of its charged parts into the interior of the membrane. Once immersed in the hydrophobic core of the membrane, these charges are effectively insulated from the electrical double layer of the membrane surface and do not further influence the protonation state of FPE or the surface potential upon which the latter depends. This phase could also indicate a change in the conformational state of the peptide. The fluorescence changes with mutant penetratin (reported not to undergo internalization) showed a quick recovery in fluorescence around the insertion phase compared to penetratin, which displays a gradual decrease in fluorescence. The significance of these findings is such that mutant penetratin binds very quickly to the membrane surface but undergoes little or no insertion probably due to its amino acid mutations. This in turn implies the importance of tryptophan in the penetratin sequence, which is crucial in the internalization process of penetratin.

The FPE and di-8-ANEPPS measurements (figure 3.25 and 3.26 respectively) both indicate that biotin-penetratin binds to the membrane with a higher affinity than

penetratin. The FPE results show the binding of all the penetratin peptides tested (native, mutant and biotinylated of both) bind to the membrane surface. There is no great difference between the binding of the native sequence and that of mutant penetratin, whereas biotinylated penetratin peptides enhance the binding clearly in terms of affinity.
The Di-8-ANEPPS dye measures changes in the "dipole potential", originated by molecular dipoles present mainly at the water-membrane interface, such as the dipole of the carbonyl group of the ester bond from the phospholipid headgroup. This potential is different from the surface potential and is positive towards the interior of the membrane. The results show that only the native sequence (biotin-labelled and unlabelled) causes a variation of the dipole potential. This implies that the wild type causes a higher perturbation of the membrane than the mutant sequence, which appears to only mostly bind. The higher disturbance caused by native penetratin suggests insertion of the peptide into the membrane.

3.5 SUMMARY

The use of BODIPY FL as a fluorescent probe proved problematic due to its big size and unstable characteristic. ADMP provided an alternative, which was found to reduce interference caused by bulky and unstable fluophores.
The uptake and intracellular movement of penetratin and its mutant version was investigated using electron and confocal microscopy. Both techniques exhibit data to confirm that penetratin peptides were taken up into B16 cells by endocytosis as seen clearly by the presence of gold particles engulfed by vesicular cell structures as well as the punctate cytoplasmic distribution of fluorescence. The mutant penetratin showed some entry into B16 cells, which was not as intense as penetratin.
The peptide membrane measurements only indicate that the peptides bind to the membrane, that is, a clear interaction between charged peptides and the lipid membranes. The fluorescence variation as a function of peptide concentration gave an accurate measure of the affinity these peptides have for the membranes but does not exhibit information as to whether the membrane is being penetrated.

CHAPTER 4

INTERCELLULAR SPREAD OF VP22 IN ANIMAL TISSUE.

4.1 INTRODUCTION

The introduction of nucleic acids, peptides/proteins, and small molecules into the appropriate target cells and tissues is being developed as a therapeutic approach to a range of diseases. Currently, the potential uses of biotherapeutic agents are compromised by problems of achieving intracellular delivery *in vivo*. It has been previously reported VP22 exhibits the unusual property of transport between cells (Elliott and O'Hare, 1997). Transport was observed after introduction of the VP22 gene by several routes, including transfection or microinjection of the isolated gene in plasmid constructs or by infection with a non-replicating herpesvirus encoding the native VP22 gene. One of the features of transport was that in cells actively synthesizing the protein, VP22 was located predominantly in the cytoplasm, where it could be observed in filamentous arrays colocalizing with bundled microtubules (Elliott and O'Hare, 1998), while in the surrounding cells, VP22 was observed mainly in the nucleus, where it could also be observed colocalizing with chromatin in mitotic cells. A short C-terminal deletion mutant of VP22 lacking 34 residues was expressed normally and exhibited unaltered cytoplasmic localization in the primary cells expressing VP22 but failed to spread to surrounding cells (Brewis *et al.*, 2000).

This chapter investigates the ability of VP22 to spread out into many cells in cell culture and animal tissues, namely muscle and tumour.

4.2 MATERIALS AND METHODS

4.2.1 Plasmid constructs

The reporter plasmids used during the course of the animal work were pRSVlacZ and pVP22. The pRSVlacZ is a 7.8 kb plasmid where the E.coli lacZ gene is under the transcriptional control of the Rous sarcoma virus (RSV) promoter/enhancer sequence. The pVP22 (kindly provided by Jeff Drew, Marie Curie Institute) incorporated two expression cassettes, one for the lacZ gene and the other for VP22. The plasmid maps for both plasmids may be found in appendix D.

4.2.2 Preparation of plasmid DNA/PEI complexes for *in vitro* studies

The concentration of DNA was monitored using the absorbance of DNA at 260 nm. PEI was used at an optimum and suboptimal N/P ratio (+/- 9.0 and +/- 3.0 respectively) as necessary. Appropriate mixtures of PEI were prepared prior to DNA complexation and diluted to a final volume of 250 μl with Hepes buffered saline (HBS). 3 μg of both plasmids was diluted to a volume of 250 μl with HBS. In each case the PEI solution was added to the DNA solution and immediately mixed by vortexing. The mixture was left to incubate for 20 minutes prior to addition to the cells. Transfection was carried out in the presence of serum-free media for four hours at 37°C after which time the transfection medium was replaced with fresh complete culture medium and cells were cultured for a further 48 hours before harvesting, fixed and stained for immunohistochemical analysis.

4.2.3 Formulation of DNA for animal studies

Following extraction and purification of DNA, the quantification revealed on a number of occasions a DNA concentration too dilute for use for animal studies. The required concentration of DNA for injection is usually 50 μg in 20 μl or 2.5 mg/ml. However, the volume injected also had to be isotonic and therefore a DNA concentration closer to 3 mg/ml was required to allow a small amount of dilution with NaCl. Since a minimum

volume of Milli-Q water must be added to the pelleted DNA to achieve complete dissolution, a poor DNA yield from the maxi kit will result in a DNA solution not sufficiently concentrated.

4.2.4 Animal administrations

Animal experiments were conducted under the supervision of Dr Pauline Wood, the Home Office license holder. Female C3H mice were obtained from Charles River at 6-7 weeks age and then allowed to acclimatize for a further two weeks prior to experiments. Before implanting murine fibrosarcoma RIF-1 cells (Twentyman *et al.*, 1980) the fur from the lower half of the mouse back was removed using clippers. The RIF-1 cells were previously cultured in RPMI 1640 (Roswell Park Memorial Institute) medium supplemented with 15% foetal calf serum, penicillin and streptomycin, and were not passaged more than 7 times prior to trypsinization for implantation. RIF-1 cells were injected intradermally mid way along the back of the mouse. To obtain an acceptable tumour implant care was taken to ensure that the cell suspension left a spherical bump at the implant site, devoid of any tracks caused by the leakage of cell suspension on needle removal. Tumours were visible after approximately seven days and were ready for gene delivery experiments 12-14 days post-implantation. One day before treatment with DNA the mice were weighed and the dimensions of the tumour recorded. The average tumour was approximately 6-9 mm in diameter and 270 mg in weight.

The intramuscular injections were made into the right hind leg of each mouse. The expression levels resulting from the two different tissues could then be directly compared. These intramuscular injections were carried out five days before intratumoural injections, so that tumour dosing occurred on day five of a typical experiment. Tissues were harvested following the killing (cervical dislocation) of the mice on day seven. To facilitate intramuscular injection the mice were anaesthetized using a combination of Hypnovel (midazolam 5 mg/ml) and Hypnorm (1 ml of Hypnovel + 1 ml of Hypnorm + 2 ml sterile water, inject 0.1 ml intraperitoneally) and the right thigh shaved with an electric shaver. Muscle injections were made using a sterile Hamilton syringe fitted with a 31 G, ½ inch needle and calibrated dosing clamp. This

clamp insured that each mouse was injected with 20 µl of formulation. The needle was left in place for a few seconds to prevent formulation being expelled by the tissue. The same procedure was carried out for the dosing of the implanted tumour five days later but without anaesthetizing the mice prior to injection. Each 20 µl injection contained 35 µg of DNA alone.

4.2.5 Tissue preparation and immunohistochemical analysis

Muscle and tumour specimens were frozen to cork blocks in Tissue-Tek mounting medium (Miles, Elkhart, Indiana) by immersion in liquid nitrogen-cooled isopentane. Four-µm sections were then cut in a Bright OTF/AS-001 motorized cryostat (Bright, Huntingdon, UK). Sections were mounted on glass slides before air-drying at room temperature for one hour. The staining procedure for frozen sections was then followed. Sections were fixed with acetone after which the slides were transferred into PBS buffer for 5 minutes. Sections were incubated for 20 minutes with diluted normal horse serum and then incubated for one hour in primary antibody in 0.05% w/v BSA at room temperature. The two primary antibodies used were monoclonal anti-β-galactosidase (SigmaAldrich) and polyclonal anti-VP22 (kindly donated by O'Hare at the Marie Curie Institute). Slides were washed for 5 minutes in PBS buffer. Sections were then incubated with biotinylated horse anti-mouse solution for 30 minutes, rinsed five times with PBS, and then incubated for 30 minutes with VECTASTAIN® ABC reagent (horseradish peroxidase-conjugated ABC). Sections were again washed in PBS and then developed using either diaminobenzidine (DAB) or fast-red (SigmaAldrich), until desired stain intensity develops. Both are substrate solutions for DAB (horseradish peroxidase) and fast-red (alkaline phosphatase) respectively. Sections are then rinsed in tap water and counterstained with haematoxylin and mounted.

4.3 RESULTS

4.3.1 Transfection of B16 cells *in vitro* using pRSVlacZ and pVP22

In vitro transfection was performed with complexes of plasmid DNA (2 μg per well) and PEI at two different N/P ratios. Expression levels following a two-day transfection period were evaluated using immunohistochemistry.

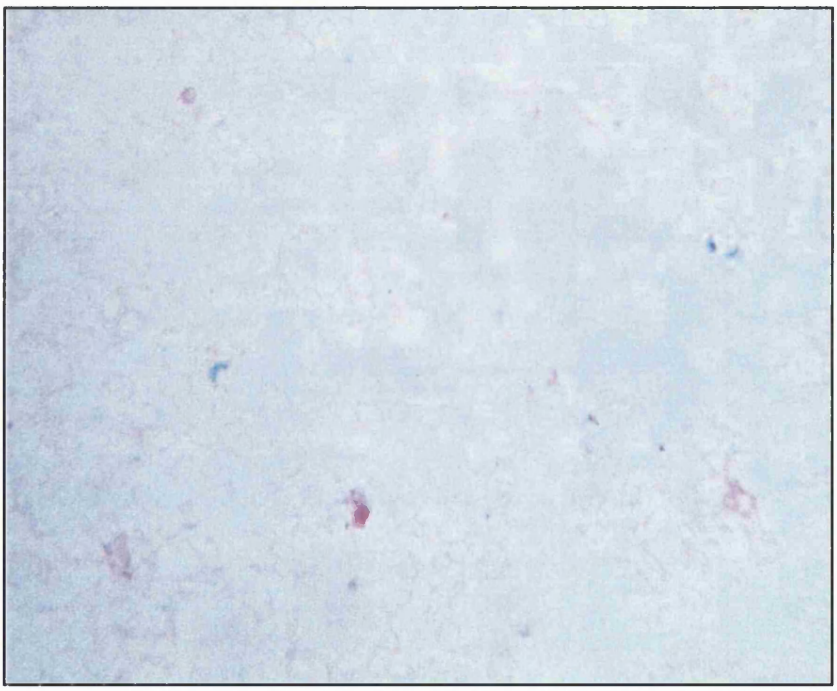

Figure 4.1. B16 cells were not transfected with expression vectors. Post transfection, the cells were fixed with 100% ethanol and stained with the monoclonal antibody to β-galactosidase using Sigma fast-red to develop staining for alkaline phosphatase. When the degree of staining intensity was reached, the reaction was terminated by washing in distilled water.

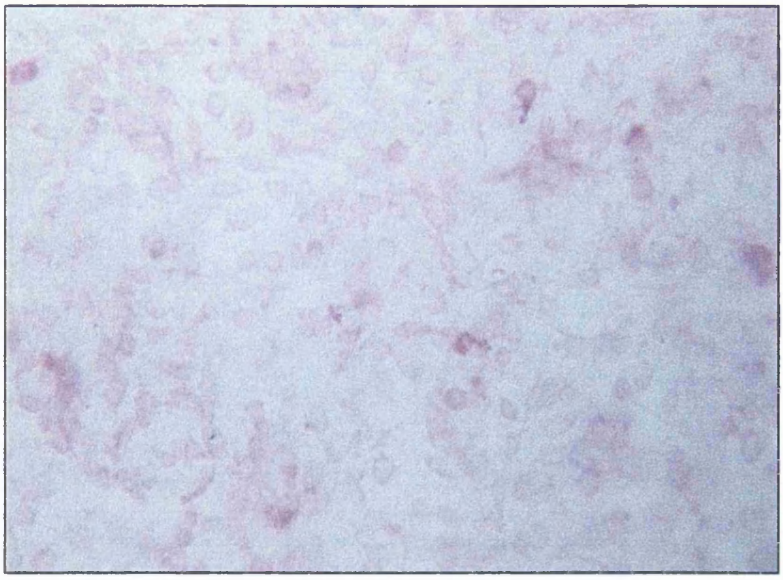

Figure 4.2. B16 cells were transfected with a complex of pRSVLacZ and PEI (N/P = 3.0). Forty-eight hours after transfection, the cells were fixed and processed for detection of β-galactosidase expression. A x40 objective was used for examination.

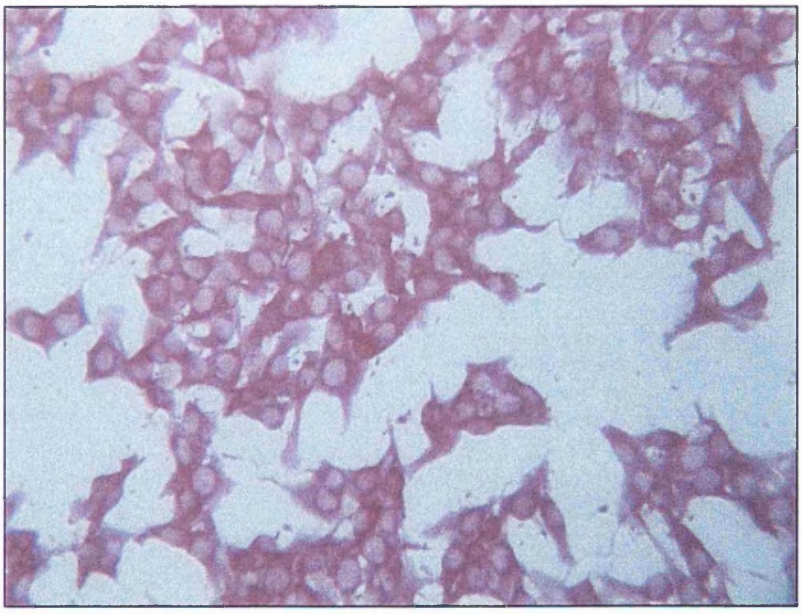

Figure 4.3. B16 cells were transfected with a complex of pRSVLacZ and PEI (N/P = 9.0). Cells were processed for β-galactosidase expression 48 hours post transfection. A x40 objective was used for examination.

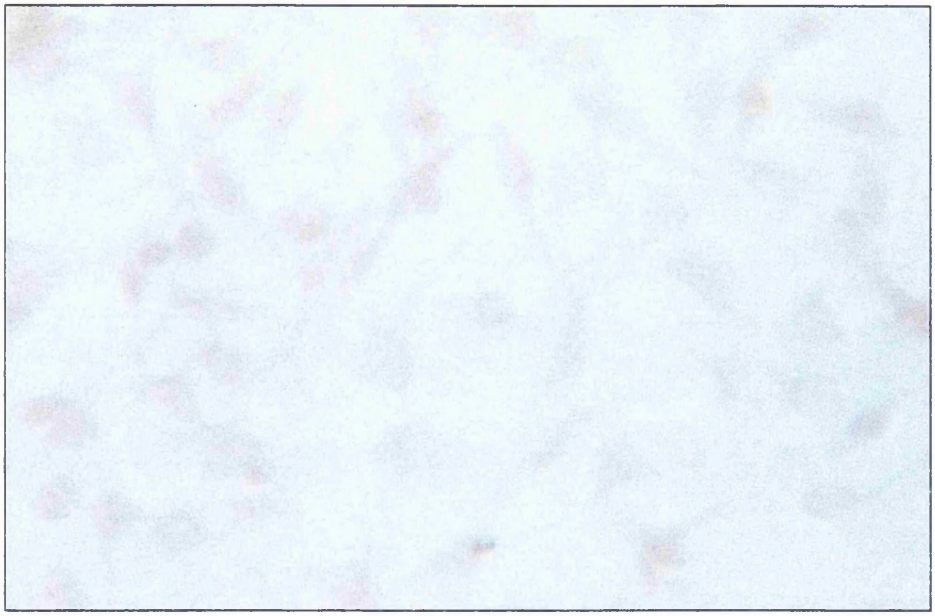

Figure 4.4. Untransfected B16 cells were fixed and processed for detection of pVP22 expression using DAB to develop staining for peroxidase, hence the brown colour.

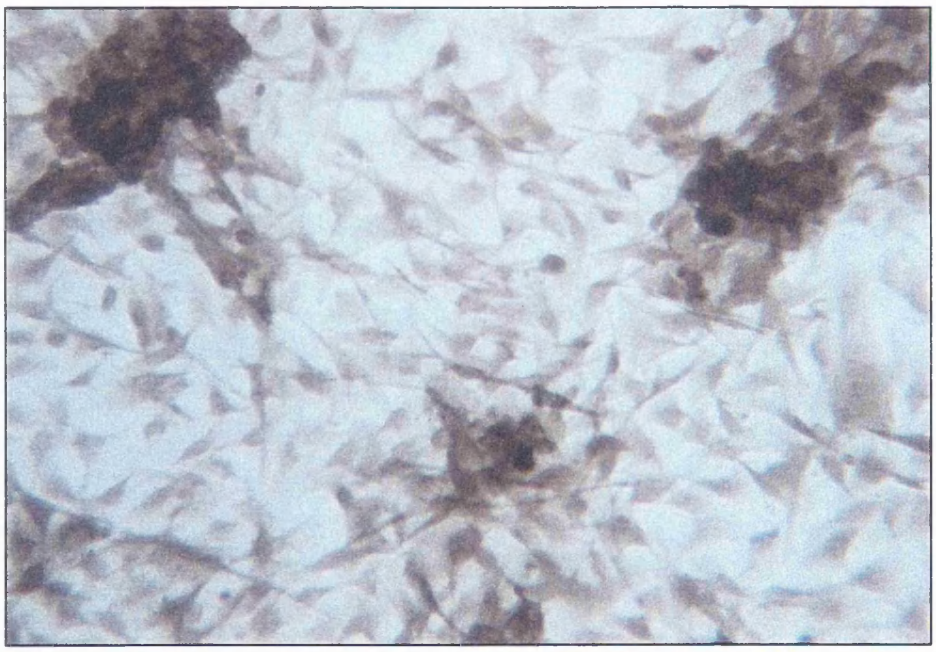

Figure 4.5. B16 cells transfected with PEI (N/P = 3.0) and pVP22 were fixed after 48 hours, and immunofluorescence carried out with a rabbit anti-VP22 polyclonal antibody. A x63 objective was used for examination.

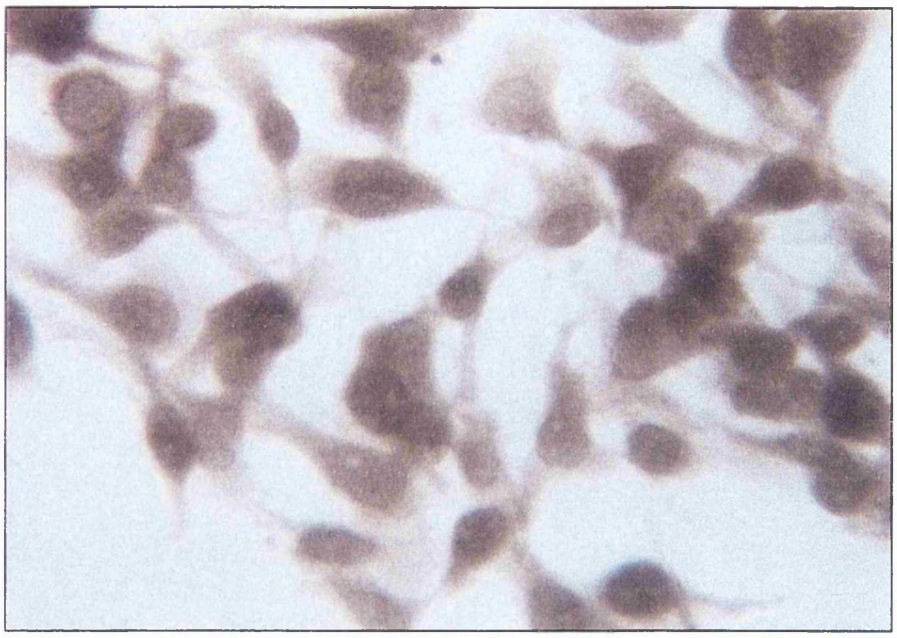

Figure 4.6. Plasmid expressing VP22 was transfected with PEI (N/P = 9.0), into B16 cells and 48 hours after transfection, the cells were fixed with 100% ethanol. Transfected monolayers were subsequently stained with a rabbit anti-VP22 polyclonal antibody. For horseradish peroxidase, cells were incubated with diaminobenzidine (Sigma) according to the manufacturer's instructions. When the desired degree of staining intensity was reached, the reaction was terminated by washing in distilled water. A x40 objective was used for examination.

Untransfected cells were used as suitable controls for visualisation of expression levels using immunofluorescence. Expression was detected in all transfected cells. Expression levels of both β-galactosidase and VP22 were estimated at only 50% in cell monolayers transfected with sub-optimal doses of PEI, but were almost doubled in cells transfected with optimal PEI doses.

4.3.2 Introduction of pRSVlacZ and pVP22 *in vivo*

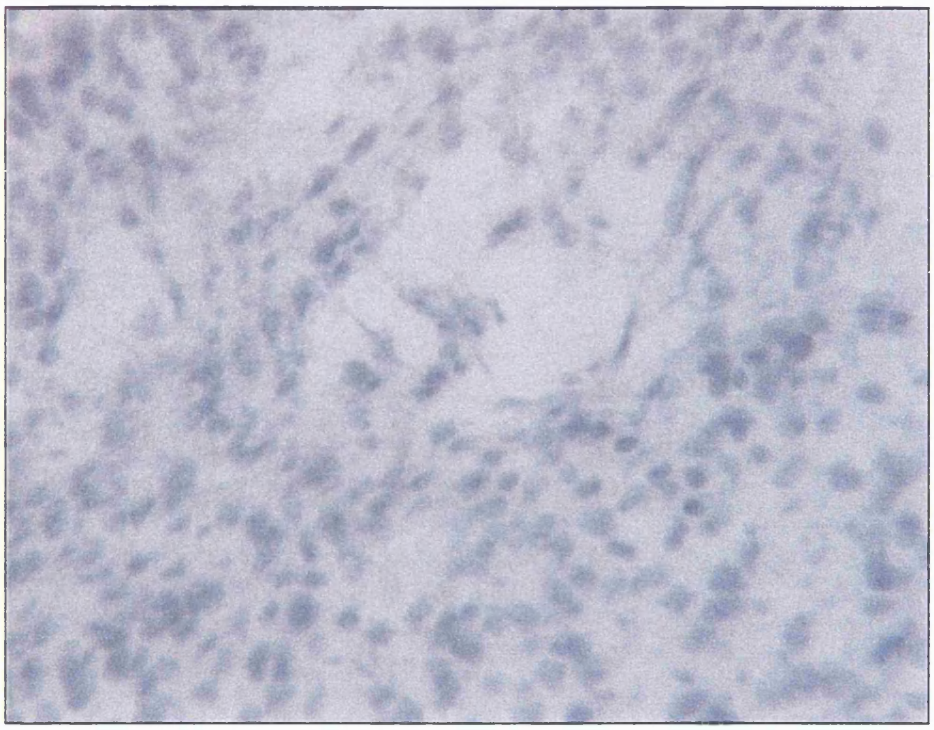

Figure 4.7. Histochemical staining of tumour tissue with X-gal. A section of mouse tumour tissue was fixed in 4% paraformaldehyde, washed three times in PBS and then developed for 36 hours in X-gal.

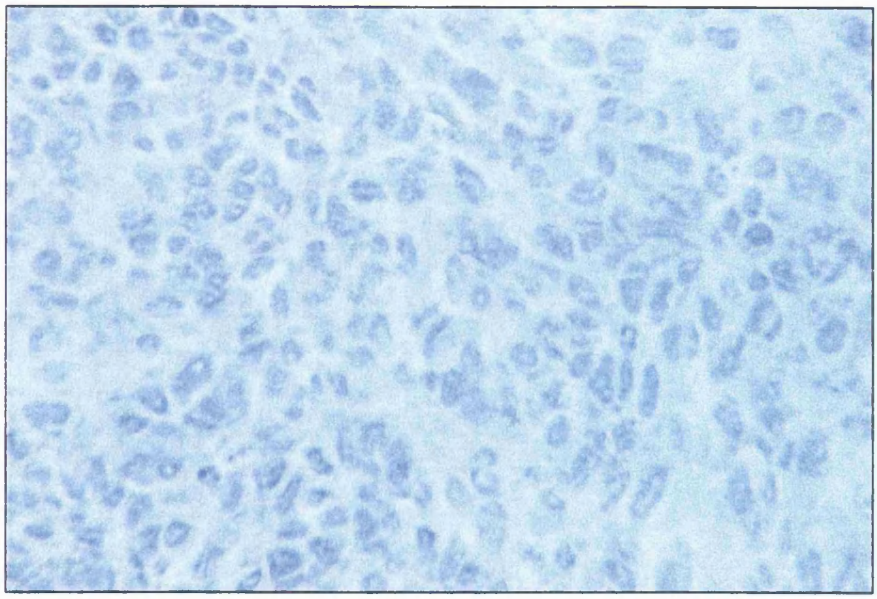

Figure 4.8. Uninjected tumour tissue fixed with acetone and stained with haematoxylin and eosin (H&E).

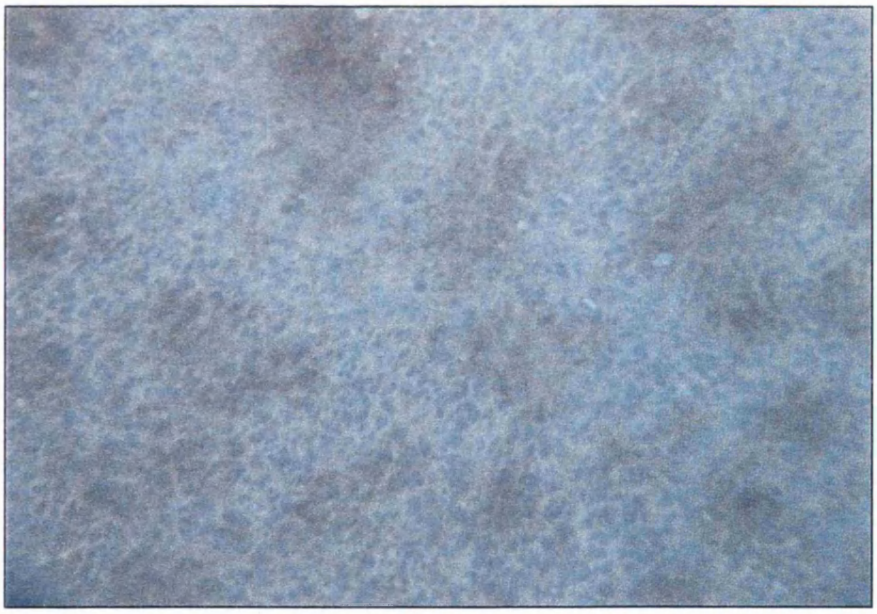

Figure 4.9. Mouse tumour tissue fixed with acetone and subsequently stained with a rabbit anti-VP22 polyclonal antibody. Expression of pVP22 was detected using DAB to develop staining for horseradish peroxidase followed by H&E stain.

4.4 DISCUSSION

Elliott *et al.*, 1997 observed transport of VP22 between cells after introduction of the gene by several routes including transfection or microinjection of the isolated gene in plasmid constructs.

The aim of this study was to detect the distribution of VP22 *in vivo* using immunohistochemistry techniques. Initially, i*n vitro* testing of the VP22 and β-gal plasmids was performed using B16 cells to confirm that the method of detection worked. Transport of VP22 has not been found to be restricted to distinct cell types or species. Wybranietz *et al.*, 1999 reported the spread of VP22 in fifteen commonly used mammalian cell lines. In addition, the use of primary and secondary antibodies provided high levels of detection in B16 cell line defining the proportion of cells containing VP22 or β-gal following transfection. This observation was also recognized in experiments carried out by other groups such as Fang *et al.*, 1998 and Elliott and O'Hare, 1999. These groups demonstrated significant increases in the sensitivity of detecting spread of VP22 fusion proteins with the use of antibodies although Fang *et al.*, 1998 did not observe the dramatic increase in the intercellular trafficking of a VP22 fusion protein in transfection experiments. This was explained by differences in the methods of fixation leading to different concentration effects and/or removal of interfering or quenching components. Brewis *et al.*, 2000 found evidence to suggest that the use of paraformaldehyde for fixing cells resulted in the significant quenching of fluorescence in recipient cells although this was partially but incompletely restored on rehydration with PBS. The distribution of VP22 in B16 cells appeared as foci of VP22-containing cells as evidenced by the brown clusters surrounded by patches of blue cells (Figure 4.5). A similar pattern of distribution was also seen in the mouse tumour tissue (Figure 4.9). The brown clusters represent intensely stained cells with a largely cytoplasmic distribution and some nuclear staining surrounded by less intensely stained cells. This pattern was observed in all the batches of tumour tissues injected with the VP22 vector. Apart from this pattern observed in tumour tissue sections, the distribution of VP22 was not detected in mouse muscle tissue. One explanation might be the fact that only a very small proportion of muscle tissue was transfected. Hence, it is possible that this area of

transfected tissue was missed during sectioning and processing of the tissue for staining. Work done by Davies *et al.*, 1993 using plasmid DNA for direct gene transfer into mouse muscle reported only 1-2% of muscle was transfected and these areas was restricted to the injection site. Similar findings were reported by Winegar *et al.*, 1996 with an intramuscular plasmid vaccine. In addition, conditions optimal for the tumour cells may be different from those for the muscle cells. Compared to muscle cells, tumour cells divide rapidly implying expression is more likely in tumour cells. The VP22 expression protein may have a more stable half-life than β-gal as well as the fact that β-gal is located intracellularly (and not secreted) as opposed to VP22, which is distributed intercellularly. Hence, VP22 may be easier to detect.

Detection of β-galactosidase was attempted by histochemical staining with X-gal. Unfortunately, little or no expression of β-gal was observed in any of the tumour and muscle tissue sections except tumour tissue which had VP22 injected into it (Figure 4.7). The presence of blue parts of the tissue sections as seen in figure 4.7, is indicative of background staining, which becomes blue after prolonged incubation with X-gal. X-gal incubations for as long as 36 hours resulted in this blue wash, suggesting that the tissue expressed relatively small amounts of the gene or more likely this implies a low level of non-specific activity. The lack of β-gal expression can possibly be due to the lack of plasmid stability within the tissue. However, considering that the half-life of β-galactosidase is eight hours, it is unlikely that protein instability within the tissue is the cause. Also, since muscle cells are nondividing compared to tumour cells, one would expect more plasmid persistence in the muscle. Wolff *et al.*, 1992 made this observation during experiments to study expression in mouse muscle. The expression of pRSVluc reporter gene was sustained for 19 months.

A more likely explanation for a lack of performance of both VP22 and β-gal plasmids *in vivo* is the fact that since only 30 μg of plasmid DNA was injected into the tissue, the chances of detecting gene expression would be overall very low. Although, the decision to use 30 μg of plasmid arose from low yields constantly achieved during plasmid preparations as well as cost and time available, it was expected that this dose of DNA would be sufficient to detect expression. Yang and Huang, 1996 carried out intratumour injections with 30 μg of free DNA and reported protein expression levels (1.9 ng of

protein) as high as those expressed in skeletal muscle observed by Wolff *et al.*, 1990. Lack of *in vivo* expression may also be caused by differences in the plasmid promoter component as well as slow DNA transport. Luby-Phelps *et al.*, 1987 found that cytoplasmic diffusion of macromolecules is slow. For instance, a molecule of molecular weight 500000 would take an approximate time of 4 days to diffuse 1 mm. Also, intramuscular injection through the skin without observation of the exact injection site may result in administration to non-muscle tissue such as adipose or other muscle groups. Insufficient penetration of the needle may also yield poor distribution as well as localizing the injected DNA mainly in the interfascicular muscle space. Occasionally, some sample got lost during the injection procedure.

Another possibility is that the relatively small injection volume of 20 µl used in these experiments may not achieve high enough expression. Davies *et al.*, 1993 observed less variability and higher gene expression in muscle tissue when they injected a larger volume of plasmid DNA. Yang *et al.*, 1996 confirmed that gene expression in BL6 tumour was almost four-fold higher with 100 µl of injection volume compared with 10 µl of injection volume, although the former resulted in tissue toxicity. A higher injection volume would spread the injected DNA to a wider area at the injection site, achieving a greater number of transfected cells. In addition, it was found that there was poor diffusion of complexes within the tumour mass post injection with a syringe. Hence, the mode of delivery may require modifications to incorporate a micropump, which would enable slow injection. Cells *in vivo* can be considered to be in a quiescent state, entry of DNA into cell nuclei becomes problematic since cell division aids uptake of DNA as is evident from *in vitro* transfection data.

4.5 SUMMARY

This study attempted to observe distribution of VP22 in animal muscle and tumour tissue. Although the spread of VP22 was observed only in tumour tissue sections, these data show the marked levels of experimental variability, which needs to be taken into account when interpreting *in vivo* studies. There was a lack of obvious β-galactosidase expression above background levels.

CHAPTER 5

RELATIVE MOBILITY OF MEMBRANE TRANSLOCATING PEPTIDES.

5.1 INTRODUCTION

Drug delivery to selected cells and tissues remains an area of active research. One potential way to improve the efficacy of gene therapy is to construct plasmids, which express fusions of therapeutic proteins with membrane translocating peptides (MTPs). Such fusion proteins may be able to translocate from transfected cells to other cells in the vicinity, producing a bystander effect, or generally improve the biodistribution of the gene product within the target tissue. The mechanism whereby these MTPs are able to target and to traverse lipid membranes currently remains unknown and though there are several putative MTPs in the literature it is difficult to assess which are the most promising for use in gene therapy. One published protein, the Drosophila pAntennapedia (pAntp) a homeotic transcription factor, has a cationic domain, which is known to include an MTP, (-RQIKIWFQNRRMKWKK-). This MTP is able to carry linear polypeptides across biological membranes, though the limits to the size of the payload have only been studied qualitatively.

This chapter investigates the generation of two fusion constructs with the enhanced green fluorescent protein (EGFP-N1), one consisting of the gene coding for the native pAntp MTP and the other carries a mutated version of pAntp MTP. These fusion constructs could show pAntp's ability to promote transfection in mammalian cells in culture and possibly protein transduction to other surrounding cells. The mutant version (-RQIKIFFQNRRMKFKK-, where two amino acid residues have been changed) may share this transduction ability but only to a smaller extent, interrupting the translocation functions of native pAntp.

5.2 MATERIALS AND METHODS

This work was done in collaboration with Dr Mick Arnott, a postdoc at the Department of Pharmacy, University of Bath.

5.2.1 Materials

The oligonucleotides required for the fusion constructs incorporated EcoR1 sites at the 5' end and BamH1 sites at the 3' end, both of which were digested. The oligonucleotides were ordered from Sigma Genosys on a 3 OD scale and were phosphorylated before use.

Native pAntp MTP Sense Primer

5'AATTCATgCgCCAgAATAAAgATTTggTTCCAgAATCggCgCATgAAgTggAAgA
Agggg 3'

Native pAntp MTP Antisense Primer

5'gATCCCCCTTCTTCCACTTCATgCgCCgATTCTggAACCAAATCTTTATCTggCg
CATg 3'

Mutant pAntp Sense Primer

5'AATTCATgCgCCAgATAAAgATTTTCTTCCAgAATCggCgCATgAAgTTCAAgAA
gggg 3'

Mutant pAntp Antisense Primer

5'gATCCCCCTTCTTgAACTTCATgCgCCgATTCTggAAgAAAATCTTTATCTggCg
CATg 3'

5.2.2 Phosphorylation and annealing of oligonucleotides

To achieve optimal cloning efficiency the oligonucleotides were phosphorylated using the following reaction mix:

137 pmoles oligo		1 µl
ATP, 0.1 mM (Boehringer)		1 µl
T4 Polynucleotide Kinase (10 U/µl, Promega)		1.5 µl
Kinase 10x buffer		4 µl
Nuclease free water	up to	50 µl

The kinase reaction was incubated at 37°C for one hour and heat inactivated by boiling at 100°C for two minutes. The reaction was allowed to cool slowly to room temperature. To anneal the oilgonucleotides together, the wild type sense and antisense primers were mixed together in a microcentrifuge tube while the mutant sense and antisense primers were also mixed in a separate reaction. Both reactions were carried out in the presence of 10 mM Tris-HCl, 10 mM $MgCl_2$, 50 mM NaCl, 1 mM EDTA, at pH 7.9 and left at 95°C for 2 minutes. The oligonucleotide mix was allowed to cool to room temperature gradually overnight. To confirm that the annealing occurred a 15% acrylamide gel was set up.

5.2.3 Preparation of the cloning vector pEGFP-N1

A large-scale digest of pEGFP-N1 with EcoR1 and BamH1 was performed overnight at 37°C to ensure optimum digestion of the vector. The vector was digested sequentially with EcoR1 and BamH1 restriction enzymes, and then run on a 1% agarose minigel. The single band was excised from the gel and purified.

5.2.4 Ligation

The following ligation reaction mixture was used:

Vector pEGFP-N1 (digested with BamH1 and EcoR1)	1.3 µl
Wild type/Mutant annealed oligos	20 µl
10x ligation buffer	2.5 µl
Ligase	1 µl

Ligations were left for 2 hours at 37°C.

Dr. P. Jones carried out DNA sequencing at the automated sequencing facility at the University of Bath using d-Rhodamine terminator dye chemistry (labeled ddNTP's) and FS Taq polymerase (PE Applied Biosystems). The AB1377 DNA sequencer and cycle sequencer used were both from PE Applied Biosystems. The DNA samples for sequencing were supplied in PCR tubes containing 10 pmoles of primer, made up to final volumes of 6 µl with Milli-Q water.

5.2.5 Cell culture and transfection of cells

One cell line was employed in this study. B16 cells were routinely cultured as adherent monolayers in MEM as described in chapter 2. Complexes of pEGFP-N1 fusions with a sub-optimal dose of PEI (N/P = 4) were prepared 30 minutes prior to use. These complexes were then incubated with 3 µg DNA per well (in 0.5 ml Opti-MEM™) on B16 cells grown on coverslips in six-well plates, in the presence of 1.5 ml Opti-MEM™. After 4 hours, the transfection medium was removed and replaced with 2 ml growth medium.

5.2.6 Immunofluorescence analysis

Immunofluorescence analysis for transfected cells was performed. After 48 hours of transfection, cells were washed with PBS, fixed for 10 minutes at room temperature with

100% methanol. The samples were then blocked with 10% foetal calf serum in PBS for 15 minutes at room temperature. Rabbit anti-GFP polyclonal antibody was added to the same solution at a concentration of 1: 500, as recommended by the manufacturer (Insight Biotechnology Ltd). The samples were then incubated for 20 minutes, washed three times with PBS, and incubated for another 10 minutes with blocking solution containing an anti-rabbit IgG antibody labeled with Rhodamine red (Insight Biotechnology Ltd). Samples were then washed three times with PBS. The coverslips were mounted on slides using DABCO antibleaching agent. Fluorescence images were obtained with a Zeiss LSM-510 confocal laser-scanning microscope (Zeiss LSM-510 system with inverted Axiovert 100M microscope) equipped with a krypton-argon laser. Excitation was set at 488 nm, and the emitted light was filtered with an appropriate filter set at 510 nm. Photomultiplier gain and laser power were identical within each experiment to allow comparison of samples against untreated samples.

5.3 RESULTS

5.3.1 Sequencing of wildtype pAntp clone.

The sequence is shown below in Figure 5.1. The EcoR1 site of the wildtype pAntp is underlined in the sequence.

5'

TTTTAANTTTCNGTTTNGNGTTCCCCAGATCCGCTANCGCTCCGGACTCAGAT
CTCGAGCTCAAGCTTCGAATTCATGCGCCAGATAAAGATTTGGTTCCAGAATC
GGCGCATGAAGTGGAAGAAGGGGGATCCACCGGTCGCCACCATGGTGAGCA
AGGGCGAGGAGCTGTTCACCGGGGTGGTGCCCATCCTGGTCGANCTTGACCG
GNGACCTNAACCGGNCACAAGTTCAACCGTNTNCNGCAAGGCCAAGGCCAA
NCCNNCTNCCGGAAAGCTTGCCCTTGANGTCATTTTGNCAACCGNCAACTTG
CCGTNCCTTGCCAACCTTGTNNACAACCTTGACTTCGGGTTCAATTGTTTAAN
CNGTTACCCGNACCCCTTGAANCANCNCAATTTNTTNAATTCCGCATTGCCC
AAAGGTTACNTCCAAGANCNCACCATTTTTTTTTAAGGGACAACGGNACTTN
CAANACCCTNNCCGAGGTGAANTTCNANGGCNACACCCTTGTTGAACCGNAT
NNAAGCTGAANGGCNTCAATTTAAAGGAGGACNGGAACATTCCTGGGGCAA
AAGCTTGGANTCCAACTTCCANCAGNCACAACGTTTTTNTCATTGGCCNA

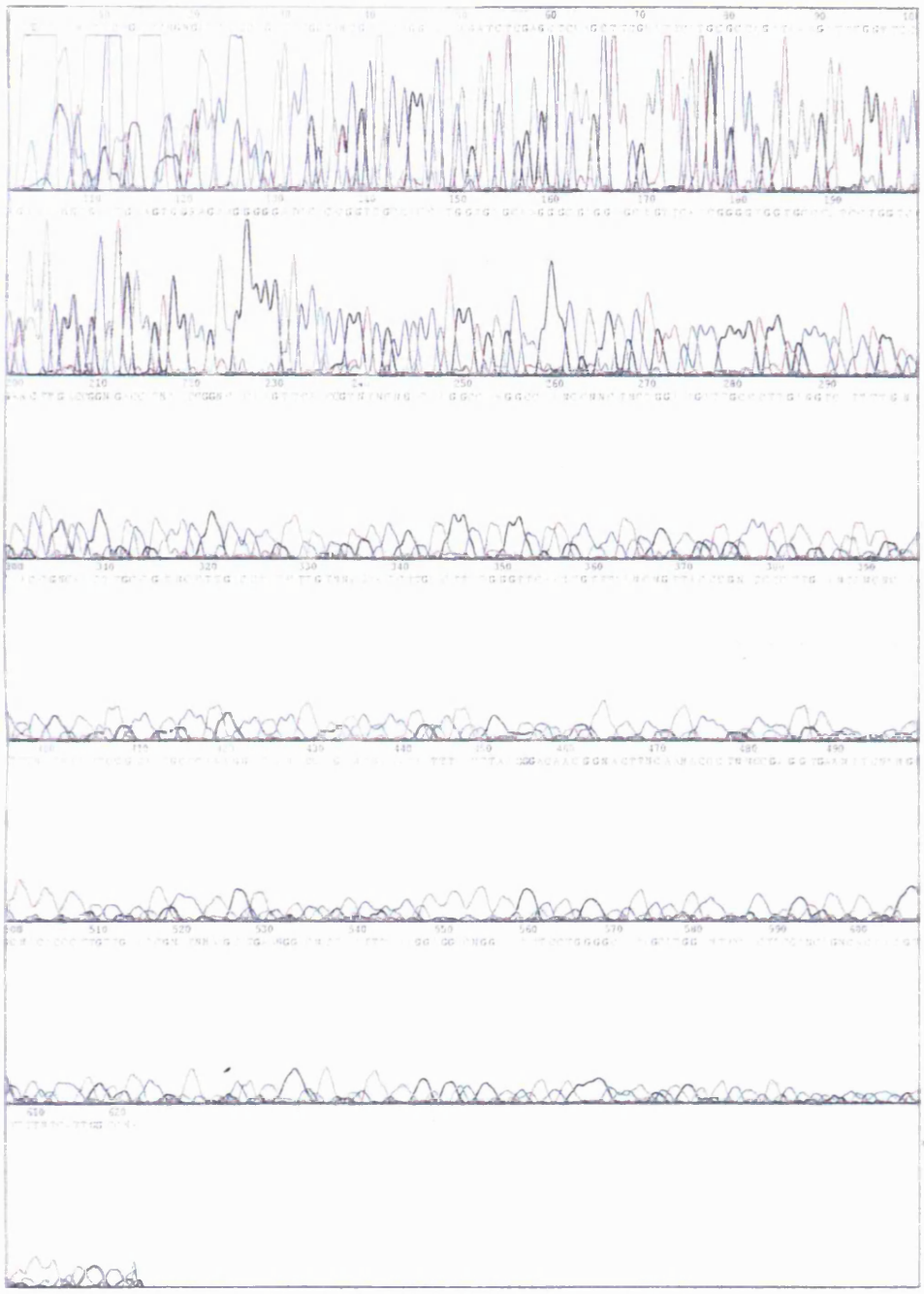

Figure 5.1. Sequencing report for wild type pAntp clone.

5.3.2 Sequencing of mutant pAntp clone.

The sequence is shown in Figure 5.2. The 5' EcoR1 site of the mutant sequence is underlined.

5'

TAACTTNCTGGTTTAGTGAACCGTCAGATCCGCTAGCGCTACCGGACTCAGAT
CTCGAGCTCAAGCTTCGAATTCATGCGCCAGATAAAGATTTTCTTCCAGAATC
GGCGCATGAAGTTCAAGAAGGGGGATCCACCGGTCGCCACCATGGTGAGCA
AGGGCGAGGAGCTGTTCACCGGGGTGGTGCCCATCCTGGTCGAGCTGGACGG
CGACGTAAACGGCCACAAGTTCAGCGTGTCCGGCGAGGGCGAGGGCGATGC
CACCTACGGCAAGCTGACCCTGAAGTTCATCTGCACCACCGGCAAGCTGCCC
GTGCCCTGGCCCACCCTCGTGACCACCCTGACCTACGGCGTGCAGTGCTTCAG
CCGCTACCCCGACCACATGAAGCAGCACGACTTCTTCAAGTCCGCCATGCCC
GAAGGCTACGTCCAGGAGCGCACCATCTTCTTCAAGGACGACGGCAACTACA
AGACCCGCGCCGAGGTGAAGTTCGAGGGCGACACCCTGGTGAACCGCATCG
AGCTGAAGGGCATCGACTTCAAGGAGGACGGAACATCCTGGGGCACAAGCT
GGAGTCAACTNCAACAGNCACAACGTNTATATCATGGCCGACAAGCNNAAG
AACGGGNTCAAGGTGAACTTNAAGATCCGCACACATNNAGGACNGNNNCN

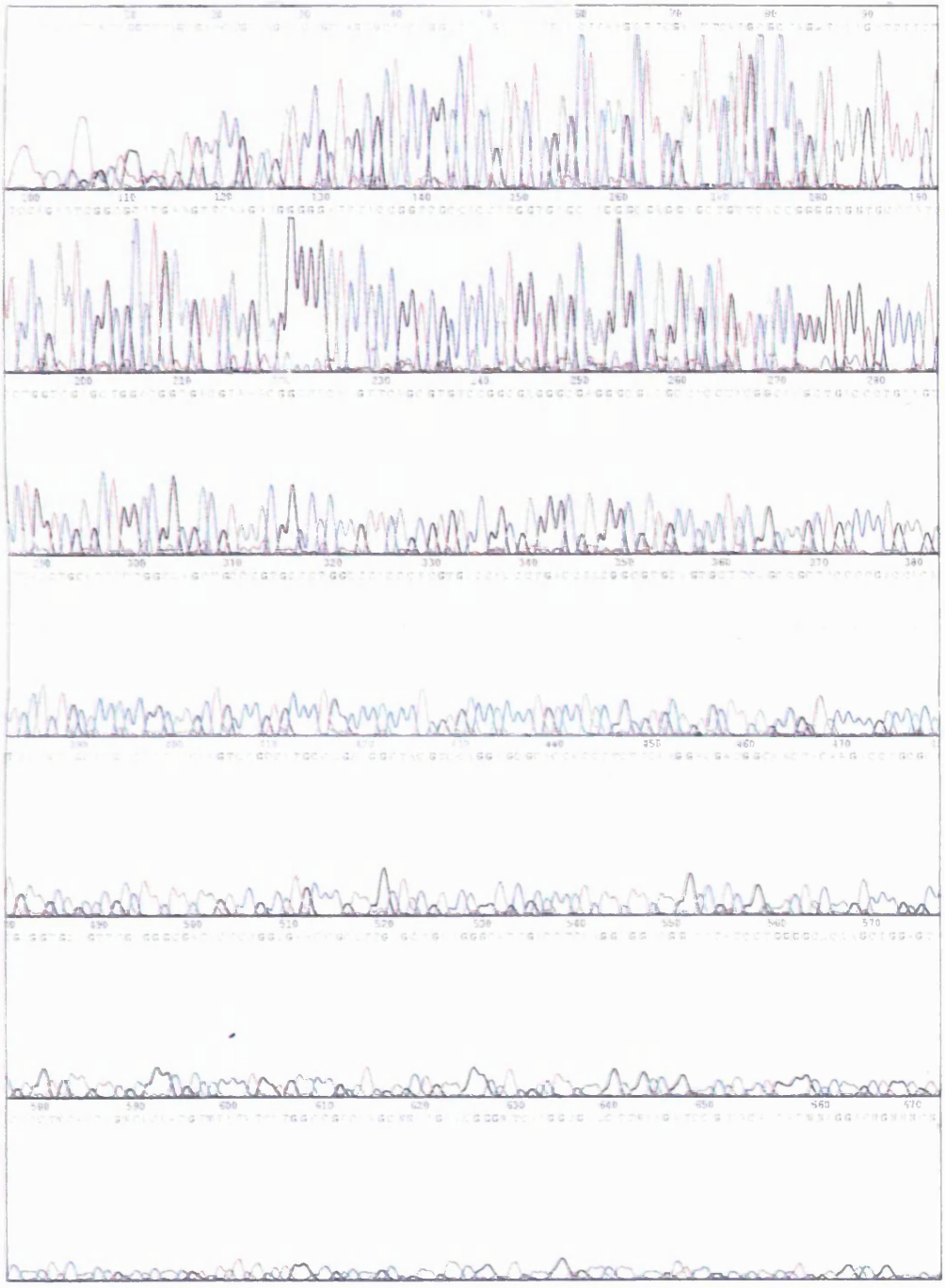

Figure 5.2. Sequencing report for mutant pAntp clone.

Both the wildtype and mutant pAntp genes were cloned into the vector pEGFP-N1 successfully as seen from the sequencing information (Figure 5.1 and 5.2).

5.3.3 Transfection of EGFP-pAntp clones.

Fusions of the N-terminus of EGFP retain the fluorescent properties of the native protein allowing the localization of the fusion protein *in vitro* and *in vivo*. The target gene is cloned into pEGFP-N1 so that it is in frame with the EGFP coding sequences.

For these results, cells were examined only with a x 40 oil immersion objective. It was not possible to obtain images of the cells at lower magnification (using a x 10 objective) because of a lack of fluorescence. No transfected cells were detected in cells exposed to pEGFP-N1 only and complexes of pEGFP-N1 and PEI. Both samples displayed similar levels of fluorescence (figures 5.3 and 5.4 respectively). Images obtained of cells exposed to complexes of the wildtype pAntp fusions displayed higher levels of fluorescence than those exposed to mutant pAntp fusions (figure 5.5).

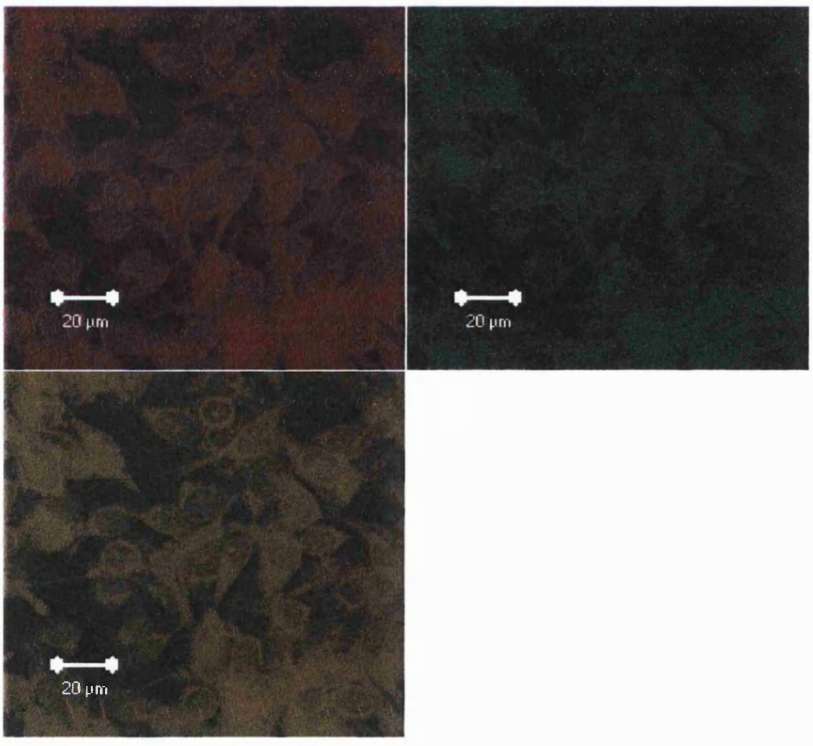

Figure 5.3. Confocal images (split display) of untransfected cells.

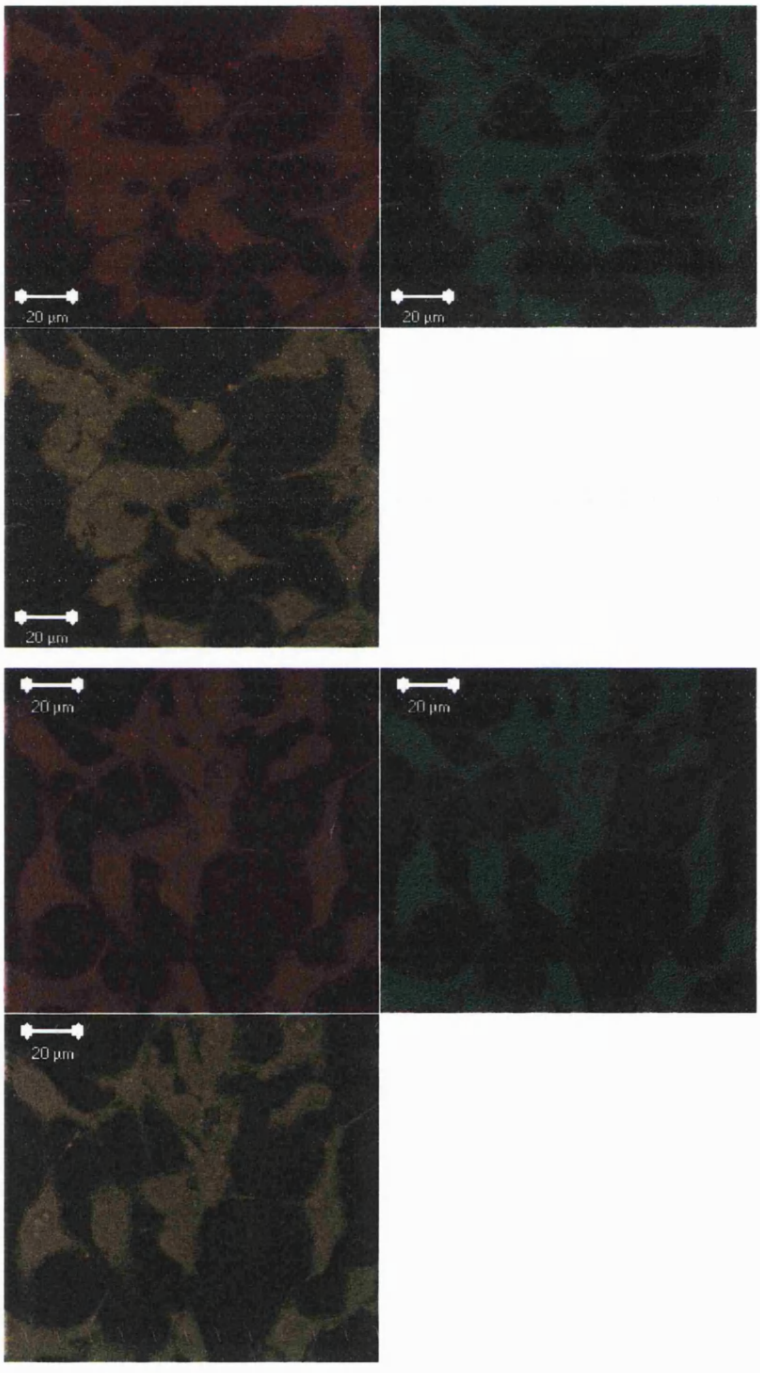

Figure 5.4 (top and bottom panels). Images of cells transfected with pEGFP-N1/PEI only. A x 40 oil immersion objective was used to captured these images.

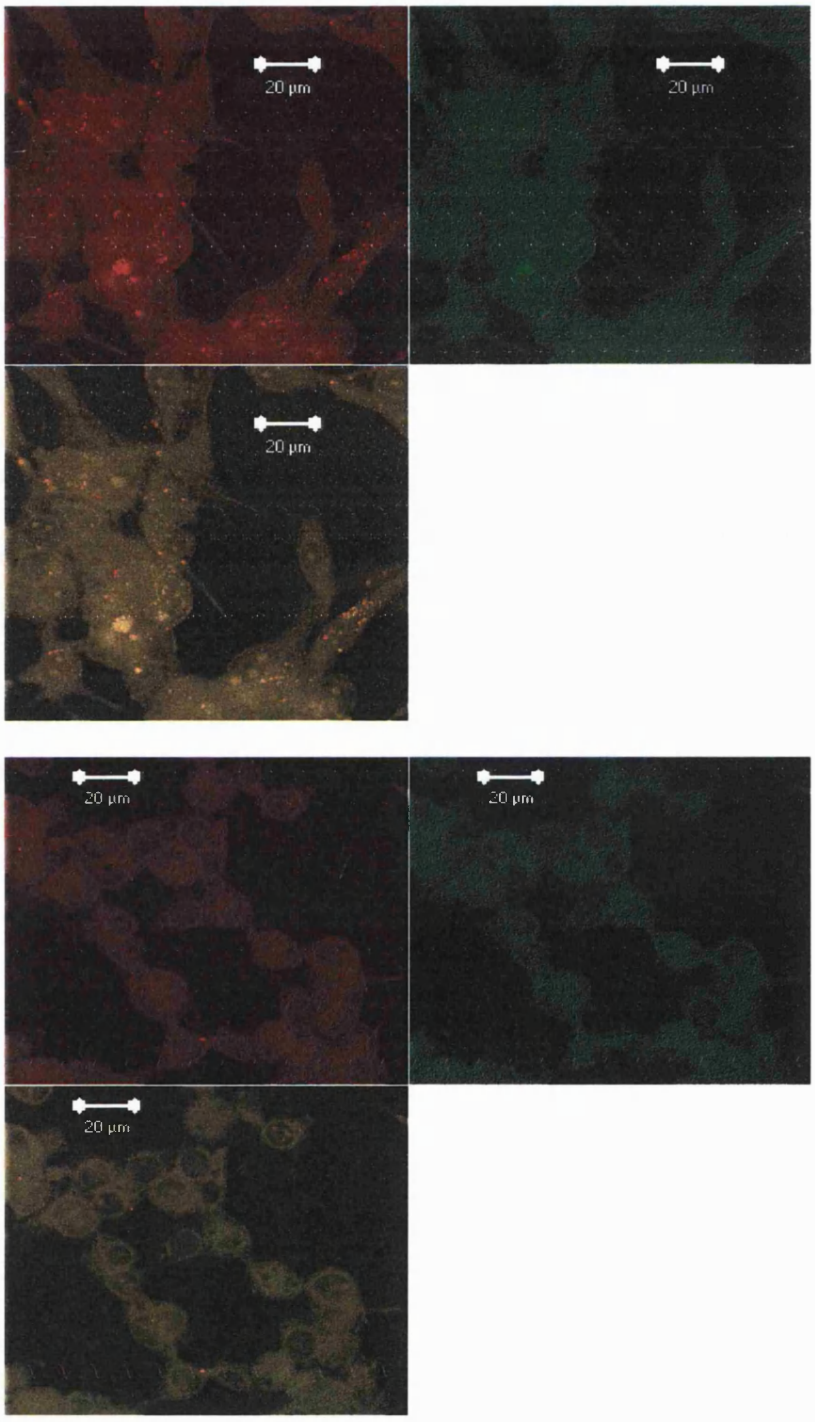

Figure 5.5. Images of cells incubated with wildtype EGFP-pAntp fusion (top) and mutant EGFP-pAntp fusion (bottom).

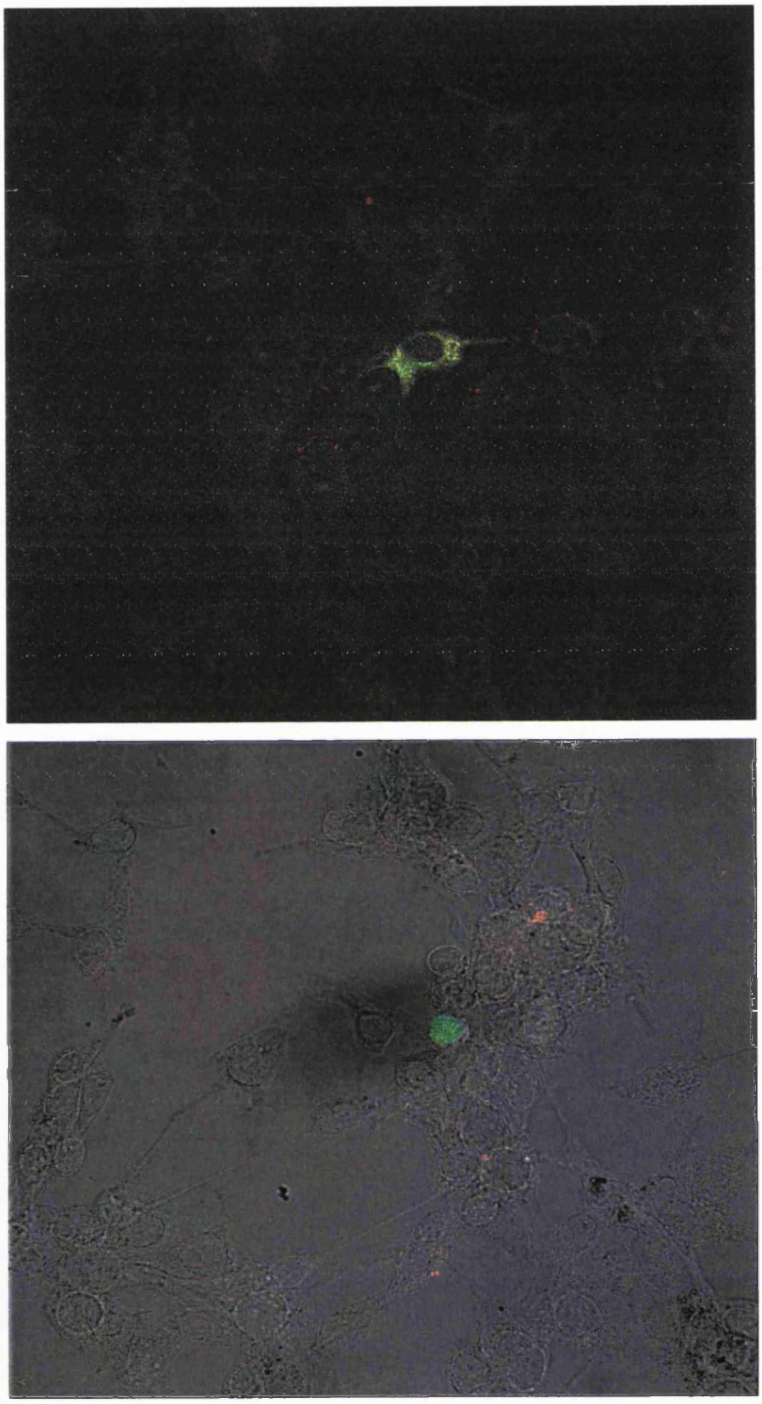

A and B

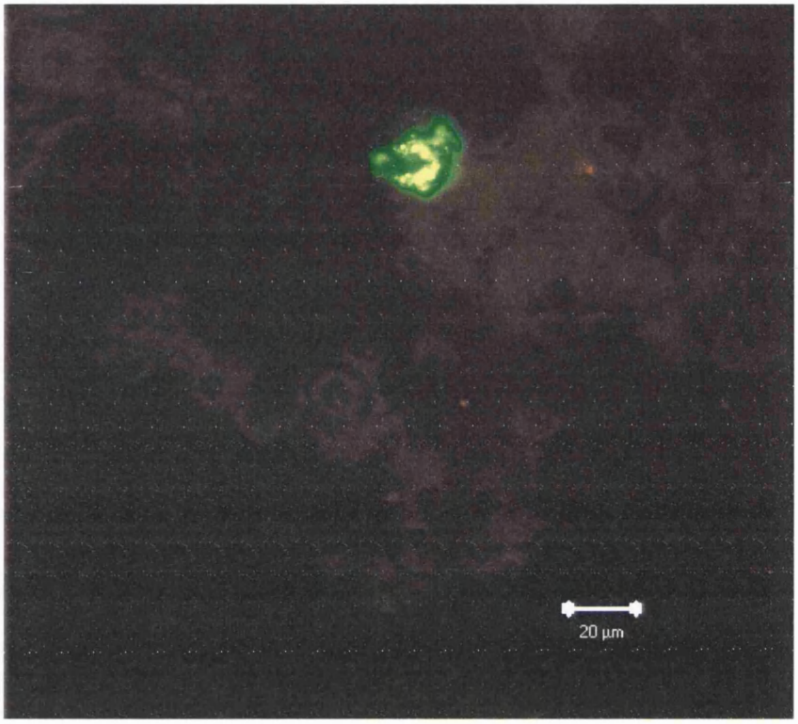

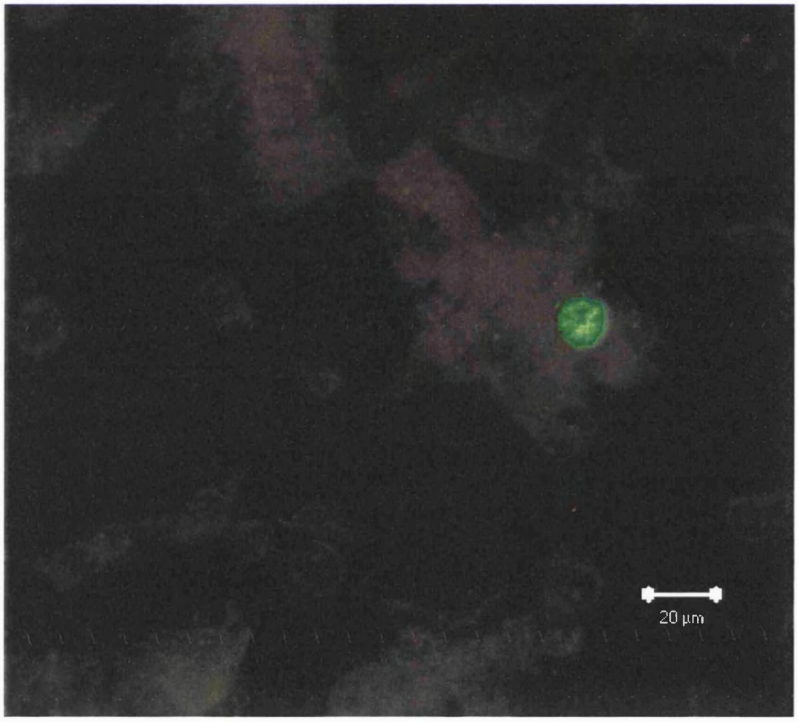

C and D

Figure 5.6. Confocal images of transfected cells using the mutant EGFP-pAntp/PEI complexes. Images were captured with a x 40 oil immersion objective.

Images taken of cells incubated with complexes of the mutant EGFP-N1 and PEI displayed few transfected cells. Figures 5.6A to D show some of these transfected cells, which were situated far apart from each other. The distances between transfected cells were too great to obtain a full view of them on the same image, hence it was only possible to take pictures of isolated transfected cells. Figure 5.6A shows a cell where transfection has occurred as seen only in the cytoplasmic region. Figure B represents an image where a dual channel (rhodamine/fluorescein) filter image of a transfected cell has been superimposed on a transmitted light image of the same cell. This superimposed attempt gives a clear picture of the proximity of surrounding cells around the transfected cell. Figure 5.6C and D display more cells that express EGFP (seen using the fluorescein filter).

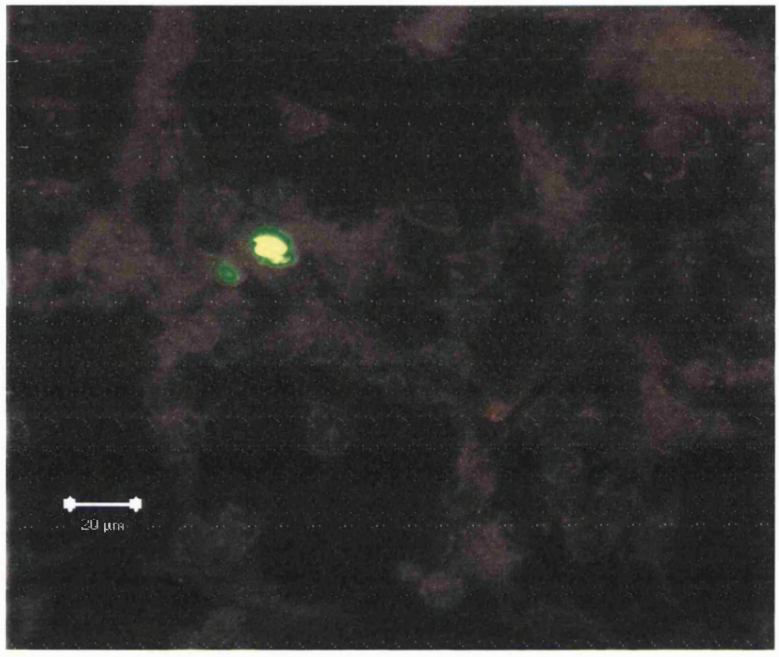

A

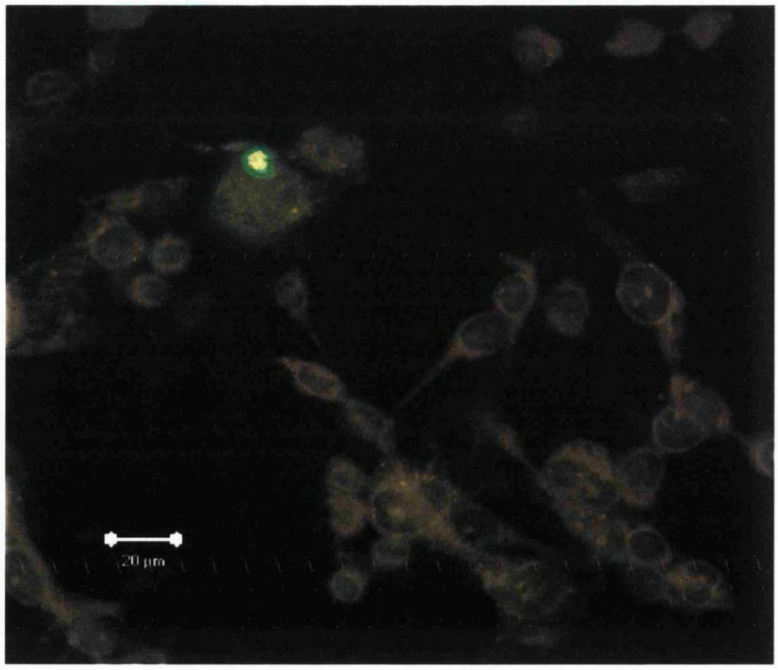

B

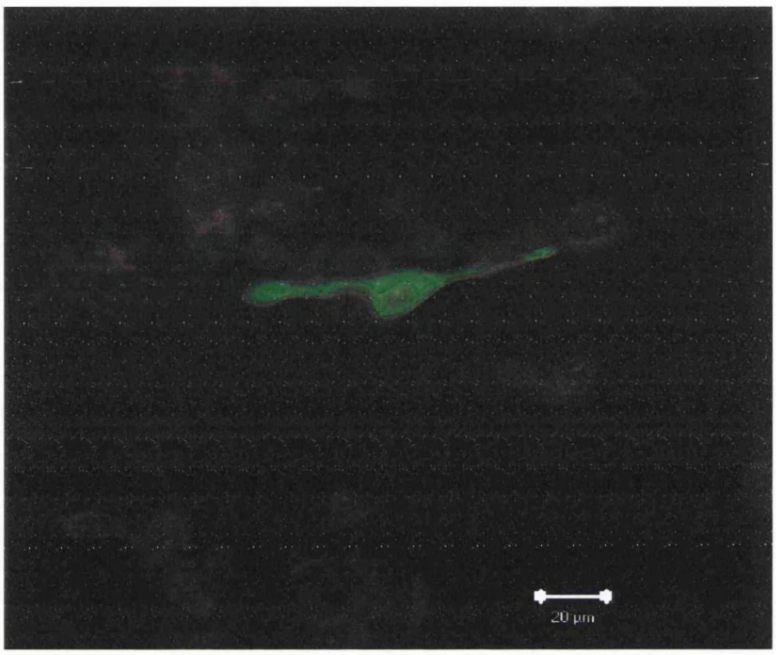

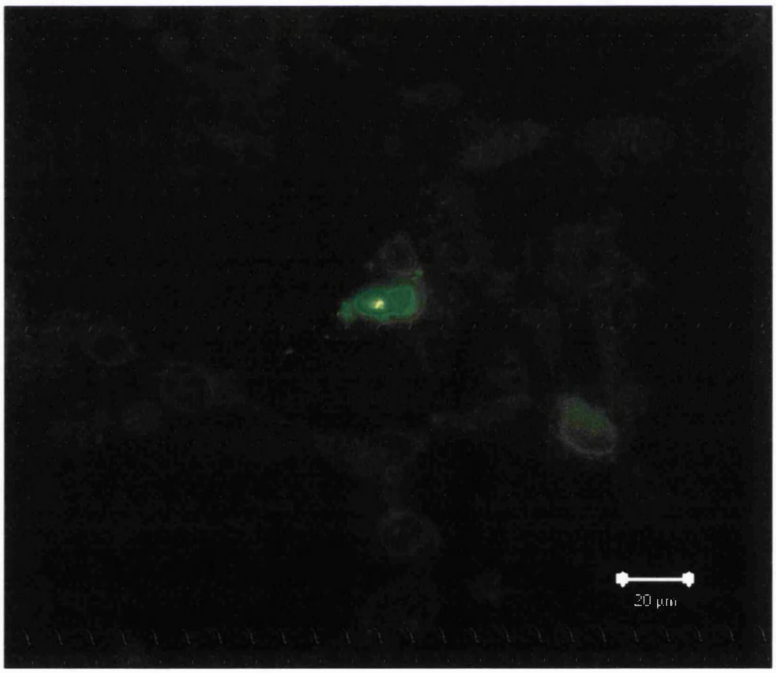

C and D

Figure 5.7. A panel of images taken from cells that were incubated with wildtype EGFP-pAntp fusion complexed with PEI. A x 40 oil immersion objective was used.

Figures 5.7A to D represent images of cells that were exposed to complexes of wildtype EGFP-N1 pAntp fusion with PEI. As with the mutant, images show a few transfected cells obtained from different fields of view from the slides. However, there seemed to be a few cells transfected by the wildtype complexes as evident from figure 5.7A where two cells are transfected. Figure 5.7D also displays more than one transfected cell in the same field, one cell (bottom right of the picture) has cytoplasmic distribution of EGFP whereas the centrally displayed cell exhibits transfection in the nucleus. In addition, there appeared to be a spread of EGFP fluorescence in the immediate vicinity (top) of this centrally placed transfected cell (figure 5.7D). The cell showed in figure 5.7B is yet another cell with nuclear expression of EGFP and spread of EGFP around it.

5.4 DISCUSSION

In order to get a reasonable visual impression of the number of transfected cells in a population of cells, it was intended to obtain images at low magnification. However, this proved difficult to achieve since the overall fluorescence of the cells was too low to allow images of the cells to be detected. The lowest magnification possible and applied was x40. This level of magnification was sufficient to observe individual cells that had been transfected. In the case of wildtype EGFP-pAntp, it was possible to detect an image with two isolated transfected cells in the same field. Generally, the proximity of the transfected cells detected was too far apart with both the mutant EGFP-pAntp and wildtype EGFP-pAntp. The low fluorescence seen with the EGFP fusions implies an overall low transfection efficiency, which may be enhanced by the use of higher N/P ratios of PEI close to ratios required for optimum transfection. Another possible explanation for the low fluorescence detected may be due to the fact that the fusion of these translocating sequences to the N-terminus of EGFP, may reduce their ability to perform their intended duties, namely to transduce proteins. Although over 20 different oligonucleotides and a similar number of peptides have been linked to pAntp, there is a strong size constraint whereby fusions with the pAntp translocating sequence appears only to be active in proteins with less than 100 residues. This is a significant contrast to other protein-transduction domains including TAT and VP22, which have been shown to transduce much larger molecules, including β-galactosidase (>1000 amino acids) (Fawell *et al.*, 1994). Schwarze *et al.*, 1999 delivered a biologically active enzyme to all cells and tissues of mice by intraperitoneal delivery of the 120-kDa β-galactosidase protein, fused to the protein transduction domain from the HIV TAT protein. This resulted in readily detectable β-gal activity in all tissues assayed, such as the bone marrow. Phelan *et al.*, 1998 transfected a VP22-p53 fusion expression vector and observed transduction of the VP22-p53 protein to the surrounding tumour cells as well as subsequent induction of apoptosis. Apoptosis of tumor cells was induced as a result of this intercellular delivery of p53 by VP22.

Recently, it has been suggested that transduction of GFP fusions across the cellular membrane is an inflexible process, which requires the partial or complete unfolding of a

protein and this in turn needs refolding once *in vivo*. Mammalian cells do not appear to have the ability to refold the GFP protein into its enzymatically active conformation (Schwarze *et al.*, 2000). This cellular handicap results in a significant loss of GFP emission. Hence, it is also conceivable that the process of translocating cell membranes can result in the denaturation of the protein. Bonifaci *et al.*, 1995 observed that transduction of full-length TAT-protein transduction domain fusion proteins across the cell membrane results in an inactivation of the protein. In this latter study, TAT was used to ferry dihydrofolate reductase into cells and results implied that unfolding of the protein might be necessary.

An alternative approach to improve the ability of pAntp to transduce proteins in mammalian cells may be to generate a construct using a bacterial expression vector. For instance, a fusion between TAT and herpes simplex virus TK protein will transduce into cells and has its highest enzymatic activity when purified from the soluble bacterial fraction. This protocol has been successfully used to transduce green fluorescent protein (Schwarze *et al.*, 2000). However, since the expression of some proteins are poor in bacteria combined with the fact that some may require posttranslational modifications, other systems such as yeast and baculovirus may provide better transduction efficiency.

5.5 SUMMARY

From the data obtained in this study, it can be deduced that no evidence yet exists to confirm that translocation by pAntp occurs from a transfected cell to other surrounding cells in the immediate vicinity. The threshold of detection of transfected cells may be too low to observe this. In addition, the emission of EGFP may decrease as it goes through the membrane. Hence, another method of marking transfection may be required such as use of alkaline phosphatase or β-gal in immunohistochemistry.

PART II

GENE DELIVERY USING BIFUNCTIONAL PEPTIDES

CHAPTER 6

GENE TRANSFER USING A BIFUNCTIONAL PEPTIDE COMPRISING A MEMBRANE TRANSLOCATING SEQUENCE COUPLED TO A CATIONIC DNA-BINDING DOMAIN.

6.1 INTRODUCTION

Current self-assembly gene delivery systems are only moderately efficient methods for gene transfer to mammalian cells and consequently efficient uptake into the nucleus, leaving much scope for improvement. In general, particulate gene delivery systems achieve cellular gene delivery by the process of endocytosis, which involves internalisation by membrane vesicles. There are several intracellular barriers for gene transfer and it is well established that escape from the endosomal compartment following internalisation of transfection complexes is one of the rate-determining steps (Zabner *et al.*, 1995). Hence, various groups have reported the use of endosomolytic agents including chloroquine (Erbacher *et al.*, 1996) or fusogenic peptide sequences such as influenza haemagglutinin subunit 2 (Schoen *et al.*, 1999), to achieve endosomal escape. Two gene delivery vectors, which were reported to have endosomolytic activity, were employed in these experiments: polyethyleneimine (PEI) and K_{25}HA2.

This chapter investigated the use of penetratin in gene delivery. The uptake mechanism of this translocating peptide is by an alternative pathway to endocytosis. This is of particular interest since endocytosis by differentiated cells *in vivo* is appreciably slower than dividing cells in culture (Matsui *et al.*, 1997; Fasbender *et al.*, 1997). The 16 amino acid sequence from pAntp has been used as an internalization vector for peptides and oligonucleotides (Schutze-Redelmeier *et al.*, 1996) but has not yet been fully evaluated for plasmid DNA delivery. This chapter evaluates the ability of penetratin and its derivative to interact with plasmid DNA, display membrane activity and modulate gene expression in a variety of cultured cell lines.

6.2 MATERIALS AND METHODS

6.2.1 Cationic vectors employed

6.2.1.1 Penetratin and its derivative

All peptides were synthesized using solid phase peptide synthesis as described in chapter 2. The penetratin sequence was synthesized as follows:

H_2N-RQIKIWFQNRRMKWKK-COOH

The penetratin derivative with an oligo-lysyl chain, K_{25}penetratin, was synthesized as follows:

H_2N-K_{25}-RQIKIWFQNRRMKWKK-COOH

6.2.1.2 Polylysine (K_{25})

This oligolysine chain was synthesized and used as a control for these experiments. The peptide appeared as a white fluffy lyophilized solid, which was stored at -20°C prior to use.

6.2.1.3 Influenza haemaglutinin subunit 2 (HA2)

This fusogenic peptide sequence was a kind gift from Alfred Agyeman (School of Pharmacy, University of Bath, UK). It was synthesized such that the native sequence was coupled to an oligolysine chain (K_{25}), which was at the amino terminal end of the HA2 sequence. The peptide was presented as a white fluffy lyophilised solid which was stored at -20°C prior to use.

H_2N-GLSEAIAGFIENGWEGMIDGWYG-COOH

6.2.1.4 Polyethyleneimine (PEI)

This gene delivery vector was commercially available and was supplied by SigmaAldrich Chemical Company. It appeared as a viscous solution. PEI average molecular weight 25000 (average degree of polymerisation 580 assuming a MW of 43 Da for the repeating unit) was used to prepare a 20 mM aqueous stock solution. The stock solution was neutralised with hydrochloric acid and filtered through a 0.2 μm Millipore filter. PEI stock solutions were stored at 4°C and used within one month of preparation.

6.2.2 Mammalian cell lines

The cell lines used in this study were as follows;

B16 cells, a murine melanoma cell line, was donated by L.R. Kelland, Institute of cancer research, Sutton.

A549 cells, a human adenocarcinoma cell line derived from the alveolar region of the lungs (alveolar type II), was obtained from M. Watson, School of Pharmacy, University of Bath, UK. For routine culture, cells were subcultured 1 in 4 twice weekly.

16HBE14o- cells, an SV40 transformed human bronchial epithelial cell line was obtained from D. Greunert, University of California, San Francisco, USA. For routine culture, cells were subcultured 1 in 2 weekly.

FEK_4 cells, a human foreskin primary cell line, was obtained from J. Brown, School of Pharmacy, University of Bath, UK. For routine culture, cells were subcultured 1 in 4 weekly.

HeLa cells, a human epithelial carcinoma cell line, was obtained from the European Collection of Animal Cell Cultures (ECACC, Porton Down, Salisbury, UK). For routine culture, cells were subcultured 1 in 10 weekly.

HEK293 cells, a human embryonal kidney cell line, was obtained from ECACC, UK. For routine culture, cells were subcultured 1 in 10 weekly.

6.2.3 Transfection of mammalian cells

6.2.3.1 Preparation of transfection complexes

Plasmid DNA (6.4 μg of pCMV*luc*, pCMV*β* or pEGFP-N1 where appropriate) was diluted to 800 μl with HBS in a sterile polystyrene tube (Costar, UK). Variable quantities of the GDV (gene delivery vector) were separately diluted to 800 μl with HBS. Complexes were prepared by adding the 800 μl of GDV solution to the 800 μl of DNA. Gentle mixing of the two solutions was executed by pipetting the solution up and down five times using a 1 ml Gilson pipette.

6.2.3.2 Exponentially growing cells

For transfection of exponentially growing cultures, cells were seeded at a density such that at the time of transfection monolayers were 70% confluent. For the various cell types studied, seeding densities on 35 mm well plates were as shown in table 6.1;
Following seeding, cells were grown for 16 - 20 hours under standard conditions in the appropriate culture medium prior to transfection.

Cell line	**Cell number per 35 mm well plate**
B16	1×10^5
16HBE14o-	5×10^5
HEK293	2×10^5
FEK_4	2×10^5
A549	2×10^5
HeLa	1×10^5

Table 6.1. Seeding densities for various cell lines.

6.2.3.3 Peripheral Mononuclear Cell Preparation

This standard method described by Favour, 1964 was employed to isolate lymphocytes.

6.2.4 Methods for quantifying expression

The transfection efficiency was calculated as a mean value of luciferase activity (ng) per quantity of protein in mg (Chapter 2).

6.2.4.1 FACS analysis of EGFP expression

At 24 hours post transfection, adherent cells were washed twice with 1.0 ml of PBS and then detached using 0.02% w/v EDTA in PBS. Cells were transferred to a 1.5 ml micro-centrifuge tube, collected by centrifugation, washed and resuspended in 1.0 ml of PBS. Control cells were untransfected. Cell fluorescence intensity relative to control cells was measured at each time point. The fluorescence analysis of cell populations was performed using a Becton Dickinson FACSVantage instrument at an excitation of 488 nm and an emission wavelength of 530 nm (±15 nm) using an argon ion laser. A minimum of 10^4 cellular events was analysed for each sample. Cell viability was assessed with propidium iodide and dead cells were excluded from analysis.

6.2.4.2 Cytochemical staining for β-galactosidase activity

The determination of the efficiency of β-galactosidase expression employed 5-bromo-4-chloro-3-indolyl-β-D-galactosidase (X-Gal), (Melford Laboratories Ltd, Ipswich, England). Staining for β-galactosidase activity in whole cells was carried out as described by MacGregor *et al.*, 1991. The distribution of expression within a cell population can be determined with histochemical staining using the substrate 5-bromo-4-chloro-3-indoly-β-D-galactoside (X-gal). Cells expressing β-gal hydrolyze this substrate to galactose and soluble indolyl substances, which undergo oxidation to insoluble blue precipitates. The solutions required were as follows;

Phosphate buffered saline (pH 7.3)	
Fixative solution	1% (v/v) glutaraldehyde
	1mM magnesium chloride
	0.1M sodium phosphate pH 7.3
X-gal solution	0.2% (w/v) 5-bromo-4-chloro-3-indolyl-β-galactoside (X-gal) in dimethylformamide
	1mM magnesium chloride
	150mM sodium chloride
	3.3mM potassium ferrocyanide, $K_4Fe(CN)_6$
	3.3mM potassium ferricyanide, $K_3Fe(CN)_6$
	0.1M sodium phosphate

Forty-four hours post transfection, cell monolayers were rinsed twice with 2 ml of PBS and then permeabilised by overlaying with 2 ml of fixative solution followed by a 5 minute incubation at 4°C. The fixative solution was aspirated, the cells were rinsed once with PBS and then overlaid with 1 ml of X-gal solution, followed by incubation overnight at 37°C in the dark. Cells were then washed twice with PBS and viewed under an inverted light microscope. Cells expressing the β-galactosidase enzyme were stained blue against a background of unstained cells. Where appropriate, photographs were taken using a Nikon F-301 camera with fujichrome 200 or 400 DX film.

6.2.5 Determination of cell viability.

A modified MTT assay (Mosmann, 1983) was used to establish the toxicity of penetratin, K_{25}penetratin, K_{25} and PEI. B16 cells were plated into 96-well tissue culture plates at a density of 4000 cells per well in 100 µl media. Peptides to be tested were made up in 100 µl of PBS and added to the wells. After treatment and a three day incubation, the medium was removed by inversion and the cells washed twice with serum free Opti-MEM™. A 200 µl aliquot of 1 mg/ml MTT formazan, (SigmaAldrich, UK) was added to each well, and the plate incubated at 37°C for 3 hours. After this time, the MTT solution was removed. 200 µl DMSO was added to each well followed by agitation on an orbital mixer for 10 minutes. Plates were read at 540 nm on a Titre plate reader (Dynatech MR 580). The optical density in wells containing treated cells was compared with that of control wells containing untreated cells to allow the percentage viability to be established.

6.2.6 Gel mobility shift assay

This assay was used to assess the interaction between penetratin and DNA. Plasmid DNA (3 µg pCMV*luc*) were diluted to 125 µl HBS in a sterile micro-centrifuge tube. Variable quantities of the peptide were separately diluted to 125 µl in sterile micro-centrifuge tubes. Hence different charge ratios were prepared. All micro-centrifuge tubes were subsequently pulse centrifuged (Jouan microfuge, France) to concentrate samples to the bottom of the tube. The peptide was then added to the DNA solution by gentle mixing. The mixture was then incubated at room temperature for 25 minutes. After this time, 40 µl of solution were diluted to 50 µl with electrophoresed loading buffer. Ten to 12 µl of this sample were then loaded on to a 1% (w/v) agarose gel in 1x TAE and electrophoresed at 80 volts for one hour in 1x TAE. The agarose gel was then viewed under an ultra-violet transilluminator and photographed using a Polaroid 55 film fitted into a Polaroid CU-5 camera.

6.2.7 Ethidium Bromide Exclusion Assay

The fluorescent properties of ethidium bromide (figure 6.1) allow it to be used as a fluorescent probe, following intercalation between double-stranded DNA.

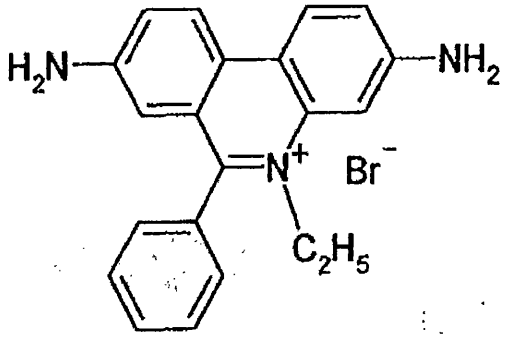

Figure 6.1. Structure of ethidium bromide: 2, 7-diamino-9-phenyl-10-ethylphenanthridinium bromide.

The peptide-DNA complexes were prepared and complexation was analysed using a method adapted from Gershon *et al.*, 1993. Six μg of pCMV*luc* was diluted to 125 μl with HBS in a sterile micro-centrifuge tube. Variable quantities of the peptide were separately diluted to 125 μl in sterile micro-centrifuge tubes. Samples were mixed, incubated for 15-30 minutes and then diluted to 3 ml with 20 mM sodium chloride solution. The fluorescence was monitored at $\lambda_{excitation}$ 260 nm and $\lambda_{emission}$ 600 nm immediately following addition of 3 μl of a 0.5 mg/ml solution of ethidium bromide (final concentration of 0.5 μg/ml), on a RF-540 spectrofluorimeter (Shimadzu, UK) using 1 cm cuvettes with slit settings of 5 nm for both the excitation and emission monochromators. The degree of complexation was reported as a percentage of the fluorescence obtained from a control sample containing 6 μg of uncomplexed DNA. The fluorescence of the control sample was normalised to 100%. A reduction in fluorescence was seen relative to the control as the intercalation of ethidium bromide between base pairs of DNA was prevented by complexation with the peptide.

6.2.8 Erythrocyte lysis assay

The method of Plank *et al.*, 1994 was followed. Freshly prepared human erythrocytes were washed with HBS and resuspended in a 2 x assay buffer of pH 5 or 7 (300 mM NaCl, 30 mM sodium citrate) at a concentration of approximately 5 x 10^7 cells/ml. An aliquot of 75 µl was added to 75 µl of a serial dilution of the peptide in water in a 96-well microtitre plate and incubated for 1 hour at 37°C with constant shaking. After removal of the unlysed erythrocytes by centrifugation (1000 x *g*, 5 min), 100 µl of the supernatant were transferred to a new microtitre plate, and haemoglobin absorption was determined at 450 nm (background correction at 750 nm). 100% lysis was determined by adding 1 µl of a 10% Triton-X solution prior to centrifugation.

6.3 RESULTS

6.3.1 Gel Mobility shift assay

The interaction between penetratin and DNA was first analyzed by agarose gel electrophoresis using the gel mobility shift assay. Following incubation of the peptide with DNA, the electrophoretic movement of complexes across the agarose gel was examined after staining with ethidium bromide. As the quantity of penetratin increased, the mobility of plasmid DNA decreased. The plasmid DNA was neutralised at the lowest charge ratio where the DNA was completely immobilised within the well origin. At charge ratios above 3.0, penetratin completely immobilised DNA at the well origin (Figure 6.2).

Figure 6.2. Determination of charge ratio of penetratin required to neutralize pCMV*luc* using the gel mobility shift assay. The DNA/penetratin complexes were run against a Molecular weight marker (M) and free DNA (D) with increasing charge ratios as shown from left to right.

6.3.2 Ethidium bromide/DNA Fluorescence assay

The interaction of the various cationic peptides with plasmid DNA was more extensively studied using a fluorescence assay. DNA neutralisation was taken to be the charge ratio at which fluorescence first reached a minimum. This point varies with each of the peptides tested. In the case of polylysine (K_{25}), this point occurred at a charge ratio (+/-) of 1.5 (Figure 6.3).

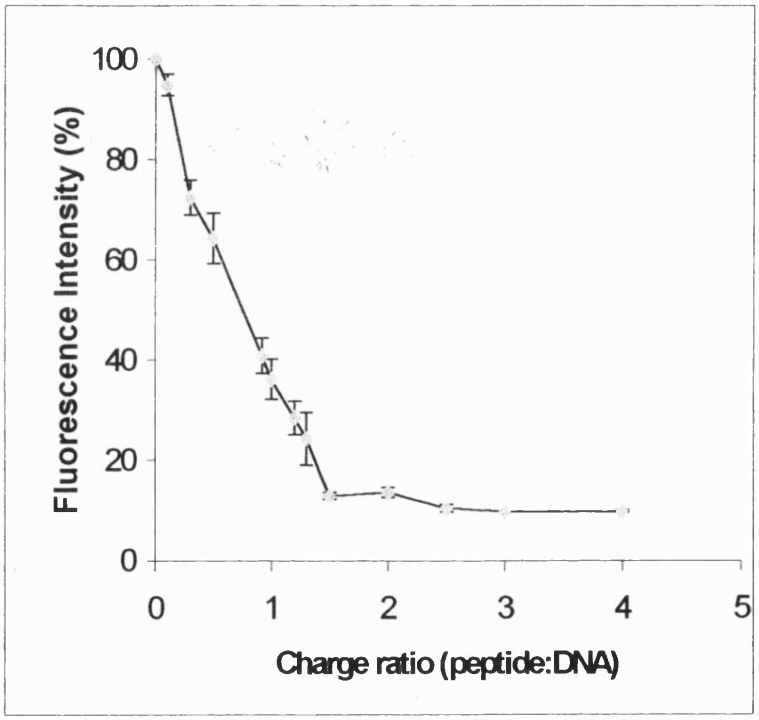

Figure 6.3. The effect on ethidium bromide fluorescence on complexing pCMV*luc* with polylysine (K_{25}). The data points represent the mean of three replicate evaluations.

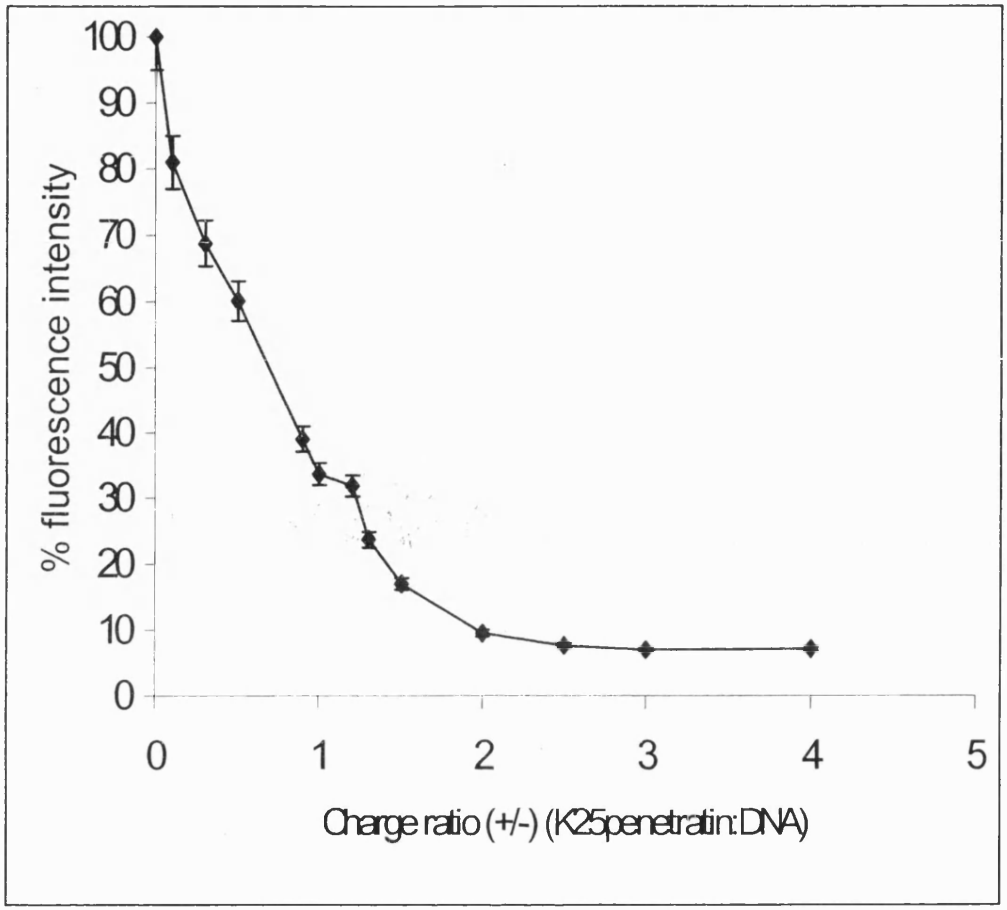

Figure 6.4. The effect on ethidium bromide fluorescence on complexing pCMV*luc* with K_{25}penetratin. The data points represent the mean of three replicate evaluations.

The interaction of DNA with the bifunctional peptide, K_{25}penetratin is shown in Figure 6.4. The charge ratio at which DNA neutralisation occurred was 2.0.

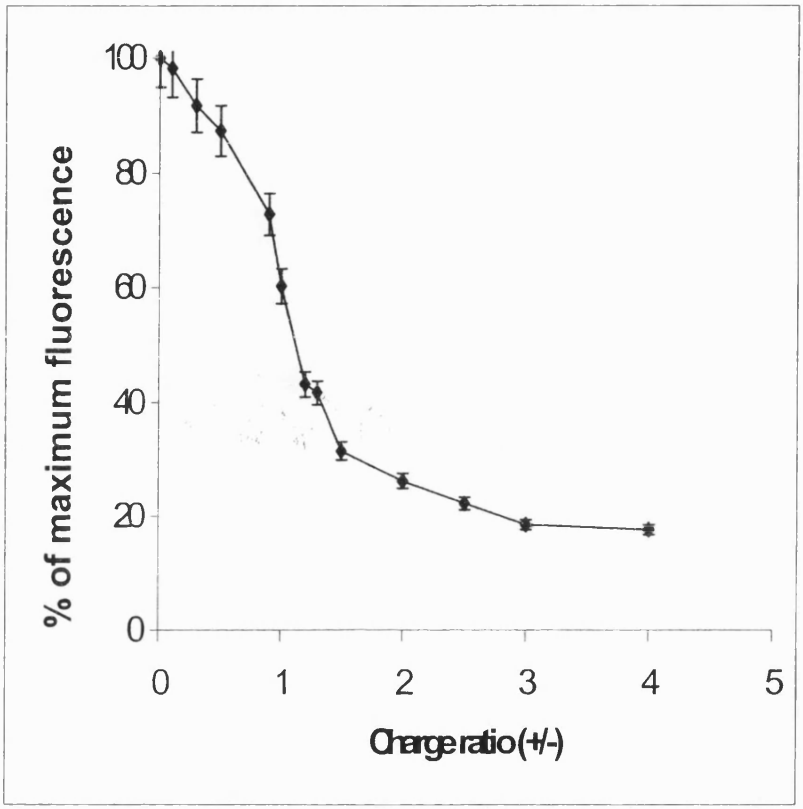

Figure 6.5. The effect on ethidium bromide fluorescence on complexing pCMV*luc* with penetratin. Each data point is the mean of three replicate evaluations.

K_{25}penetratin appeared to show a stronger binding ability with DNA compared with penetratin where larger mass excess was needed. The critical point of DNA neutralization for penetratin was at a charge ratio of 3.5 (Figure 6.5).

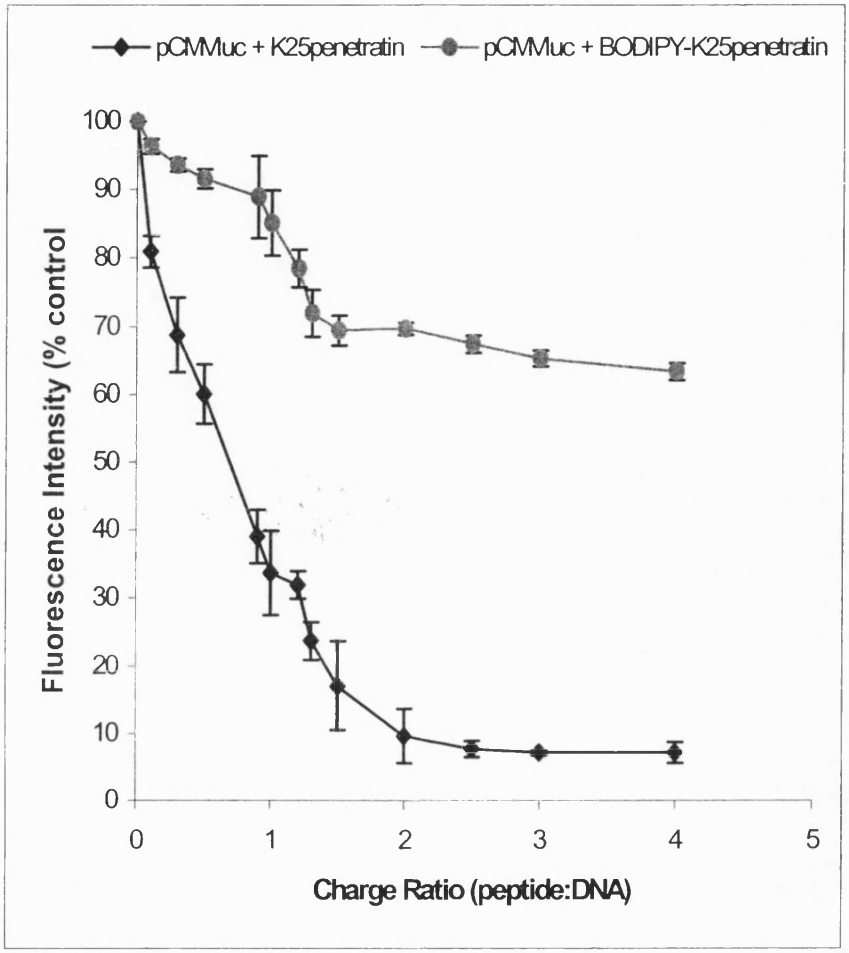

Figure 6.6. Complexation of DNA using K_{25}penetratin and BODIPY-K_{25}penetratin. The pCMV*luc* was mixed separately with increasing quantities of unlabelled K_{25}penetratin or with K_{25}penetratin linked to BODIPY. The degree of complexation was measured as a decrease in fluorescence relative to the control, which was free DNA. The exclusion of ethidium bromide is plotted against charge ratio of the DNA complexes (peptide: DNA). Each data point represents the mean ± SD of three replicate evaluations.

To investigate whether labelled peptide molecules were interacting with DNA in a similar manner to unlabelled peptides, their abilities to complex plasmid DNA were examined using the ethidium bromide exclusion assay. Labelling with BODIPY resulted in a reduction in the peptide's ability to interact with DNA (Figure 6.6). K_{25}penetratin

complexed DNA in a similar manner to K_{25}. Fluorescence dropped to 10% at a charge ratio between 1.0 and 2.0. There was little exclusion of ethidium bromide by the labelled peptide even at higher charge ratios, and the slope was clearly shallower at low charge ratios.

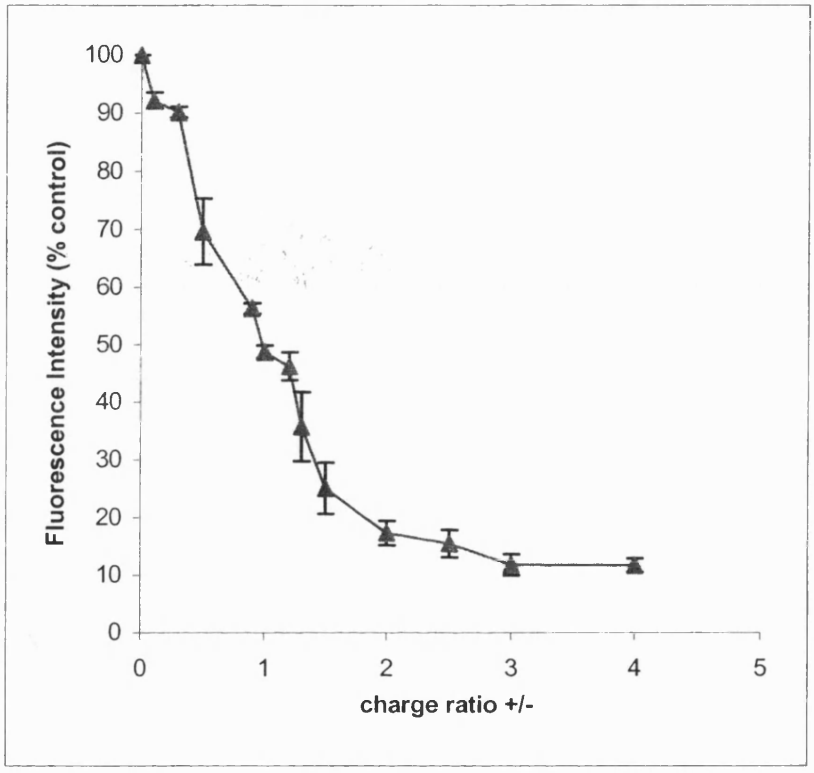

Figure 6.7. Complexation of DNA using ADMP-K_{25}penetratin. The pCMV*luc* was mixed with increasing quantities of ADMP linked to K_{25}penetratin. The degree of complexation was measured as a decrease in fluorescence relative to the control, which was free DNA. The exclusion of ethidium bromide is plotted against charge ratio of the DNA complexes (labelled peptide: DNA). Each data point represents the mean ± SD of three replicate evaluations.

Figure 6.7 indicates that ADMP-K_{25}penetratin was able to exclude ethidium bromide causing a decrease in the fluorescence intensity similar to the unlabelled peptide.

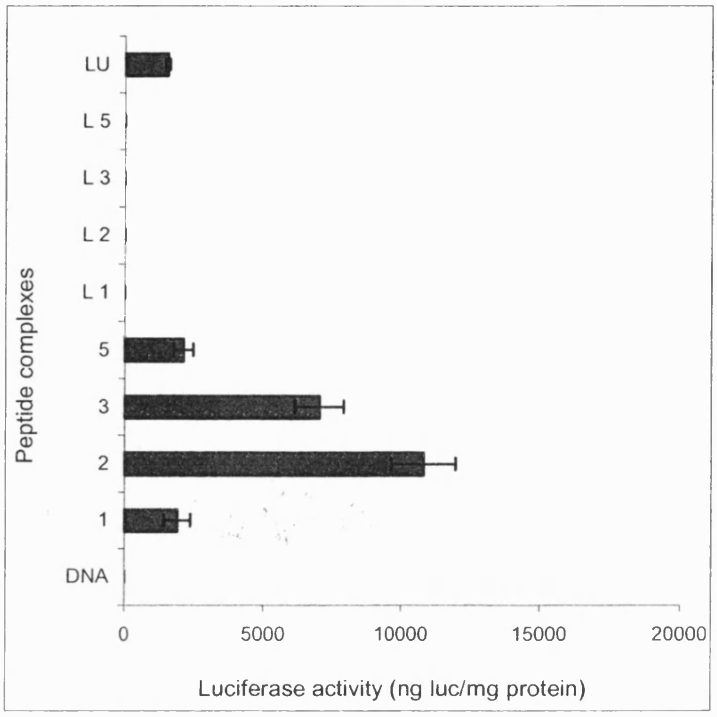

Figure 6.8. Comparative transfection efficiency of unlabelled K_{25}penetratin and K_{25}penetratin labelled with BODIPY FL CASE. Luciferase expression following transfection of B16 murine melanoma cells using pCMV*luc* (2 μg) alone or complexed separately at various charge ratios (+/-), with labeled (L1, L2, L3 and L5) and unlabelled K_{25}penetratin (1, 2, 3, and 5). At the same time, cells were also treated with DNA complexed with a 50: 50 mixture of labelled and unlabelled K_{25}penetratin (LU). Transfection was carried out for four hours in the presence of 100 μM chloroquine. Expression was assayed 24 hours post transfection. Data points represent the mean ± SD of three replicates. Free DNA was used as a negative control.

A transfection experiment (figure 6.8) helped to confirm that there was very poor binding occurring between the labelled peptide and plasmid DNA. At all charge ratios tested for the labelled peptide, there was little evidence of gene expression compared to the reasonably high transfection efficiency displayed by the unmodified peptide. The data also shows the marked reduction in transfection efficiency when the labelled peptide is

combined with the unlabelled peptide in the same ratio. This was assumed to be due to poor or imcomplete condensation of the plasmid DNA by the labelled peptide.

6.3.3 Optimisation of chloroquine

B16 cells were transfected with K_{25}penetratin at an optimum charge ratio (+/-) of 2.0 in the presence of increasing concentrations of chloroquine. The optimum concentration of chloroquine that gave high transfection levels of K_{25}penetratin was found to be 100 μm (Figure 6.9). This concentration was used in subsequent transfection experiments with the gene delivery vectors, where appropriate.

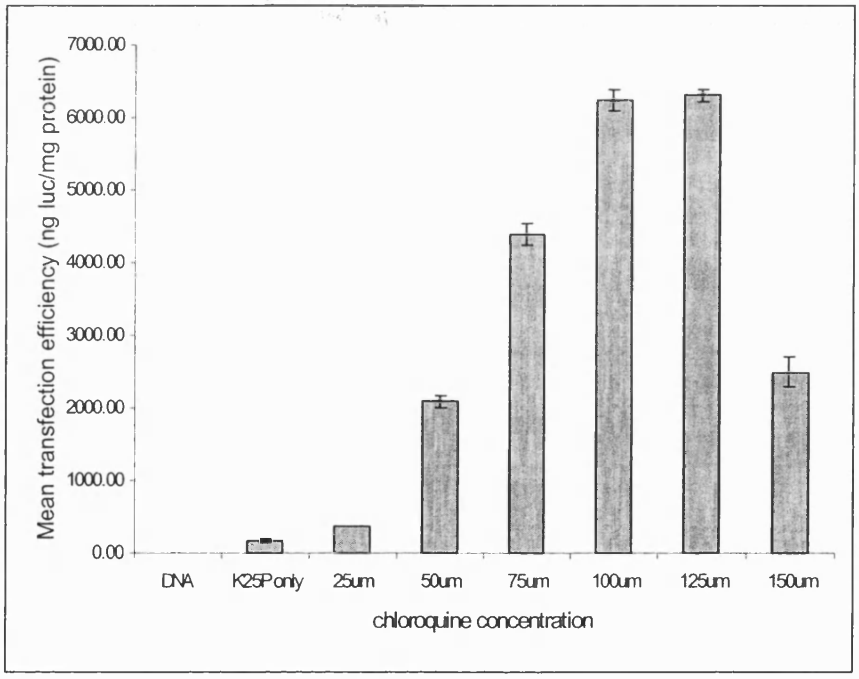

Figure 6.9. Optimisation of chloroquine concentration for transfection of B16 cells with K_{25}penetratin at a charge ratio (+/-) of 2.0. B16 cells were transfected with 2 μg of pCMV*luc* complexed with K_{25}penetratin (+/- 2.0) for four hours and cells harvested 24 hours post initiation of transfection for analysis. Data represent the mean of triplicate samples ± SD.

6.3.4 Charge ratio of transfection complexes

For the transfection experiments, the optimum charge ratio of all cationic gene delivery systems tested was determined in B16 cells. Table 6.2 gives an overview of the optimum charge ratios. Plasmid DNA, 2 μg of pCMV*luc* was complexed with various quantities of the gene delivery vectors and transfected for four hours. Chloroquine at 100 μM was added where appropriate, prior to each transfection experiment.

Gene delivery system	Optimum charge ratio (+/-)
Penetratin	3.5
K_{25}penetratin	2.0
K_{25}	1.5
PEI	1.0 (≡ N/P ratio of 6.0)
K_{25}HA2	1.0

Table 6.2. Optimum charge ratios for various gene delivery systems for transfections in cell culture. The cationic vectors were transfected in the presence of chloroquine.

6.3.5 Transfection of penetratin and its derivative

The transfection efficiency of K_{25}penetratin was about six times higher than that of penetratin alone, although the level of luciferase expression was very low. Both penetratin and K_{25} showed little efficacy, even in the presence of chloroquine. Cells transfected with naked DNA had no measurable luciferase activity.

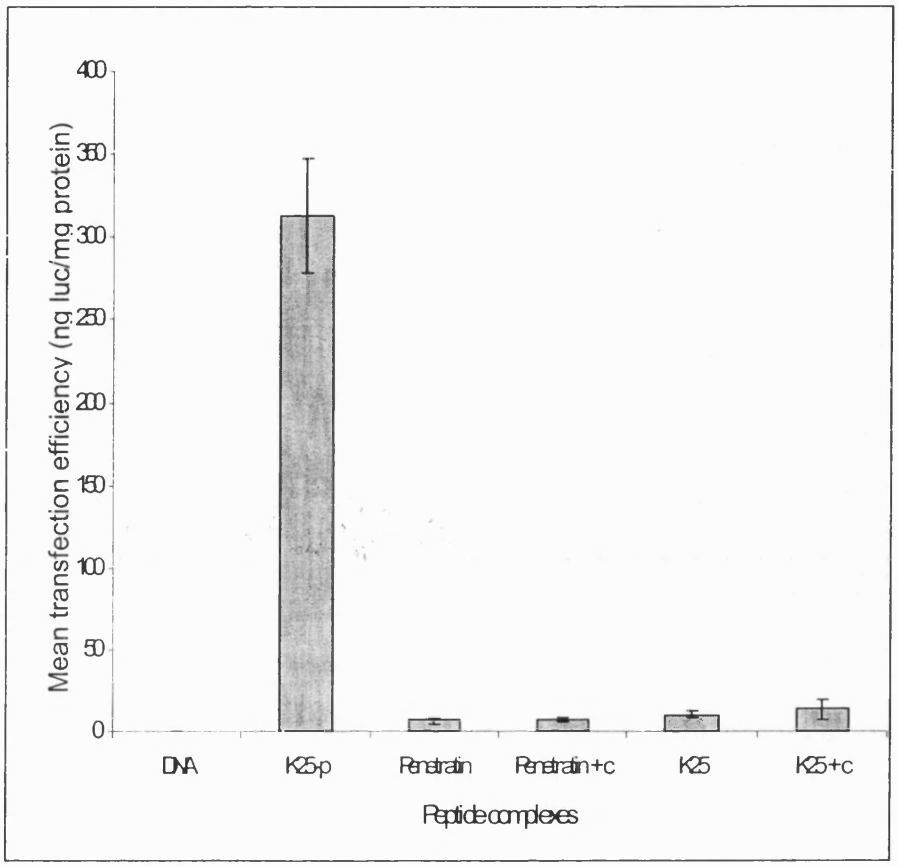

Figure 6.10. Transfection of B16 cells with various peptides. Luciferase expression following transfection using 2 μg pCMV*luc* complexed with K_{25}penetratin (+/- 2.0), penetratin (+/- 3.5) and polylysine (K_{25} +/- 1.5) in the presence or absence of 100 μM chloroquine (c). Expression was assayed 24 hours after transfection. Data points represent the mean ± SD of three replicates.

6.3.6 A comparison of penetratin with endosomolytic agents in different mammalian cell lines

Also, in all cell lines employed, transfection of the various gene delivery vectors was carried out in the presence of 100 μM chloroquine. The conditions optimized in B16 cells were used in all other cell lines and each vector was used at its optimum charge ratio for transfection. Naked DNA was used as a negative control in all cases.

6.3.6.1 B16 cells

The efficiency of transfection in B16 cells is shown in Figures 6.11A and B. All the gene delivery vectors were able to mediate gene expression in this cell line. PEI gave the highest transfection efficiency, especially without the presence of chloroquine, displaying twice as much activity as K_{25}HA2 and about three times as much efficiency as K_{25}penetratin with chloroquine. However, the efficiency of PEI seemed to decrease in the presence of chloroquine. The activity of K_{25}penetratin in the presence of chloroquine was significantly higher than that of K_{25}penetratin alone, which was higher than K_{25}. Polylysine (K_{25}) had little measurable activity, even in the presence of chloroquine. Naked DNA showed no measurable luciferase activity.

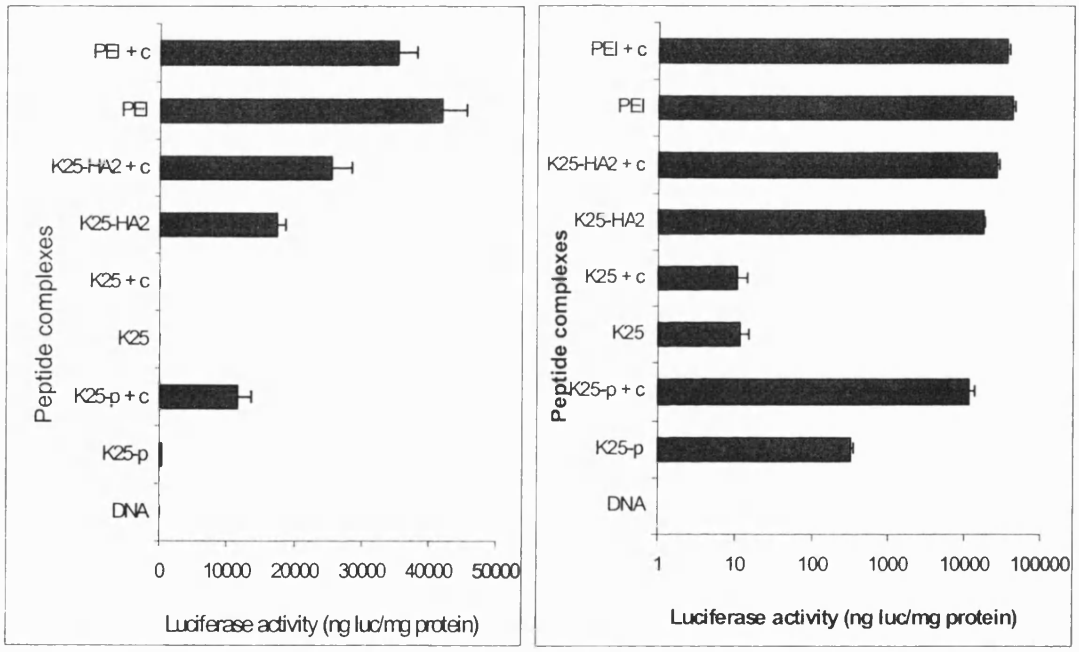

A B

Figures 6.11A and B. Both graphs show the same data for the transfection of B16 cells except that graph B is a log plot. Luciferase expression following transfection of pCMV*luc* (2 μg) complexed with various gene delivery vectors at their respective optimum charge ratios (+/-). Complexes were transfected in the absence and presence of 100 μM chloroquine (c). Expression was assayed 24 hours post initiation of transfection.

Data points represent the mean ± SD of three replicates. Free DNA was used as a negative control.

Histochemical staining of B16 cells with X-gal was used to assess the percentage of B16 cells expressing β-galactosidase after transfection with pCMVβ complexed with PEI, K_{25}HA2 and K_{25}penetratin at their optimum charge ratios (Figure 6.12). The cell population transfected with the cationic polymer, PEI, had markedly higher expression levels than those observed for the peptides. The influenza haemagglutinin peptide derivative, K_{25}HA2, also gave high numbers of β-gal^{+ve} cells compared to K_{25}penetratin.

A  B 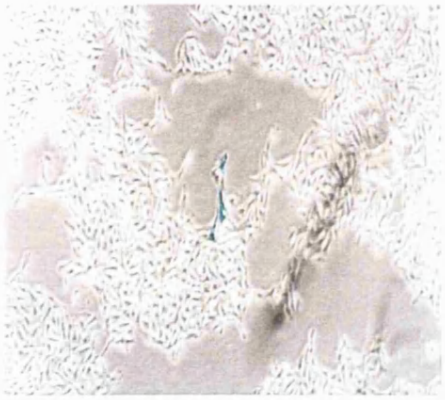

C 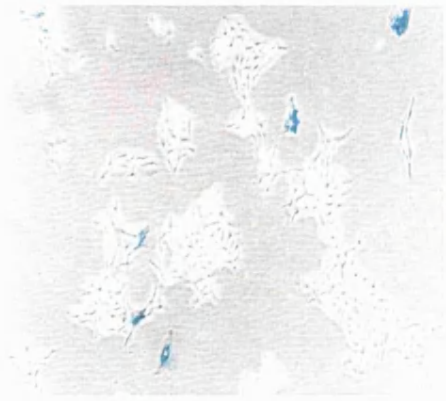 D 

E

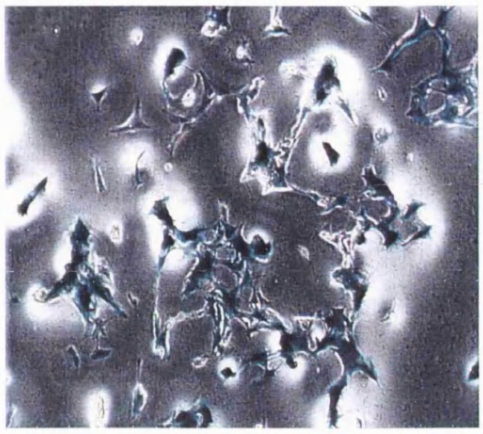

Figure 6.12. Histochemical staining of B16 cells with X-gal. (A) Cells incubated with naked DNA only. Complexes were formed between pCMVβ and (B) K_{25}penetratin, (C) K_{25}penetratin in the presence of chloroquine, (D) K_{25}HA2, (E) PEI. All complexes were incubated at 37°C for four hours and cells were treated with X-gal stain 48 hours post transfection. β-galactosidase expressing cells were stained blue.

This method of analysis involves counting the number of cells that are stained and therefore can be subject to error. Hence, expression was quantified more accurately using flow cytometry analysis or fluorescence activated cell sorting (FACS), which proves to be a more sensitive method. Figure 6.13 shows that K_{25}penetratin alone achieved only about 1% expression compared to 30% in the presence of chloroquine. It is noteworthy that with FACS analysis, chloroquine displays small amounts of autofluorescence and this should be taken into account when interpreting expression levels in the presence of chloroquine. PEI achieved over 55% of expression without the need for chloroquine, almost twice as much as K_{25}penetratin with chloroquine. Both methods of determining the percentage of cell expression levels exhibited similar trends in B16 cells with all the delivery vectors tested.

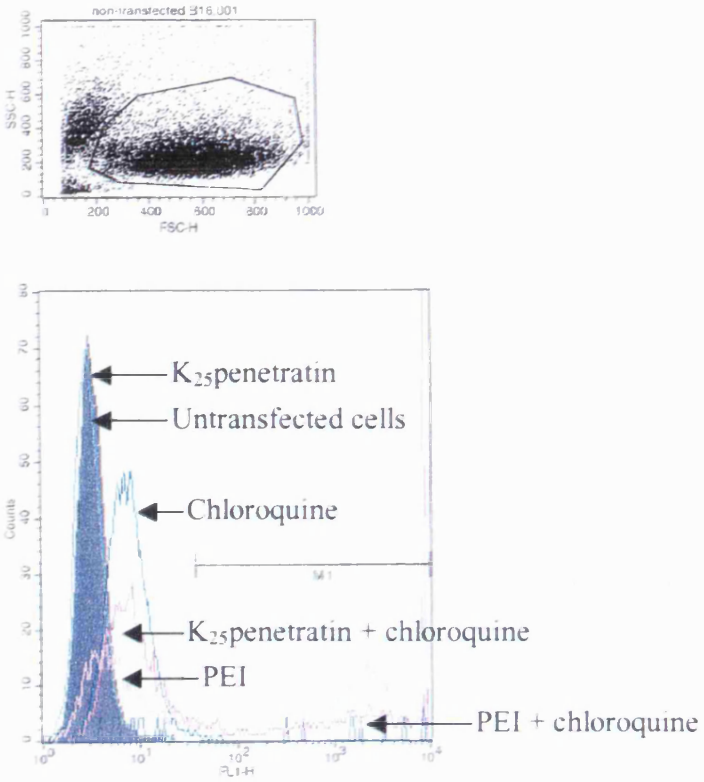

SAMPLE	% Gated (M1)
Untransfected cells	0.02
Chloroquine only	0.69
K_{25}penetratin	0.11
K_{25}penetratin+ chloroquine	33.96
PEI	58.95
PEI + chloroquine	51.23

Figure 6.13. FACS analysis of B16 cells transfected with K_{25}penetratin and PEI at their optimum charge ratios. The pEGFP-N1 (2 µg) was complexed with the gene transfer agents and incubated at 37°C for four hours in the presence of 100 µM chloroquine where necessary. FL-1-Height on the x-axis represents the fluorescence intensity at 530 nm ± 15 nm and Events on the y-axis represents the cell counts. Table shows the percentage values for gated cells.

6.3.6.2 *HEK293 cells*

The transfection efficiency in HEK293 cells for the various gene transfer agents was, in most cases, about twice the activity obtained in B16 cells with all vectors (with or without chloroquine) including K_{25} alone. PEI transfected with chloroquine in this cell line gave high expression levels similar to PEI alone.

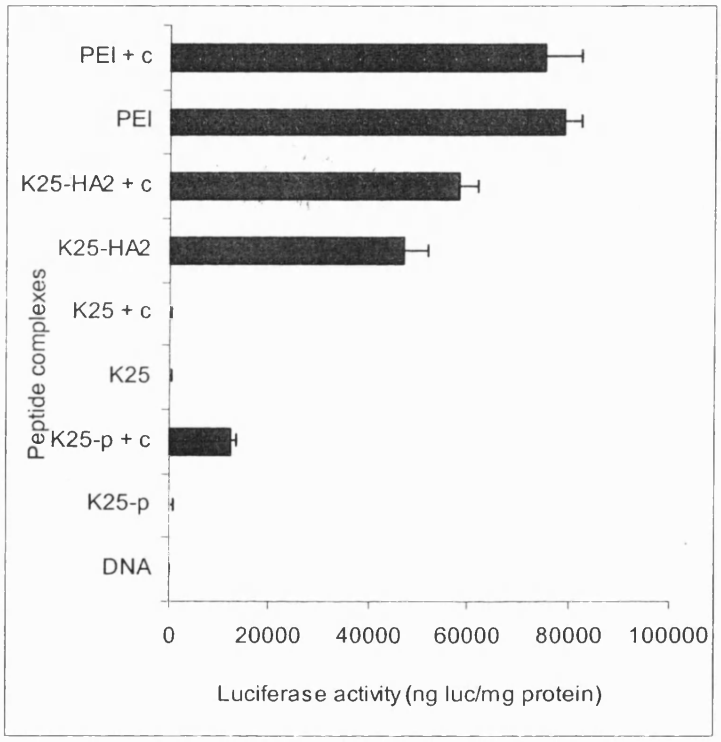

Figure 6.14A. Comparative transfection studies in HEK293 cells. Luciferase expression following transfection of pCMV*luc* (2 μg) complexed with various gene delivery vectors at their respective optimum charge ratios (+/-). Complexes were transfected in the absence and presence of 100 μM chloroquine (c). Expression was assayed 24 hours post initiation of transfection. Data points represent the mean ± SD of three replicates. DNA only was used as a negative control.

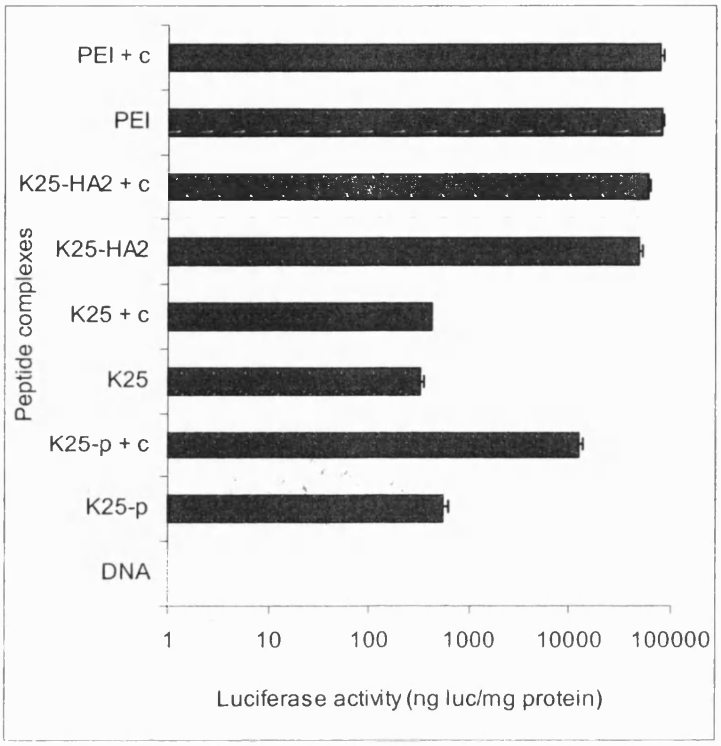

Figure 6.14B. Comparative transfection studies in HEK293 cells in a log representation.

6.3.6.3 HeLa cells

Figure 6.15 shows comparative transfection results in HeLa cells. PEI and K_{25}HA2 were very efficient transfection agents although PEI achieved about two times the transfection activity of K_{25}HA2. Expression levels were similar to those obtained in HEK293 cells. However, there was a marked decrease in the transfection activity of PEI in the presence of chloroquine while the transfection of K_{25}HA2 was enhanced by chloroquine. K_{25}penetratin expressed relatively low levels of luciferase even in the presence of chloroquine.

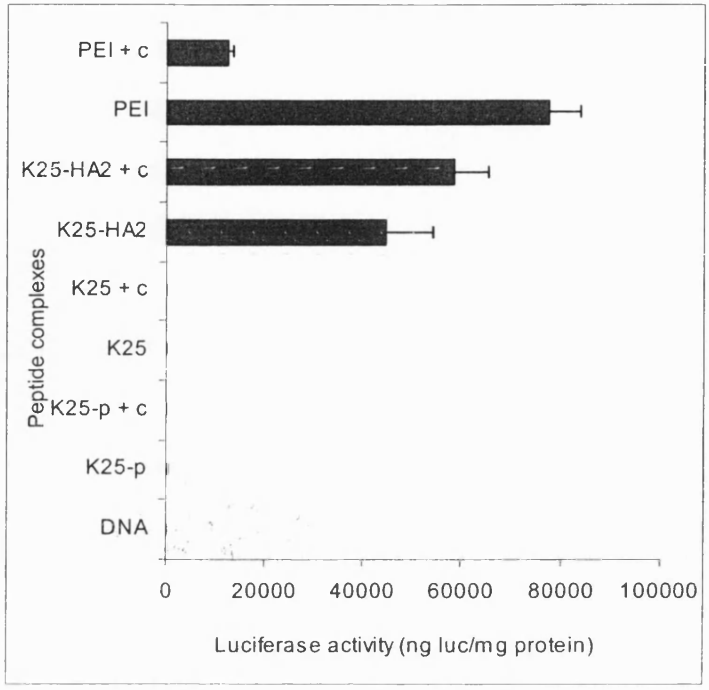

A

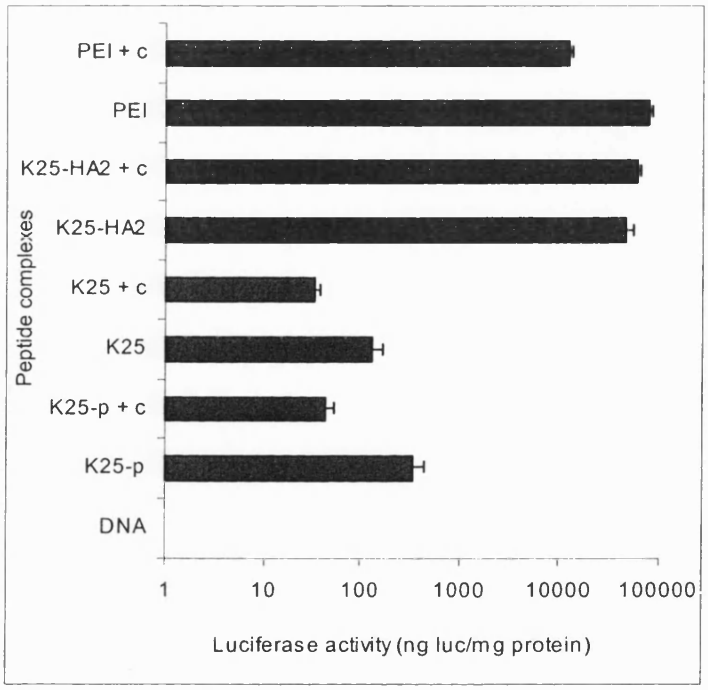

B

Figure 6.15A and B. Transfection in HeLa cells. Luciferase expression following transfection of pCMV*luc* (2 μg) complexed with various gene delivery vectors at their

respective optimum charge ratios (+/-). Complexes were transfected in the absence and presence of 100 μM chloroquine (c). Expression was assayed 24 hours post initiation of transfection. Data points represent the mean ± SD of three replicates. DNA only acted as a negative control. B is a log plot of the data.

6.3.6.4 A549 cells

Generally, the levels of luciferase expressed in this cell line were lower than in previous cell lines studied. PEI proved to be the best efficient transfection agent without the presence of chloroquine. The difference in transfection efficiency between K_{25}HA2 and PEI was much greater, with the latter almost three times more efficient than the former. K_{25}penetratin mediated some transfection on its own as well as in the presence of chloroquine.

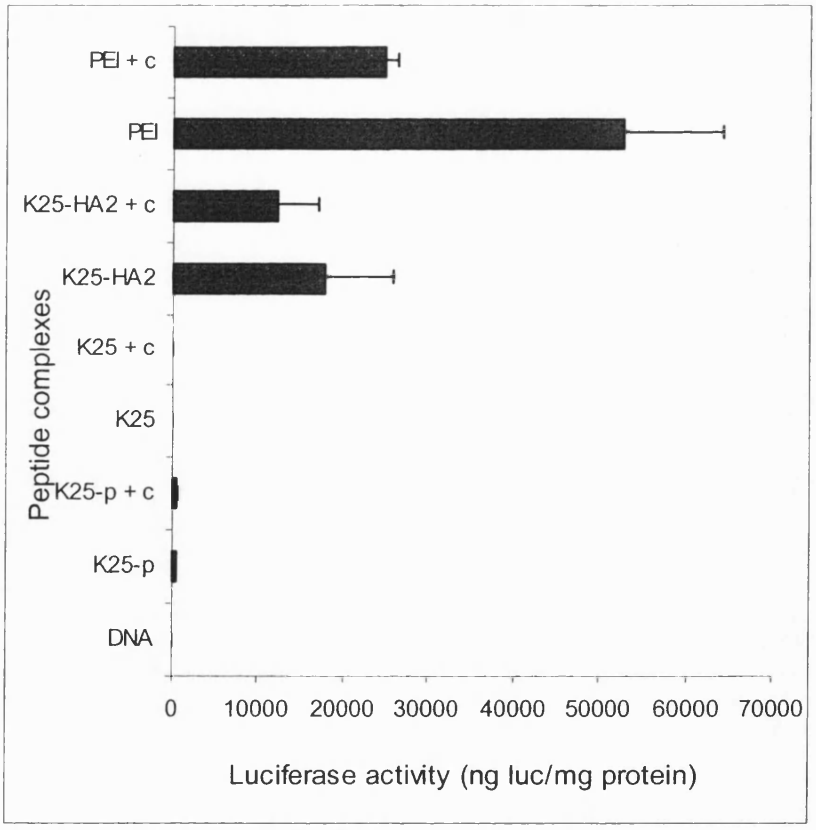

A

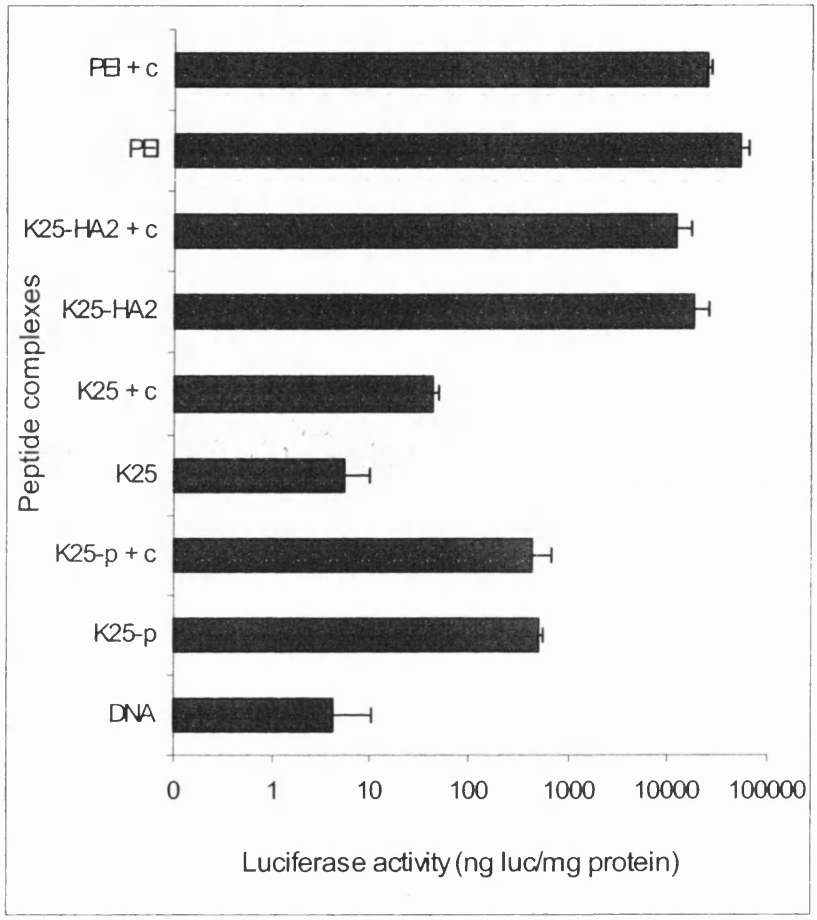

B

Figure 6.16A and B. Transfection in A549 cells. Luciferase expression following transfection of pCMV*luc* (2 μg) complexed with various gene delivery vectors at their respective optimum charge ratios (+/-). Complexes were transfected in the absence and presence of 100 μM chloroquine (c). Expression was assayed 24 hours post initiation of transfection. Data points represent the mean ± SD of three replicates. Free DNA was incorporated as a negative control. B is a log representation of the data.

6.3.6.5 16HBE14o⁻ cells

In this cell line the levels of luciferase activity were relatively very low. The gene transfer agents, including PEI, displayed about half as much expression as with previous cell lines. Luciferase activity was two-fold higher in PEI transfected cells compared with K_{25}HA2 alone or in the presence of chloroquine.

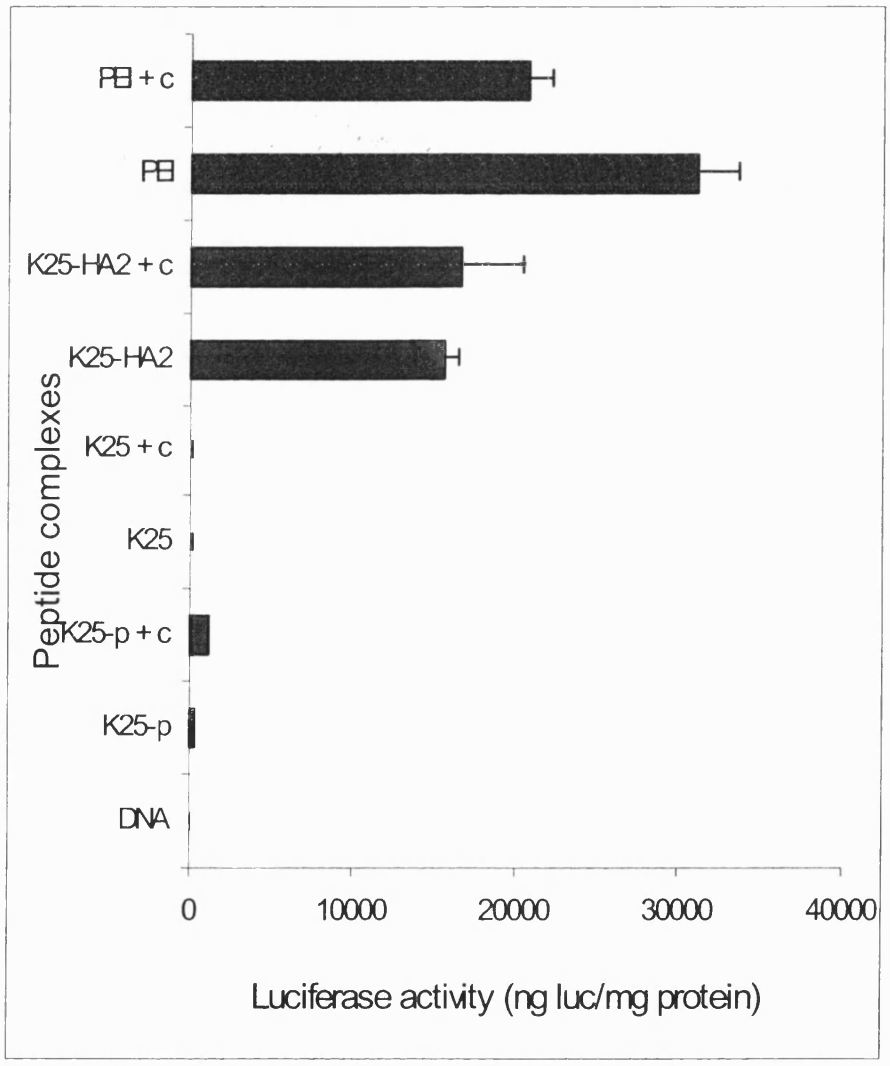

A

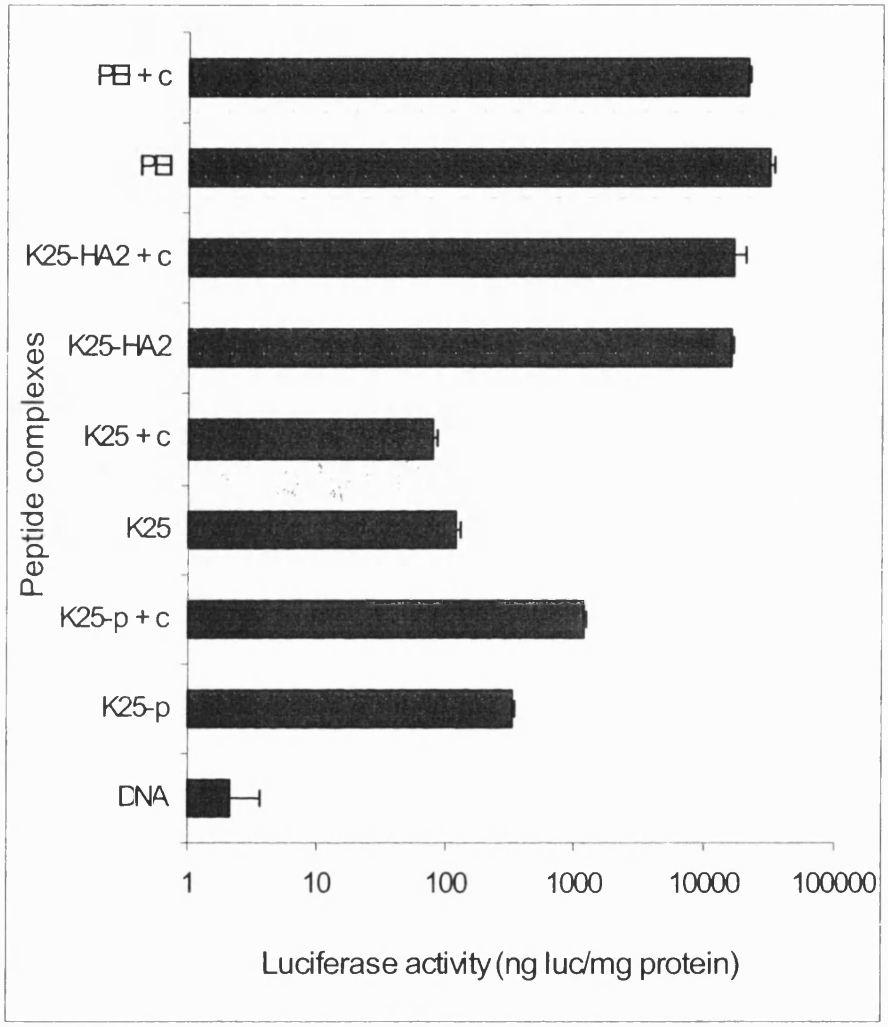

B

Figure 6.17A and B. Transfection in 16HBE14o$^-$ cells. Luciferase expression following transfection of pCMV*luc* (2 μg) complexed with various gene delivery vectors at their respective optimum charge ratios (+/-). Complexes were transfected in the absence or presence of 100 μM chloroquine (c). Expression was assayed 24 hours post initiation of transfection. Data points represent the mean ± SD of three replicates. Free DNA only was used as a negative control. B represents a log plot of the transfection data.

6.3.6.6 *FEK$_4$ cells*

A comparative transfection study in FEK_4 cells is shown in Figure 6.18. The transfection levels were relatively very low. Both PEI and K_{25}HA2 proved to be more efficient with PEI displaying the highest activity by an appreciable margin. Transfection with K_{25}penetratin in the presence of chloroquine gave similar activity to that of PEI and chloroquine.

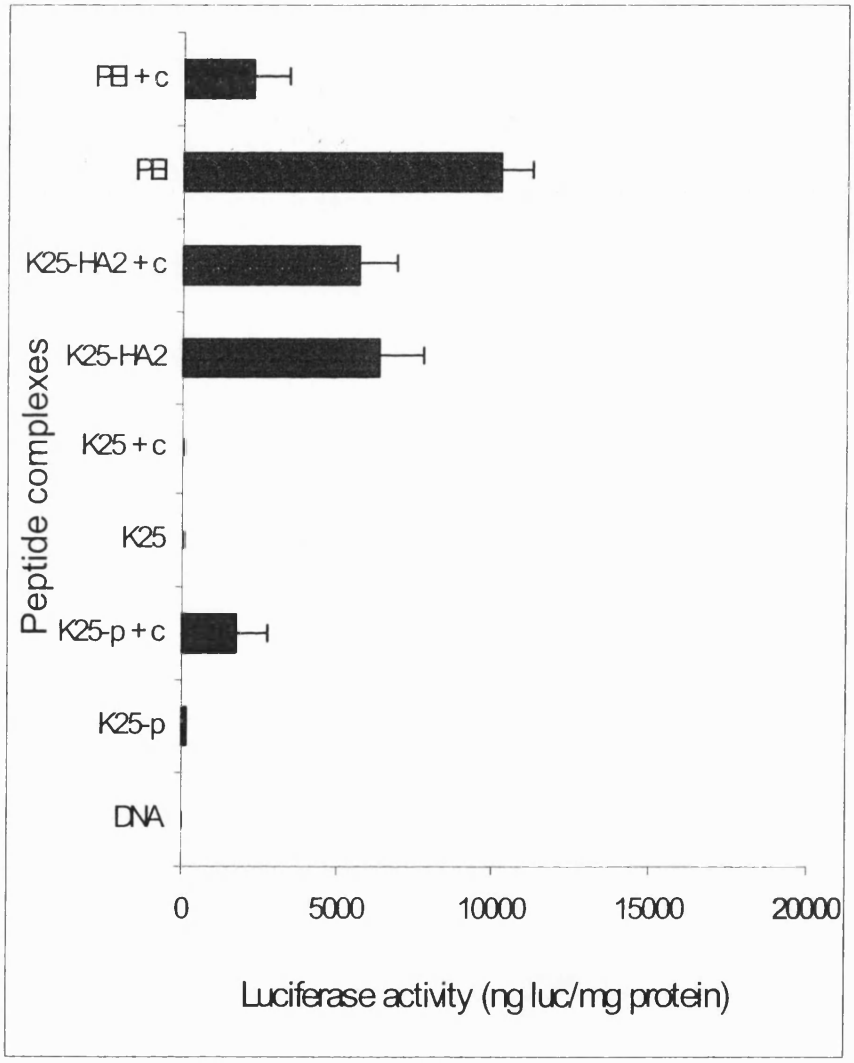

A

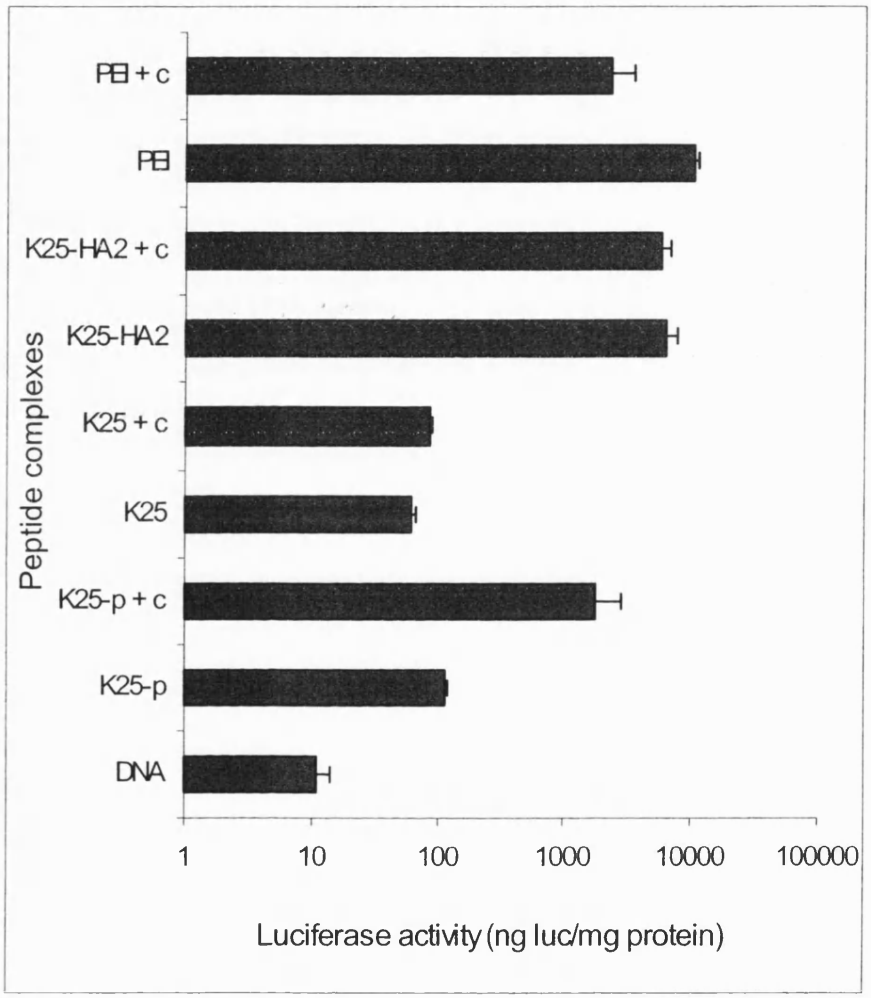

B

Figure 6.18A and B. Transfection in FEK_4 cells. Luciferase expression following transfection of pCMV*luc* (2 μg) complexed with various gene delivery vectors at their respective optimum charge ratios (+/-). Complexes were transfected in the absence or presence of 100 μM chloroquine (c). Expression was assayed 24 hours post initiation of transfection. Data points represent the mean ± SD of three replicates. DNA alone served as a negative control. B is a log plot representation of the transfection data.

6.3.7 Multi-component transfection systems

The gene transfer agents, PEI and K_{25}HA2 employed in this study, were both co-complexed with penetratin or K_{25}penetratin. The combination of PEI with either K_{25}penetratin or penetratin reduced transfection activity of the polymer. However, the combination of K_{25}HA2 with either K_{25}penetratin or penetratin appeared to enhance transfection activity but this was not statistically significant.

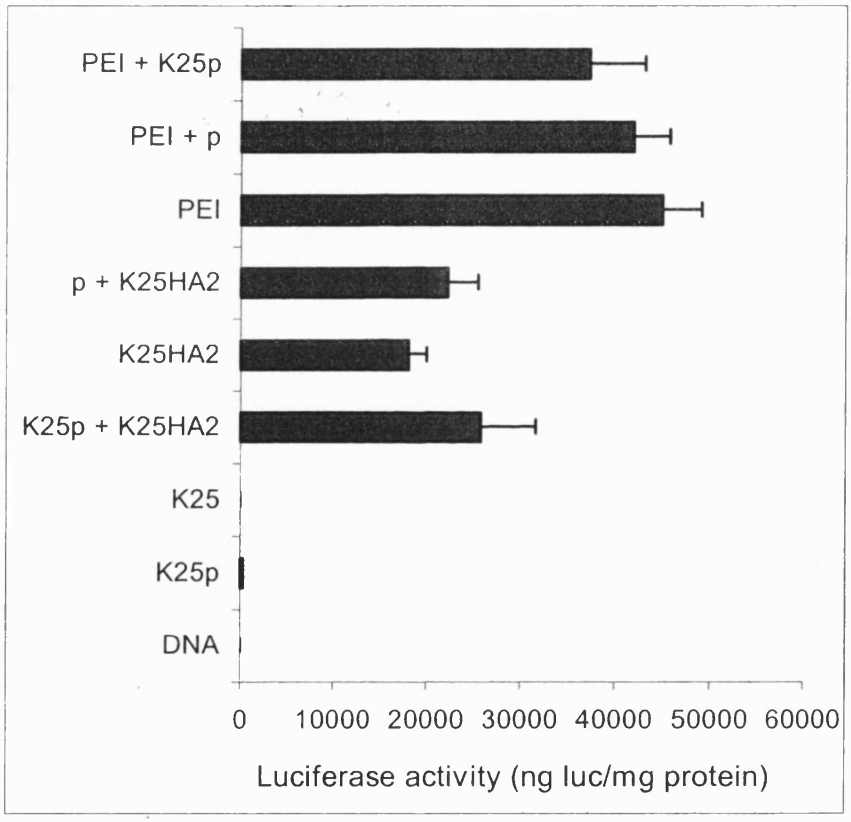

Figure 6.19. Transfection of multi-component systems in B16 cells. Luciferase expression following transfection of pCMV*luc* (2 μg) complexed with two gene delivery vectors at the same time. Expression was assayed 24 hours post initiation of transfection. Data points represent the mean ± SD of three replicates. Naked DNA was used as a negative control.

6.3.8 Effect of centrifugation on transfection efficiency in B16 cells

The effect of centrifugation (300 *g* for 5 minutes) on the efficiency of transfection mediation by gene transfer agents was investigated in B16 cells and is shown in Table 6.3. The gene delivery vectors were complexed with pCMV*luc* and transfected at their optimum charge ratios with or without centrifuging the cell culture plates. The results showed that this process of spinning the culture plates before incubation proved to be beneficial for all the gene transfer agents. However, the increase of transfection efficiency due to spinning was only significant for K_{25}penetratin.

Gene delivery vector	Mean transfection efficiency (ng luc/mg protein)		% increase on spinning	P value
	No spin	Spin		
K_{25}penetratin	343.98	2275.13	84.9	0.0062
K_{25}penetratin + c	7918.79	9641.97	17.9	0.3000
K_{25}HA2	16996.01	23564.25	27.9	0.0790
K_{25}HA2 + c	28199.19	34088.21	17.3	0.1600
PEI	37855.63	38749.72	2.3	0.8800

Table 6.3. Effect of centrifugation on transfection in B16 cells. Luciferase expression following transfection of pCMV*luc* (2 μg) complexed with various gene delivery vectors at their respective optimum charge ratios. Transfection of B16 cells was carried out with or without centrifugation. Data points represent the mean ± SD of three replicates. Free DNA (+/-spin) only was used as a negative control. P values ≤ 0.05 are significant.

6.3.9 Toxicity of polymer/peptides.

The MTT assay was used to determine levels of toxicity of various gene delivery agents. Figure 6.20 shows a comparison of the percentage of B16 cells viable after 3 hours with the peptides and PEI. The peptides, K_{25}, K_{25}penetratin and penetratin all displayed similar levels of percentage cell viability, especially at lower peptide concentrations. K_{25}penetratin showed slightly lower cell viability than K_{25} and penetratin at higher concentrations of peptides. PEI displayed the highest level of toxicity. The charge ratio calculated for PEI is only theoretical and is based on its protonation outline where one in six amines are charged under physiological conditions.

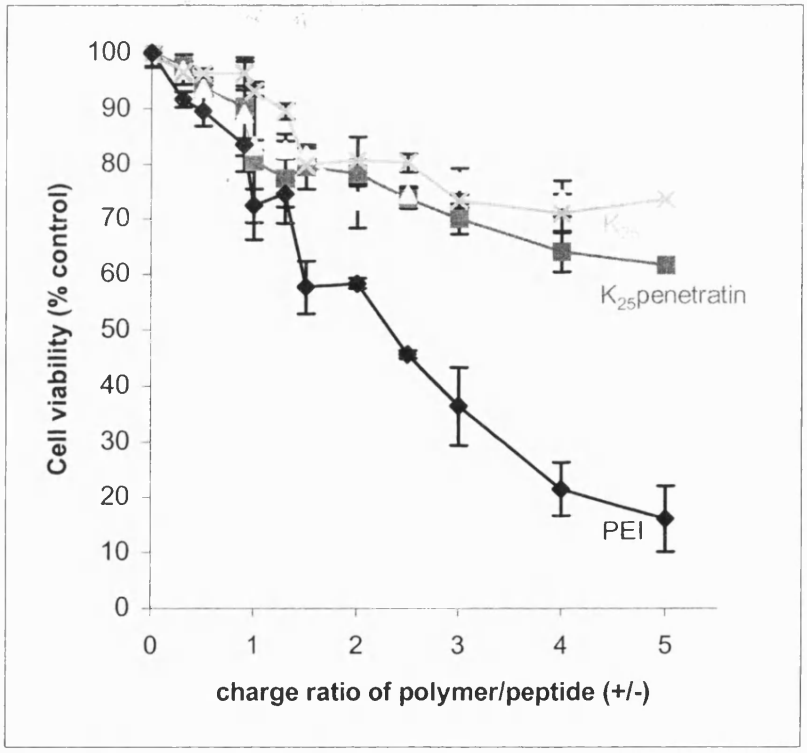

Figure 6.20. Determination of toxicity of uncomplexed gene delivery agents in B16 melanoma cells. Various additions of peptides/polymer were made to the wells equivalent to concentrations similar to that used in transfection experiments. Cell viability was determined by comparison with a control population of cells, plated out 16 hours before the MTT assay, using the calibration curve (Appendix G). Data points represent an average of triplicate evaluations.

All peptides displayed comparable toxicity levels, with higher charge ratios giving higher toxicity. The polycations were found to be non-toxic at concentrations giving optimum transfection efficiency: B16 cells exhibited over 60% viability at the range of charge ratios tested, for all peptides. PEI showed a higher toxicity level in comparison at a similar range in the absence of DNA. However, levels of PEI toxicity on B16 cells was generally low and occurred at charge ratios higher than that required for optimal transfection efficiency. This can be explained by the fact that the cationic charges are not neutralized under these conditions.

6.3.10 Particle size analysis

A comparative analysis of particle size exhibited by peptide-DNA complexes at their respective optimum charge ratios used for transfection is shown in Table 6.4. The measurements were made in 5% glucose using the ZetaPlus Particle Sizing Software by Brookhaven Instruments Corp.

Peptides	Optimum charge ratio	1	2	3	Mean diameter (nm)
Polylysine (K_{25})	1.5	87.7	85.3	115.5	96.2
K_{25}penetratin	2.0	99.5	88.0	91.0	92.8
Penetratin	3.5	104.1	89.1	112.4	101.9

Table 6.4. Determination of particle size analysis of polycation-DNA complexes. Complexes were prepared using pCMV*luc* and appropriate quantities of peptides equivalent to their optimum charge ratios used for transfection experiments. Complexes were incubated for 20 minutes at room temperature. Measurements were made at 20°C and five runs were recorded per sample, n = 3.

6.3.11 Erythrocyte Lysis Assay

K_{25}HA2 demonstrates enhanced and pH-specific activity in the lysis of erythrocytes relative to K_{25}penetratin.

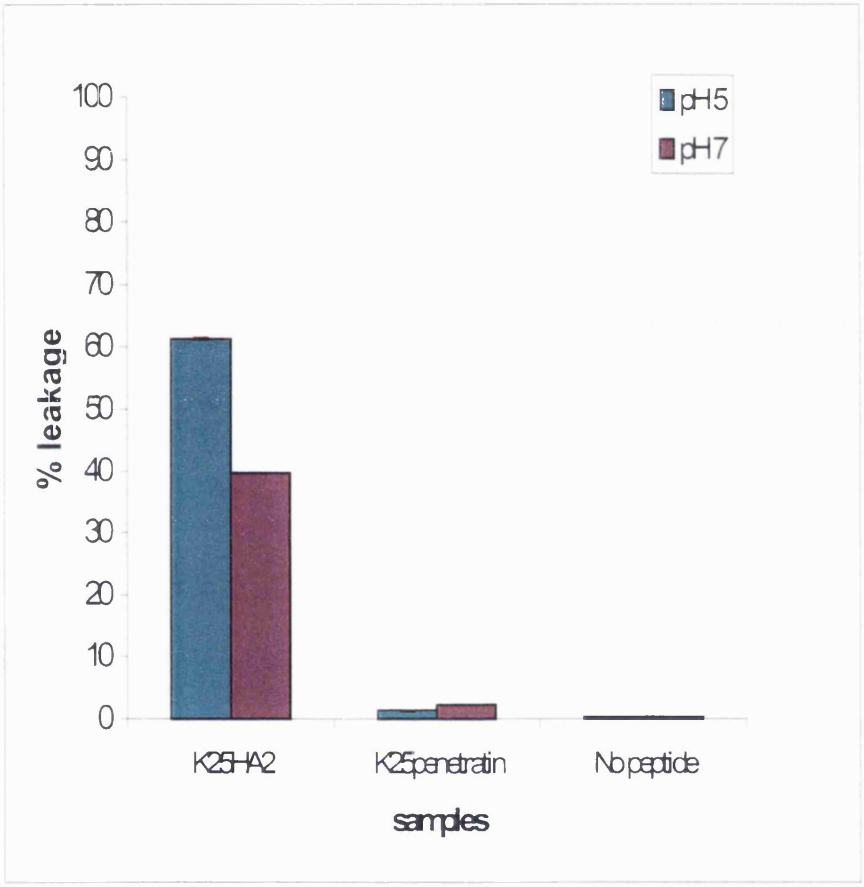

Figure 6.21. Erythrocyte leakage activity of K_{25}penetratin and K_{25}HA2. The absorption of haemoglobin is plotted using 10% Triton X-100 to give 100% lysis. Values are normalised to 100%. n = 1.

6.4 DISCUSSION

6.4.1 DNA binding

Plasmid DNA has difficulty gaining access to the cytoplasm and nucleus of eukaryotic cells because of its large size and polyanionic property. Hence, it is necessary to neutralise the excess negative charges of DNA as well as condense DNA to a size that facilitates cell entry. The neutralisation of excess negative charges on DNA with polycations has been investigated by various techniques such as gel mobility shift assay (Wagner *et al.*, 1990, Vitiello *et al.*, 1996) and the ethidium bromide spectrofluorimetric assay (Gershon *et al.*, 1993). The interaction between penetratin derivative and plasmid DNA in this study was investigated using both techniques.

It has been previously shown that the interaction between cationic polymers/polycations and plasmid DNA is electrostatic (Bloomfield, 1996). The extent of plasmid DNA binding by penetratin was determined by gel mobility assay. This requirement for a high charge ratio implies that penetratin does not have a strong electrostatic interaction with plasmid DNA. This was supported by data obtained using the ethidium bromide fluorescence assay. There is a distinct fluorescence enhancement when ethidium bromide intercalates with double-stranded DNA. The dye binds at a stoichiometry of one dye per 4-5 base pairs of DNA and its fluorescence is enhanced by 20- to 30-fold. Ultraviolet radiation is absorbed by the DNA and transmitted to the bound dye, the energy being re-emitted in the red-orange region of the visible spectrum (Sambrook *et al.*, 1989). Spectrofluorimetric quantitation of displacement from its intercalation site was used to quantitate the charge ratio at which these peptides competitively displace ethidium bromide from DNA. Comparative studies with K_{25}penetratin showed that the electrostatic interaction with plasmid DNA proved to be stronger than that of penetratin. A relatively low mass of K_{25}penetratin was required to neutralise DNA. This suggests that the attachment of the polylysine chain (K_{25}) to penetratin creating a peptide with a cluster of positively charged amino promoted a 1: 1 interaction with DNA phosphate groups. Thus K_{25}penetratin binds more strongly probably resulting in a smaller and more compact structure, while promoting effective DNA uptake into the cell. Olins *et al.*, 1968

have shown that a minimum of eight linear lysines is required in order to induce the biphasic melting behaviour on complexation of DNA that is characteristic of polylysines. The advantage of using K_{25} is that it avoids poorly defined heterogeneous complexes that are difficult to characterise on a molecular basis, often achieved with commercial polylysines that have been found to be polydisperse. This is a longer oligolysine chain than that used by Gottschalk *et al.*, 1996 who developed a peptide with 10 lysines, which apparently still binds to DNA. In this study, K_{25} provided a good comparison with the endosomolytic agent, K_{25}HA2. Differences were seen between the amounts of each peptide required to achieve plasmid DNA condensation. Profiles were related to the net charge of each peptide as well as the accessibility of their charged residues to interact with plasmid DNA. Condensation of DNA is an important factor as it not only enhances expression in the penetratin system, but has been shown to improve gene delivery and expression in various other systems (Wagner *et al.*, 1991; Fominaya and Wels, 1996). The lysine chain may contribute to a resistance to degradation of the DNA-peptide complex by cellular processes, possibly due to a lack of accessibility of the DNA to lysosomal nucleases because of tight binding to the lysine moiety.

The ethidium bromide exclusion profiles on DNA complexation were investigated in an attempt to confirm that both the labelled and unlabelled peptides were behaving in a similar manner. The ability of K_{25}penetratin to condense DNA was dramatically reduced by the presence of BODIPY FL (Figure 6.6). BODIPY-labelled K_{25}penetratin caused a much lower reduction in fluorescence and was unable to exclude ethidium bromide from plasmid DNA even at higher charge ratios compared to the peptide alone. The difference in the interaction with plasmid DNA between the labelled and unlabelled peptides was further confirmed in transfection studies. The ability to transfer DNA into cells was totally abolished in the presence of BODIPY (Figure 6.8). One explanation for these differences in behaviour is the fact that the presence of BODIPY prevents the peptide from interacting with plasmid DNA. BODIPY is a molecule of relatively large size (MW = 641.5), which exerts significant steric hindrance on the interaction with plasmid DNA. The use of BODIPY as an extrinsic probe proved to be intrusive and led to changes in the functional and structural properties of the labelled peptide. It would be to great

advantage to have a chemically and biologically stable, non-intrusive fluophore, which could be incorporated in a peptide.

6.4.2 Endosomal release

For efficient transfection, escape from the endosome and delivery to the cytoplasm are required. Various groups have observed similar approaches to cytoplasmic delivery involving the endosomal pathway, where the endosome is disrupted and allows DNA access to the cytoplasm prior to fusion of the endosome with the lysosome (Behr *et al.*, 1994; Gao and Huang, 1995). In the presence of chloroquine, cultured cells expressed the reporter gene following transfection with peptide-condensed plasmid DNA. The luciferase activity was maximal when the transfection was conducted in the presence of 100 μM chloroquine. This result was in agreement with those obtained for transfections of an erythroblast cell line HD3 using plasmid/transferrin-polylysine complexes (Zenke *et al.*, 1990).

Although the mode of action of chloroquine is not clear, it is thought that apart from neutralizing the pH of endocytotic vesicles as a weak base (Poole and Okhuma, 1981), it prevents fusion of endosomes with the lysosomes where complexes get degraded. Its buffering of the endosomal pH causes a rise in the osmolarity of the vesicle such that lysis may take place leading to the release of DNA into the cytoplasm. Chloroquine has also been shown to induce dissociation of plasmid DNA/peptide complexes in vesicular compartments (Erbacher *et al.*, 1996). This may help explain why the activity of the bifunctional peptide, K_{25}penetratin, was dramatically enhanced when chloroquine was present in the transfection stage. The critical requirement for chloroquine is a significant finding as it implies that most of the K_{25}penetratin/DNA complexes enter the cells by endocytosis. Chloroquine has been shown to increase the egress of complexes from endosomes and mediate efficient gene transfer by several other groups (Hedin and Thyberg, 1985; Taxman *et al.*, 1993; Midoux *et al.*, 1993; Cotten *et al.*, 1990). Cell lines differ considerably with respect to the need for chloroquine for efficient transfection, implying that there are variations in the integrity of endosomal membrane components.

Other groups have demonstrated the use of membrane-active peptides in enhancing DNA delivery (Midoux *et al.*, 1993; Haensler and Szoka, 1993). K_{25}HA2 is a membrane-active amphipathic helical peptide. The membrane-disrupting action is demonstrated in the erythrocyte lysis study, which had a strong correlation with luciferase gene transfer efficiency. These results are in line with those reported by Plank *et al.*, 1994. Penetratin, on the other hand, is only very partially amphipathic, and amphiphilicity is not a requirement for its internalization (Prochaintz *et al.*, 1996). K_{25}penetratin displays little measurable lytic activity at pH 5 and 7 despite the fact that binding of penetratin to the membrane will occur since the membrane of erythrocytes possess negatively charged, sialic acid-modified glycoproteins. Investigations by Joliot *et al.*, 1991b reported clear interactions of penetratin with polysialic acid groups present on neuronal membrane surfaces. Singh *et al.*, 1992 also studied the interaction of polycations with negative charges on epithelial cell surfaces, which appears to be due to carboxylic acids of the sialic acid of glycoproteins and sulphate groups of proteoglycans. Schutze-Redelmeier *et al.*, 1996 reported data that suggest polysialic acid groups bind penetratin through electrostatic interactions, concentrating the peptide at the cell surface and protecting it from proteolytic degradation. This may help explain why penetratin has been found to exhibit very efficient translocating properties. Although the mode of action of penetratin is yet to be confirmed, preliminary studies have reported that cell entry does not involve endocytosis as it occurs at both 37°C and 4°C (Derossi and Prochiantz, 1995). This deviates from transfection results achieved in this study as the delivery of penetratin was enhanced significantly in the presence of chloroquine, implying endosomal uptake. Among peptide vectors that have been proposed for intracellular delivery, those involving receptor-mediated mechanisms have been successful in gene delivery (Perales, 1994). It is noteworthy that preliminary studies done to establish a mechanism of action for penetratin have not assessed interactions with plasmid DNA, that is complexed systems, which creates a different molecular environment compared to the peptide on its own.

Polycation-mediated gene transfer is thought to involve DNA aggregation and binding of the resulting particles to anionic residues on the plasma membrane (Behr *et al.*, 1994). The complexes should exhibit an overall net positive charge to be efficient. PEI consistently proved to be the best gene delivery agent in all experiments and all cell lines

tested in this study, without the need for chloroquine. The buffering capacity of PEI is substantial at any pH making it a highly efficient vector for delivering plasmids *in vitro* and *in vivo* (Boussif *et al.*, 1995). The penetratin peptide showed no significant effect on PEI transfection, perhaps due to a saturation of positive charges, and hence achieves no additional benefit. The interaction between penetratin and PEI is not a covalent one, hence it is difficult to conclude if penetratin can actually exert an enhancement of PEI activity.

6.4.3 Transfection efficiency of gene delivery vectors

Preliminary transfection data with penetratin in B16 cells showed that there was little gene expression at all charge ratios tested, although it was able to condense plasmid DNA at high charge ratios. The improvement in transfection efficiency achieved with K_{25}penetratin was due to the inclusion of a chain of lysines. Fritz *et al.*, 1996 observed a similar result, which involved gene transfer using a lysine-rich histone/DNA complex in the presence of chloroquine. Presumably, K_{25}penetratin derives its DNA transfection efficiency from both the penetrating ability of penetratin and the known properties of the added polylysine cationic peptide. Apart from the fact that HEK293 cells have weaker endosomal membranes making them much more readily transfected. Wolfert and Seymour, 1998 also observed that HEK293 were readily transfected with polylysine/DNA complexes *in vitro*. In all other cell lines tested, the expression level of PEI was dramatically reduced with chloroquine. In particular, HeLa cell line were much more sensitive to toxicity and may require <100 μM chloroquine as this amount of chloroquine plus PEI proved too toxic. The transfection efficiency of the endosomolytic peptide, K_{25}HA2, was increased with chloroquine in all cell lines with the exception of A549s and FEK_4 cells. Although it is possible that < 100 μM of chloroquine may result in better transfection of K_{25}HA2 in these cells, the transfection efficiency of K_{25}penetratin was consistently improved with chloroquine at this concentration. The transfection efficiency of K_{25}penetratin alone was relatively similar in all cell lines although FEK_4s, A549s and 16HBE14o- cells generally proved to be more resistant to transfection. The transfection of these delivery peptides in primary cells proved very

inefficient implying the very high resistance these groups of cells have to transfection probably due to decreased cell binding. Bahnson *et al.*, 1995 observed refractory transfection efficiency with peripheral blood mononuclear cells because they lack cation-binding surface components. These cationic vectors bind to anionic sugars present on the membrane of adherent cells only. Derossi and Prochiantz, 1995 reported the significance of these interactions in permitting or facilitating the internalization process of various polypeptides. Labat-Moleur *et al.*, 1996 showed the difficulty in transfecting peripheral blood mononuclear cells due to the absence of these membrane components. Wyman *et al.*, 1996 reported a lack of transfection mediation in primary epithelial cells using the cationic amphipathic peptide KALA. A variation in transfection efficiency in cell lines tested may be the result of differences in cell surface composition that affect the binding of complexes.

Transfection efficiency was further improved in B16 cells when the culture plates were centrifuged after the delivery vectors have been added to the wells. Transfection of cells in culture involves the random movement of complexes in suspension to the close proximity of the cell surface. Spinning the culture plates allows smaller polycation/DNA complexes to come into closer proximity with the surface of the cells. This makes a greater amount of these complexes available for uptake into the cells, which in turn results in higher expression levels. Similar data were observed by Boussif *et al.*, 1996 in a study to optimize conditions used in transfection. There was no beneficial effect on PEI/DNA complexes probably due to their bigger particle population most of which settle on to the cells without the need for centrifugation. Swaney *et al.*, 1997 reported a synergistic effect in the transfection efficiencies of cationic complexes when combined with centrifugation.

6.4.4 Characterization studies

Particle size analysis of polycation/DNA complexes demonstrated that the complexes were between 90 – 101 nm mean diameter. The use of 5% glucose in these experiments provides isotonic conditions found *in vivo*. It is necessary to control the size of complexes such that they are small enough to access target cells. Most forms of triggered

membrane penetration act via the endosomal membrane following endocytosis, and pinocytic internalization is usually limited to materials of less than 100 nm diameter (Wagner *et al.*, 1991, Perales *et al.*, 1994a). Receptor-mediated gene transfer was found to be far more effective when DNA was condensed into particles of approximately 80 – 100 nm (Ogris *et al.*, 1998). Preliminary measurements were carried out in HBS in an attempt to mimic transfection conditions as close as possible. However, the measurements with HBS proved to be problematic as extremely large (>1600 nm) aggregated particles were formed. A similar observation was also found by Tang and Szoka, 1997. Sometimes it was not possible to interpret results with HBS, as the interference of the light scattering path was too great.

6.5 SUMMARY

Penetratin has considerable potential for delivery of small polypeptides (and possibly oligonucleotides) by direct transfer of the molecule across the plasma membrane. Fahraeus *et al.*, 1996 observed entry into S phase of HaCaT cells was blocked by a p16-derived peptide when it was coupled to penetratin. Although K_{25}penetratin is capable of mediating transfection in a variety of cell lines, this internalization process is not efficient for larger species such as plasmids used in this study. The K_{25} moiety helps to anchor penetratin to DNA, which does not display as high endosomolytic activity as amphipathic helical peptides. K_{25}penetratin appears to be membrane-active but most of the DNA is taken up primarily by endocytosis, which contradicts results from other groups (Derossi and Prochiantz, 1995). The cationic polymer, polyethyleneimine shows very effective DNA-binding, mediating efficient gene transfer, without the addition of chloroquine.

CHAPTER 7

SYNTHETIC VIRUS-LIKE PARTICLES FOR INTEGRIN-MEDIATED TARGETING

7.1 INTRODUCTION

Cationic polyplexes interact in a non-specific manner with most cells. If formulated with an endosomolytic polymer, such as PEI, cationic polyplexes are adequate for transfection *in vitro*. There are practical problems with the use of such polyplexes *in vivo*. When injected directly into solid tissues they tend to bind to any negatively charged surfaces causing them to be immobilised close to the injection site. One way to circumvent this problem may be to design negative or neutral particles, which use a selective ligand to promote uptake into target cells. This chapter investigates the design and assembly of polyplexes (or virus-like particles) for non-viral gene delivery. In their core polyplexes must contain the appropriate condensed DNA, and their design must include a mechanism for endosome escape. This chapter explores whether targeting of neutral or negative polyplexes could be achieved, and how the efficiency of targeting related to their total polycation content. Hart *et al.*, 1994 showed that particles in the form of filamentous phage could be targeted to cells using cyclic RGD peptides. Later an integrin-binding RGD peptide was coupled to polylysine (Hart *et al.*, 1996) to produce a polymer which was capable of targeting DNA to cells which expressed appropriate integrins. This study aims to combine an RGD peptide with PEI, a polymer that was first identified as a transfection reagent by Boussif *et al.*, 1995 and has been regarded as the reagent of choice for transfection of cells *in vitro* and *in vivo* (Coll *et al.*, 1999). The objective was to partly-neutralise the DNA with PEI, to mediate endosome escape, and then to add cationic peptides with or without a targeting function to the system. The integrin-binding moiety GACDCRGDCFCA (Pasqualini *et al.*, 1997) was used as a model ligand for this purpose.

7.2 MATERIALS AND METHODS

7.2.1 Materials

Cyclic-GRGDSPA was obtained from Bachem, UK and was employed in inhibition experiments.

The other materials used in this study include the reporter plasmid pCMV*luc*, PEI, K_{25} and K_{25}RGD, which have already been described in detail in chapter 2. The sequence of K_{25}RGD was as follows;

H_2N-K_{25}-GACDC**RGD**CFCA-COOH

7.2.2 Preparation of complexes

Appropriate mixtures of PEI and K_{25} or PEI and K_{25}RGD were prepared prior to DNA complexation and diluted to a final volume of 250 µl with Hepes buffered saline (HBS). 3 µg pCMV*luc* was diluted to a volume of 250 µl with HBS. In each case the PEI/peptide solution (or PEI alone for controls) was added to the DNA solution and immediately mixed by vortexing. For experiments involving DNA/PEI/peptide complexes the PEI content was kept constant at two N/P ratios of 4 and 2. Complexes were labeled according to the additional charge resulting from the cationic peptide content [ratio of lysine groups added per phosphate; equivalent to the additional charge ratio (+/-)]. The additional charge ratio relating to the K_{25} or K_{25}RGD content was varied within the range 0.1 to 1.0 (+/-) to produce DNA/PEI/peptide complexes with net negative as well as net positive charge.

7.2.3 Cell culture and transfection of cells

Two cell lines were employed in this study. Cos7 and B16 cells were routinely cultured as adherent monolayers in MEM as described in chapter 2. Cos7 cells, a fibroblast-like cell line established by SV40 transformation of CV-1 African green monkey kidney cells,

were obtained from the European Collection of Animal Cell Cultures (ECACC), UK. For routine culture, cells were subcultured 1 in 5 twice weekly. Cells were seeded onto six-well plates in 2 ml growth medium 24 hours before transfection. Complexes of pCMV*luc* with polycations were prepared 30 minutes prior to use, then transfections were carried out with 3 μg DNA per well (in 0.5 ml HBS) in the presence of 1.5 ml Opti-MEM. For competitive inhibition experiments, the cells were first incubated with 600 μg of cyclic-GRGDSPA per well, for 5 minutes, prior to addition of complexes. After 4 hours, the transfection medium was removed and replaced with 2 ml growth medium. Cells were harvested 24 hours after transfection and analysed using the Promega luciferase assay system. Luminescence generated in each sample was determined over 10 seconds using a Turner Design 20/20 luminometer. The concentration of protein in cell extracts was measured using the Bio-Rad Dc protein assay kit.

7.2.4 Zeta potential measurements

Zeta potential measurements of PEI-K_{25}RGD-DNA and PEI-DNA complexes formed were determined using an electrophoretic light scattering technique in the form of a Brookhaven ZetaPALS (zeta phase analysis light scattering), Zeta Potential Analyser (Brookhaven Instruments Corporation, USA). Measurements were made on PEI complexes formed in a tris 0.01 M solution pH 7.0. All sample vials, glass and plasticware were washed using prefiltered water to reduce particulate contamination. Measurements were made in a micro-electrophoresis cell thermostatically controlled at 25°C. The model or method of calculating zeta potential from the measured mobility using the dielectric constant and viscosity of the suspending fluid is based on the Smoluchowsky equation.

7.3 RESULTS

Complexes of pCMV*luc* with PEI transfected B16 (figure 7.1) and Cos7 (figure 7.2) cells spontaneously with N/P ratios between 6 and 9 showing the most efficiency. The transfection data showing the optimum N/P range was in agreement with published results Boussif *et al.*, 1995, and this is equivalent to a range of charge ratio (+/-) between 1 – 1.5.

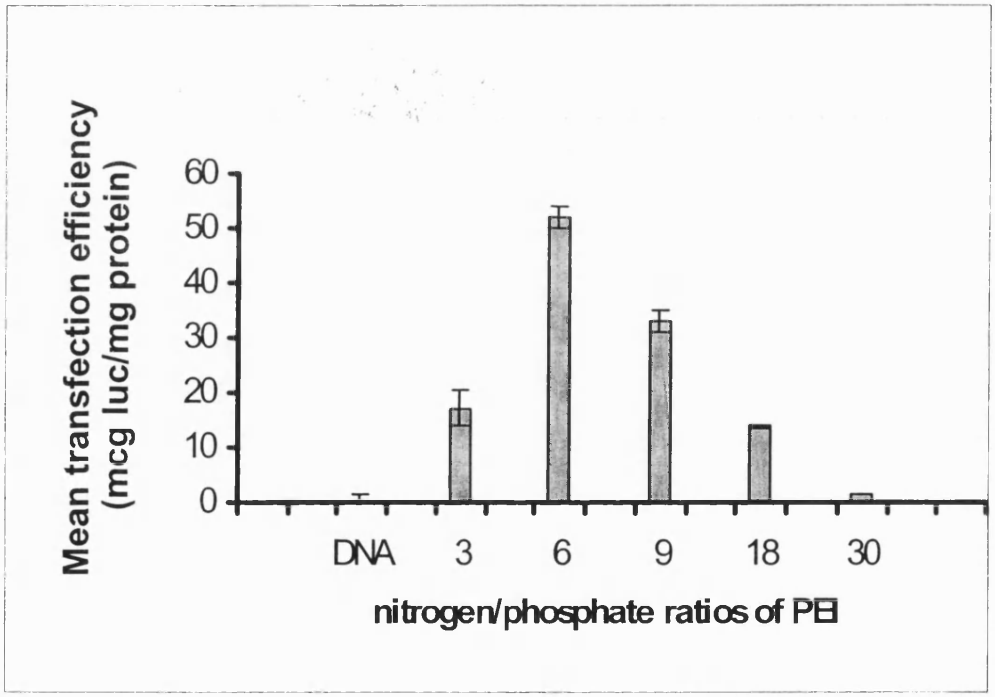

Figure 7.1. Luciferase expression in B16 cells as a function of the PEI content of polyplexes (mean ± sd, n=3). Complexes were formed between pCMV*luc* and PEI in the absence of additional peptide. PEI content is expressed as the nitrogen/phosphate (N/P) ratio within the complex. An N/P of 6 is approximately equivalent to charge-neutralisation. At N/P ratios <6 the particles were expected to be anionic. At the N/P ratio of 9 the particles were cationic.

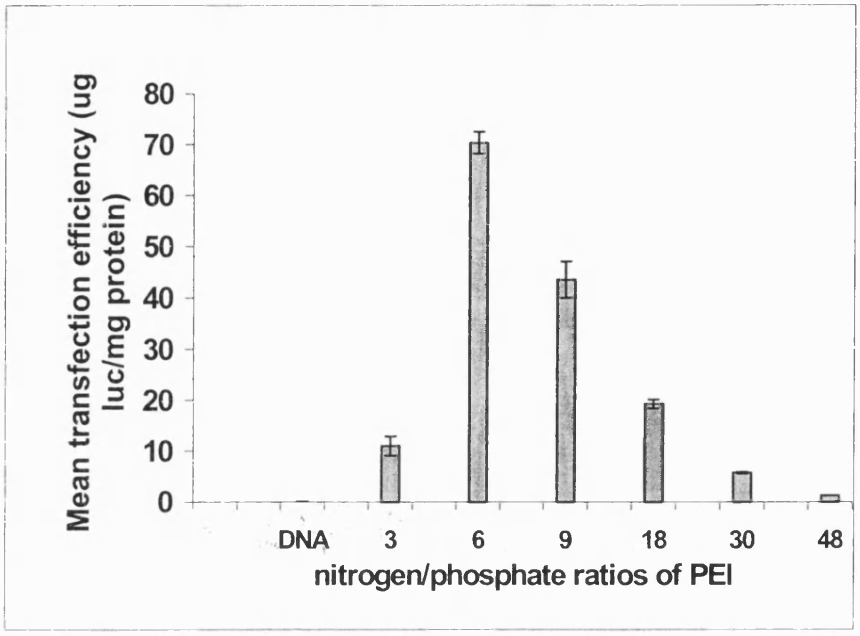

Figure 7.2. Luciferase expression in Cos7 cells as a function of the PEI content of polyplexes (mean ± sd, n=3). Complexes were formed between pCMV*luc* and PEI in the absence of additional peptide.

This study employed a longer oligolysine chain (K_{25}) as opposed to a K_{16} used by Hart *et al.*, 1997 to ensure that DNA binding was strong. K_{25}RGD was shown to condense DNA stochiometrically using the ethidium exclusion assay in a similar manner to K_{25} (figure 7.3). Polyplexes formed by co-condensing pCMV*luc* with K_{25}RGD were in all cases more active in Cos7 cells than the corresponding complexes containing K_{25} as evident in figures 7.4a and 7.5a. Figure 7.4a and 7.4b represent the biological activity of complexes prepared with slightly positive and substantially positive excesses. The activity of complexes prepared with lower peptide contents, exhibiting negative charge excesses is shown in figures 7.5a and 7.5b. Complexes containing K_{25} had similar activities in Cos7 cells irrespective of their net charge excess, whereas those containing K_{25}RGD resulted in 5 – 10 fold higher levels of gene expression. In each graph, the suffix in each case represents the additional charge ratio (+/-) conferred by the peptide

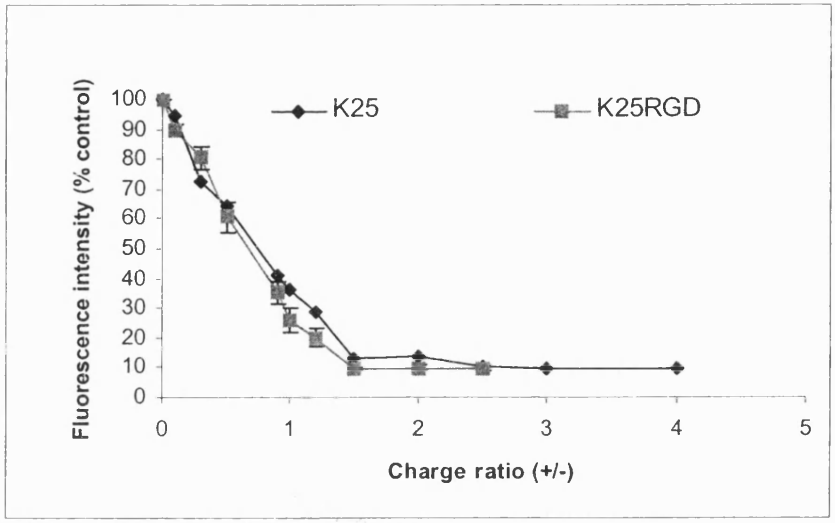

Figure 7.3. Ethidium bromide exclusion assay for K_{25}RGD and K_{25}.

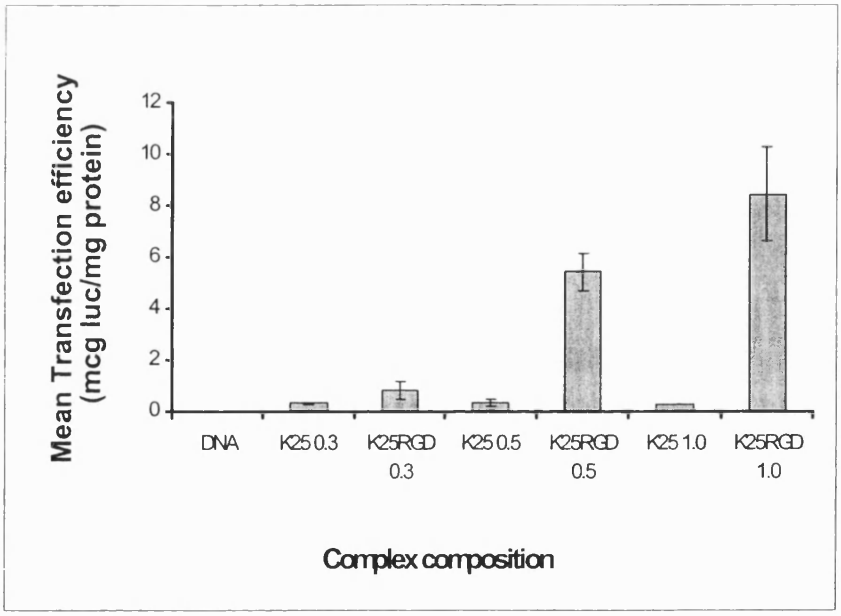

Figure 7.4a. Luciferase expression after transfection of Cos7 with polyplexes formed by complexation of pCMV*luc* with PEI/peptide mixtures (mean ± sd, n=3). PEI content was constant at N/P = 4. PEI/K_{25} or PEI/K_{25}RGD = polyplexes produced with mixtures of PEI and K_{25} or PEI and K_{25}RGD. Complexes with additional 0.3 (+/-) had negative charge excess; 0.5 (+/-) = slight positive charge excess; 1.0 (+/-) = clear positive charge excess.

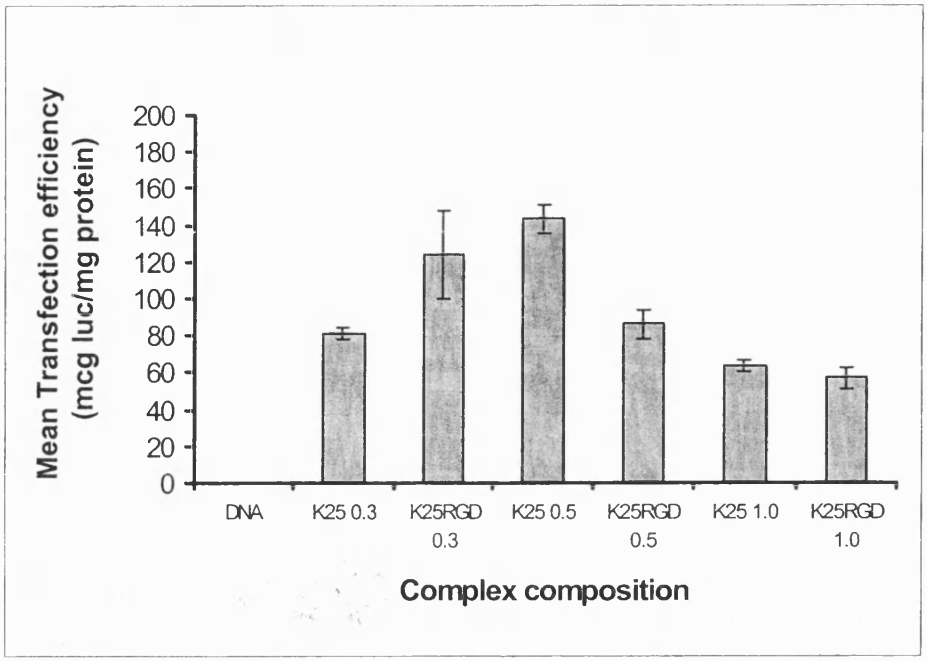

Figure 7.4b. Luciferase expression after transfection of B16 cells with polyplexes formed by complexation of pCMV*luc* with PEI/peptide mixtures (mean ± sd, n = 3).

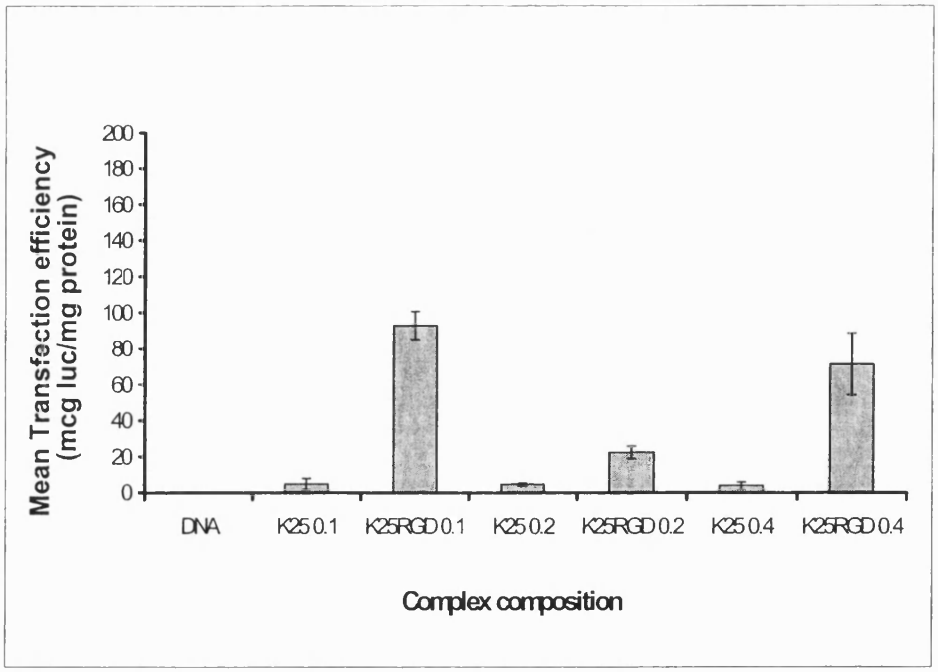

Figure 7.5a. Luciferase expression after transfection of Cos7 cells with polyplexes formed by complexation of pCMV*luc* with PEI/peptide mixtures (mean ± sd, n = 3). Complexes with additional 0.1 and 0.2 (+/-) had negative charge excess; 0.4(+/-) = close to charge neutralization/slightly positive charge.

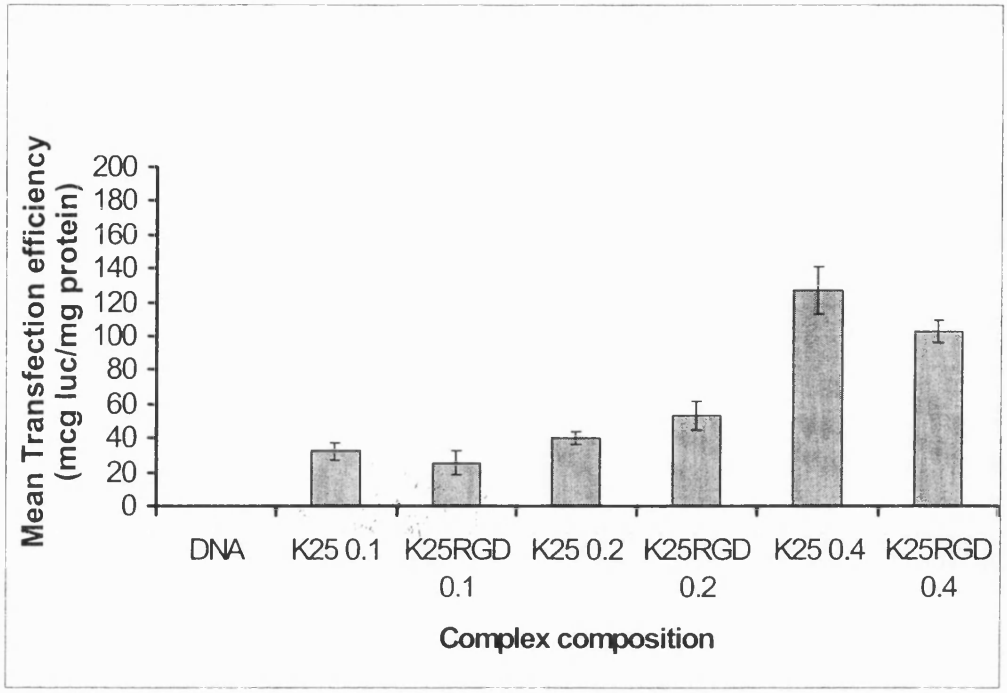

Figure 7.5b. Luciferase expression after transfection of B16 cells with polyplexes formed by complexation of pCMV*luc* with PEI/peptide mixtures (mean ± sd, n=3).

Complexes with higher additional cationic charge, particularly those with cationic charge excess generally resulted in the highest levels of gene expression, but this was not always the case in some experiments. For example, the data shown in figure 7.5a suggests that transfection with PEI/K_{25}RGD 0.1 (which had negative charge excess) resulted in a very high level of gene expression in Cos7 cells. This is indicative of variability that is inherent in using partially complexed systems. There was no significant advantage in using RGD peptides for transfection of B16 cells, whether the polyplexes had excess anionic or cationic charge, despite the reported expression of integrins by B16 cells (figures 7.4b and 7.5b). The optimum gene expression in B16 cells appeared to occur at net (total) charge ratios (+/-) of approximately 1.0 – 1.2 (complexes denoted PEI/K_{25}RGD 0.3-0.5) with no further advantage gained by increasing the level of cationic charge excess.

7.3.1 Competitive inhibition

Figure 7.6 shows the inhibition of integrin-mediated uptake in the presence of the synthetic cyclic oligopeptide, GRGDSPA. This is consistent with the increase in gene expression conferred by use of K_{25}RGD. In the presence of the competitive inhibitor the levels of expression were reduced to levels similar to those produced by the corresponding PEI/K_{25} complex.

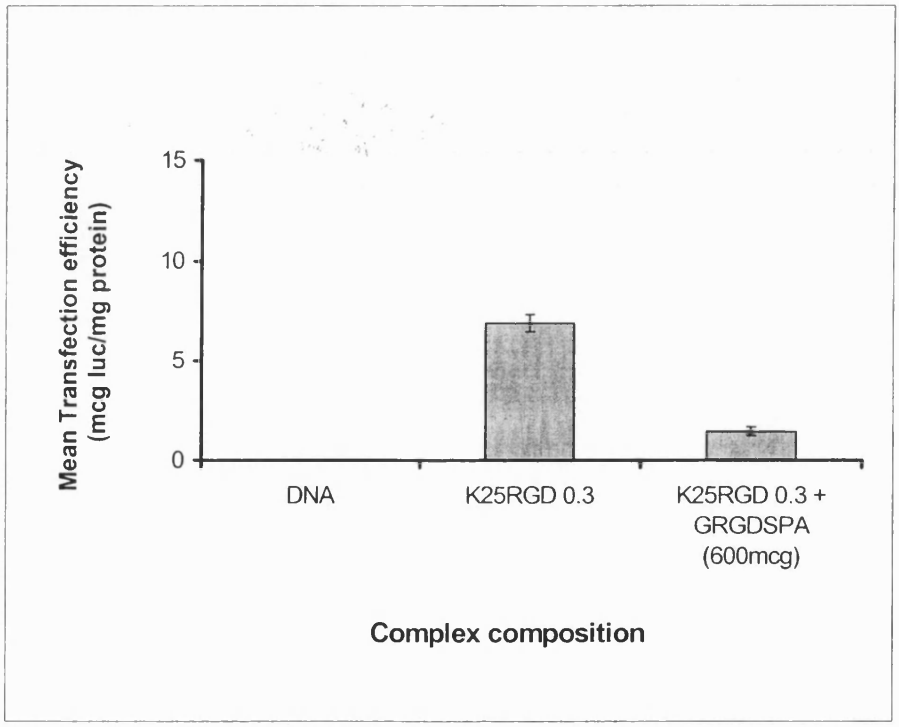

Figure 7.6. Inhibition of transfection of Cos7 cells with RGD-polyplexes in the presence of free cyclic RGD peptide formed by complexation of pCMV*luc* with PEI/peptide mixtures (mean ± sd, n=3). PEI/K25RGD 0.3 particles comprised DNA, PEI (at N/P ratio of 4), and K_{25}RGD at a charge ratio of 0.3 (+/-).

7.3.2 Effect of serum on transfection efficiency

The transfection efficiency of polyplexes was tested in the presence of foetal calf serum (FCS) as a model for what might be encountered in biological fluids. Figure 7.7 shows the advantage of using K_{25}RGD for transfection of Cos7 cells was lost in the presence of FCS and in all cases the level of gene expression was very much lower than in the absence of FCS.

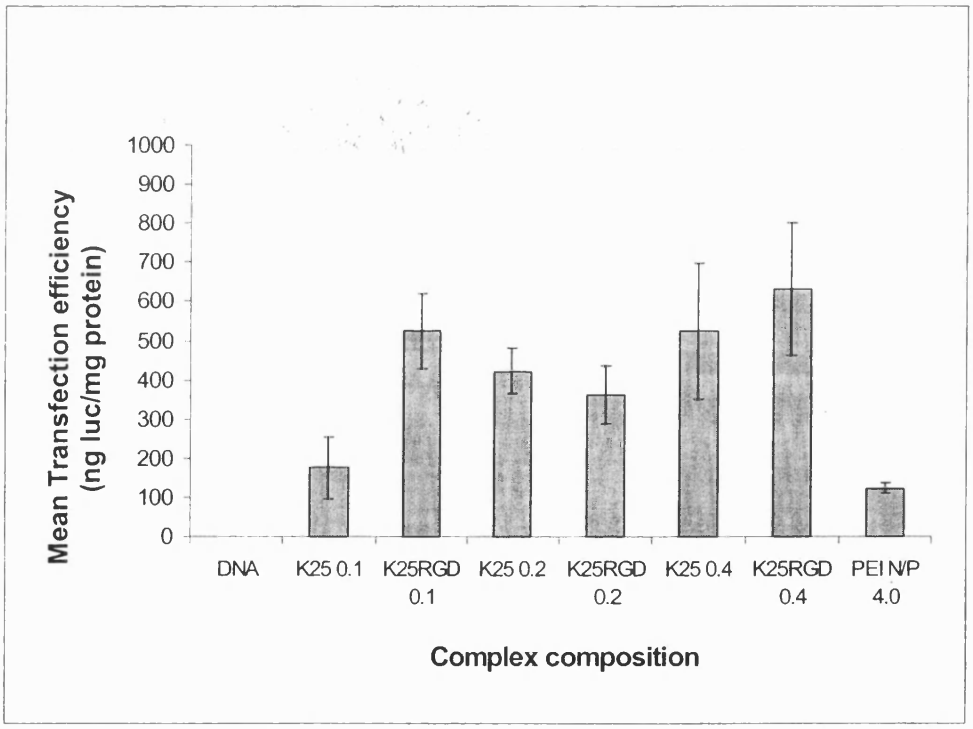

Figure 7.7. Luciferase expression after transfection of Cos7 cells with polyplexes in the presence of fetal bovine serum (mean ± sd, n=3). PEI content was constant at N/P = 4. PEI/K_{25} or PEI/K_{25}RGD = polyplexes produced with mixtures of PEI and K_{25} or PEI and K_{25}RGD. The suffix in each case represents the additional charge ratio (+/-) conferred by the peptide. Complexes with additional 0.1 and 0.2 (+/-) had negative charge excess; 0.4 (+/-) = close to charge neutralisation/slightly positive.

7.3.3 Zeta potential studies

Figure 7.8 shows the zeta potential measurements of polyethyleneimine at various nitrogen/phosphate (N/P) ratios.

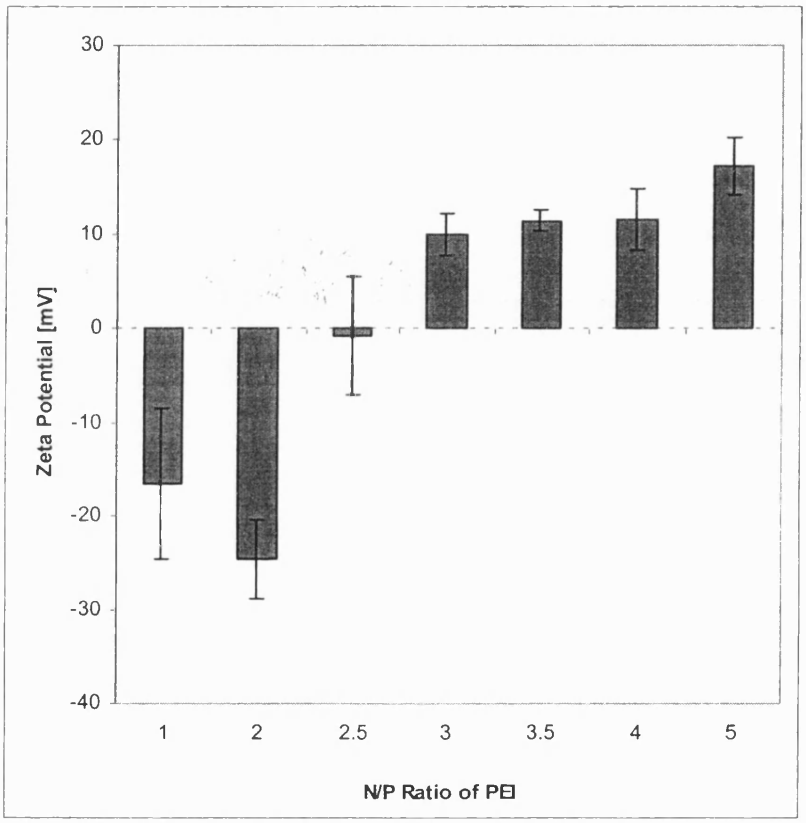

Figure 7.8. Effect of N/P ratio on the zeta potential measurements of PEI/DNA complexes. Complexes were incubated for 30 minutes at room temperature. Zeta potential was determined using an electrophoretic light scattering technique. Measurements were made in a thermostatically controlled electrophoresis cell equilibriated to 25°C. Each value represents the mean ± standard deviation for three replicate measurements.

The binding of nucleic acids to PEI shifts its protonation profile. Recent reports by Erbacher *et al.*, 1999a suggest that particles were neutral at an N/P (PEI nitrogen atoms to DNA phosphates) ratio = 3.5 – 4.0. This ratio differs from previous published data that showed particles were neutral at an N/P ratio of 6.0 (Boussif *et al.*, 1995). Based on these new data, zeta potential measurements were carried out on complexes formed using PEI at an N/P ratio of 2.0.

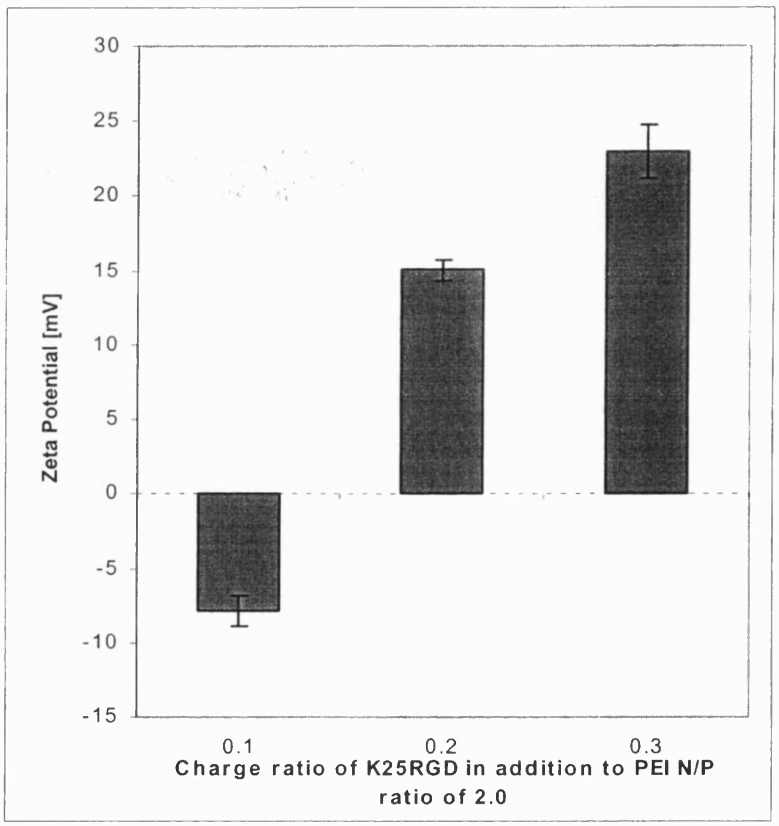

Figure 7.9. The zeta potential measurements of PEI/K_{25}RGD complexes at an N/P ratio of 2.0 while varying peptide charge ratios. The suffix in each case represents the additional charge ratio (+/-) conferred by the peptide. Complexes with additional 0.1 (+/-) had negative charge excess and 0.2 (+/-); 0.3 (+/-) = slightly positive

7.3.4 Transfection efficiency of polyplexes using PEI at N/P of 2.0

Based on the data on the zeta potential measurements identifying negative complexes at PEI N/P ratio of 2.0, Cos7 cells were transfected with polyplexes with PEI at an N/P ratio of 2.0, which was shown to give negative charge particles.

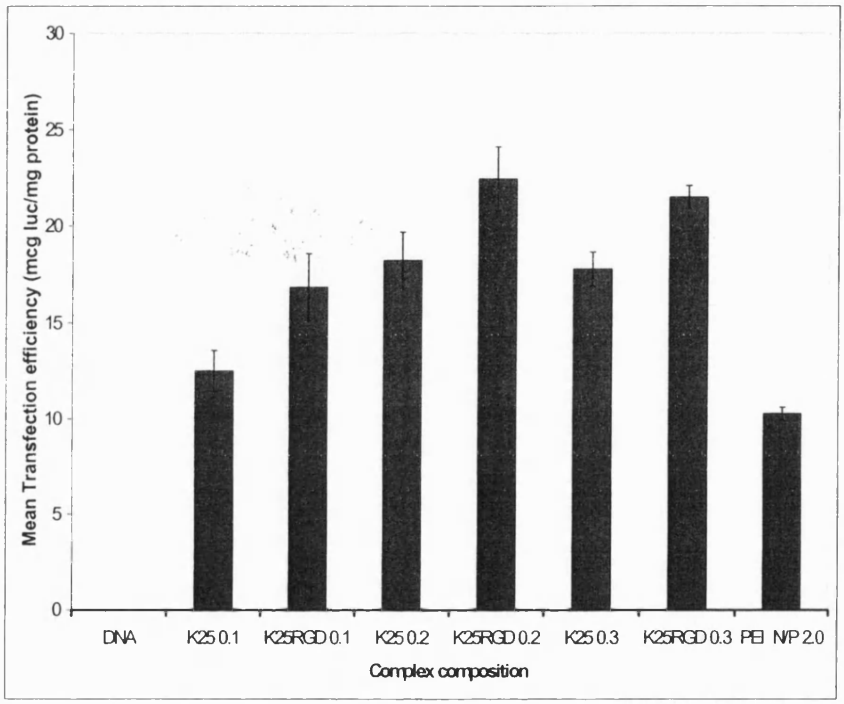

Figure 7.10. Luciferase expression after transfection of Cos7 cells with polyplexes (mean ± sd, n=3). PEI content was constant at N/P = 2. PEI/K_{25} or PEI/K_{25}RGD = polyplexes produced with mixtures of PEI and K_{25} or PEI and K_{25}RGD. The suffix in each case represents the additional charge ratio (+/-) conferred by the peptide. Complexes with additional 0.1 (+/-) had negative charge excess and 0.2; 0.3 (+/-) = close to charge neutralisation and slightly positive excess.

7.4 DISCUSSION

Establishing a negative or neutral surface is a key objective in polyplex design in order to avoid parasitic interactions, a problem typical of positively charged complexes. The protonation of PEI occurs over a wide pH range, unlike other polycations such as polylysine, and is very sensitive to change at pH values close to neutrality. This makes it impractical to calculate precise charge ratios for complexes formed at neutral pH. The estimation of net charge excess was initially based on the assumption that most samples of PEI are approximately one-sixth protonated at pH 7.4. This implies that the most effective complexes of PEI and DNA (figure 7.1) are formed just above charge neutralisation when the particles will have a positive zeta potential. Transfection is optimal when complexes are positively charged since anionic cell-surface proteoglycans of adherent cells mediate their attachment and spontaneous endocytosis. At high N/P ratios the activity typically decreases in a similar manner to polyplexes formed by other polycations, whether or not they have endosomolytic potential (Lucas *et al.*, 1999). This may possibly be due to the fact that after a certain ratio of PEI nitrogens to DNA phosphates, no more anionic charge remains for PEI to bind. Another suggestion may be changes in particle size or aggregation state which affect the biological activity of the complexes. Also, there may be direct toxic effect on the cells. The moderate activity of complexes formed by PEI complexes at N/P = 3 in both B16 cells and Cos7 cells is interesting (Figures 7.1 and 7.2). Polylysine complexes are completely inactive, even in the presence of chloroquine, until the charge ratio (+/-) exceeds unity and the zeta potential becomes positive (Lucas *et al*, 1999). One hypothesis is that complexation of polylysine with DNA is a random process, and that condensation is required for biological activity. Thus complexes which are half-neutralized are inactive. If complexation of PEI with DNA was random then one would expect that at N/P = 3 the DNA would have been uniformly in a state of half-neutralization, and partial condensation. This implies that cells took up partially condensed complexes, and that they delivered enough PEI to the endosome to allow endosomolysis to occur. However an alternative explanation is that the binding of PEI to DNA was co-operative, such that

at a N/P ratio of 3, the resulting mixture consisted of some 50% fully condensed plasmids and 50% free DNA (Nwachuku and Pouton, manuscript in preparation).

The zeta potential measurements of PEI/DNA complexes gave a similar trend to zeta potential data from Erbacher *et al.*, 1999. For PEI/DNA particles between N/P = 2 and N/P = 5, the surface charge varied from -25 mV to +17 mV respectively. The employment of K_{25}RGD as a targeting moiety was shown to be advantageous in the transfection of Cos7 cells. In some cases there was up to 10-fold increase in transfection efficiency in Cos7 cells over non-targeted DNA (figures 7.4a and 7.5a). Erbacher *et al.*, 1999 found that grafting an RGD-containing peptide to PEI improved transfection in HeLa cells by two orders of magnitude. Such results could make a significant difference to the feasibility of non-viral gene delivery systems *in vivo* if an identical benefit was obtained. There was still an added advantage to be gained in Cos7 cells even when polyplexes were strongly positive as evident in the high efficiency shown by PEI/K_{25}RGD 1.0 complexes. In such cases, it is possible that ligand-mediated binding is facilitated by ionic interaction between the particles and the cell surface, allowing closer access to integrins. However, in the transfection of B16 cells, the activity of integrin-targeted polyplexes were not stronger than corresponding non-targeted polyplexes. It has been established that variations in transfection data in various cells may arise from differences in cellular membrane integrity and internal endosomal conditions. Although, cell line variability is often seen in numerous transfection experiments, this was unexpected considering that B16 cells are integrin-expressing cells. It is not clear at present what proportion of cells expressing integrins will respond favourably to a targeting system such as RGD peptide. B16 cells take up cationic particles more readily than most cells, which in this case may have reduced the significance of the targeting ligand. B16 cells showed extensive gene expression even when they were transfected with PEI/K_{25} complexes, so it is possible that *in vitro* the output of B16 cells was saturated, even after transfection with less favourable delivery systems. An additional explanation for this variability is the fact that different integrin receptors are present on different cell lines. For instance, Cos7 cells express $\alpha 5$ integrins but not $\alpha 4$ integrins. RGD peptides target $\alpha 5$ integrins. Hence, the results obtained in this study are in line with the receptor expression pattern for Cos7 cells. It is possible that the type of integrins

present on B16 cells are not responsive to the specific RGD peptide used here. The specificity of integrin peptides, and their affinity of binding, has been found to be influenced by the amino acid sequences flanking the –RGD- group (Hart *et al.*, 1997). Overall, a broad range of cell lines would need to be investigated to determine the significance of integrin-mediated endocytosis.

Facilitating tissue dispersion after intramuscular or intratumoral injection and preventing tissue sequestration close to the injection site are issues that can be overcome with the formulation of negatively charged or neutral particles. However, the beneficial effects shown by the RGD targeting moiety in Cos7 cells may be reduced when polyplexes come into contact with plasma proteins. Still, the possibility of co-operative condensation between PEI/DNA and K_{25} or K_{25}RGD remains.

7.5 SUMMARY

This study has shown that targeting of neutral or negative polyplexes to cell surfaces can be achieved. Combining the high transfection potential of PEI with the efficient and specific mechanism of receptor-mediated endocytosis improves gene transfer efficiency and offers the possibility for specific targeting of gene delivery.

CHAPTER 8

CONCLUDING REMARKS AND FURTHER WORK

One of the main goals of continuing research in gene delivery is the work on the barriers that hamper the development of efficient gene delivery vectors. The first hurdle that delivery systems need to overcome is getting across the plasma membrane of living cells, which may be problematic in the gene therapy of some inherited or acquired diseases, for example, solid tumours. The plasma membrane of eukaryotic cells is inherently impermeable to peptides and proteins that lack specialized membrane receptors or transport proteins. The hydrophobic nature of the lipid bilayer makes it difficult for hydrophilic compounds to target the cytoplasm and nucleus of cells. Some proteins are endowed with properties to cross the plasma membrane and gain entry into the living cell. These include the homeodomain of Antennapedia (pAntp), the Herpes virus 22 protein VP22 and the Tat protein of HIV (Prochiantz, 1996; Phelan *et al.*, 1998; Schwarze *et al.*, 1999). The identification of these proteins and their respective abilities to undergo internalization into cells has opened new possibilities for the study of intracellular functions.

The work discussed in this thesis focussed on investigating the behaviour and properties of these membrane-translocating sequences in an attempt to determine their mode of internalization while assessing their potential for gene therapy and as a general means of introducing proteins into cells.

Chapter three presented significant data on trafficking of labeled peptides in B16 cells. Initially, confocal microscopy employing fluorescently labeled peptides revealed that most of the pAntp (penetratin) particles were taken up into endocytotic-type vesicles. In addition, EM images using gold-labeled pAntp have revealed an entry process typical of endocytosis. The results gave an indication of how long these peptides take to get into cells. The use of ADMP, showed that some of the labeled wildtype pAntp were instantaneously internalized up to the first five minutes of incubation. Plus, intracellular staining became more widespread after a further few hours. Fenton *et al.*, 1998 studied

import of pAntp peptide into primary B and T lymphocytes and found that some of the cells took up the peptide within 10 minutes of its addition to the culture medium. The majority of the cells were stained positive after two hours. The work done on the interaction of peptides with lipid membranes reported in chapter two gave evidence of binding affinities of various peptides. However, further work will need to be done to determine which amino acid residues play a role in the mechanism of entry of a protein into a cell and how conformational changes of the sequence affects the cellular internalization. For instance, some pore-forming proteins undergo a dramatic partial unfolding to form an extended, largely helical structure that lies on the surface of the bilayer. Then, under the influence of the transmembrane potential, a large fraction of the polypeptide chain is translocated into the bilayer where it regroups to form ion channels with more than one possible structure (Fernandez and Bayley, 1998).

Elliott and O'Hare, 1997 reported on the potential usefulness of VP22 in gene therapy by studying its distribution *in vitro*. They showed that VP22 had the remarkable property of intercellular transport, which is so rapid and efficient that following expression in a subpopulation the protein spreads to every cell in a monolayer, where it concentrates in the nucleus. Phelan *et al.*, 1998 also reported on the widespread delivery of functional p53 protein to a human tumour cell line inducing apoptosis. However, no study of VP22 in animal tissues has yet been reported. This was attempted and discussed in chapter four. In this study, it was possible to see *in vivo* activity of VP22 in tumour where the pattern of distribution appeared similar to that achieved *in vitro*. Overall, there was a lack of expression in animal tissue compared to transfection of cells in culture, which may explain why there has not been any studies *in vivo* published yet. This study also highlighted how the manipulation of procedures for animal experimentation is fraught with a vast amount of experimental variability. *In vivo* experiments performed by other groups such as Manthorpe *et al.*, 1993 also reported high variability in gene expression. They showed that there was a marked decline of muscle expression up to 14 days post injection of a plasmid containing a CMV promoter, whereas a luciferase plasmid containing the RSV promoter maintained an almost constant level of expression for four months. The study also indicated how various injection protocols resulted in high variability of reporter gene expression. For instance, the administration of luciferase

plasmid by longitudinal injection mediated 200-fold higher expression levels than perpendicular injection (Levy *et al.*, 1996). Further work on VP22 *in vivo* should initially employ two-fold higher concentration of expression vector that can be achieved in solution.

The ability of the membrane-translocating peptides to undergo intercellular spread in cells in culture was tested using fusions of pAntp with the enhanced green fluorescent protein (EGFP). Such fusions were prepared successfully and shown to transfect cells but efficiency was too low to confirm whether pAntp does undergo intercellular spread. Also, from the point of view of the mutant pAntp, which has been reported not to undergo internalization, it is of great interest to confirm whether the mutant distorts the expression levels and spreading efficiency. One potential disadvantage of this system is the reported size limitation of the fusion peptides that can be introduced by the pAntp peptide (Chatelin *et al.*, 1996). A study in which 30 kDa proteins were linked to the pAntp peptide, no uptake was observed confirming the limit to the size and/or constraint on the cargo structure that pAntp can translocate (Perez *et al.*, 1994). However, Rojas *et al.*, 1998 reported on another membrane-translocating sequence able to import proteins (as a fusion construct) as large as 45 kDa into living cells. These fusion proteins are easy to produce, highly stable and have low cytotoxicity. Such a novel technique will find widespread use in intracellular functional study and in drug and vaccine development.

The utility of noninvasive delivery of membrane-translocating sequences and proteins has been established and offers lots of possibilities in probing and protein-protein and protein-DNA interactions. Some of the limitations inherent in currently used invasive methods such as microinjection or the use of membrane-permeabilizing reagents are overcome by advantages of using cell-permeable peptides that include the speed and ease of translocation across the plasma membrane, low immunogenicity, a wide range of cell types, free movement to cytoplasmic target proteins as well as easy detection (Hawiger, 1999).

Since viral vectors can cause nonspecific inflammation and anti-vector immune responses, non-viral systems present a more attractive alternative, as they are more amenable to engineering to overcome immune and other toxic effects as well as tackle production challenges. However, low efficiency compared to viral systems is a major

limitation. Non-viral systems are based on DNA compaction by electrostatic interaction between the polyanion and cationic polymers (polyplexes). The ability of the membrane-translocating peptide, pAntp peptide (penetratin) to transfer genes to cells in culture was examined in chapter six. Initial experiments were performed in which the peptide-mediated retardation of plasmid DNA was examined using ethidium bromide exclusion assays. A bifunctional peptide (K_{25}penetratin) was synthesized that was able to have stronger binding affinity for DNA compared to penetratin alone. Above charge ratios of (+/-) 1.5, complexes had mean particle diameters of between 92 – 102 nm, which represents a size range amenable for cellular uptake. Although the transfection efficiency of pAntp peptide was improved by this modification, the gene expression data suggested that K_{25}penetratin was not as efficient as other endosomolytic peptides such as K_{25}HA2 and PEI. Results also suggested variations in transfection efficiency, in the presence and absence of chloroquine, with the different cell lines tested. Such observations imply differences in the integrity of cell membranes as well as variations in the endosomal environment. Hart *et al.*, 1997 found that transfection with Cos7 cells was enhanced in the presence of chloroquine whereas the same effect on ECV304 cells was achieved without chloroquine. Wagner *et al.*, 1992 found that HepG2 cells did not achieve as high transfection levels as erythroid leukemic K-562 cells, which are unusual cells, since they lack regulation of endosomal regulation and have a low endosomal pH. Results with chloroquine in this chapter suggested that most of the complexes were taken up by the endocytotic process. Further transfection studies on pAntp should include inhibitors of endocytosis such as cytochalasin B. Although preliminary transfection data suggested that penetratin might not offer any more benefit to an endosomolytic agent such as PEI, penetratin can be chemically linked to PEI perhaps via a disulphide linkage to test whether the translocating sequence can infer any additional benefit on the activity of PEI. This is important since transfection systems are often poorly characterised mixtures and not consistently well-defined. Such systems may facilitate entry of pAntp peptides to the nucleus. It is well established that the entry of plasmid DNA into the nucleus is one of the steps limiting non-viral gene transfer (Dowty *et al.*, 1995). Nuclear pores only allow proteins of < 60 kDa to gain access to the nucleus unless they display a nuclear

localization signal (NLS) (Jans and Hubner, 1996). Hence, the incorporation of an NLS could be considered for examining nuclear uptake of pAntp peptides.

On the other hand, the exploitation of a mutant pAntp (does not accumulate in the nucleus) or linking of proteins to pAntp, may prove useful for the delivery of proteins to non-nuclear locations. Derossi *et al.*, 1996 reported on various mutants of pAntp peptide including mutants that had one amino acid replaced by a proline residue. This proline mutant was concentrated solely in the cytoplasm and not the nucleus compared to the native pAntp peptide. Electrostatic cell-membrane binding and entry pathways are efficient and extensively exploited for *in vitro* transfection. In addition to intracellular barriers, physical restrictions and immunological barriers have to be overcome for the development of vectors applicable to *in vivo* gene transfer. Ideally, transfection complexes should be highly soluble, specific for binding to the target cells, but inert against parasitic interactions with body fluids or tissues. The most efficient synthetic *in vitro* DNA delivery systems are dependent on a net positive charge, which is one of the major barriers for targeted *in vivo* delivery. Positively charged particles prepared for transfection can bind in a non-specific manner to cell surfaces as well as activate the complement system (Plank *et al.*, 1994). Results from chapter seven showed that PEI complexes formed with either cationic or anionic charge excess can be targeted using K_{25}RGD, which implies that it will be possible to deliver negatively charged particles by ligand-mediated endocytosis. Although the exact mechanism of PEI remains to be elucidated (Godbey *et al.*, 1999), further work should involve testing this system using an *in vivo* model. Arap *et al.*, 1998 showed preferential targeting of an RGD-containing peptide to a toxin of tumour blood vessels in a mouse model. Such results might become applicable to cancer gene therapy. Recently, ligands have been coupled to PEI to produce polyplexes, which can target cell surfaces, and as a result are partially selective transfection systems (Diebold *et al.*, 1999a, 1999b). Such cell-binding ligands include transferrin, which may stabilize complexes in solution around electroneutrality. It may be possible to design transfection delivery systems that can target specific integrins that are prevalent on certain cell types in an attempt to give integrin-mediated transfection complexes a degree of specificity. Since the cyclic structure of the peptide is important for maintaining affinity by keeping the RGD domain in the correct conformation for

maximal integrin-binding, the formation of two pairs of disulphide bridges between flanking cysteine residues in the peptide structure might favour higher binding affinities of transfection complexes. The widespread distribution of target integrin ligands makes *in vivo* use of RGD peptides as DNA vectors problematic. However, these vectors can be employed for *ex vivo* gene transfer to tissues such as the cornea.

Barry *et al.*, 1996 used a general and systematic approach for generating phage libraries to select peptides that bind and enter several different cell types. Because of their small size, cell-binding peptides such as these could be incorporated into biological or physical gene therapy vectors. This process requires no prior knowledge of the biology of the target cells and hence may be useful for gene therapy and drug-targeting strategies.

Overall, peptides have many advantages as ligands for transfection complexes. They are not only easy to synthesize to a good degree of purity but sequences can be designed on the basis of known ligands. The functions of some peptides, such as membrane-destabilization by the influenza hemagglutinin HA-2 fusogenic peptide, can be incorporated into peptide-targeted transfection complexes.

Further work may include a comparison of all the internalizing sequences and a search for conserved structural traits. This should lead to the synthesis of peptidomimetic molecules, which will be of interest both in fundamental and applied pharmaceutical research.

Although the use of penetratin may not improve the efficiency of DNA transfection systems with endosomolytic activity such as PEI, constructs consisting of penetratin and established nuclear localization sequences can be assembled to achieve efficient transfection to the nucleus. The ability of penetratin and VP22 to translocate across cell membranes presents a great potential to target pharmacologically active substances into live cells.

ABSTRACTS AND PUBLICATIONS

1998; Annual American Pharmaceutical Scientists meeting (AAPS)

Abstract: Gene transfer using a bifunctional peptide.

1999; American Society of Gene Therapy (ASGT)

Abstract: Transfection efficiency of virus-like particles, comprising DNA plasmids, endosomolytic peptides and integrin-targeting ligands.

Transfection complexes (polyplexes) produced by co-condensation of DNA plasmid with polyethyleneimine and K_{25}-integrin-binding peptide.

Manuscript by Julia N Nwachuku and Colin W Pouton

Manuscript in preparation 2000

REFERENCES

Abdallah, B., Hassan, A., Benoist, C., Goula, D., Behr, J.-P., and Demeneix, B. A. (1996) A powerful nonviral vector for in vivo gene transfer into the adult mammalian brain: Polyethyleneimine. *Human Gene Therapy* 7, 1947-1954.

Addison, C. L., Braciak, T., Ralston, R., Muller, W. J., Gauldie, J., and Graham, F. L. (1995) Intratumoral injection of an adenovirus expressing interleukin 2 induces regression and immunity in a murine breast cancer model. *Proceedings of the National Academy of Sciences of the United States of America* **92**, 8522-8526.

Aihara, H. and Miyazaki, J.-I. (1998) Gene transfer into muscle by electroporation in vivo. *Nature Biotechnology* **16**, 867-870.

Alton, E. W., Middleton, P. G., Caplen, N. J., Smith, S. N., Steel, D. M., Munkonge, F. M., Jeffrey, P. K., Geddes, D. M., Hart, S. L., Williamson, R., Fasold, K. I., Miller, A. D., Dickinson, P., Stevenson, B. J., MacLachlan, G., Dorin, J. R., and Porteous, D. J. (1993) Non-invasive liposome-mediated gene delivery can correct the ion transport defect in cystic fibrosis mutant mice. *Nature Genetics* **5**, 135-142.

Anderson, W. F. (1992) Human Gene Therapy. *Science* **256**, 808-813.

Arap, W., Pasqualini, R., and Rouslahti, E. (1998) Cancer treatment by targeted drug delivery to tumor vasculature in a mouse model. *Science* **276**, 377-380.

Atherton, E. and Sheppard, R. C. (1989) Solid Phase Peptide Synthesis. IRL Press (Oxford University).

Bahnson, A. B., Dunigan, J. T., Baysal, B. E., Mohney, T., Atchison, R. W., Nimgaonkar, M. T., Ball, E. D., and Barranger, J. A. (1995) Centrifugal enhancement of retroviral-mediated gene transfer. *Journal of Virology Methods* **54**, 131-143.

Baker, A. and Cotten, M. (1997) Useful delivery of Bacterial Artificial Chromosomes into mammalian cells using psoralen-inactivated adenovirus carrier. *Nucleic Acids Research* **25**, 1950-1956.

Barry, M. A., Dower, W. J., and Johnston, A. (1996) Toward cell-targeting gene therapy vectors: selection of cell-binding peptides from random peptide-presenting phage libraries. *Nature Medicine* **2**, 299-305.

Behr, J.-P., Demeneix, B., Loeffler, J. P., and Perez-Mutul, J. (1989) Efficient gene transfer into mammalian primary endocrine cells with lipopolyamine-coated DNA. *Proceedings of the National Academy of Sciences of the United States of America* **86**, 6982-6986.

Behr, J.-P. (1994) Gene transfer with synthetic cationic amphiphiles: prospects for gene therapy. *Bioconjugate Chemistry* **5**, 382-389.

Bennett, F. A., Barlow, D. J., Dodoo, A. N .O., Hider, R. C., Lansley, A. B., Lawrence, M. J., Marriott, C., and Bansal, S. (1999) Synthesis and properties of (6,7-dimethoxy-4-coumaryl)alanine: A fluorescent peptide label. *Analytical Biochemistry* **270**, 15-23.

Birnboim, H. C. and Doly, J. (1979) A rapid alkaline extraction procedure for screening recombinant plasmid DNA. *Nucleic Acids Research* **7**, 1513-1522.

Bloomfield, V. A. (1996) DNA condensation. *Current Opinion in Structural Biology* **6**, 334-341.

Bonifaci, N., Sitia, R., Rubartelli, A. (1995) Nuclear translocation of an exogenous fusion protein containing HIV Tat requires unfolding. *AIDS* **9**, 995-1000.

Boussif, O., Lezoualc'h, F., Zanta, M. A., Mergny, M. D., Scherman, D., Demeneix, B., and Behr, J.-P. (1995) A versatile vector for gene and oligonucleotide transfer into cells in culture and in vivo: Polyethyleneimine. *Proceedings of the National Academy of Sciences of the United States of America* **92**, 7297-7301.

Boussif, O., Zanta, M. A., and Behr, J.-P. (1996) Optimized galenics improve in vitro gene transfer with cationic molecules up to 1000-fold. *Gene Therapy* **3**, 1074-1080.

Brewis, N., Phelan, A., Webb, J., Drew J., Elliott, G., and O'Hare, P. (2000) Evaluation of VP22 spread in tissue culture. *Journal of Virology* **74**, 1051-1056.

Brody, S. L., Metzger, M., Danel, C., Rosenfeld, M. A., and Crystal, R. G. (1994) Acute responses of non-human primates to airway delivery of an adenovirus vector containing the human cystic fibrosis transmembrane conductance regulator cDNA. *Human Gene Therapy* **5**, 821-836.

Budker, V., Zhang, G., Danko, I., Williams, P., and Wolff, J. A. (1998) The efficient expression of intravascularly delivered DNA in rat muscle. *Gene Therapy* **5**, 272-276.

Budker, V., Zhang, G., Knechtle, S., and Wolff, J. A. (1996) Naked DNA delivered intraportally expresses efficiently in hepatocytes. *Gene Therapy* **3**, 593-598.

Bukrinsky, M. I., Haggerty, S., Dempsey, M. P., Sharova, N., Adzhubel, A., Spitz, L., Lewis, P., Goldfarb, D., Emerman, M., and Stevenson, M. (1993) A nuclear-localization signal within HIV-1 matrix protein that governs infection of nondividing cells. *Nature* **365**, 666-669.

Caplen, N. J., Alton, E.W.F.W., Middleton, P. G., Dorin, J. R., Stevenson, B. J., Durham, S. R., Gao, X., Jeffery, P. K., Hodson, M. E., Coutelle, C., Huang, L., Porteous, D. J., Williamson, R., and Geddes, D. M. (1995) Liposome-mediated CFTR gene transfer to the nasal epithelium of patients with cystic fibrosis. *Natural Medicines* **1**, 39-46.

Cavazzana-Calvo, M., Hacein-Bey, S., de Saint Basile, G., Gross, F., Yvon, E., Nusbaum, P., Selz, F., Hue, C., Certain, S., Casanova, J.-L., Bousso, P., Le Deist, F., Fischer, A. (2000) Gene therapy of human severe combined immunodeficiency (SCID)-X1 disease. *Science* **288**, 669-672.

Chatelin, L., Volovitch, M., Joliot, A. H., Perez, F., and Prochiantz, A. (1996) Transcription factor Hoxa-5 is taken up by cells in culture and conveyed to their nuclei. *Mechanisms of Development.* **55**, 111-117.

Chen, S. H., Shine, H. D., Goodman, J. C., Grossman, R. G., and Woo, S. L. C (1994) Gene therapy for brain tumours: regression of experimental gliomas by adenovirus-mediated gene transfer in vivo. *Proceedings of the National Academy of Sciences of the United States of America* **91**, 3054-3057.

Cheng, P.-W. (1996) Receptor-ligand-facilitated gene transfer: enhancement of liposome-mediated gene transfer and expression by transferrin. *Human Gene Therapy* **7**, 275-282.

Cole, N. B. and Lippincott-Schwartz, J. (1995) Organisation of organelles and membrane traffic by microtubules. *Current Opinion in Cell Biology* **7**, 55-64.

Coll, J. L., Chollet, P., Brambilla, E., Desplanques, D., Behr, J.-P., and Favrot, M. (1999) In vivo delivery to tumors of DNA complexed with linear polyethyleneimine. *Human Gene Therapy* **10**, 1659-1666.

Conary, J. T., Parker, R. E., Christman, B. W., Faulks, R. D., King, G. A., Meyrick, B. O., Brigham, K. L. (1994) Protection of rabbit lungs from endotoxin injury by in vivo hyperexpression of the prostaglandin G/H synthase gene. *Journal of Clinical Investigation* **93**, 1834-1840.

Coonrod, A., Li, F.-Q., and Horwitz, M. (1997) On the mechanism of DNA transfection: efficient gene transfer without viruses. *Gene Therapy* **4**, 1313-1321.

Cotten, M., Langle-Rouault, F., Kirlappos, H., Wagner, E., Mechtler, K., Zenke, M., Beug, H., and Birnstiel, M. L. (1990) Transferrin-polycation-mediated introduction of DNA into human leukemic cells: Stimulation by agents that affects the survival of transfected DNA or modulate transferrin receptor levels. *Proceedings of the National Academy of Sciences of the United States of America* **87**, 4033-4037.

Cotten, M. and Wagner, E. (1997) Non-viral approaches to gene therapy. *Current Opinion in Biotechnology* **4**, 705-710.

Crystal, R. G. (1995) The gene as the drug. *Nature Medicine* **1**, 15-17.

Culver, K. W., and Blaese, R. M. (1994) Gene therapy for adenosine deaminase deficiency and malignant tumours. In: *Gene Therapeutics: Methods and Applications of Direct Gene Transfer.*, 263-280. Edited by Wolff, J.A., Boston, Birkhauser.

Dai, Y., Schwarz, E. M., Gu, D., Zhang, W.-W., Sarvetnick, N., and Verma, I. M. (1995) Cellular and humoral immune responses to adenoviral vectors containing factor IX gene: tolerization of factor IX and vector antigens allows for long-term expression. *Proceedings of the National Academy of Sciences of the United States of America* **92**, 1401-1405.

Dash, P. R., Toncheva, V., Schacht, E., and Seymour, L. W. (1997) Synthetic polymers for vectorial delivery of DNA: Characterization of polymer-DNA complexes by photon correlation spectroscopy and stability to nuclease degradation and disruption by polyanions in vitro. *Journal of Controlled Release* **48**, 269-276.

Davies, H. L., Brazolot, M. C., and Watkins, S. C. (1997) Immune-mediated destruction of transfected muscle fibers after direct gene transfer with antigen-expressing plasmid DNA. *Gene Therapy* **4**, 181-188.

Davies, H. L., Demeneix, B. A., Quantin, B., Coulombe, J., and Whalen, R. G. (1993) Plasmid DNA is superior to viral vectors for direct gene transfer into adult mouse skeletal muscle. *Human Gene Therapy* **4**, 733-740.

Davies, H. L., Whalen, R. G., and Demeneix, B. A. (1993) Direct gene transfer into skeletal muscle in vivo: Factors affecting efficiency of transfer and stability of expression. *Human Gene Therapy* **4**, 151-159.

Deisseroth, A. B., Kavanagh, J., and Champlin, R. (1994) Use of safety-modified retroviruses to introduce chemotherapy resistance sequences into normal hematopoietic cells for chemoprotection during the therapy of ovarian cancer: a pilot trial. *Human Gene Therapy* **5**, 1507-1522.

DeKruijff, B., Rietveld, A., Telders, N., and Vaandrager, B. (1985) Molecular aspects of the bilayer stabilization induced by poly(-L-)lysines of varying size in cardiolipin liposomes. *Biochimica et Biophysica Acta* **820**, 295-304.

Derossi, D., Calvet, S., Trembleau, A., Brunissen, A., Chassaing, G., and Prochiantz, A. (1996) Cell internalization of the third helix of the Antennapedia homeodomain is receptor-independent. *Journal of Biological Chemistry* **271**, 18188-18193.

Derossi, D., Joliot, A. H., Chassaing, G., and Prochiantz, A. (1994) The third helix of the Antennapedia homeodomain translocate through biological membranes. *Journal of Biological Chemistry* **269**, 10444-10450.

Derossi, D. and Prochiantz, A. (1995) Internalization of macromolecules by live cells. *Restorative Neurology and Neuroscience* **8**, 7-10.

Diebold, S. S., Kursa, M., Wagner, E., Cotten, M., and Zenke, M. (1999a) Mannose polyethyleneimine conjugates for targeted DNA delivery into dendritic cells. *Journal of Biological Chemistry* **274**, 19087-19094.

Diebold, S. S., Lehrmann, H., Kursa, M., Wagner, E., Cotten, M., and Zenke, M. (1999b) Efficient gene delivery into human dendritic cells by adenovirus polyethyleneimine and mannose polyethyleneimine transfection. *Human Gene Therapy* **10**, 775-786.

Dietrich, G., Bubert, A., Gentschev, I., Sokolovic, Z., Simm, A., Catic, A., Kaufmannn, S. H. E., Hess, J., Szalay, A. A., and Goebel, W. (1998) Delivery of antigen-encoding plasmid DNA into the cytosol of macrophages by attenuated suicide *Listeria monocytogenes*. *Nature Biotechnology* **16**, 181-185.

Dilber, M. S., Phelan, A., Aints, A., Mohamed, A. J., Elliott, G., Smith, C. I. E., and O'Hare, P. (1999) Intercellular delivery of thymidine kinase prodrug activating enzyme by the herpes simplex virus protein, VP22. *Gene Therapy* **6**, 12-21.

Dodoo, A. N. O., Bansal, S., Barlow, D. J., Bennett, F. A., Hider, R. C., Lansley, A. B., Lawrence, M. J., and Marriott, C. (2000) Systematic investigations of the influence of molecular structure on the transport of peptides across cultured alveolar cell monolayers. *Pharmaceutical Research* **17**, 7-14.

Dowty, M. E., Williams, P., Zhang, G., Hagstrom, J. E., and Wolff, J. A. (1995) Plasmid DNA entry into postmitotic nuclei of primary rat myotubes. *Proceedings of the National Academy of Science of the United States of America* **92**, 4572-4576.

Eissa, N. T., Chu, C. S., Danel, C., Crystal, R. G. (1994) Evaluation of the respiratory epithelium of normal and individuals with cystic fibrosis for the presence of adenovirus E1a sequences relevant to the use of E1a-adenovirus vectors for gene therapy for the respiratory manifestations of cystic fibrosis. *Human Gene Therapy* **5**,1105-1114.

Elliott, G. and O'Hare, P. (1997) Intercellular trafficking and protein delivery by a herpesvirus structural protein. *Cell* **88**, 223-233.

Elliott, G. and O'Hare, P. (1998) Herpes simplex virus type 1 tegument protein VP22 induces the stabilization and hyperacetylation of microtubules. *Journal of virology* **72**, 6448-6455.

Elliott, G. and O'Hare, P. (1999) Intercellular trafficking of VP22-GFP fusion proteins. *Gene Therapy* **6**, 149-151.

Erbacher, P., Bettinger, T., Belguise-Valladier, P., Zou, S., Coll, J.-L., Behr, J.-P., and Remy, J.-S. (1999a) Transfection and physical properties of various saccharide, poly(ethylene glycol), and antibody-derivatized polyethyleneimines (PEI). *Journal of Gene Medicine* **1**, 210-222.

Erbacher, P., Remy, J.-S., and Behr, J.-P. (1999b) Gene transfer with synthetic virus-like particles via the integrin-mediated endocytosis pathway. *Gene Therapy* **6**, 138-145.

Erbacher, P., Roche, A. C., Monsigny, M., and Midoux, P. (1996) Putative role of chloroquine in gene transfer into a hepatoma cell line by DNA/lactosylated polylysine complexes. *Experimental Cell Research* **225**, 186-194

Fahraeus, R., Paramio, J.M., Ball, K.L., Lain, S., and Lane, D.P. (1996) Inhibition of pRb phosphorylation and cell-cycle progression by a 20-residue peptide derived from $p16^{CDKN2/INK4A}$. *Current Biology* **6**, 84-91.

Fang, B., Eisensmith, R. C., Wang, H., Kay, M. A., Cross, R. E., Landen, C. N., Gordon, G., Bellinger, D. A., Read, M. S., Hu, P. C., Brinkhous, K. M., and Woo, S. L. C. (1995) Gene therapy for haemophilia B: host immunosuppression prolongs the therapeutic effect of adenovirus-mediated factor IX expression. *Human Gene Therapy* **6**, 1039-1044.

Fang, B., Xu, B., Koch, P., and Roth, J. A. (1998) Intercellular trafficking of VP22-GFP fusion proteins is not observed in cultured mammalian cells. *Gene Therapy* **5**, 1420-1424.

Farhood, H., Serbina, N., and Huang, L. (1995) The role of dioleoyl phosphatidylethanolamine in cationic liposome-mediated gene transfer. *Biochimica et Biophysica Acta* **1235**, 289-295.

Fasbender, A., Zabner, J., Zeiher, B. G., and Welsh, M. J. (1997) A low rate of cell proliferation and reduced DNA uptake limit cationic lipid-mediated gene transfer to primary cultures of ciliated human airway epithelia. *Gene Therapy* **4**, 1173-1180.

Favour, C. B. (1964) Antigen-antibody reactions in tissue culture. *Immunological methods*, ed. J. R. Ackroyd, 195-223. Blackwell Scientific Publication, Oxford.

Fawell, S., Seery, J., Daikh, Y., Moore, C., Chen, L. L., Pepinsky, B., and Barsoum, J. (1994) Tat-mediated delivery of heterologous proteins into cells. *Proceedings of the National Academy of Sciences of the United States of America* **91**, 664-668.

Felgner, P. L. (1996) Improvements in cationic liposomes for in vivo gene transfer. *Human Gene Therapy* 7, 1791-1793.

Felgner, J. H., Kumar, R., Sridhar, C. N., Wheeler, C. J., Tsai, Y., Border, R., Ramsey, P., Martin, M., and Felgner, P. L. (1994) Enhanced gene delivery and mechanism studies with a novel series of cationic lipid formulations. *Journal of Biological Chemistry* **269**, 2550-2561.

Felgner, P. L. and Ringold, G. M. (1989) Cationic liposome mediated transfection. *Nature* **331**, 461-462.

Fenton, M., Bone, N., and Sinclair, A. J. (1998) The efficient and rapid import of a peptide into primary B and T lymphocytes and a lymphoblastoid cell line. *Journal of Immunological Methods* **212**, 41-48.

Fernandez, T. and Bayley, H. (1998) Ferrying proteins to the other side. *Nature Biotechnology* **16**, 418-420.

Flotte, T. R., Barraza-Ortiz, X., Solow, R., Afione, S. A., Carter, B. J., and Guggino, W. B. (1995) An improved system for packaging recombinant adeno-associated virus vectors capable of *in vivo* transduction. *Gene Therapy* **2**, 29-37.

Fominaya, J. and Wels, W. (1996) Target cell-specific DNA transfer mediated by a chimeric multidomain protein. *Journal of Cell Biology* **271**, 10560-10568.

Friedmann, T., Felgner, P. L., Blaese, R. M., Ho, D. Y., Sapolsky, R. M., Mirsky, S., and Rennie, J. (1997) Making gene therapy work. *Scientific American* 95-123.

Fritz, J. D., Herweijer, H., Zhang, G., and Wolff, J. A. (1996) Gene transfer into mammalian cells using histone-condensed plasmid DNA. *Human Gene Therapy* **7**, 1395-1404.

Furth, P. A., Shamay, A., Wall, R. J., and Henninghausen, L. (1992) Gene transfer into somatic tissues by jet injection. *Analytical Biochemistry* **20**, 365-368.

Gao, X. and Huang, L. (1995) Cationic liposome-mediated gene transfer. *Gene Therapy*, **2**, 710-722.

Gao, X. and Huang, L. (1996) Potentiation of cationic liposome-mediated gene delivery by polycations. *Biochemistry* **35**, 1027-1036.

Gershon, H., Ghirlando, R., Guttman, S. B., and Minsky, A. (1993) Mode of formation and structural features of DNA-cationic liposome complexes used for transfection. *Biochemistry* **32**, 7143-7151.

Godbey, W. T., Wu, K. K., and Mikos, A. G. (1999) Tracking the intracellular path of poly(ethyleneimine)/DNA complexes for gene delivery. *Proceedings of the National Academy of Sciences of the United States of America* **96**, 5177-5181.

Golding, C., Senior, S., Wilson, M. T., and O'Shea, P. (1996) Time resolution of binding and membrane insertion of a mitochondrial signal peptide: Correlation with structural changes and evidence for cooperativity. *Biochemistry* **35**, 10931-10937.

Gottschalk, S., Sparrow, J. T., Hauer, J., Mims, M. P., Leland, F. E., Woo, S. L. C., and Smith, L. C. (1996) A novel DNA-peptide complex for efficient gene transfer and expression in mammalian cells. *Gene Therapy* **3**, 448-457.

Goula, D., Remy, J.-S., Erbacher, P., Wasowicz, M., Levi, G., Abdallah, B., and Demeneix, B. A. (1998) Size, diffusibility and transfection performance of linear PEI/DNA complexes in the mouse central nervous system. *Gene Therapy* **5**, 712-717.

Grillot-Courvalin, C., Goussard, S., Huetz, F., Ojjicius, D. M., and Courvalin, P. (1998) Functional gene transfer from intracellular bacteria to mammalian cells. *Nature Biotechnology* **16**, 862-866.

Gruenberg, J. and Maxfield, F. R. (1995) Membrane transport in the endocytic pathway. *Current Opinion in Cell Biology* **7**, 552-563.

Gustafsson, J., Arvidson, G., Karlsson, G., and Almgren, M. (1995) Complexes between cationic liposomes and DNA visualized by cryo-TEM. *Biochimica et Biophysica Acta* **2**, 305-312.

Haensler, J., and Szoka, F. C. (1993) Polyamidoamine cascade polymers mediate efficient transfection of cells in culture. *Bioconjugate Chemistry* **4**, 372-379.

Hamm-Alvarez, S. R. (1998) Molecular motors and their role in membrane traffic. *Advanced Drug Delivery Reviews* **29**, 229-242.

Hancock, W. S. and Battersby, J. E. (1976) A new micro-test for the detection of incomplete coupling reactions in solid-phase synthesis using 2, 4, 6-trinitrobenzenesulphonic acid. *Analytical Biochemistry* **71**, 260-264.

Hart, S. L., Collins, L., Gustafsson, K., and Fabre, J. W. (1997) Integrin-mediated transfection with peptides containing arginine-glycine-aspartic acid domains. *Gene Therapy* **4**, 1225-1230.

Hart, S. L., Harbottle, R. P., Cooper, M. J., Miller, A., Williamson, R., and Coutelle, C. (1996) Gene delivery and expression mediated by an integrin-binding peptide. *Gene Therapy* **3**, 1032-1033.

Hart, S. L., Knight, A. M., Harbottle, R. P., Mistry, A., Hunger, H. D., Cutler, D. F., Williamson, R., and Coutelle, C. (1994) Cell binding and internalization by filamentous phage displaying a cyclic Arg-Gly-Asp-containing peptide. *Journal of Biological Chemistry* **269**, 12468-12474.

Hartikka, J., Sawdey, M., Cornefert-Jensen, F., Margalith, M., Barnhart, K., Nolasco, M., Vahlsing, H. L., Meek, J., Marquet, M., Hobart, P., Norman, J., and Manthorpe, M. (1996) An improved plasmid DNA expression vector for direct injection into skeletal muscle. VR1012 construction. *Human Gene Therapy* **7**, 1205-1217.

Hashida, M., Mahato, R. I., Kawabata, K., Miyao, T., Nishikawa, M., and Takakura, Y. (1996) Pharmacokinetics and targeted delivery of proteins and genes. *Journal of Controlled Release* **41**, 91-97.

Hawiger, J. (1999) Noninvasive intracellular delivery of functional peptides and proteins. *Current Opinion in Chemical Biology* **3**, 89-94.

Hedin, U. and Thyberg, J. (1985) Receptor-mediated endocytosis of immunoglobulin-coated colloidal gold particles in cultured mouse peritoneal macrophages. Chloroquine and monensin inhibit transfer of the ligand from endocytotic vesicles to lysosomes. *European Journal of Cell Biology* **39**, 130-135.

Heller, R., Jaroszeski, M., Atkin, A., Moradpour, D., Gilbert, R., Wands, J., and Nicolau, C. (1996) In vivo gene electroporation and expression in rat liver. *Febs Letters* **389**, 225-228.

Hengge, U. R., Walker, P. S., and Vogel, J. C. (1996) Expression of naked DNA in human, pig, and mouse skin. *Journal of Clinical Investigation* **97**, 2911-2916.

Hodgson, C. P. (1995) The vector void in gene therapy. *Biotechnology* **13**, 222-225.

Hyde, S. C., Gill, D. R., Higgins, C. F., Trezise, A. E., Macvinish, L. J., Cuthbert, A. W., Ratcliff, R., Evans, M. J., and Colledge, W. H. (1993) Correction of the ion transport defect in cystic fibrosis transgenic mice by gene therapy. *Nature* **362**, 250-255.

Isner, J. M. (1998) Arterial gene transfer of naked DNA for therapeutic angiogenesis: early clinical results. *Advanced Drug Delivery Reviews* **30**, 185-197.

Isner, J. M. and Asahara, T. (1999) Angiogenesis and vasculogenesis as therapeutic strategies for postnatal neovascularization. *Journal of Clinical Investigation* **103**, 1231-1236.

Jans, D. A. and Hubner, S. (1996) Regulation of protein transport to the nucleus: Central role of phosphorylation. *Physiological Reviews* **76**, 651-685.

Jiao, S., Williams, P., Berg, R. K., Hodgeman, B. A., Liu, L., Repetto, G., and Wolff, J. A. (1992) Direct gene transfer into nonhuman primate myofibers in vivo. *Human Gene Therapy* **3**, 21-33.

Joliot, A., Pernelle, C., Deagostini-Bazin, H., and Prochiantz, A. (1991a) Antennapedia homeobox peptide regulates neural morphogenesis. *Proceedings of the National Academy of Sciences of the United States of America* **88**, 1864-1868.

Joliot, A., Trembleau, A., Raposo, G., Calvet, S., Volovitch, M., and Prochiantz, A. (1997) Association of engrailed homeoproteins with vesicles presenting caveolae-like properties. *Development* **124**, 1865-1875.

Joliot, A., Triller, A., Volovitch, M., Pernelle, C., and Prochiantz, A. (1991b) Alpha-2, 8-polysialic acid is the neuronal surface receptor of antennapedia homeobox peptide. *New Biology* **3**, 1121-1134.

Kabanov, A. V. and Kabanov, V. A. (1995) DNA complexes with polycations for the delivery of genetic material into cells. *Bioconjugate Chemistry* **6**, 7-20.

Kaiser, E., Colescott, R. L., Bossinger, C. D., and Cook, P. I. (1970) Color test for detection of free terminal amino groups in the solid-phase synthesis of peptides. *Analytical Biochemistry*, **34**, 595.

Kalderon, D., Robertson, B. L., Richardson, W. D., and Smith, A. E. (1984) A short amino acid sequence able to specify nuclear location. *Cell* **39**, 499-509.

Kawabata, K., Takakura, Y., and Hashida, M. (1995) The fate of plasmid DNA after intravenous injection in mice: involvement of scavenger receptors in its hepatic uptake. *Pharmaceutical Research* **12**, 825-830.

Kay, M A., Manno, C. S., Ragni, M. V., Larson, P. J., Couto, L. B., McClelland, A., Glader, B., Chew, A. J., Tai, S. J., Herzog, R. W., Arruda, V., Johnson, F., Scallan, C., Skarsgard, E., Flake, A. W., and High, K. A. (2000) Evidence for gene transfer and expression of factor IX in haemophilia B patients treated with an AAV vector. *Nature Genetics* **24**, 257-261.

Kay, M. A., Rothenburg, S., Landen, C. N., Bellinger, D. A., Leland, F., Toman, C., Finegold, M., Thompson, A. R., Read, M. S., Brinkhous, K. M., and Woo, S. L. C. (1993) *In vivo* gene therapy of haemophilia B:sustained partial correction in factor IX-deficient dogs. *Science* **262**, 117-119.

Kayatose, S., and Kataoka, K. (1998) Remarkable increase in nuclease resistance of plasmid DNA through supramolecular assembly with poly(ethylene glycol)-poly(L-lysine) block copolymer. *Journal of Pharmaceutical Sciences* **87**, 160-163.

Kessler, P. D., Podsakoff, G. M., Chen, X. J., McQuiston, S A., Colosi, P. C., Matelis, L. A., Kurtzman, G. J., and Byrne, B. J. (1996) Gene delivery to skeletal muscle results in sustained expression and systemic delivery of a therapeutic protein. *Proceedings of the National Academy of Sciences of the United States of America* **93**, 14082-14087.

Kichler, A., Behr, J.-P., and Erbacher, P. (1999) Polyethyleneimines: A family of potent polymers for nucleic acid delivery. In: *Nonviral Vectors for Gene Therapy*, 191-206. Edited by Huang, L., Hung, M.-C., and Wagner, E., San Diego, Academic Press.

Kircheis, R., Kichler, A., Wallner, G., Kursa, M., Ogris, M., Feizmann, T., Buchberger, M., and Wagner, E. (1997) Coupling of cell-binding ligands to polyethyleneimine for targeted delivery. *Gene Therapy* **4**, 409-418.

Kircheis, R., Schuller, S., Brunner, S., Ogris, M., Heider, K.-H., Zauner, W., and Wagner, E. (1999) Polycation-based DNA complexes for tumor-targeted gene delivery in vivo. *Journal of Gene Medicine* **1**, 111-120.

Knowles, M. R., Hohneker, K. W., Zhou, Z., Olsen, J. C., Noah, T. L., Hu, P-C., Leigh, M. W., Engelhardt, J. F., Edwards, L. J., Jones, K. R., Grossman, M., Wilson, J. M., Johnson, L. G., and Boucher, R. C. (1995) A controlled study of adenoviral vector mediated gene transfer in the nasal epithelium of patients with cystic fibrosis. *New England Journal of Medicine* **333**, 823-831.

Kon, O. L., Sivakumar, S., Teoh, K. L., Loh, S. K., Long, Y. C. (1999) Naked plasmid-mediated gene transfer to skeletal muscle ameliorates diabetes mellitus. *Journal of Gene Medicine* **1**, 186-194.

Kotin, R. M. (1994) Prospects for the use of adeno-associate virus as a vector for human gene therapy. *Human Gene Therapy* **5**, 793-801.

Kukowska-Latallo, J. F., Bielinska, A. U., Johnson, J., Spindler, R., Tomalia, D. A., and Baker, J. R. (1996) Efficient transfer of genetic material into mammalian cells using Starburst polyamidoamine dendrimers. *Proceedings of the National Academy of Sciences of the United States of America* **93**, 4897-4902.

Labat-Moleur, F., Steffan, A.-M., Brisson, C., Perron, H., Feugeas, O., Furstenberger, P., Oberling, F., Brambilla, E., and Behr, J.-P. (1996) An electron microscopy study into the mechanism of gene transfer with lipopolyamines. *Gene Therapy* **3**, 1010-1017.

Ledley, F. D. (1994) Non-viral gene therapies. *Current Opinion in biotechnology* 5, 626-636.

Ledley, F. D. (1995) Non-viral gene therapy: the promise of genes as pharmaceutical products. *Human Gene Therapy* **6**, 1129-1144.

Legendre, J.-Y. and Szoka, J. F. C. (1992) Delivery of plasmid DNA into mammalian cell lines using pH-sensitive liposomes: comparison with cationic liposomes. *Pharmaceutical Research* **9**, 1235-1242.

Lemmon, M. J., Van Zijl, P., Fox, M. E., Mauchline, M. L., Giacca, A. J., Minton, N. P., and Brown, J. M. (1997) Anaerobic bacteria as a gene delivery system that is controlled by the tumour microenvironment. *Gene Therapy* **4**, 791-796.

Leong, K. W., Mao, H.-Q., Truong-Le, V. L., Roy, K., Walsh, S. M., August, J. T. (1998) DNA-polycation nanospheres as non-viral gene delivery vehicles. *Journal of Controlled Release* **53**, 183-193.

Leventis, R., and Silvius, J. R. (1990) Interactions of mammalian cells with lipid dispersions containing novel metabolizable cationic amphiphiles. *Biochimica et Biophysica* Acta **1023**, 124-132.

Levy, M. Y., Barron, L. G., Meyer, K. B., and Szoka, J. FC. (1996) Characterization of plasmid DNA transfer into mouse skeletal muscle: Evaluation of uptake mechanism, expression and secretion of gene products into blood. *Gene Therapy* **3**, 201-211.

Lew, D., Parker, S. E., Latimer, T., Abai, A. M., Kuwahara-Rundell, A., Doh, S. G., Yang, Z.-Y., Laface, D., Gromkowski, S. H., Nabel, G. J., Manthorpe, M., and Norman, J. (1995) Cancer gene therapy using plasmid DNA: pharmacokinetic study of DNA following injection in mice. *Human Gene Therapy* **6**, 553-564.

Lewin, M., Carlesso, N., Tung, C.-H., Tang, X.-W., Cory, D., Scadden, D. T., and Weissleder, R. (2000) Tat peptide-derivatized magnetic nanoparticles allow in vivo tracking and recovery of progenitor cells. *Nature Biotechnology* **18**, 410-414.

Liljestrom, P. (1995) Alphavirus vectors for gene delivery. *Gene Therapy* **2**, 569-569.

Liu, Y., Liggitt, D., Zhong, W., Tu, G., Gaensler, K., and Debs, R. (1995) Cationic liposome mediated intravenous gene delivery. *Journal of Biological Chemistry* **270**, 24864-24870.

Loeffler, J. P., Barthel, F., Feltz, P., Behr, J.-P., Sassone-Corsi, P., and Feltz, A. (1990) Lipopolyamine-mediated transfection allows gene expression studies in primary neuronal cells. *Journal of neurochemistry* **54**, 1812-1815.

Logan, J. J., Bebok, Z., Walker, L. C., Peng, S., Felgner, P. L., Siegal, G. P., Frizzell, R. A., Dong, J., Howard, M., Matalon, S., Lindsey, J. R., DuVall, M., and Sorscher, E. J. (1995) Cationic lipids for reporter gene and CFTR transfer to rat pulmonary epithelium. *Gene Therapy* **2**, 38-49.

Luby-Phelps, K., Castle, P. E., Taylor, D. L., and Lanni, F. (1987) Hindered diffusion of inert tracer particles in the cytoplasm of mouse 3T3 cells. *Proceedings of the National Academy of Sciences of the United States of America* **84**, 4910-4913.

Lucas, P., Milroy, D. A., Thomas, B. J., Moss, S. H., and Pouton, C. W. (1999) Pharmaceutical and biological properties of poly(amino acid)/DNA polyplexes. *Journal of Drug Targeting* **7**, 143-156.

MacGregor, G. R., Nolan, G. P., Fiering, S., Roederer, M., and Herzenberg, L. A. (1991) Use of *E.coli lacZ* (β-galactosidase) as a reporter gene. *Methods in Molecular Biology* **7**, 217-235.

Manthorpe, M., Cornefert-Jensen, F., Hartikka, J., Felgner, J., Rundell, A., and Margalith, M. (1993) Gene therapy by intramuscular injection of plasmid DNA: studies on firefly luciferase gene expression in mice. *Human Gene Therapy* **4**, 411-418.

Marshall, E. (1995) Gene therapy's growing pains. *Science* **269**, 1050-1055.

Marshall, P., Malik, N., and Larin, Z. (1999) Transfer of YACs up to 2.3 Mb intact into human cells with polyethyleneimine. *Gene Therapy* **6**, 1634-1637.

Mastrangeli, A., Harvey, B.-G., Yao, J., Wolff, G., Kovesdi, I., Crystal, R. G., and Falck-Pedersen, E. (1996) "Sero-switch" adenovirus-mediated in vivo gene transfer: circumvention of anti-adenovirus humoral immune defences against repeat adenovirus vector administration by changing the adenovirus serotype. *Human Gene Therapy* **7**, 79-87.

Matsui, H., Johnson, L. G., Randell, S. H., and Boucher, R. C. (1997) Loss of binding and entry of liposome-DNA complexes decreases transfection efficiency in differentiated airway epithelial cells. *Journal of Biological Chemistry* **272**, 1117-1126.

Mayer, L. D., Hope, M. J., and Cullis, P. R. (1986) Vesicles of variable sizes produced by a rapid extrusion procedure. *Biochim Biophysica Acta* **858**, 161-168.

McLachlan, G., Davidson, H., Davison, D., Dickinson, P., Dorin, J., and Porteous, D. (1994) DOTAP as a vehicle for efficient gene delivery in vitro and in vivo. *Biochemistry* **11**, 19-21.

Mendell, J. R., Kissel, J. T., Amato, A. A., King, W., Signore, L., Prior, T. W., Sahenk, Z., Benson, S., McAndrew, P. E., Rice, E., Nagaraja, H., Stephens, R., Lantry, L., Morris, G. E., and Burghes, A. H. M. (1995) Myoblast transfer in the treatment of Duchenne's muscular dystrophy. *New England Journal of Medicine* **333**, 832-838.

Meyer, K. B., Thompson, M. M., Levy, M. Y., Barron, L. G., and Szoka, F. C. (1995) Intratracheal gene delivery to the mouse airway: characterisation of plasmid DNA expression and pharmacokinetics. *Gene Therapy* **2**, 450-460.

Meyer, K. B., Uyechi, L. S., and Szoka, F. C. (1997) Manipulating the intracellular trafficking of nucleic acids. In: *Gene Therapy for Diseases of the Lung*, 135-180. Edited by Brigham, K. L., New York, Marcel dekker.

Midoux, P., Mendes, C., Legrand, A., Raimond, J., Mayer, R., Monsigny, M., and Roche, A. C. (1993) Specific gene transfer mediated by lactosylated poly-L-lysine into hepatoma cells. *Nucleic Acids Research* **21**, 871-878.

Miller, A. D. (1990) Retrovirus packaging cells. *Human Gene Therapy* **1**, 5-14.

Miller, A. D. (1992) Human gene therapy comes of age. *Nature* **357**, 455-460.

Mosmann, T. (1983) Rapid colorimetric assay for cellular growth and survival: application to proliferation and cytotoxicity assays. *Journal of immunological Methods* **65**, 55-63.

Mumper, R. J., Barron, M. K., Anwer, K., Lessard, R. L., Liu, Q., Nitta, H., Alila, H., and Rolland, A. (1995) Interactive polymeric gene delivery systems for enhanced muscle expression. *Pharmaceutical Research* **12**, 80.

Mumper, R. J., Duguid, J. G., Anwer, K., Barron, M. K., Nitta, H., and Rolland, A. (1996) Polyvinyl derivatives as novel interactive polymers for controlled gene delivery to muscle. *Pharmaceutical Research* **13**, 701-709.

Nabel, G. J., Nabel, E. G., Yang, Z.-Y., Fox, B. A., Plautz, G. E., Gao, X., Huang, L., Shu, S., Gordon, D., and Chang, A. E. (1993) Direct gene transfer with DNA-liposome complexes in melanoma: Expression, Biologic activity and lack of toxicity in humans. *Proceedings of the National Academy of Science of the United States of America* **90**, 11307-11311.

Nishida, K., Mihara, K., Takino, T., Nakane, S., Takakura, Y., Hashida, M., and Sezaki, H. (1991) Hepatic disposition characteristics of electrically charged macromolecules in rat in vivo and in the perfused liver. *Pharmaceutical Research* **8**, 437-444.

Nordstrom, J. (1999) Expression plasmids for non-viral gene therapy. In: *Advanced Gene Delivery: from concepts to pharmaceutical products*, 15-43. Edited by Rolland, A., Harwood.

Ogris, M., Steinlein, P., Kursa, M., Mechtler, K., Kircheis, R., and Wagner, E. (1998) The size of DNA/transferrin-PEI complexes is an important factor for gene expression in cultured cells. *Gene Therapy* **5**, 1425-1433.

Ogris, M., Brunner, S., Schuller, S., Kircheis, R., and Wagner, E. (1999) PEGylated DNA/transferrin-PEI complexes: reduced interaction with blood components, extended circulation in blood and potential for systemic gene delivery. *Gene Therapy* **6**, 595-605.

Ohashi, T., Boggs, S., Robbins, P., Bahnson, A., Patrene, K., Wei, F.-S., Wei, J.-F., Li, J., Lucht, L., Fei, Y., Clark, S., Kimak, M., He, H., Mowery-Rushton, P., and Barranger, J. A. (1992) Efficient transfer and sustained high expression of the human glucocerebrosidase gene in mice and their functional macrophages following transplantation of bone marrow transduced by a retroviral vector. *Proceedings of the National Academy of Sciences of the United States of America* **89**, 11332-11336.

Olins, D. E., Olins, A. L., and Hippel, P. H. (1968) On the structure and stability of DNA-protamine and DNA-polypeptide complexes. *Journal of Molecular Biology* **33**, 265-281.

Page, R. L., Butler, S. P., Subramanian, A., Gwazdauska, F. C., Johnson, J. L., and Velander, W. H. (1995) Transgenesis in mice by cytoplasmic injection of polylysine/DNA mixtures. *Transgenic Research* **4**, 353-360.

Pante, N. and Aebi, U. (1996) Toward the molecular dissection of protein import into nuclei. *Current Opinion in Cell Biology* **8**, 397-406.

Perales, J. C., Ferkol, T., Beegan, H., Ratnoff, O. D., and Hanson, R. W. (1994b) Gene transfer *in vivo*: Sustained expression and regulation of genes introduced into the liver by receptor-targeted uptake. *Proceedings of the National Academy of Sciences of the United States of America* **91**, 4086-4090.

Perales, J. C., Ferkol, T., Molas, M., and Hanson, R. W. (1994a) An evaluation of receptor-mediated gene transfer using synthetic DNA-ligand complexes. *European Journal of Biochemistry* **226**, 255-266.

Perez, F., Lledo, P. M., Karagogeos, D., Vincent, J. D., Prochiantz, A., and Ayala, J. (1994) Rab3A and Rab3B carboxy-terminal peptides are both potent and specific inhibitors of prolactin release by rat anterior pituitary cells. *Molecular Endocrinology* **8**, 1278-1287.

Pasqualini, R., Koivunen, E., and Ruoslahti, E. (1997) Alpha v integrins as receptors for tumor targeting by circulating ligands. *Nature Biotechnology* **15**, 542-546.

Phelan, A., Elliott, G., and O'Hare, P. (1998) Intercellular delivery of functional p53 by the herpesvirus protein VP22. *Nature Biotechnology* **16**, 440-443.

Plank, C., Oberhauser, B., Mechtler, K., Koch, C., and Wagner, E. (1994) The influence of endosome-disruptive peptides on gene transfer using synthetic virus-like gene transfer systems. *Journal of Biological Chemistry* **269**, 12918-12924.

Plank, C., Mechtler, K., Szoka, F. C., Jr., and Wagner, E. (1996) Activation of the complement system by synthetic DNA complexes: A potential barrier for intravenous gene delivery. *Human Gene Therapy* **7**, 1437-1446.

Plank, C.,Zatloukal, K., Cotten, M., Mechtler, K., Wagner, E. (1992) Gene transfer into hepatocytes using asialoglycoprotein receptor-mediated endocytosis of DNA complexed with an artificial tetra-antennary galactose ligand. *Bioconjugate Chemistry* **3**, 533-539.

Podsakoff, G., Wong, K. K., and Chatterjee. S. (1994) Efficient gene transfer into nondividing cells by adeno-associated virus-based vectors. *Journal of virology* **68**, 5656-5666.

Pollard, H., Remy, J.-S., Loussouarn, G., Demolombe, S., Behr, J.-P., and Escande, D. (1998) Polyethyleneimine but not cationic lipids promotes transgene delivery to the nucleus in mammalian cells. *Journal of Biological Chemistry* **273**, 7507-7511.

Pooga, M., Soomets, U., Hallbrink, M., Valkna, A., Saar, K., Rezaei, K., Kahl, U., Hao, J.-X., Xu, X.-J., Wiesenfeld-Hallim, Z., Hokfelt, T., Bartfai, T., and Langel, U. (1998) Cell penetrating PNA constructs regulate galanin receptor levels and modify pain transmission in vivo. *Nature Biotechnology* **16**, 857-861.

Poole, B. and Okhuma, O. (1981) Effect of weak bases on the intralysosomal pH in mouse peritoneal-macrophages. *Journal of Cell Biology* **90**, 665-669.

Pouton, C. W. (1998) Nuclear import of polypeptides, polynucleotides and supramolecular complexes. *Advanced Drug Delivery Reviews* **34**, 51-64.

Pouton, C. W. and Seymour, L. W. (1998) Key issues in non-viral gene delivery. *Advanced Drug Delivery Reviews* **34**, 3-19.

Prochiantz, A. (1996) Getting hydrophilic compounds into cells: lessons from homeopeptides. *Current Opinion in Neurobiology* **6**, 629-632.

Qin, L., Ding, Y., Pahud, D. R., Chang, E., Imperiale, M. J., and Bromberg, J. S. (1997) Promoter attenuation in gene therapy: interferon-γ and tumour necrosis factor-α inhibit transgene expression. *Human Gene Therapy* **8**, 2019-2029.

Rapaport, D. and Shai, Y. (1994) Interaction of fluorescently labeled analogs of the amino-terminal fusion peptide of sendai virus with phospholipid membranes. *Journal of biological chemistry* **269**, 15124-15131.

Riddell, S. R., Greenberg, P. D., Overell, R. W., Loughran, T. P., Gilbert, M. J., Lupton, S. D., Agosti, J., Scheeler, S., Coombs, R. W., and Corey, L. (1992) Phase I study of cellular adoptive immunotherapy using genetically modified CD8+ HIV-specific T cells for HIV seropositive patients undergoing allogeneic bone marrow transplant. *Human Gene Therapy* **3**, 319-328.

Robards, W. A. and Wilson, A. J. Ed (1989) Procedures in electron microscopy. John Wiley and son Press, UK.

Robinson, M. S., Watt, C., and Zerial, M. (1996) Membrane dynamics in endocytosis. *Cell* **84**, 13-21.

Rojas, M., Donahue, J. P., Tan, Z., and Lin, Y.-Z. (1998) Genetic engineering of proteins with cell membrane permeability. *Nature Biotechnology* **16**, 370-375.

Rosenfeld, M. A., Yoshimura, K., Trapnell, B., Yoneyama, K., Rosenthal, E., Dalemans, W., Fukayama, M., Stier, J., Stratford-Perricaudet, L. D., Perricaudet, M., Guggina, W., Pavirani, A., Lecocq, P.-P., and Crystal, R. G. (1992) In vivo transfer of the human cystic fibrosis transmembrane conductance regulator gene to the airway epithelium. *Cell* **68**, 143-155.

Rosenkranz, A. A., Yachmenev, S. V., Jans, D. A., Serebryakova, N. V., MuravEv, V. I., Peters, R., and Sobolev, A. S. (1992) Receptor-mediated endocytosis and nuclear transport of a transfecting DNA construct. *Experimental Cell Research* **199**, 323-329.

Rother, R. P., Fodor, W. L., Springhorn, J. P., Birks, C. W., Setter, E., Sandrin, M. S., Squinto, S. P., and Rollins, S. A. (1995) A novel mechanism of retrovirus inactivation in human serum mediated by anti-alpha-galactosyl natural antibody. *Journal of Exp Medicine* **182,** 1345-1355.

Rother, R. P., Squinto, S. P., Mason, J. M., and Rollins, S. A. (1995) Protection of retroviral vector particles in human blood through complement inhibition. *Human Gene Therapy* **6**, 429-435.

Sambrook, J., Fritsch, E. F., and Maniatis, T. (Eds.) (1989) *Molecular Cloning – A laboratory manual.*, New York, Cold Spring Harbor Laboratory Press.

Schoen, P., Chonn, A., Cullis, P. R., Wilschut, J., and Scherrer, P. (1999) Gene transfer mediated by fusion protein haemagglutinin reconstituted in cationic lipid vesicles. *Gene Therapy* **6**, 823-832.

Schutze-Redelmeier, M.-P., Gournier, H., Garcia-Pons, F., Moussa, M., Joliot, A. H., Prochiantz, A., and Lemonnier, F. A. (1996) Introduction of exogenous antigens into the MHC class I processing and presentation pathway by Drosophila antennapedia homeodomain primes cytotoxic T cells *in vivo*. *Journal of Immunology* **157**, 650-655.

Schwarze, S. R., Ho, A., Vocero-Akbani, A., and Dowdy, S. F. (1999) In vivo protein transduction: delivery of biologically active protein into the mouse. *Science* **285**, 1569-1572.

Schwarze, S. R., Hruska, K. A., and Dowdy, S. F. (2000) Protein transduction: unrestricted delivery into all cells? *Trends in Cell Biology* **10**, 290-295.

Sgouras, D. and Duncan, R. (1990) Methods for the evaluation of biocompatibility of soluble synthetic polymers which have potential for biomedical use: Use of the tetrazolium based colorimetric assay (MTT) as a preliminary screen for evaluation of in vitro cytotoxicity. *Journal of Material Science:* Materials in Medicine **1**, 61-68.

Shai, Y. (1995) Molecular recognition between membrane-spanning polypeptides. *Trends in Biochemical Sciences* **20**, 460-464.

Singh, D., Davis, J. H., and Grant, C. W. (1992) Behaviour of a glycosphingolipid with unsaturated fatty acid in phosphatidylcholine bilayers. *Biochimica et Biophysica Acta – Biomembranes* **1107**, 23-30.

Sternberg, B., Sorgi, F. L., and Huang, L. (1994) New structures in complex formation between DNA and cationic liposomes visualized by freeze-fracture electron microscopy. *Febs Letters* **356**, 361-366.

Stolnik, S., Illum, L., and Davis, S. S. (1995) Long circulating microparticulate drug carriers. *Advanced Drug Delivery Reviews* **16**, 195-214.

Stribling, R., Brunette, E., Liggit, D., Gaensler, K., and Debs, R. (1992) Aerosol gene delivery in vivo. *Proceedings of the National Academy of Science of the United States of America* **89**, 11277-11281.

Suh, J., Paik, H., and Hwang, B. K. (1994) Ionization of polyethyleneimine and polyalkylamine at various pHs. *Bioorganic Chemistry* **22**, 318-327.

Swaney, W. P., Sorgi, F. L., Bahnson, A. B., and Barranger, J. A. (1997) The effect of cationic liposome pretreatment and centrifugation on retrovirus-mediated gene transfer. *Gene Therapy* **4**, 1379-1386.

Tabata, Y. and Ikada, Y. (1988) Macrophage phagocytosis of biodegradable microspheres composed of L-lactic acid/glycolic acid homo- and copolymers. *Journal of Biomedical Materials Research* **22**, 837-858.

Tang, M. X., Redemann, C. T., and Szoka, F. C., Jr. (1996) In vitro gene delivery by degraded polyamidoamine dendrimers. *Bioconjugate Chemistry* **7**, 703-714.

Tang, M. X. and Szoka, F. C. (1997) The influence of polymer structure on the interactions of cationic polymers with DNA and morphology of the resulting complexes. *Gene Therapy* **4**, 823-832.

Taxman, D. J., Lee, E. S., and Wojchowski, D. M. (1993) Receptor-targeted transfection using stable maleimido-transferrin/thio-poly-L-lysine conjugates. *Analytical Biochemistry* **213**, 97-103.

Temin, H. M. (1990) Safety considerations in somatic gene therapy of human disease with retrovirus vectors. *Human Gene Therapy* **1**, 111-123.

Theodore, L., Derossi, D., Chassaing, G., Llirbat, B., Kubes, M., Jordan, P., Chneiweiss, H., Godement, P., and Prochiantz, A. (1995) Intraneuronal delivery of protein kinase C pseudosubstrate leads to growth cone collapse. *Journal of neuroscience* **15**, 7158-7167.

Thierry, A. R. and Dritschilo, A. (1992) Intracellular availability of unmodified, phosphorothioated and liposomally encapsulated oligodeoxynucleotides for antisense activity. *Nucleic Acids Research* **20**, 5691-5698.

Thierry, A. R., Lunardi-Iskander, Y., Bryant, J. L., Rabinovich, P., Gallo, R. C., and Mahan, L. C. (1995) Systemic gene therapy: biodistribution and long-term expression of a transgene in mice. *Proceedings of the National Academy of Sciences of the United States of America* **92**, 9742-9746.

Thierry, A. R., Rabinovich, P., Peng, B., Mahan, L. C., Bryant, J. L., and Gallo, R. C. (1997) Characterization of liposome-mediated gene delivery: expression, stability and pharmacokinetics of plasmid DNA. *Gene Therapy* **4**, 226-237.

Tomlinson, E. and Rolland, A. (1996) Controllable gene therapy: pharmaceutics of non-viral gene delivery systems. *Journal of Controlled Release* **39**, 357-372.

Trapnell, B. C. (1993) Adenoviral vectors for gene transfer. *Advanced Drug Delivery Reviews* **12**, 185-199.

Troy, C. M., Derossi, D., Prochiantz, A., Greene, L. A., and Shelanski, M. L. (1996) Downregulation of Cu/Zn Superoxide Dismutase leads to cell death via the nitric oxide-peroxynitrite pathway. *Journal of Neuroscience* **16**, 253-261.

Twentyman, P. R., Brown, J. M., Gray, J. W., Franko, A. J., Scoles, M. A., and Kallman, R. F. (1980) A new mouse tumor model system (RIF-1) for comparison of end-point studies. *Journal of National Cancer Institute* **64**, 595-604.

Ulmer, J. B., Donnelly, J. J., Parker, S. E., Rhodes, G. H., Felgner, P. L., Dwarki, V. J., Gromkowski, S. H., Deck, R. R., DeWitt, C. M., Friedman, A., Hawe, L. A., Leander, K. R., Martinez, D., Perry, H. C., Shiver, J. W., Montgomery, D. L., and Liu, M. A. (1993) Heterologous protection against influenza by injection of DNA encoding a viral protein. *Science* **259**, 1745-1749.

Utvik, J. K., Nja, A., and Gundersen, K. (1999) DNA injection into single cells of intact mice. *Human Gene Therapy* **10**, 291-300.

Van derWoude, I., Visser, H. W., Ter Beest, M. B. A., Wagenaar, A., Ruiters, M. H. J., Engberts, J. B. F. N., and Hoekstra, D. (1995) Parameters influencing the introduction of plasmid DNA into cells by the use of synthetic amphiphiles as a carrier system. *Biochimica et Biophysica Acta* **1240**, 35-40.

Vile, R. G. and Hart, I. R. (1993) *In vitro* and *in vivo* targeting of gene expression to melanoma cells. *Cancer Research* **53**, 962-967.

Vitiello, L., Chonn, A., Wasserman, J. D., Duff, C., and Worton, R. G. (1996) Condensation of plasmid DNA with polylysine improves liposome-mediated gene transfer into established and primary muscle cells. *Gene Therapy* **3**, 396-404.

Vrionis, F. D., Wu, J. K., Qi, P., Waltzmann, M., Cherington, V., and Spray, D. C. (1997) The bystander effect exerted by tumor cells expressing the herpes simplex virus thymidine kinase (HSVtk) gene is dependent on connexin expression and cell communication via gap junctions. *Gene Therapy* **4**, 577-585.

Wagner, E., Cotten, M., Foisner, R., and Birnsteil, M. L. (1991) Transferrin-polycation DNA complexes: the effect of polycations on the structure of the complex and DNA delivery to cells. *Proceedings of the National Academy of Science of the United States of America* **88**, 4255-4259.

Wagner, E., Curiel, D., and Cotten, M. (1994) Delivery of drugs, proteins and genes into cells using transferrin as a ligand for receptor-mediated endocytosis. *Advanced Drug Delivery Reviews* **14**, 113-135.

Wagner, E., Plank, C., Zatloukal, K., Cotten, M., and Birnstiel, M. L. (1992b) Influenza virus hemagglutinin HA-2 N-terminal fusogenic peptides augment gene transfer by transferrin-polylysine-DNA complexes: Toward a synthetic virus-like gene transfer vehicle. *Proceedings of the National Academy of Science of the United States of America* **89**, 7934-7938.

Wagner, E., Zatloukal, K., Cotten, M., Kirlappos, H., Mechtler, K., Curiel, D. T., and Birnstiel, M. L. (1992) Coupling of adenovirus to transferrin-polylysine/DNA complexes greatly enhances receptor-mediated gene delivery and expression of transfected genes. *Proceedings of the National Academy of Science of the United States of America* **89**, 6099-6103.

Wagner, E., Zenke, M., Cotten, M., Beug, H., and Birnsteil, M. L. (1990) Transferrin-polycation conjugates as carriers for DNA uptake into cells. *Proceedings of the National Academy of Science of the United States of America* **87**, 3410-3414.

Wall, J. S., Golding, C., Van Veen, M., and O'Shea, P. S. (1995) The use of fluoresceinphosphatidylethanolamine as a real-time probe for peptide membrane interactions. *Molecular Membrane Biology* **12**, 183-192.

Walker, S., Sofia, M. J., Kakarla, R., Kogan, N. A., Wierichs, L., Longley, C. B., Bruker, K., Axelrod, H. R., Midha, S., Babu, S., and Kahne, D. (1996) Cationic facial amphiphiles: a promising class of transfection agents. *Proceedings of the National Academy of Science of the United States of America* **93**, 1585-1590.

Wheeler, C. J., Sukhu, L., Yang, G., Tsai, Y., Bustamente, C., Norman, J., and Manthorpe, M. (1996) Converting an alcohol to an amine in a cationic lipid dramatically alters the co-lipid requirement, cellular transfection activity and the ultrastructure of DNA-cytofectin complexes. *Biochimica et Biophysica Acta – Biomembranes* **1280**, 1-11.

Wilke, M., Fortunati, E., Van den Broek, M., Hoogeveen, A. T and Scholte, B. J. (1996) Efficacy of a peptide-based gene delivery system depends on mitotic activity. *Gene Therapy* **3**, 1133-1142.

Williams, R. S. (1995) Human gene therapy-of tortoises and hares. *Nature Medicine* **1**, 1137-1138.

Winegar, R. A., Monforte, J. A., Suing, K. D., O'Loughlin, K. G., Rudd, C. J., Macgregor, J. T. (1996) Determination of tissue distribution of an intramuscular plasmid vaccine using PCR and in situ DNA hybridization. *Human Gene Therapy* **7**, 2185-2194.

Wohlgemuth, J. G., Kang, S. H., Bulboaca, G. H., Nawotka, K. A., and Calos, M. P. (1996) Long-term gene expression from autonomously replicating vectors in mammalian cells. *Gene Therapy* **3**, 503-512.

Wolfert, M. A., Schacht, E. H., Toncheva, V., Ulbrich, K., Nazarova, O., and Seymour, L. W. (1996) Characterization of vectors for gene therapy formed by self-assembly of DNA with synthetic block co-polymers. *Human Gene Therapy* **7**, 2123-2133.

Wolfert, M. A. and Seymour, L. W. (1996) Atomic force microscopy analysis of the influence of the molecular weight of poly(L)lysine on the size of polyelectrolyte complexes formed with DNA. *Gene Therapy* **3**, 269-273.

Wolfert, M. A. and Seymour, L. W. (1998) Chloroquine and amphipathic peptide helices show synergistic transfection in vitro. *Gene Therapy* **5**, 409-414.

Wolff, J. A., Dowty, M. E., Jiao, S., Repetto, G., Berg, R. K., Ludtke, J., Williams, P., and Slautterback, D. B. (1992) Expression of naked plasmids by cultured myotubes and entry of plasmids into T-tubules and caveolae of mammalian skeletal muscle. *Human Molecular Genetics* **1**, 363-369.

Wolff, J. A., Malone, R. W., Williams, P., Wang, C., Acsadi, G., Jani, A., and Felgner, P. L. (1990) Direct gene transfer into mouse muscle in vivo. *Science* **247**, 1465-1468.

Wrobel, I. and Collins, D. (1995) Fusion of cationic liposomes with mammalian cells occurs after endocytosis. *Biochimica et Biophysica Acta* **1235**, 296-304.

Wu, G. Y. and Wu, C. H. (1988) Receptor-mediated gene delivery and expression in vivo. *Journal of Biological Chemistry* **263**, 14261-14264.

Wu, G. Y. and Wu, C. H. (1993) Liver-directed gene delivery. *Advanced Drug Delivery Reviews* **12**, 159-167.

Wybranietz, W. A., Prinz, F., Speigel, M., Schenk, A., Bitzer, M., Gregor, M., and Lauer, U. (1999) Quantification of VP22-GFP spread by direct fluorescence in 15 commonly used cell lines. *Journal of Gene Medicine* **1**, 265-274.

Wyman, T. B., Nicol, F., Zelphati, O., Scaria, P. V., Plank, C., and Szoka, F. C. (1997) Design, synthesis and characterization of a cationic peptide that binds to nucleic acids and permeabilizes bilayers. *Biochemistry* **36**, 3008-3017.

Xiao, X., Li., J., and Samulski, R. (1996) Efficient long-term gene transfer into muscle tissue of immunocompetent mice by adeno-associated virus vector. *Journal of Virology* **70**, 8098-8108.

Yang, J.-P. and Huang, L. (1996) Direct gene transfer to mouse melanoma by intratumor injection of free DNA. *Gene Therapy* **3**, 542-548.

Yang, N.-S., Burkholder, J. K., Roberts, B., Martinell, B., and McCabe, D. (1990) *In vivo* and *in vitro* gene transfer to mammalian somatic cells by particle bombardment. *Proceedings of the National Academy of Sciences of the United States of America* **87**, 9568-9572.

Yang, Y., Li, Q., Ertl, H. C., and Wilson, J. M. (1995) Cellular and humoral immune responses to viral antigens creates barriers to lung-directed gene therapy with recombinant adenoviruses. *Journal of virology* **69**, 2004-2015.

Yang, Y., Nunes, F. A., Berenesi, K., Goneczol, E., Engelhardt, J. F., and Wilson, J. M. (1994) Inactivation of E2a in recombinant adenoviruses improves the prospect for gene therapy in cystic fibrosis. *Nature Genetics* **7**, 362-369.

Yei, S., Mittereder, N., Wert, S., Whitsett, J. A., Wilmott, R. W., and Trapnell, B. C. (1994) *In vivo* evaluation of the safety adenovirus-mediated transfer of the human cystic fibrosis transmembrane conductance regulator cDNA to the lung. *Human Gene Therapy* **5**, 731-744.

Yu, M., Leavitt, M.C., Maruyama, M., Yamada, O., Young, D., Ho, A.D., and Wong-Staal, F. (1995) Intracellular immunization of human fetal cord blood stem/progenitor cells with a ribozyme against human immunodeficiency virus type 1. *Proceedings of the National Academy of Sciences of the United States of America* **92**, 699-703.

Zabner, J., Fasbender, A. J., Moninger, T., Poellinger, K. A., and Welsh, M. J. (1995) Cellular and molecular barriers to gene transfer by a cationic lipid. *Journal of Biological Chemistry* **270**, 18997-19007.

Zanta, M. A., Boussif, O., Adib, A., and Behr, J.-P. (1997) In vitro gene delivery to hepatocytes with galactosylated polyethyleneimine. *Bioconjugate Chemistry* **8**, 839-844.

Zauner, W., Ogris, M., and Wagner, E. (1998) Polylysine-based transfection systems utilizing receptor-mediated delivery. *Advanced Drug Delivery Reviews* **30**, 97-113.

Zelphati, O., Liang, X., Hobart, P., and Felgner, P. L. (1999) Gene chemistry: Functionally and conformationally intact fluorescent plasmid DNA. *Human Gene Therapy* **10**, 15-24.

Zenke, M., Steinlein, P., Wagner, E., Cotton, M., Beug, H., and Birnstiel, M. L. (1990) Receptor-mediated endocytosis of transferrin-polycation conjugates: An efficient way to introduce DNA into hematopoietic cells. *Proceedings of the National Academy of Sciences of the United States of America* **87**, 3655-3659.

Zhou, X. and Huang, L. (1994) DNA transfection mediated by cationic liposomes containing lipopolylysine: characterisation and mechanism of action. *Biochimica et Biophysica Acta* **1189**, 195-203.

APPENDIX A

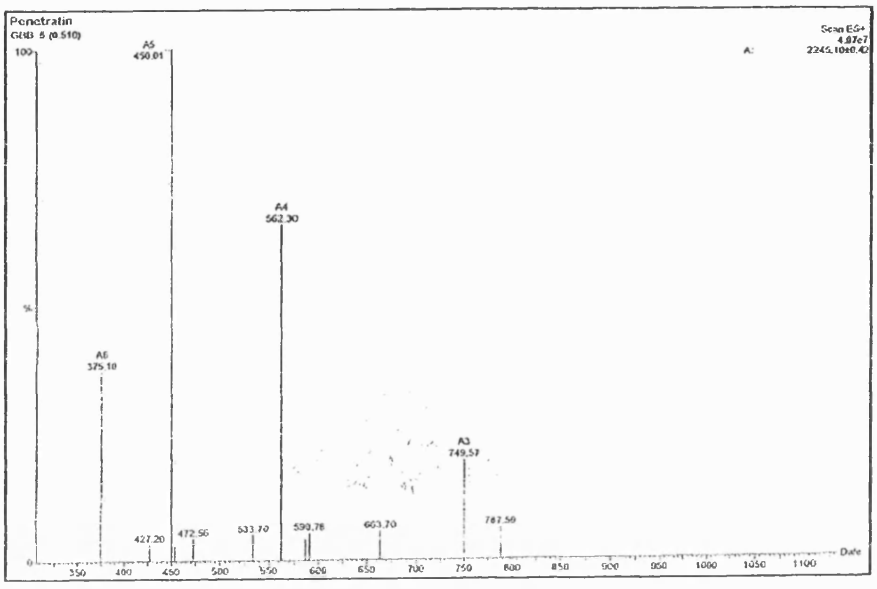

Figure A1: Electrospray mass spectrometry for penetratin. Expected mass = 2246

Observed mass = 2245.10

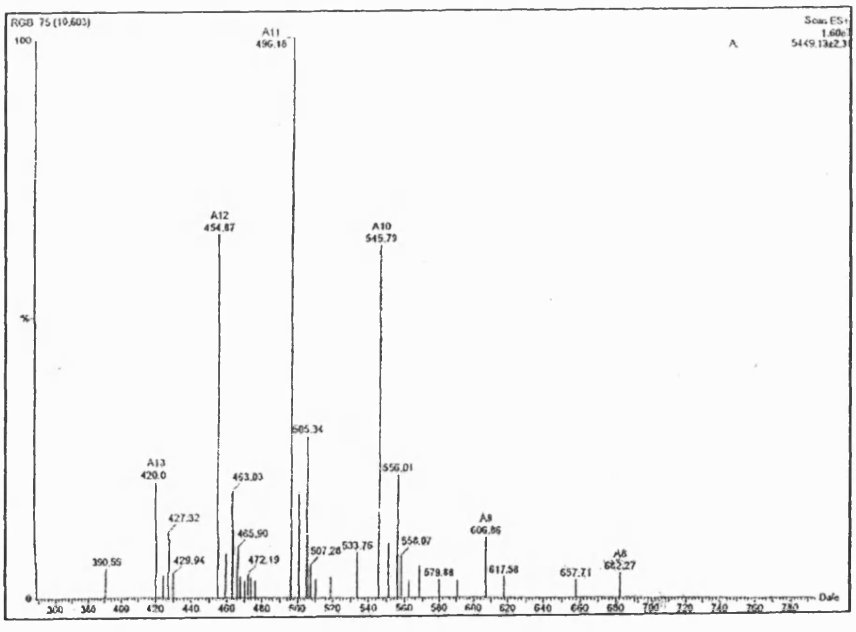

Figure A2: Electrospray mass spectrometry for K_{25}penetratin. Expected mass = 5451

Observed mass = 5449

APPENDIX B

1. Antibiotics

Ampicillin sodium (Sigma, UK) was prepared as a 100 mg/ml solution in water and filter sterilised using a 0.2 μm pore membrane (Millipore, UK) and stored at -20°C for up to three months. Working concentration 100 μg/ml.

Tetracycline (Sigma, UK) was prepared as a 25 mg/ml solution in methanol and stored at -20°C for up to three months.

2. Chloroquine

Chloroquine (Baxter, UK) was prepared as a 10 mM aqueous stock solution, filter sterilised via a 0.2 μm pore membrane (Millipore, UK) and stored at -20°C for up to one month.

APPENDIX C

TAE buffer 0.04 mM Tris-acetate
0.01 mM EDTA

TE buffer 10 mM Tris.Cl (pH 8)
1 mM EDTA (pH 8)

Electrophoresis loading buffer (5x) 0.25% bromophenol blue
0.25% Xylene cyanol FF
15% Ficoll (type 400, Pharmacia)

Electrophoresis loading buffer containing sodium dodecyl sulphate (5x)

Na_2EDTA	6.7% w/v
Glycerol	50% v/v
Bromophenol blue	0.2% w/v
Sodium dodecyl sulphate	1% w/v

Luria Bertani Medium (LB)

Bacto-tryptone		10 g
Bacto-yeast extract		5 g
Sodium chloride		10 g
DDDW	to	1000 ml

LB Agar

Bacto-tryptone		10 g
Bacto-yeast extract		5 g
Sodium chloride		10 g
Agar Technical		12 g
DDDW	to	1000 ml

Reagents for preparing LB were obtained from DIFCO, UK. Solutions were sterilised by autoclaving at 121°C and 15 psi for 15 minutes on a liquid cycle in a swingate Type SFT-LAB oven (British Steriliser Co. Ltd., UK)

APPENDIX D

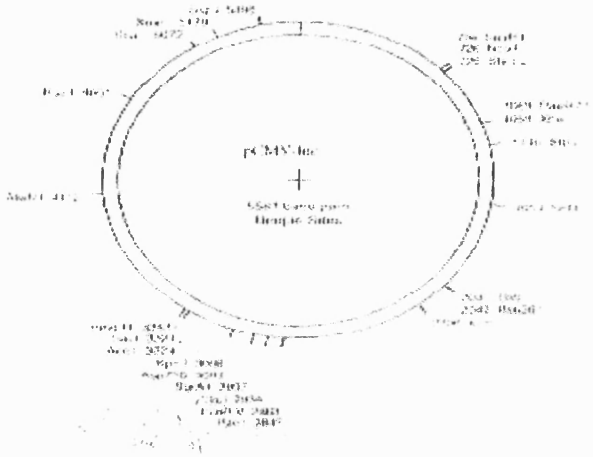

Figure D1. Plasmid map for pCMV*luc*

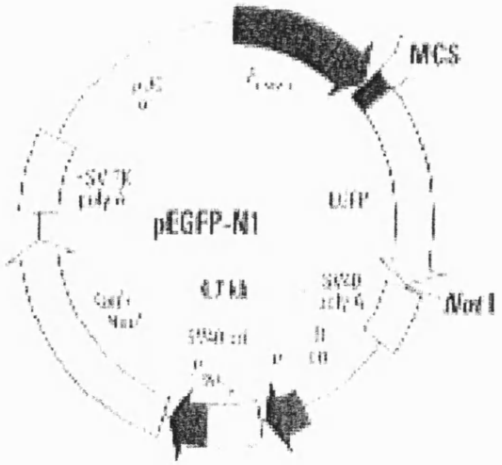

Figure D2. Plasmid map for pEGFP-N1

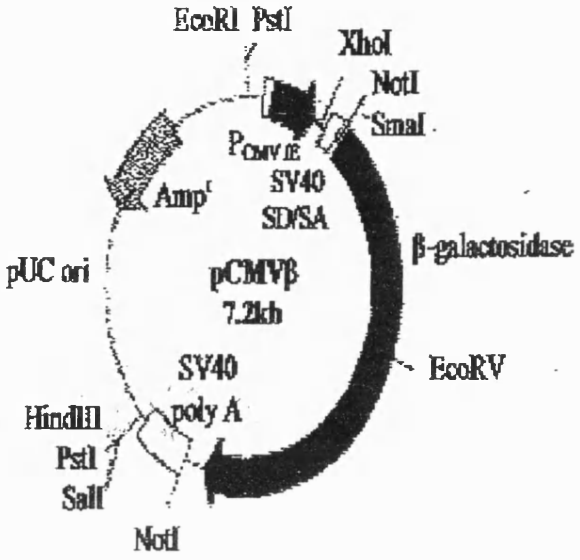

Figure D3. Plasmid map for pCMVβ.

APPENDIX E

Calibration curve for luciferase by dilution of purified luciferase (Promega) stock with 1x lysis buffer (Promega). Analysis was performed as described previously in 2.6.2.1. The linear regression analysis was as follows:

Gradient (m) = 685.15

Intercept (c) = 0

Correlation coefficient (r) = 0.9994

APPENDIX F

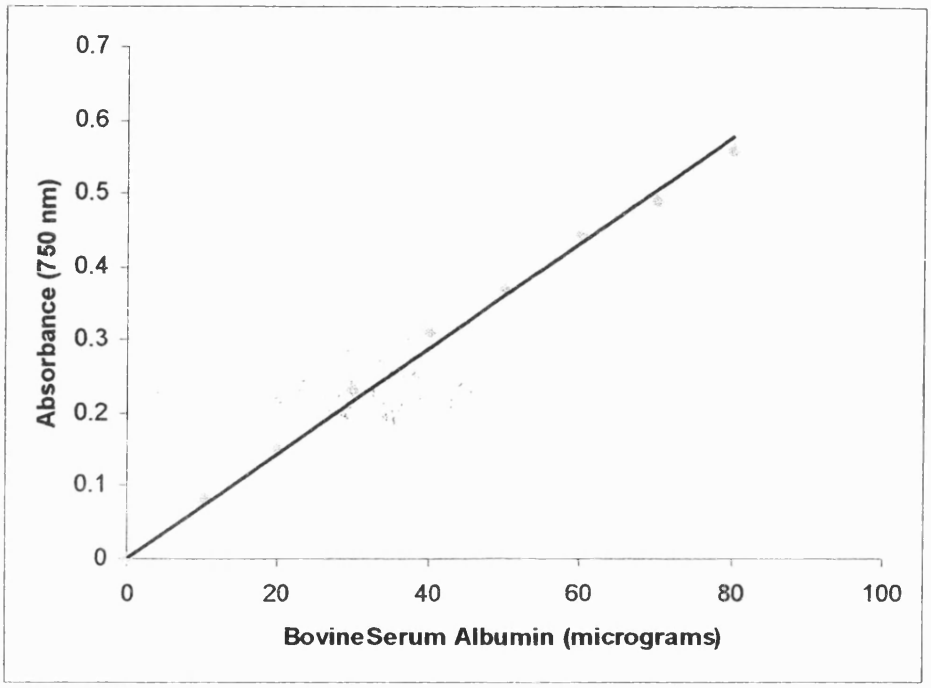

Calibration curve for protein using bovine serum albumin (BSA) as a standard and the Bio-Rad Dc protein assay kit. A stock solution of 1mg/ml of BSA (SigmaAldrich, UK) was prepared from which 100 µl aliquots in 0.1 M sodium phosphate buffer (pH 7.4) containing various amounts of protein.

Gradient (m) = 0.0072

Intercept (c) = 0.0159

Correlation coefficient (r) = 0.9961

APPENDIX G

A calibration curve was constructed for B16 cells by plating known numbers of cells into 96-well plates, before using the MTT method. Figure below shows linear regression analysis obtained for absorbance against cell number.

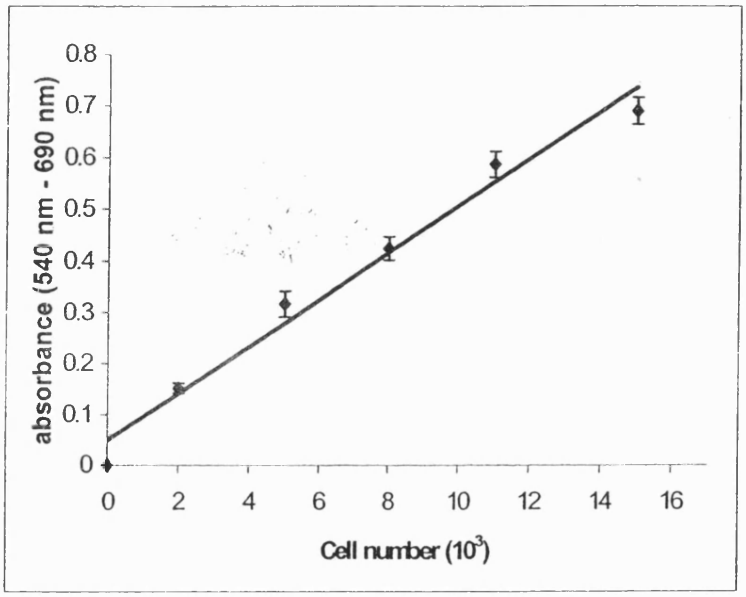

Calibration curve for the MTT assay for B16 cell number. Each data point represents the mean absorbance values (540 nm – 690 nm) ± SD of three evaluations.

Gradient (m) = 0.0457

Intercept (c) = 0.0491

Correlation coefficient (r) = 0.9784

APPENDIX H

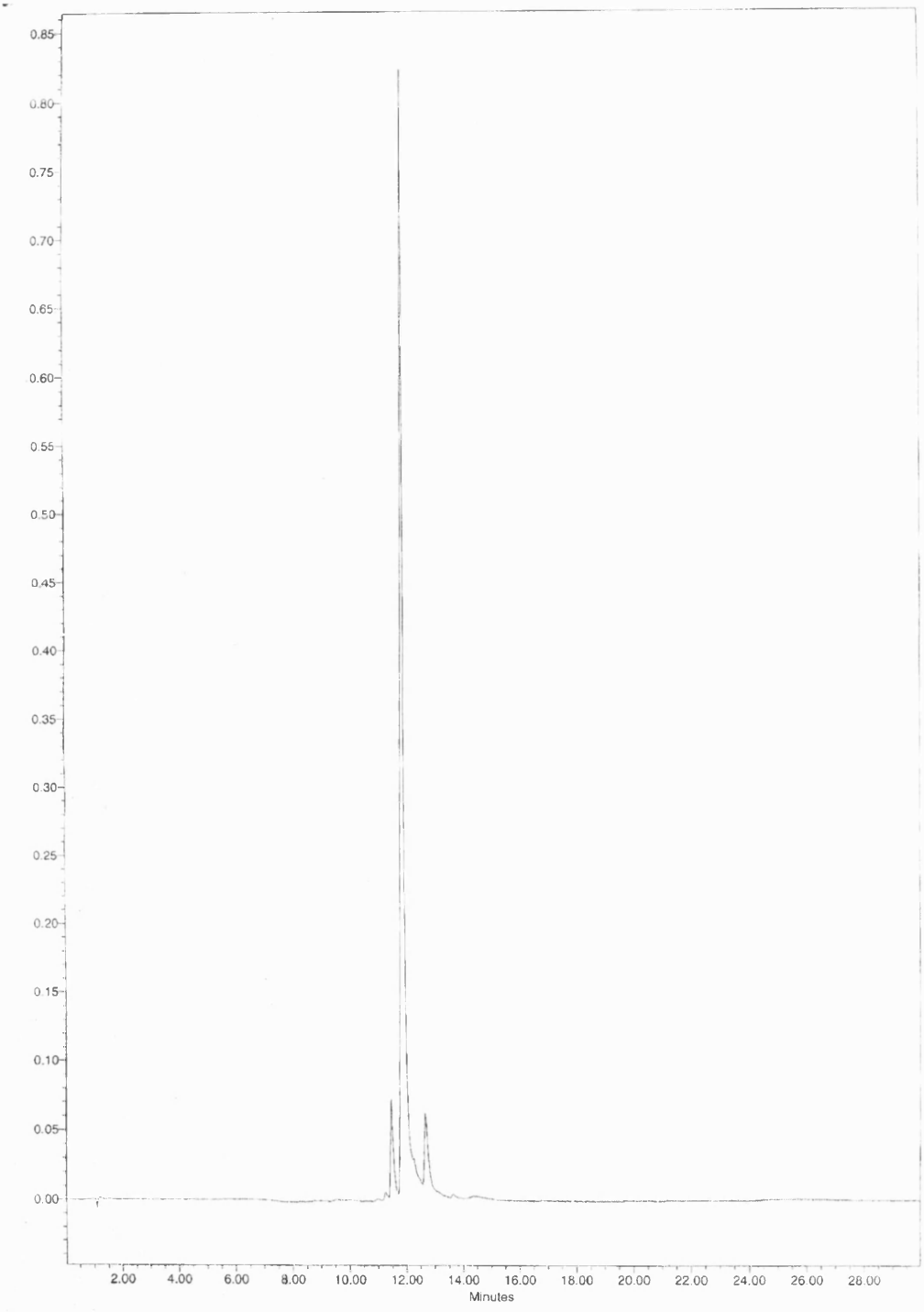

HPLC trace for ADMP. Column: Vydac 218TP53 3.2 cm x 250 mm

Flow rate = 0.5 ml/min λ of detection = 230 nm Material pore size = 3 μm

Solvent A = 0.1% Trifluoroacetic acid Solvent B = 10%A + 90% acetonitrile

Gradient = 10%B to 90%B in 30 minutes

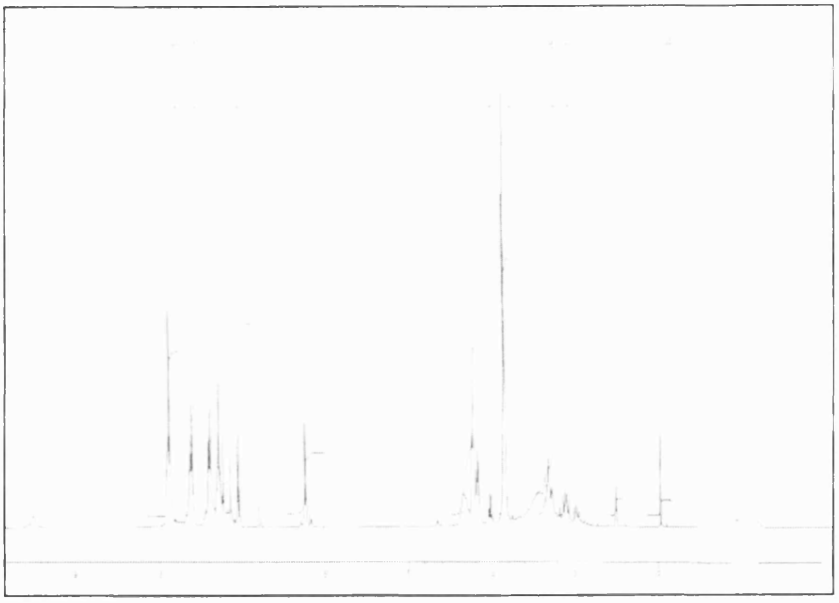

Nuclear Magnetic Resonance (NMR) for fluorescent ADMP

APPENDIX I

Molecular Weight Markers

For agarose gel electrophoresis, the marker used was *Eco*R I/Hind III cut λ DNA (NBL Gene Sciences Ltd, UK).

1	21226
2	5148
3	4973
4	4268
5	3530
6	2027
7	1904
8	1584
9	1375
10	947
11	831
12	564
13	125

APPENDIX J

Incubation time for the expression of luciferase

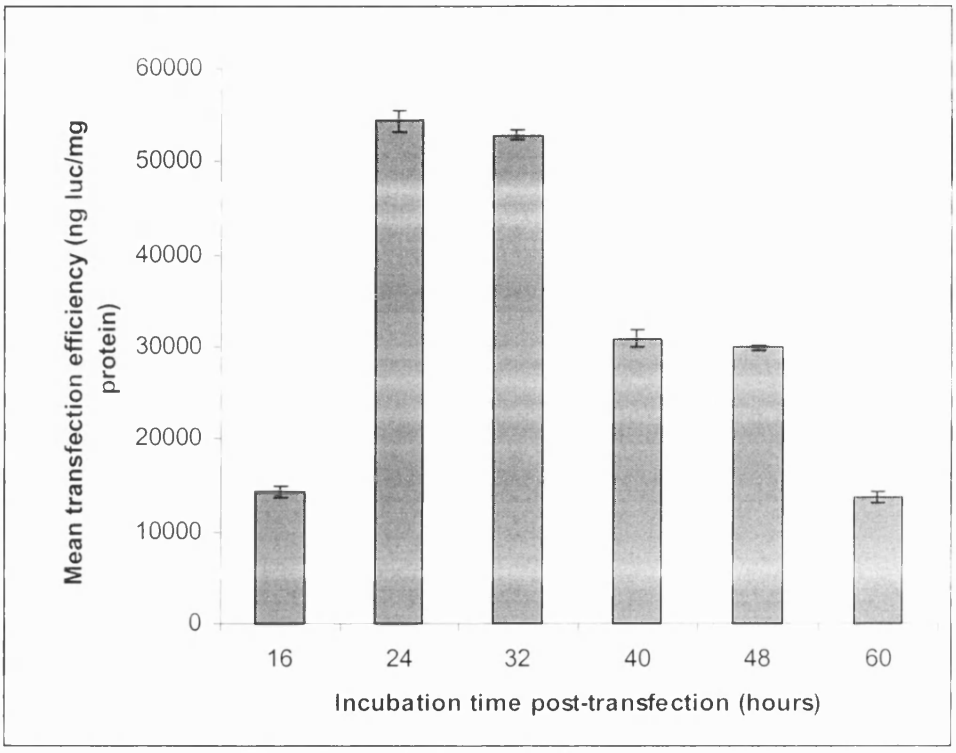

Incubation time for the expression of luciferase. B16 murine melanoma cells were transfected with 2 μg of pCMV*luc* complexed with DOTAP (+/- 2.4) for four hours and cells harvested at various time points post transfection for analysis. Analysis was carried out as described in 2.6.2.1. Data points represent the mean triplicate samples ± SD.

APPENDIX K

The DNA encoded amino acids: structure, abbreviations, and properties

Name	Structure	Abbreviation		pI	Charge of side chain		Key feature of side chain		Molecular formula	Molecular weight
		3-Letter	1-Letter		Acidity/ basicity	Affinity for water				
Alanine		Ala	A	6.02	N	O	Alkyl	—R	$C_3H_7NO_2$	89
Arginine	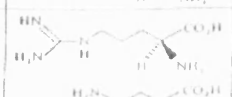	Arg	R	10.76	B	O	Guanidino		$C_6H_{14}N_4O_2$	174
Asparagine		Asn	N	5.41	N	H	Amide	$—CONH_2$	$C_4H_8N_2O_3$	132
Aspartic acid	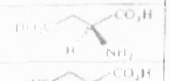	Asp	D	2.98	A	H+	Acid	$—CO_2H$	$C_4H_7NO_4$	133
Cysteine	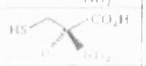	Cys	C	5.02	N*	H	Thiol	—SH	$C_3H_7NO_2S$	121
Glutamic acid	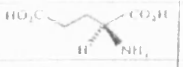	Glu	E	3.22	A	H+	Acid	$—CO_2H$	$C_5H_9NO_4$	147
Glutamine	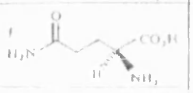	Gln	Q	5.70	N	H	Amide	$—CONH_2$	$C_5H_{10}N_2O_3$	146
Glycine		Gly	G	5.97	N	H	H	—H	$C_2H_5NO_2$	75
Histidine		His	H	7.59	N*	H	Aromatic	Ar	$C_6H_9N_3O_2$	155
Isoleucine	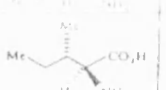	Ile	I	6.02	N	L+	Alkyl	R	$C_6H_{13}NO_2$	131
Leucine		Leu	L	5.98	N	L	Alkyl	R	$C_6H_{13}NO_2$	131
Lysine		Lys	K	9.74	B	H	Amine	$—NH_2$	$C_6H_{14}N_2O_2$	146
Methionine	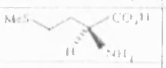	Met	M	5.06	N	L	Thioether	—SMe	$C_5H_{11}NO_2S$	149
Phenylalanine	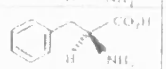	Phe	F	5.48	N	L+	Aromatic	—Ar	$C_9H_{11}NO_2$	165
Proline	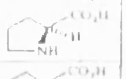	Pro	P	6.30	N	L	N*-ring		$C_5H_9NO_2$	115
Serine		Ser	S	5.68	N	H	Alcohol	—OH	$C_3H_7NO_3$	105
Threonine	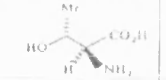	Thr	T	5.60	N	O	Alcohol	—OH	$C_4H_9NO_3$	119
Tryptophan		Trp	W	5.88	N	L+	Aromatic	—Ar	$C_{11}H_{12}N_2O_2$	204
Tyrosine		Tyr	Y	5.62	N	L	Aromatic	—Ar	$C_9H_{11}NO_3$	181
Valine	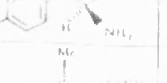	Val	V	5.97	N	L	Alkyl	R	$C_5H_{11}NO_2$	117